Analytical Kinematics

Analysis and Synthesis of Planar Mechanisms

Roger F. Gans
University of Rochester

Butterworth–Heinemann
Boston London Singapore Sydney Toronto Wellington

Library of Congress Cataloging-in-Publication Data

Gans, Roger F.
Analytical kinematics : analysis and synthesis of planar mechanisms / Roger F. Gans.
p. cm.
Includes bibliographical references and index.
ISBN 0-7506-9011-9 (casebound)
1. Machinery, kinematics of. I. Title.
TJ175.G34 1991 90-48111
621.8'11—dc20 CIP

British Library Cataloguing in Publication Data

Gans, Roger F.
Analytical kinematics.
1. Kinematics
I. Title
531.112
ISBN 0-7506-9011-9

Butterworth-Heinemann
80 Montvale Avenue
Stoneham, MA 02180

10 9 8 7 6 5 4 3 2 1

Printed in the United States of America

Contents

PART III KINEMATICS I: ANALYSIS

PART IV KINEMATICS II: SYNTHESIS

PART V FORCES AND MOMENTS

Preface

I wrote this book for the same reason I suspect most academics write books: because there was no book available that did what I wanted with the subject matter. I was looking for a computational approach that was not a cookbook or a collection of programs. I wanted to get at the way programming is done, the idea of thinking algorithmically. This was most easily attained using the compact notation possible when kinematic links are represented as complex numbers. Computation is the heart of this book, and it is made compact by the introduction of the complex variable method of representing two-dimensional vectors.

The book is suitable for a rich one-semester course in kinematics. It is designed to be self-contained. In particular, there is a complete introduction to complex variables in the book. All properties of complex variables necessary for planar kinematics (and a little more) are presented in the text. No background in complex variables is necessary. The student who has never seen complex variables can use this book with no other resource necessary. The student should have calculus, preferably including some differential equations. Chapters 10 and 11 will be easier for students who have had a first course in engineering statics.

The first seven chapters provide a foundation for the following four. Any course based on this book should include these. The first two chapters introduce, in a leisurely fashion, basic kinematic concepts. Chapter 1 introduces seven familiar elementary mechanisms that recur throughout the book. These are used to illustrate basic concepts such as mobility and kinematic inversion. Chapter 2 introduces the bar linkage and extends the ideas beyond four-bar linkages and the slider crank. The four-link mechanism is in many ways a special case. Many of the analytic techniques for analysis and synthesis do not extend automatically to more complicated linkages. The student should be aware of this. Computer power makes more complicated mechanisms less daunting. The step from four to six bars is the key to all further complication. Therefore, I have introduced six-bar linkages here and discussed briefly how one would go to eight-bar and higher linkages. (There is a later homework problem requiring the painless synthesis of a ten-bar linkage.) In these two chapters, the idea of mathematical abstraction is introduced.

The next two chapters provide some mathematical preliminaries. The idea of frame of reference and a general review of vectors are given in Chapter 3. Students well prepared in these areas can safely skim this chapter to become familiar with the notation used in this book. Chapter 4 introduces the complex variable, its arithmetic

properties, and its connection with the two-dimensional vector. The final section of Chapter 4 explains how to differentiate complex variables, which is necessary for the analysis of velocity and acceleration.

The foundations of kinematic analysis appear in Chapters 5 through 7. Chapter 5 introduces position analysis of bar linkages (including the slider-crank linkage). As in other sections of the book, extensions to six-bar linkages are given. The fundamental nonlinear nature of the analysis is explored, and the power of the complex-variable representation is demonstrated. The closing section of Chapter 5 deals with indirect, iterative methods of solution, which are used throughout the rest of the book. Modern digital computers make iterative schemes practical; however, they are not always taught before students encounter kinematics. Some students never see them in a setting in which their utility is apparent. To rectify this and to keep this book self-contained, I have introduced Newton–Raphson schemes for single equations and for systems of equations and have explicated matrix inversion through Gaussian reduction.

Chapter 6 introduces velocity and acceleration, connecting the physical nature of velocity and acceleration with their simple representation in terms of complex variables. Four-bar linkages are emphasized, with extension to six-bar and higher linkages, and there is a discussion of singular mechanisms.

Chapter 7 introduces the two most important higher pairs: gears and cams. The complex-variable approach is shown to make gear-train analysis very simple. The concept of a loop-closure variable not attached to a link is introduced and then used to write loop-closure equations for cam pairs in the second half of the chapter. Cam pairs are analyzed using a Newton–Raphson iterative scheme, for which a pseudocode listing is given. Examples of both single- and four-lobe cams are provided. The translating follower pair is thoroughly explored, and the oscillating follower pair is examined analytically.

Chapters 8 and 9 deal with synthesis. Chapters 10 and 11 deal with forces and moments, introducing the discipline of kinetics. It is difficult in a one-semester course, and probably impossible in a one-quarter course, to cover all the material in these last four chapters. A course in pure kinematics, to be followed by a second course in kinetics, should probably include Chapters 8 and 9. These present the basic concepts of synthesis. Chapter 8 introduces direct methods made possible by the formulation in terms of complex variables. Chapter 9 goes on to indirect methods of the sort necessary for more complicated systems. The transition to six-bar analysis is introduced, and quick mention is made of velocity and acceleration synthesis, as well as the concept of optimum design, which shares techniques with kinematic synthesis.

If synthesis is not a concern, because it is covered in some design sequence, then Chapters 8 and 9 can be omitted without loss of continuity, and the last two chapters can be included. Chapter 10 builds on statics and lays the groundwork for Chapter 11, which introduces such real-world phenomena as inertia and friction. The two final sections present a moderately realistic model of a one-cylinder internal combustion engine as a vehicle for exploration of true dynamic systems, those for which the input is a force and the output is motion. The engine is modeled by a slider crank, with which the student will be very familiar, and a realistic model of the driving force, based on combustion, is provided. I examine start-up from rest, equilibrium speed, variations in

speed, and how they depend on system inertia, and the shaking of the frame induced by low- and high-inertia systems. I give pseudocode for all these problems.

An alternative course including the elements of both synthesis and kinetics would utilize Chapters 8 and 10, again without loss of continuity.

I close this Preface with some comments about computation. "Real" kinematics is done computationally. Computing is central to this book. Algorithms for solving progressively more difficult problems are given throughout the book, often building on simpler algorithms presented earlier. I believe, however, that giving commercial packages to students in a first course in any engineering area obscures both the academic subject and the limits of computation. Students must write their own codes. They must understand what algorithms are and how to create them before going on to use the major commercial codes they will see in industry. Programming skills, and the algorithmic thinking that underlies these skills, are essential for anyone embarking on an engineering career today. On the other hand, it doesn't matter in what language a student programs. Fortran is perhaps the best. It is widely used in engineering and science, and it has the advantage of built-in complex variable arithmetic, but many engineering students are first introduced to computing through Basic or Pascal, languages without built-in complex arithmetic. I have elected to present the programs in pseudocode; however, all the programs in this text are easily programmed in Pascal. Many of the curves presented in the text were created using Pascal programs written following the pseudocode algorithms in the text. (Indeed, some of the pseudocode is backformed from the appropriate Pascal program.)

I am grateful to the following gentlemen for their wisdom and kind suggestions: Professor Michael Savage, University of Akron, Dr. Struan R. Robertson, University of Lowell, Professor Brian Gilmore, Pennsylvania State University at University Park, and Professor Stephen Tricamo, Stevens Institute of Technology. This book is better because of them. Of course, they are not responsible for suggestions misunderstood and wisdom ignored.

Roger F. Gans
Rochester, New York

PART I

Kinematic Preliminaries

Chapter 1

Mechanisms and Their Abstractions

One of the most important tasks for mechanical engineers is the design of machines with moving parts. These machines transform motion from one form to another and transmit power. The earliest machines are ancient indeed: the mill, the shadoof, the loom, the pot chain. Two early tasks were the conversion of reciprocating motion to rotary motion, and vice versa, and the change in direction of rotary power.

Of the former, Watt (Tann 1972) said in 1808, "The true inventor of the crank rotative motion was the man (who unfortunately has not been deified) that first contrived the common foot lathe." Whether this is true or not, crank-driven rotary motion was well known early in the fifteenth century (Usher 1929), and many of Leonardo da Vinci's sketches show crank-operated mechanisms (as do earlier sketches by Taccolo (Prager and Scaglia 1972). (For an interesting assessment of Leonardo, see Truesdell 1955.)

Gearing was developed when water power was harnessed for the grinding of grain. It was necessary to transform the rotation of the waterwheel's horizontal axle to vertical rotation to drive the millstones. Changes in speed also allowed more efficient grinding. The problem was certainly solved by the Romans before the start of the Christian Era. For an interesting collection of the state of kinematic knowledge in Europe during the late Renaissance, see the 1588 "text" by Ramelli, which shows, among many other things, 110 ways to raise water (Gnudi 1972).

The design process involves synthesizing mechanisms that will produce, without failure, given motions under the application of given forces. The design process itself is full of art, an art the design engineer keeps learning throughout his or her career.

The first task, design of a mechanism that can produce a desired motion from a simpler motion, is the main subject of this text. (It will be necessary to study how existing mechanisms work before new ones can be designed.) Some attention will be paid to the second task, the transmission and transformation of forces, but the emphasis will be on motion transformation. The study of motion, divorced from the force that produces it, is kinematics. The study of dynamics, including the forces, can be added. The resulting discipline, to which this text provides some introduction, is usually called *kinetics*.

Before mechanisms can be synthesized, existing mechanisms need to be analyzed. This is the easiest way to develop a set of tools that can be used later for synthesis. It is also a good way to become familiar with over two thousand years of kinematic lore. The more mechanisms one sees, the better chance one has of designing a good mechanism to do a given task. The great ancient and medieval mechanicians could function with primitive tools. The average engineer needs better, modern tools. These tools of the modern engineer are mathematical techniques implemented on digital computers. Therefore, of necessity, this text will eventually become quite mathematical, but we will always maintain contact with the physical world of engineering devices.

The words *design* and *synthesis* have already been used interchangeably. They are not exact synonyms. Synthesis is the more limited and well-defined word. Design includes synthesis. In this text, *synthesis* will be used fairly strictly to mean the design of a mechanism to perform a given kinematic task. Design will be used more generally. Synthesis is the design of a mechanism to take one sort of motion and transform it into another. The primary motion is simple, usually a rotation, as the output of most prime movers, motors, and engines is rotation. Occasionally, the prime motion will be reciprocal, as the motion of a piston (which is then converted into a rotating motion at the crankshaft, which can serve as the prime mover for the next mechanism).

Like all design problems, mechanism synthesis does not have a single solution. There are an infinite number of mechanisms capable of accomplishing a given task. It is the job of the designer to find the best approximation possible to the optimum mechanism. The meaning of optimum is not always clear and varies from job to job. Some criteria for "goodness" will be given in this text. Others will be discovered throughout your career.

The study of mechanism design will begin with the quick, qualitative examination of some specific mechanisms.

SEVEN MODERN MECHANISMS

Figure 1.1 shows the working parts of a set of compasses or dividers. The two legs pivot at *a*. The joints at *b* and *c* are more complicated. There is a pin normal to the page. The leg can slip with respect to this pin. The pin also has a threaded hole in the plane of the page through which the threaded control rod goes. Rotation of knob *d* pushes pins *b* and *c* apart or pulls them together. The thread shown is right-handed on one side and left-handed on the other. The motion transduction is from the rotation of knob *d* to the change in angle between the legs of the compasses. Note that this motion is not two-dimensional; the rotation axes of the two rotations are perpendicular.

Figure 1.2 shows a geared corkscrew, immediately after the cork has been withdrawn. The bottle is shown in section and severely truncated. The screw itself and the attached cork have not been shown. They are in the frame, center. There are two kinematic processes required to remove the cork. The first is rotation of the shaft about the vertical, driving the corkscrew into the cork and lifting the legs by the action of the toothed shaft on the toothed legs. The second process, withdrawal of the cork, takes place by moving the legs down and lifting the shaft, which does not turn.

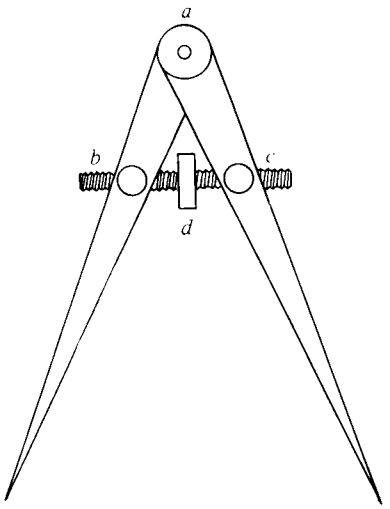

FIGURE 1.1 *Schematic of the working mechanism of a pair of dividers or a compass. The knob* d *is rotated to change the spacing of the legs.*

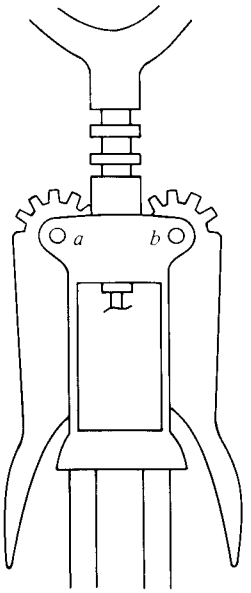

FIGURE 1.2 *A typical two-eared geared corkscrew shown immediately after pulling a cork. The bottle is shown sketchily, and the cork and screw are not shown.*

In operation, the side legs pivot about pins a and b. The gears mesh with the teeth of the vertical member, attached to the actual corkscrew and cork, moving it up and down. This is a rack-and-pinion system, in principle, exactly as advertised on the steering of sports cars. The two gears are the pinions, and the shaft is the rack.

Figure 1.3 shows another type of corkscrew, which I will call a sommelier's corkscrew, in its initial position and, in dashed lines, its final position. The process of withdrawing the cork is shown by the arrow from c to c'. The parts of the corkscrew have been labeled 2, 3, and 4. In operation, part 2 pivots on the bottle at point a. Part 3 pivots about point b, which is also moving with part 2. There is relative rotation of parts 3 and 4 about the pivot c, but part 4 moves in a straight line, constrained by the neck of the bottle. Kinematically, the cork and the corkscrew are part of the same member because there is no relative motion between them.

Figure 1.4 shows a device that allows the earpieces of a pair of eyeglasses to flex outward. The view is from above. The earpiece extends horizontally to the left, and the lenses of the glasses extend upward from point d, which is the ordinary hinge between the earpiece and the front of the glasses. In operation, earpiece segment 1 is fixed, and the remainder of the earpiece is pulled out (down in the figure), as indicated by the arrow. There is a pivot point at a and a pin at b. Block c is constrained in a channel and has a pivot, so that members 2 and 4 can slide with respect to each other and block c can also pivot. It is interesting to compare this to the second corkscrew.

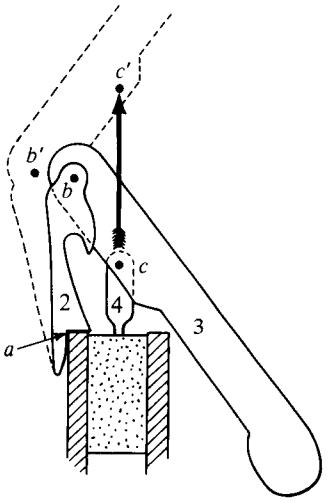

FIGURE 1.3 *The sommelier's corkscrew shown at the start of its stroke (solid lines) and then end (dashed lines). The cork and screw move together from point* c *to point* c'.

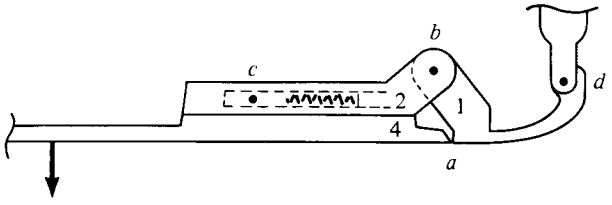

FIGURE 1.4 *A device that allows the earpiece of a pair of eyeglasses to be pulled out wider than its normal rest position. The earpiece is horizontal, labeled* 4*; the eyeglass front is vertical, directly above point* d.

The two pivots at *a* are equivalent, and the block *c* behaves like the cork. The earpiece is like the bottle. Detailed comparison awaits the development of a language in the next chapter.

Figure 1.5 is a scale drawing of the foot-brake linkage on a motorcycle, viewed from the side. Element 2 is the foot pedal. It pivots about pin *a*, connecting it to the frame of the motorcycle, here solid black and numbered 1. The motion of the pedal pulls on link 3, which rotates lever 4. Lever 4 is pivoted at *d* and operates the brake shoes inside the casing labeled 1. The casing is labeled 1 because it is rigidly attached to the frame of the motorcycle and so is kinematically the same as the other frame member labeled 1.

Figure 1.6 shows the opening mechanism for a pivoted rear automobile window. The view is from above, and this is the mechanism on the left-hand side of the car. The front of the car is to the left. Element 1 is part of the body of the car. Element 4 is the window, which pivots around a point well off the page to the left.

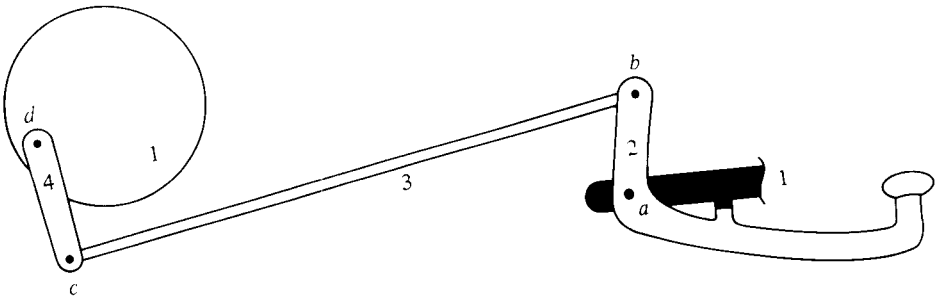

FIGURE 1.5 *Scale sketch of the foot-brake linkage for a motorcycle. The motorcycle has been omitted for clarity. The black element 1 on the right represents the frame of the motorcycle. The disk labeled* 1 *on the left represents the brake drum housing. It has the same designation as the frame because it is attached to the motorcycle and does not move with respect to the frame.*

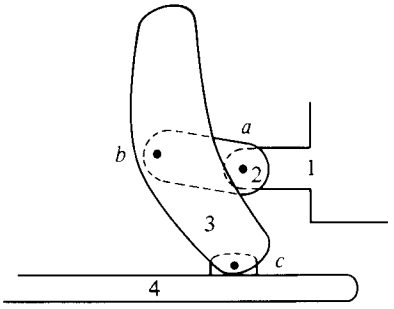

FIGURE 1.6 *A top (plan) view of the pivot mechanism for the rear window of an automobile. The link labeled* 4 *represents the window. It pivots about a point about 800 mm to the left of point* c.

The operator rotates and slides element 3. This rotates both 2 and 4. In both the closed and open positions, elements 2 and 3 are nearly parallel in the sense that the lines *ab* and *bc* are nearly parallel. Element 2 rotates approximately π rad. Element 3 rocks back and forth through a smaller angle, and 4 pivots smoothly through a very small angle. (For the vehicle in question, this angle is about 0.08 rad, or 4.5°.)

Figure 1.7 shows a pair of vise-grip pliers. The fixed jaw is labeled 1 and the movable jaw 4. The operator moves handle 3, rotating jaw 4 and element 2. In the closed position, elements 2 and 3 are nearly parallel in the same sense as for the window mechanism just described: Lines *bc* and *cd* are nearly parallel. The opening of the jaw for which this occurs is controlled by the location of pivot *d*, which is controlled by element 5, so that this mechanism is somewhat more complicated than the window mechanism. (The spring that keeps the system from coming apart when the pliers are open is not shown.)

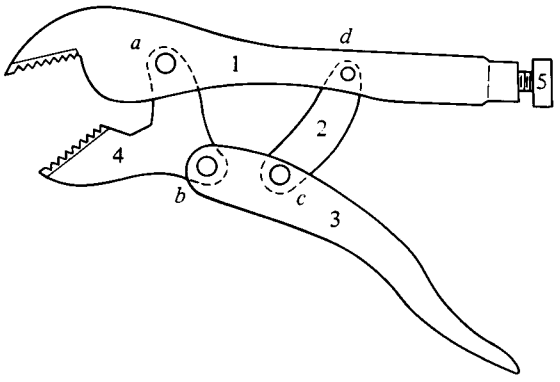

FIGURE 1.7 *A pair of locking (vise-grip) pliers. The screw* 5 *is used to adjust the position of the pivot* d, *which controls the size of the jaw opening in its locked position.*

JOINTS AND LINKS: LOWER PAIRS AND HIGHER PAIRS

The devices described so far are all complicated arrangements of parts, unsuitable to direct analysis, with the differences in their appearance obscuring the commonality they share. This formal section will demonstrate the commonality and provide language with which kinematic devices can be discussed and analyzed.

Each device is made of solid parts connected by joints of one sort or another, allowing relative movement. In what follows, the solid parts will be assumed to be ideally rigid and undeformable. This is a good approximation for machines that are working as they are meant to. Later in the text, modes of failure will be discussed briefly; for now, the ideal is good enough. The solid parts will be called *links* and the joints will be called *joints.*

Joints allow motion. The kind of motion is best classified by its number of degrees of freedom. A joint has as many degrees of freedom as the number of independent motions it allows. The word *independent* is important. A screw rotates and translates, two different motions, but these motions are not independent; they are connected by the pitch of the thread, and one variable can describe the position and orientation of the screw.

Consideration of the various joints that occur in machinery, such as nut and bolt, ball and socket, and cam and follower, leads one to note that joints are not isolated objects but pairs. A joint or connection is also called a *kinematic pair.*

Kinematic pairs are divided into lower pairs and higher pairs. The language comes from Reuleaux (1876), as does the identification of the first three lower pairs. Lower pairs are kinematic pairs, the elements of which contact along surfaces. Reuleaux called these *closed pairs.* Modern terminology recognizes six lower pairs: (1) the pin or revolute, (2) the sliding or prismatic, (3) the screw or helical, (4) the cylindric, (5) the globular or spheric, and (6) the flat or planar pair. Figure 1.8 shows sketches of the lower pairs (the first three from Reuleaux), and Table 1.1 summarizes their properties.

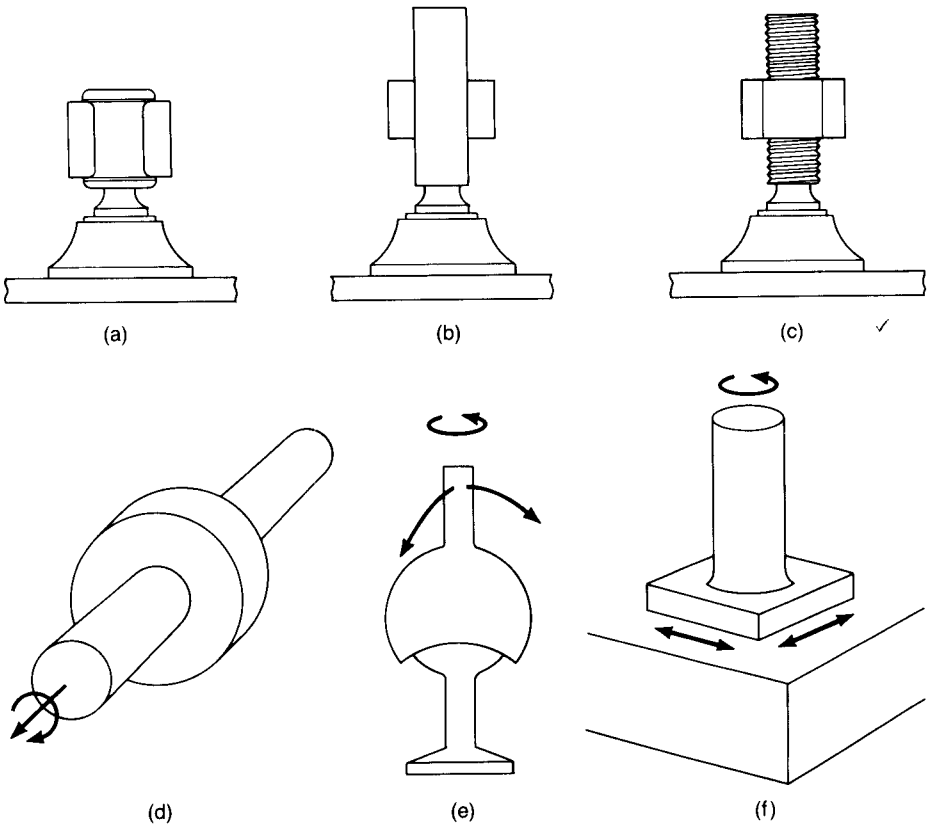

FIGURE 1.8 *The six lower pairs:* (a) *the revolute;* (b) *the prism;* (c) *the screw or helix;* (d) *the cylindric;* (e) *the spheric or globular; and* (f) *the planar, or flat. [Parts* a–c *after Reuleaux (1876).]*

Table 1.1 The Six Lower Pairs

Pair	*Symbol*	*Variable*	*Degrees of Freedom*	*Motion*
Revolute	R	θ	1	Circular
Prism	P	s	1	Linear
Screw	S	θ or s	1	Helical
Cylinder	C	θ & s	2	Cylindrical
Sphere	G	θ, ϕ, ψ	3	Spherical
Flat	F	x, y, θ	3	Planar

All other pairs, such as gears, cams, wheels, chains, and belts, are called *higher pairs.* These do not lend themselves to easy subclassification and will be dealt with as they arise.

A set of links connected by joints forms a *kinematic chain.* A closed kinematic chain, in which the last link is attached back to the first, is called a *mechanism.* Chains and mechanisms can be classified according to the nature of their movement. Chains for which all link points move in parallel planes, so that the system can be projected unambiguously onto a single plane, are called *planar.* Chains for which all motions can be described as rotation about a single point are called *spherical.* For both these systems, the motion of a point can be described by two variables, the Cartesian x and y for the planar case and the polar angles θ and ϕ for the spherical. All remaining chains are called *spatial.*

Most mechanisms in use today are planar, and this text will be restricted to planar mechanisms after this chapter. The restriction to planar mechanisms means that only two lower pairs will be considered: the revolute, which I will usually refer to as a *pin,* and the prismatic, which I will usually refer to as a *slider.* In the interest of generality, some properties of general mechanisms will be presented before the text becomes restricted.

The subject of this text is relative motion. A useful mechanism is attached to something; it has a stationary link. The compasses, the vise grip, and the eyeglasses are attached to the user. The corkscrews are attached to the bottle, which is held firmly by the wine steward. The window mechanism is attached to the car. The brake mechanism is attached to the motorcycle. Nothing about the relative motion of the links changes if the car is moving or the wine steward is in the dining car of a train (or on the Concorde). On the other hand, a mechanism can seem very different if viewed from a different perspective.

A mechanism is not fully specified until its ground link is defined. There is always one link that is stationary, and that link is called the *ground link,* or *frame link.* The positions of the other links can be defined in terms of a reference frame (coordinate system) attached to the frame link. (There is something of a deliberate pun here; *frame* has two meanings.)

Motion in Three Dimensions

A rigid object—a link—has six degrees of freedom. To define its position in space requires six numbers. These can be chosen in several ways. The most convenient for kinematic (and kinetic) analysis is to choose three to define the location of one point on the link, and three more to define the orientation of the link with respect to the frame (of reference). The location and orientation of the link can then be specified by choosing the three coordinates of the fixed point (x, y, z), and three numbers, the direction cosines, say, specifying the orientation of the line.

The usual way to specify the orientation of the line is in terms of its Euler angles. For a complete development, the reader is referred to any of several books on dynamics, such as McGill and King (1984) or Meirovitch (1970). I will outline the definitions here.

The idea is to define, unambiguously, three angles relating the orientation of a link as described in a coordinate system attached to the link to a fixed coordinate system

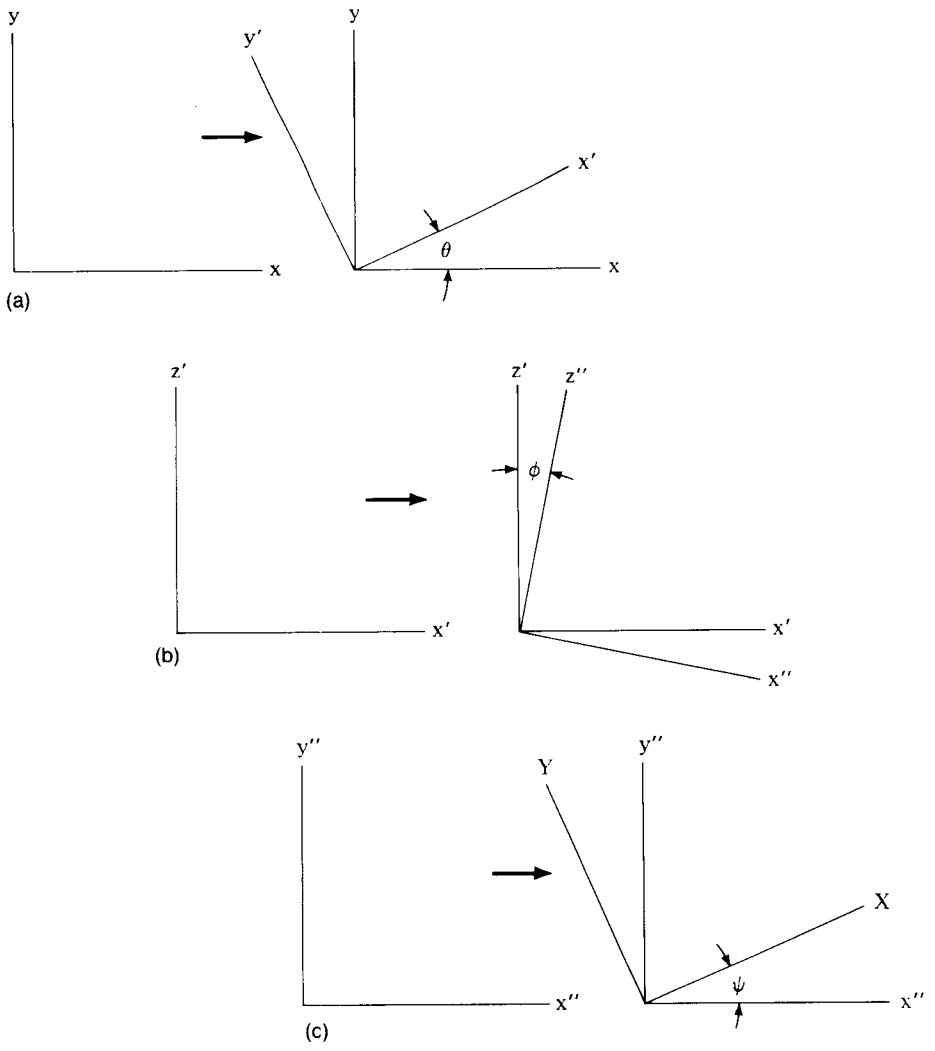

FIGURE 1.9 *Planar projections showing the three successive rotations in going from* (x, y, z) *to* (X, Y, Z) *through the intermediate coordinate systems* (x', y', z') *and* (x", y", z"): (a) *rotation about the* z *axis;* (b) *rotation about the* y' *axis;* (c) *rotation about the* z" *axis.*

attached to the frame. This is done operationally in the form of an algorithm that can be followed to bring one coordinate system into correspondence with another. Three such rotations suffice, and the magnitudes of the rotations are called the *Euler angles.*

The full three-dimensional picture is hard to draw. Figure 1.9 shows planar projections of the three rotations. Let x, y, z represent the initial coordinate system and X, Y, Z the final system. The algorithm is as follows:

1. Rotate an angle θ around z, giving an intermediate coordinate system (x', y', z'). Because the rotation was around z, z and z' are identical.
2. Rotate an angle ϕ around y', giving a second intermediate system, (x'', y'', z''). Because the rotation was around y', y' and y'' are identical.
3. Rotate an angle ψ around z'', bringing the frame into correspondence with (X, Y, Z). Because the rotation was around z'', z'' and Z are identical.

MOBILITY

Attaching two links constrains the motion of each link. They must move together. How they do this depends on the kind of pair used to join the links. To illustrate this, imagine attaching a link to the frame using each of the various lower pairs. The frame defines the frame of reference. It has no degrees of freedom. Attaching a link to the frame will remove one or more degrees of freedom, the number depending on the type of joint. Let the attachment point be the reference point on the link, and designate the link as 2, so that its coordinates are x_2, y_2, z_2, and θ_2, ϕ_2, ψ_2. The lower pairs are shown in Figure 1.8. The axes of the first four—revolute, prism, screw, and cylindric—are taken to be parallel to the z axis of a Cartesian system. The plane shown in Figure 1.8f is taken to be the x-y plane.

Using these definitions to analyze each of the lower pairs in turn leads to the following constrained motions:

1. The revolute fixes x_2, y_2, z_2 and ϕ_2—the attachment point and the plane of the motion, the x-y plane. The link can rotate around its attachment point. It is held in the x-y plane, and its position is completely specified by the angle that the link makes with the x axis, θ_2.
2. The prismatic pair fixes everything except z_2. The link can move along the z axis without rotation. Its position is completely specified by the value of z_2.
3. The helical pair fixes x_2, y_2, ϕ_2, and ψ_2 and relates θ_2 and z_2. The link rotates around, and simultaneously moves along, the z axis. Because the helix is a specified screw with a specified pitch, the rotation angle θ_2 and the axial position z_2 are related. Either variable completely specifies the position of the link. The motion is a constrained combination of the first two motions.
4. The cylindric pair fixes x_2, y_2, ϕ_2, and ψ_2. This is an unconstrained combination of the first two motions. Two numbers, θ_2 and z_2, are required to specify the position of the link.
5. The spheric pair fixes all three Cartesian coordinates and leaves all the angles free. It takes three numbers to specify the position of the link. This is a universal joint. The link can be rotated about three independent axes. (In reality, the rotation will be limited by interference between actual physical elements. The ideal of full 360° rotation about three axes is not physically realizable.)
6. The planar pair fixes z_2, θ_2, and ψ_2. It takes three numbers to specify the position of the link. The motion of the link is confined to the x-y plane but totally unconstrained in that plane. The planar pair does not constrain planar motion; it is not one of the lower pairs used in planar kinematics.

These examples illustrate the general principle that adding an n-degree-of-freedom joint to a system removes $6 - n$ degrees of freedom from that system, providing $6 - n$ *constraints.*

The point of mechanism is *relative motion.* The total degrees of freedom is not of interest. What is of interest is the number of degrees of freedom remaining when one link is fixed. Fixing one link is equivalent to choosing the frame or ground link. The number of degrees of freedom remaining is called the *mobility,* denoted by m. Let j_1 denote the number of one-degree-of-freedom joints in a mechanism j_2, the number of two-degree-of-freedom joints, and so on to j_5. Let n denote the number of links. Then the mobility is given by

$$m = 6(n - 1) - 5j_1 - 4j_2 - 3j_3 - 2j_4 - j_5 \tag{1.1}$$

This is called the *Kutzbach mobility criterion* for a spatial mechanism.

A system of no mobility cannot move. It is a structure. It is of no interest to a class in kinematics. The question arises: Can anything general be said about the number of links necessary to have a mobility greater than zero?

Consider a spatial mechanism with only lower pairs. The least restrictive lower pairs have three degrees of freedom and provide three constraints. The minimum mechanism will satisfy Equation (1.1) with $m = 1$, and j_1, j_2, j_4, j_5 all zero. To have a closed kinematic chain, there must be at least as many joints as links. Set $j_3 = n$, and solve to find $n = 7/3$. That is, of course, silly. There must be an integral number of links. The next integral number of links is three, for which the Kutzbach formula predicts a mobility of 3.

The actual mechanism just specified is not useful. Consider three rods joined in a triangle by spheric pairs. As each pair allows rotation in any direction, each rod can rotate about its own long axis independently of the others. It is a three-degree-of-freedom system (once the frame link is chosen). It is not a normal mechanism. It doesn't do anything that meets with one's intuitive feeling about mechanisms. Is a more restrictive set of joints any help?

How many links are necessary to have a useful (mobility at least unity) spatial mechanism using just one-degree-of-freedom joints? Set $m = 1$ and j_2–j_5 equal to zero, and rearrange to find

$$6n - 5j_1 - 7 = 0, \tag{1.2}$$

the so-called Gruebler criterion. A closed kinematic chain must have at least as many joints as links. Setting $j_1 = n$ gives the least number of links and the simplest such spatial mechanism, a seven-link, seven-joint mechanism.

The reduction to planar mechanisms is not direct. This is because the three spatial degrees of freedom—z_2, ϕ_2, and θ_2 in the current setting—can be removed only once. The problem of redundant reduction of freedom will be clarified shortly by a planar example. Because of the ambiguity, it is easiest to consider planar mechanisms ab initio, assuming the reduction to a plane to be given and working directly in two dimensions.

A link confined to a plane has three degrees of freedom, two translational and one rotational. Two links have six degrees of freedom. Welding them together reduces this

to three. Pinning them together removes two degrees of freedom, leaving four. Only one- and two-degree-of-freedom joints are possible in a two-dimensional system. If the number of each is denoted by j_1 and j_2, respectively, an argument parallel to that just given gives the two-dimensional Kutzbach criterion

$$m = 3(n - 1) - 2j_1 - j_2 \tag{1.3}$$

and the Gruebler criterion reduces to

$$3n - 2j_1 - 4 = 0 \tag{1.4}$$

from which the simplest mechanism is a four-link mechanism. A planar mechanism is a special case of a spatial mechanism, but the smallest spatial mechanism with one degree of freedom apparently needs seven links. What happened?

This is a pathological example of the Kutzbach and Gruebler criteria. They work most of the time and provide an essential guide to what is happening but, in special circumstances, they are incorrect. What has happened here is that some of the constraints are duplicate, redundant, when a spatial mechanism is reduced to a planar mechanism. The first $n-1$-degree-of-freedom joints remove three translational and two rotational degrees of freedom as each link is added. The remaining rotational degree of freedom for each link is parallel to those before. The argument can be rephrased mathematically as follows.

Let there be n links and j_1 single-degree-of-freedom joints. The first link is irrelevant, representing the gross motion of the mechanism. The second link has six degrees of freedom, five of which are removed by the first one-degree-of-freedom joint. The third link has five of its degrees of freedom removed when it is added. So, too, the fourth link has five of its degrees of freedom removed when it is added. At this point, there is an open kinematic chain of four links with three degrees of freedom. The system cannot rotate or translate out of the plane. The last joint, reconnecting the fourth link to the first, removes only two **new** degrees of freedom. The other three are already gone. This argument can be extended to planar systems of more than four links, but it is easier to use the reduced criteria (1.3) and (1.4).

Figure 1.10 shows several planar mechanisms involving only one-degree-of-freedom joints: sliders and pins. For each, the formal mobility is given using the Kutzbach recipe. There are a number of things to note about this diagram. Most important perhaps is the degree of abstraction. The minimum number of lines have been used to represent the essential kinematic data. The second thing to note is the introduction of the *ground,* or *frame,* link, that single link with respect to which the motion of the others is to be considered. It is symbolized by the diagonal hatching beneath it. In this figure, the ground link is drawn in a continuous fashion. This will not always be so. In the future, remember that all joints attached to diagonal hatching are attached to the same (kinematic) ground, or frame, link.

Figure 1.10c introduces one notation for a slider. The block is a link; it is a separate rigid body with two joints, a pin (revolute) and a slider (prism), connecting it to the two adjacent links.

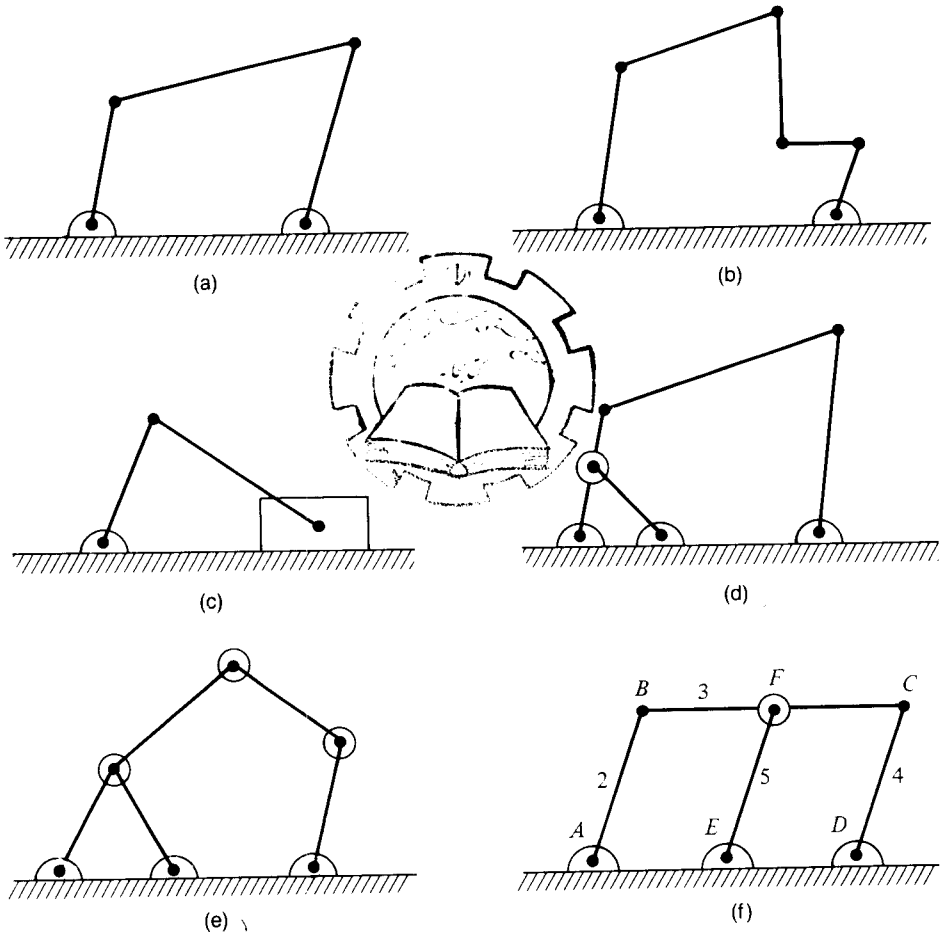

FIGURE 1.10 *Some planar mechanisms and their formal mobility according to the Kutzbach criterion:* (a) n = *4*, j_1 = *4*, m = *1;* (b) n = *6*, j_1 = *6*, m = *3;* (c) n = *4*, j_1 = *4*, m = *1;* (d) n = *5*, j_1 = *6*, m = *0;* (e) n = *6*, j_1 = *7*, m = *1;* (f) n = *5*, j_1 = *6*, m = *0.*

Figure 1.10d illustrates an immobile mechanism, a structure (actually a simple truss). This is the general situation for $m \leq 0$. Figure 1.10e shows a partially mobile mechanism. It has a formal and actual mobility of unity, but only three of the five non-ground links can move. It is effectively a four-link rather than a six-link mechanism. Figure 1.10f is a pathological example of a mechanism with a formal mobility of zero that is nonetheless mobile. A formal demonstration of this will make the idea of these redundant, pathological cases easier to understand. I will outline such a demonstration here, an imaginary assembly of the mechanism from its links.

When a contrary-to-fact answer emerges from these Kutzbach and Gruebler criteria, it suggests the need to think more clearly and precisely. One useful technique is mentally to "assemble" the mechanism, keeping track of what happens to the

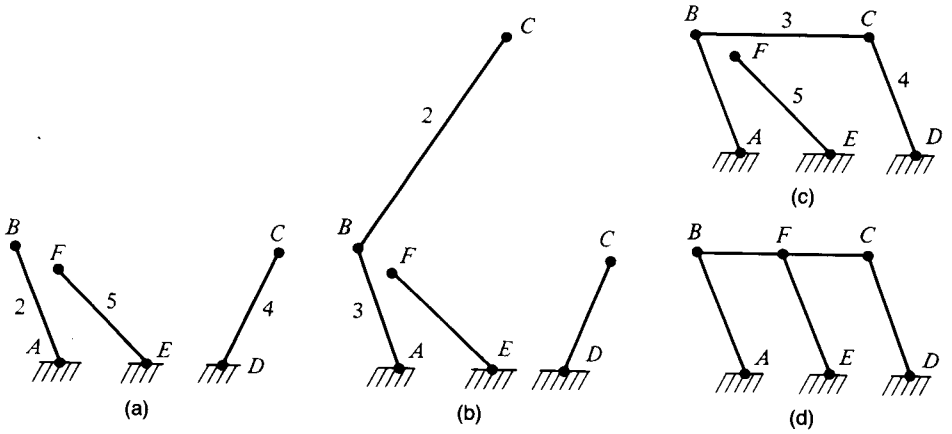

FIGURE 1.11 *The steps in the mental assembly of a pathological mechanism:* (a) *attach links* 2, 4, *and* 5 *to the ground (frame);* (b) *attach link* 3 *to link* 2; (c) *attach link* 3 *to link* 4; (d) *attach link 5 to link 3.*

degrees of freedom as the assembly proceeds. To that end, let the frame be link 1, and label the other links as shown in Figure 1.10f. Let the fixed points be A for link 2, B for link 3, D for link 4, E for link 5. Denote the length of each link by r_j, where j takes on the values 1–5. The defining coordinates will be x_j, y_j, and θ_j. Without loss of generality, I can let the frame link coincide with the x axis, and I can let A be the origin. The assembly stages are shown in Figure 1.11.

Attach links 2, 4, and 5 to the frame (Figure 1.11a). This imposes the following conditions:

$$x_2 = 0 = y_2, \qquad x_4 = r_1,\ y_4 = 0, \qquad x_5 = a,\ y_5 = 0 \tag{1.5}$$

where a is the distance from A to E. The three angles θ_2, θ_4, and θ_5 are left unspecified. The partial assembly has three degrees of freedom, a mobility of 3.

Attach link 3 to link 2 (Figure 1.11b). This determines the location of the fixed point, the end of link 3, in terms of the orientation of link 2

$$x_3 = r_2 \cos \theta_2, \qquad y_3 = r_2 \sin \theta_2 \tag{1.6}$$

and leaves θ_3 unspecified. This partial assembly has four degrees of freedom. Now, attach link 3 to link 4 (Figure 1.11c). Point C can be expressed in terms of both links 4 and 3. As the two expressions for C must be the same, this provides additional constraints. After some simple algebraic manipulation, the constraints become

$$\begin{aligned} r_2 \cos \theta_2 + r_3 \cos \theta_3 &= r_1 + r_4 \cos \theta_4 \\ r_2 \sin \theta_2 + r_3 \sin \theta_3 &= r_4 \sin \theta_4 \end{aligned} \tag{1.7}$$

These are two (nonlinear) equations in the three unknowns θ_2, θ_3, and θ_4. It happens that they are sufficient to eliminate any two of the three angles. Let θ_2 be the angle retained. This partial assembly has two degrees of freedom, conveniently retained in the two angles θ_2 and θ_5.

Now, attach the other end of link 5 to link 3 (Figure 1.11d). Point F is representable in two ways, again providing two constraints. These constraints can be written as the pair of algebraic equations

$$\begin{aligned} r_2 \cos\theta_2 + b \cos\theta_3 &= a + r_5 \cos\theta_5 \\ r_2 \sin\theta_2 + b \sin\theta_3 &= r_5 \sin\theta_5 \end{aligned} \tag{1.8}$$

Recall that θ_3 is a function of θ_2, so that these equations have two unknowns, θ_5 and b, the distance from B to F. In general, there is a unique solution, and the arrangement shown in Figure 1.10f is a structure. Note, however, that if $r_2 = r_4 = r_5$ and $r_1 = r_3$, then the two pairs of Equations (1.7) and (1.8) can be made identical by setting $b = a$, $\theta_3 = 0$, and θ_4 and θ_5 equal to θ_2. The angle θ_2 remains unspecified, and the mechanism can move. An alternative approach to mobility will be given in Chapter 6.

Figure 1.12 shows the mechanism of Figure 1.10d redrawn with the links and joints labeled. This introduces a convention to be followed in this text: links will be numbered and joints denoted by uppercase letters. Note that this mechanism remains a structure, no matter where on link 2 joint E is placed (except at A, when link 5 becomes redundantly equivalent to link 1, the frame, or ground, link). In particular, if E is placed at B, the structure remains a structure. Remember this example when counting joints. A pin that connects three links looks like a single pin on paper but is actually two pins. If link 5 connected B to F, the joint at B would be counted twice in calculating the mobility. Another way to remember this is to recall the idea of pair. The pin may be a single pin in fact (supposed to be part of link 3, say), but it has one surface that mates with a surface on link 2 and another that mates with a surface on link 5. This is shown in Figure 1.13.

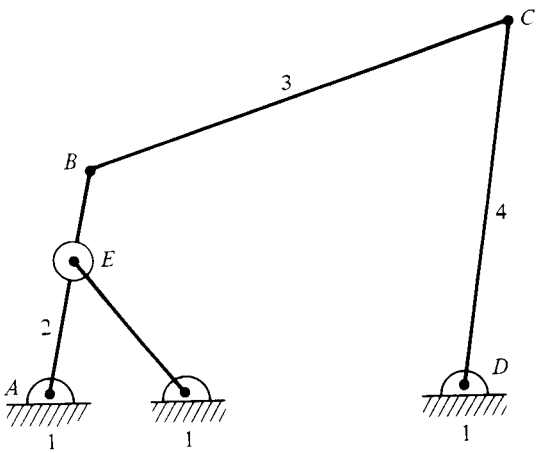

FIGURE 1.12 *A five-bar structure that has a formal and an actual mobility of zero.*

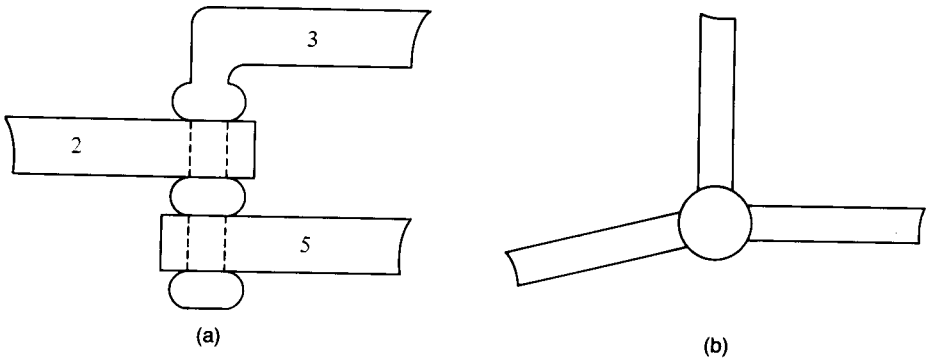

FIGURE 1.13 *Two revolute joints connecting the three bars* 2, 3, *and* 5: (a) *side view (elevation),* (b) *top (plan) view.*

Before leaving the subject of mobility, it is useful to discuss the application of pathology to real mechanisms briefly. A planar mechanism is a special case of a spatial mechanism and obeys the special Kutzbach and Gruebler criteria only insofar as it is truly planar. In the real world, truly planar objects do not exist. Fortunately, truly ideal joints also do not exist. A planar mechanism, then, will behave like an ideal planar mechanism only if the imperfections in the joints are comparable to the imperfections in the planar nature of the mechanism. That is, the (unavoidable) play in the joints must be comparable to the (unavoidable) misalignment of the mechanism.

We can get a feel for this behavior in two dimensions by looking again at Figure 1.10f. If the redundant diagonal member is misaligned, the mechanism becomes a structure, but a slight misalignment can be compensated for by a sloppy joint, allowing the link to wriggle into alignment when necessary.

EQUIVALENT MECHANISMS AND KINEMATIC INVERSION

The degrees of freedom of the "first" link are irrelevant. (By convention, the first link will be identified with the ground link, or the frame of the mechanism.) It must then follow that the identity of the first link is also irrelevant to the overall relative motion of the mechanism. That is true in principle. The abstract geometry of movement doesn't change with the choice of the first link. However, the utility of the mechanism, the observer's view of the mechanism, and the effectiveness of the mechanism in a machine depend heavily on the choice of frame member.

Mechanisms that are identical except for the choice of the frame member are called *equivalent mechanisms.* The process of changing the frame member is called *kinematic inversion.* Figure 1.14 shows the four equivalent mechanisms for the slider crank. The first is identical to the mechanism shown in Figure 1.10c. To make the process clearer, the links and joints are not relabeled from inversion to inversion. This is a temporary departure from the usual convention that the frame link is always labeled link 1.

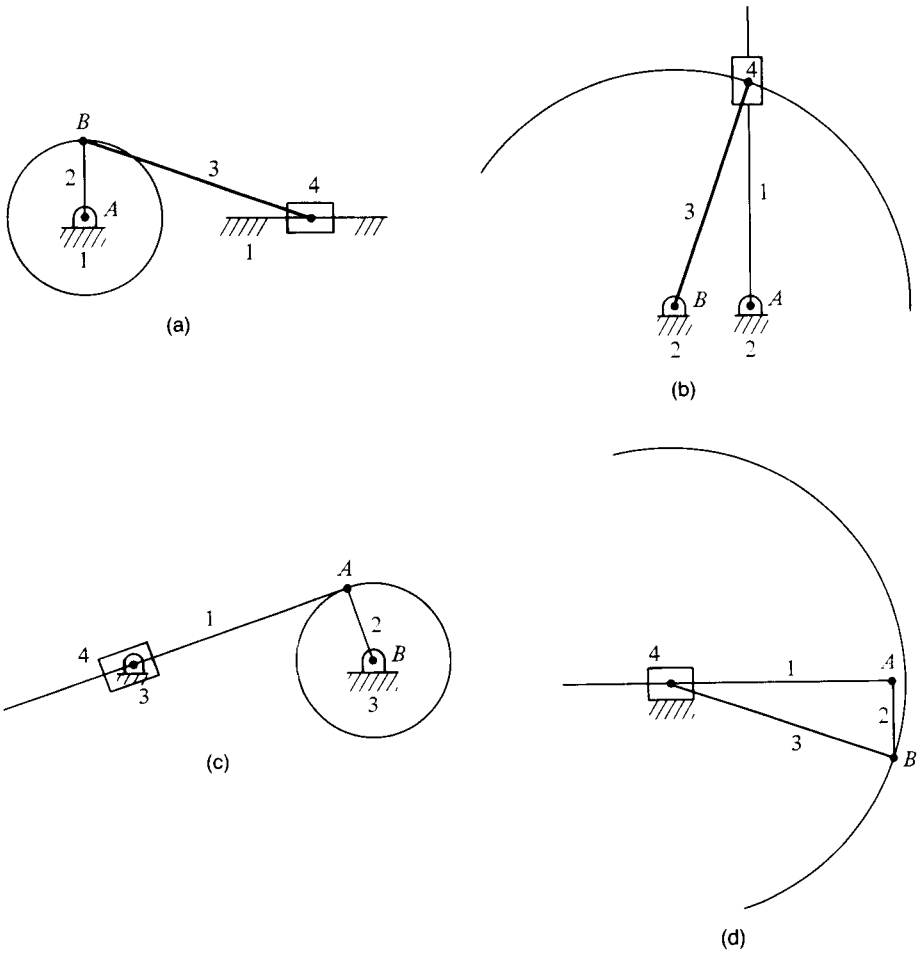

FIGURE 1.14 *The four inversions of the slider-crank mechanism:* (a) *the crank slider;* (b) *the center of the slider moves in a circle around* B; (c) *the slider pivots about its center;* (d) *the slider is stationary, and* B *moves in a circle about the center of the slider.*

The first inversion is the slider crank. Link 2 rotates with respect to the frame, and link 4 oscillates without changing its orientation. If link 4 is driven, this is a model of one cylinder of an internal combustion engine: link 1 is the block, link 2 the crankshaft, link 3 the connecting rod, and link 4 the piston. If link 2 is driven, this can be a pump. In the next inversion, both links 1 and 3 rotate. With suitable stops, this can be a model of a window closing mechnism: link 1 is the window, link 2 is the building, and links 3 and 4 form the closing mechanism. (As drawn, this is a poor mechanism, but the object of this exercise is to keep the dimensions the same to emphasize the process of inversion.) In the third inversion, link 2 rotates and links 1 and 4 rock. In the fourth inversion, link 3 rocks and link 1 moves back and forth. The mechanism closely

resembles the first and shares with it an ambiguity of motion that will be more fully explored later.

The process of kinematic inversion is general. Any mechanism can be inverted by simply changing the identity of the frame. The illustration was a very simple four-link planar mechanism. Do not let this obscure the generality of the process. Similarly, the Kutzbach and Gruebler criteria, although they fail in what the mathematician would call pathological cases, are general. The next chapter explores the less general situation of bar linkages, which are mechanisms consisting only of bars connected by pins.

ABSTRACTION OF SOME REAL MECHANISMS

Before moving on, consider the real mechanisms described qualitatively in this chapter. The language developed and the idea of abstraction will reveal the essentials of the mechanisms and their commonality. Because the first two modern mechanisms are "pathological," the discussion will begin with the third, the sommelier's corkscrew. I will return to the first two at the end of the chapter.

Examination of Figure 1.3 reveals that this mechanism, considered as a unit, with bottle and cork attached, has four links. These are (1) the bottle, (2) the pivot, (3) the handle, and (4) the screw and cork unit. There are three obvious lower pairs, the pins at *b* and *c* and the prism between the cork and the bottle. The joint at *a* is a higher pair, a complicated contact. There is slippage between bottle and corkscrew, as well as rotation; however, for most purposes, it is sufficiently close in behavior to a revolute to be replaced by a revolute for analysis. This is another example of abstraction, a more artistic abstraction or approximation. Figure 1.15 shows the abstracted mechanism drawn to scale. It is a slider-crank mechanism, and the labeling of the links in the figure is the conventional one for the slider crank.

The device shown in Figure 1.4 is very similar. It is a kinematic inversion of the slider crank, with the crank element fixed. Thus, the link labeled 1 in that figure is the crank of Figure 1.3. The joint at *a* is again actually a higher pair, but equivalent to a revolute, and replaced by a revolute in Figure 1.16, the abstraction of this mechanism. Note that the spring has been omitted in the abstraction. The spring provides a force constraint, not a geometric constraint, and the necessary language has not yet been introduced. You should convince yourself that the spring neither subtracts nor adds geometric degrees of freedom.

The next three mechanisms, Figures 1.5–1.7, are all four-bar linkages. Each has four links (remember to count the frame link) and four revolutes for a formal and actual mobility of unity. Figure 1.17 shows the abstractions for all three.

The corkscrew-bottle mechanism of Figure 1.2 must be considered as a unit, as was the first corkscrew. It has four links: the two arms, the bottle-frame combination, and the shaft–screw-cork combination. The number and type of joints depends on the attitude taken by the analyst. If there is no rotation of the cork, as is the case in practice, then the mechanism is a planar mechanism and it has two pins, two gears (higher pairs), and one prismatic joint, the cork in the neck of the bottle. All the joints are single-degree-of-freedom joints, and the formal mobility is -1. This is another pathological

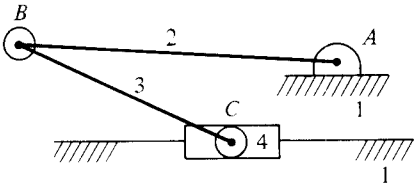

FIGURE 1.15 *A kinematic abstraction of the sommelier's corkscrew.*

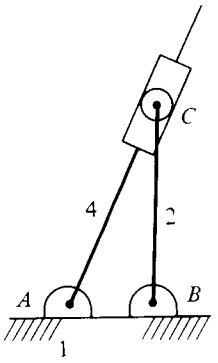

FIGURE 1.16 *A kinematic abstraction of the eyeglass earpiece mechanism.*

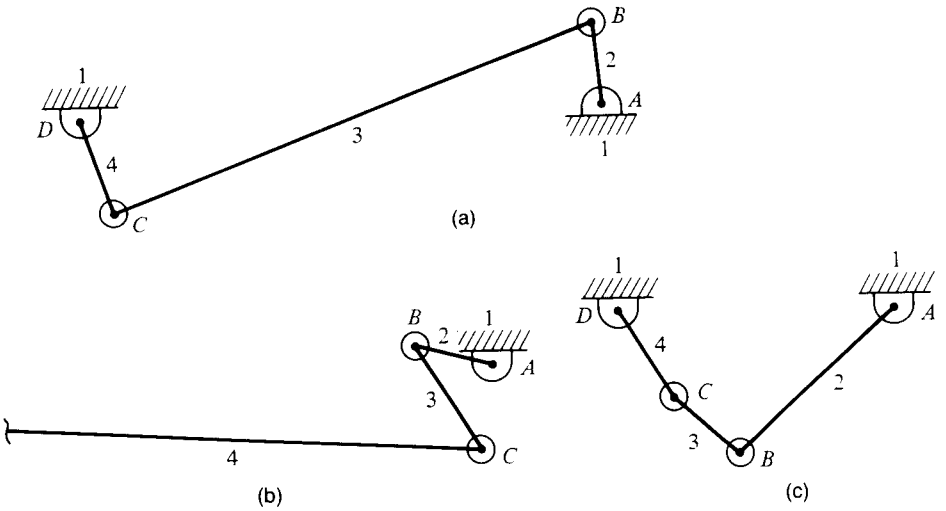

FIGURE 1.17 *Kinematic abstractions of three four-bar mechanisms, shown together to emphasize their similarity;* (a) *the motorcycle foot-brake linkage;* (b) *the auto window mechanism;* (c) *the locking pliers.*

example. The explanation here is clear, however. The two gears and the prism are redundant; they all remove the same degrees of freedom, preventing sideways motion and rotation. Thus, the true mobility is unity.

The compasses of Figure 1.1 are not a planar mechanism. This was noted in the Introduction to this chapter. Count the physical elements: two legs joined by a pin at *a*, a threaded rod, and two further pins at *b* and *c*. There are six elements, six links, and there are six one-degree-of-freedom joints, all lower pairs, four revolutes, and two helices. Alternatively, the count can omit the actual physical pins and include only two

legs and the screw element, with one one-degree-of-freedom joint, the pin at a, and two two-degree-of-freedom joints, the threaded pins at b and c. The former count, inserted into the Kutzbach criterion for three-dimensional mechanisms gives a formal mobility of zero, and the latter a formal mobility of -1. The actual mobility is unity. The compasses are a pathological mechanism.

Chapter 2

Bar Linkages

First, note that it is conventional to apply the term *linkages* to planar mechanisms involving only lower pairs. *Bar linkages* are made up of links or *bars* pinned together. Bar is a convenient term used for links with only pin joints. Bars are not necessarily bar-shaped. Bars may have more than two pin joints. The analyst may be interested in points on a bar not lying on the line joining any two pins. When either (or both) of these circumstances obtains, it is convenient to represent a bar by a polygon, frequently a triangle.

Figure 2.1 represents a four-bar linkage. Parts a and b of the figure are taken from Reuleaux. Figure 2.1a shows four bars connected by four pins. It is not yet a defined linkage because no ground line has been chosen. Figure 2.1b shows an elegant ground link. Figure 2.1c is a modern abstraction of the linkage, illustrating the convention to be followed in labeling four-bar linkages: the *frame* will be link 1; link 2 will be called the *crank*, link 3 the *coupler*, and link 4 the *follower*. The four pin joints will be labeled as shown. The Gruebler criterion for planar mechanisms, Equation (1.4), indicates that the four-bar linkage is the simplest nontrivial bar linkage. Four-bar linkages are common, and much lore has grown up about them. Some of this lore will be explored shortly.

Each additional link adds three degrees of freedom, and each additional pin subtracts two. Thus, a five-bar linkage with five pins has a mobility of 2. A five-bar linkage with more than five pins is a structure. Figure 2.2 shows a five-bar linkage with five pins and one with six pins. The latter has a double pin, labeled *B, F*. Six-bar linkages are mobile with six pins ($m = 3$) or seven pins ($m = 1$). The reader can go on in the obvious fashion. Bar linkages with an even number of bars have mobilities that are odd numbers. Bar linkages with an odd number of bars have mobilities that are even numbers. Because a mobility of 1 is of particular interest in mechanism design, allowing for control with a single input driver, bar linkages with an even number of bars are common. Those with an odd number are not.

Rules for even bar linkages of mobility 1, a small subset of bar linkages, are not plentiful. This is because the linkages become rapidly more complicated as the number of bars increases. I will discuss these briefly at the end of the chapter. Four-bar linkages are common and well understood and can be exhaustively classified.

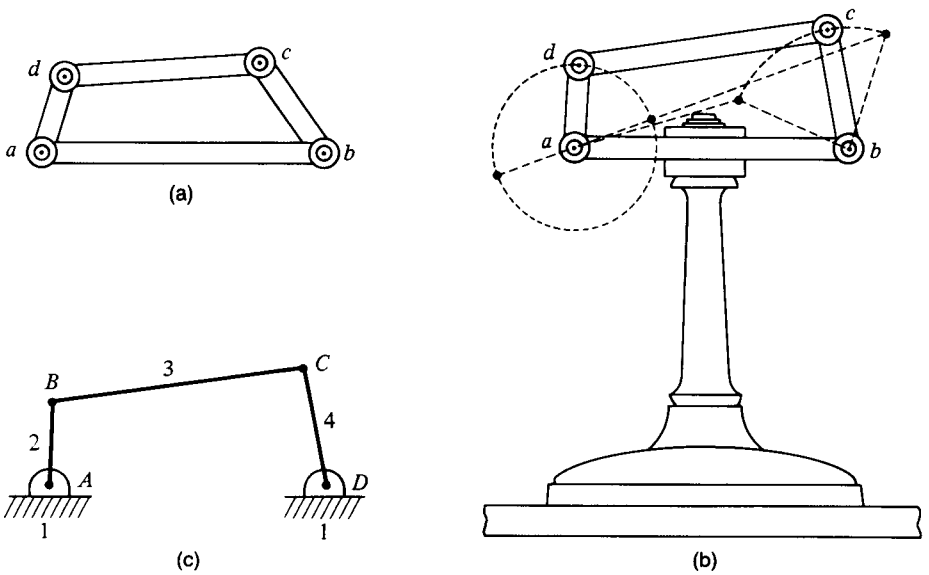

FIGURE 2.1 *Three stages in the representation of a four-bar linkage:* (a) *the free linkage, a kinematic chain, not a mechanism;* (b) *the mechanism formed by grounding the link shown;* (c) *a kinematic abstraction of the mechanism. [Parts a and b after Reuleaux (1876).]*

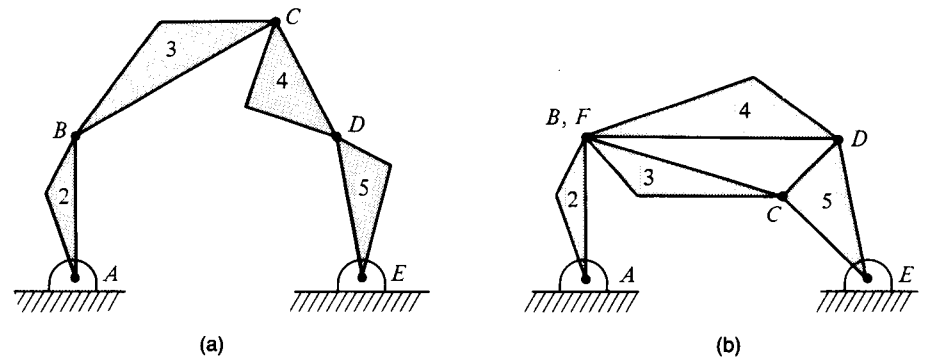

FIGURE 2.2 *A five-bar linkage with two degrees of freedom can be changed into a structure with zero degrees of freedom by adding a joint:* (a) *the linkage;* (b) *the structure.*

FOUR-BAR LINKAGES

The general four-bar linkage has four bars of different length. The behavior of the linkage depends entirely on the relative lengths of the bars. It is conventional to denote the length of the shortest bar by s, that of the longest by l, and the two intermediate

lengths by p and q. Where there is no risk of ambiguity, the bars will carry the labels used to denote their lengths. The most important property of a linkage is that any bar can perform a complete rotation with respect to the others. This is necessary for a mechanism that is to be driven by a motor, or any prime mover providing rotary motion. Grashof's criterion states that the shortest link will rotate continuously with respect to the other three if

$$s + l \leq p + q \tag{2.1}$$

If this condition is not satisfied, no link can make a complete revolution with respect to any other. Mechanisms for which the condition holds are called *Grashof mechanisms.*

The criterion is a consequence of simple geometry. Figure 2.3 shows two mechanisms. The left-hand mechanism satisfies the Grashof condition and the right-hand does not. The relative link lengths in each diagram are: 10, 5, 15, 19 and 10, 5, 15, 21. The left-hand diagram shows the mechanism at $\theta_2 = \pi/2$ (dashed lines) and $\theta_2 = 0$. The lower diagram shows $\theta_2 = \pi/2$, and at its minimum, the value of which is left as an exercise for the reader. This example is one for which complete rotation is prevented by a forbidden zone near $\theta_2 = 0$. More common is the case in which $r_1 + r_2 > r_3 + r_4$ and the forbidden zone is near $\theta_2 = \pi$.

In a Grashof mechanism, the shortest link can rotate completely with respect to the other links. Sometimes this rotation is subtle, as I will now show. Figure 2.4 shows

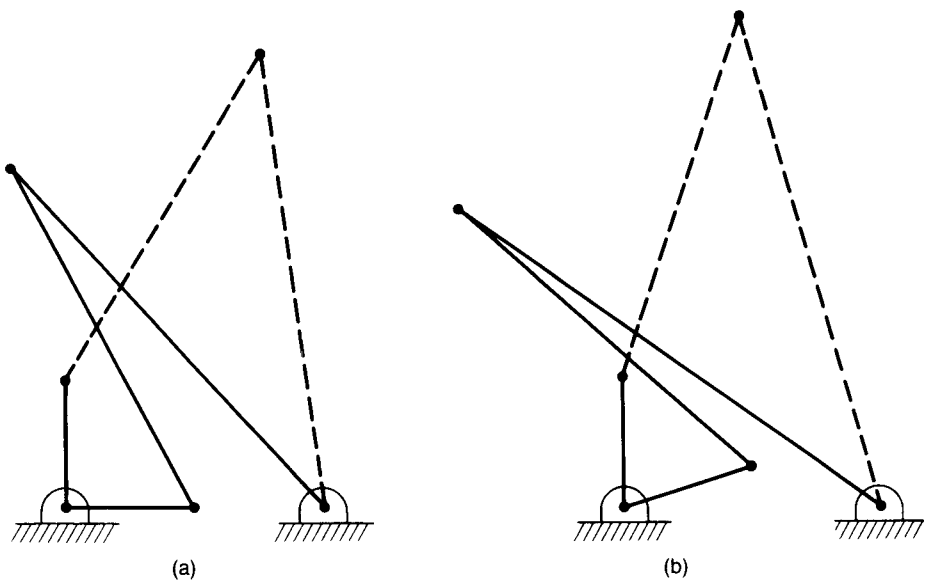

FIGURE 2.3 *A Grashof linkage can be changed into a non-Grashof linkage by slight changes in dimension:* (a) *the Grashof version;* (b) *the non-Grashof version. Here the longest link grows slightly longer. The solid lines in part b show the inner limits of rotation.*

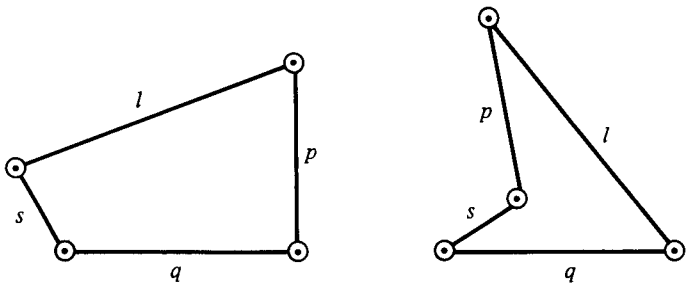

FIGURE 2.4 *The two kinematically distinct assembly positions of a Grashof chain:* (a) *the shortest and longest links are adjacent;* (b) *the shortest and longest links are opposite each other.*

two potential linkages, each with relative lengths $s{:}p{:}q{:}l = 4{:}8{:}10{:}13$. Figure 2.4a has s and l adjacent; Figure 2.4b has s and l opposite.

Consider the linkage of Figure 2.4a and fix, in turn, s, p, q, l. This is an example of kinematic inversion. Each new fixed frame link gives a new equivalent linkage. The resulting linkages are shown in Figure 2.5 a–d. The first two show the extreme cases, that of (a) a double crank, or *drag link,* and (b) a double rocker. In the latter, neither the crank nor the follower can rotate completely with respect to the frame. According to the Grashof criteria, s, here the coupler, can. The reader may find it instructive to verify this, either by a series of sketches or a model. The final two linkages show that with either q or l fixed, the crank, taken to be s, can rotate and the follower cannot. These linkages are called crank-rocker mechanisms.

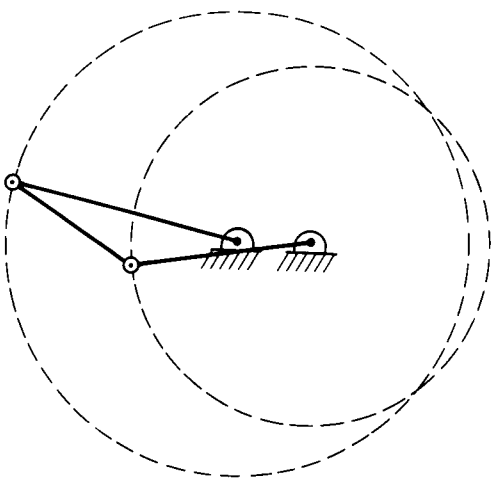

FIGURE 2.5 *The four inversions of a Grashof linkage:* (a) *The shortest link is grounded; the linkage is a double crank (drag link).* (continued)

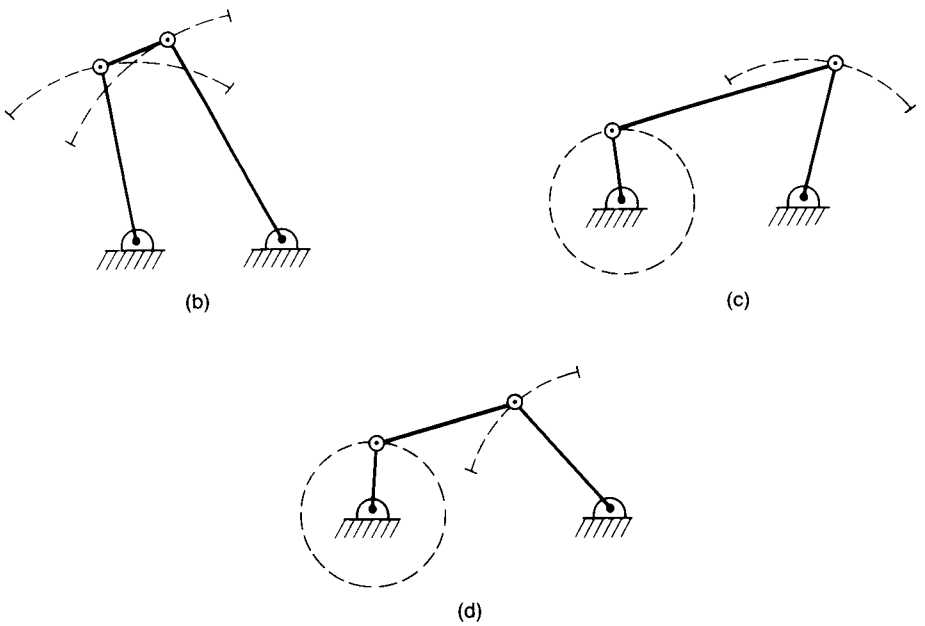

FIGURE 2.5 (continued) (b) *The link opposite the shortest link is grounded; the linkage is a double rocker.* (c) *An intermediate link* (q) *adjacent to the shortest link is grounded; the linkage is a crank rocker.* (d) *The longest link, which is adjacent to the shortest, is grounded; the linkage is a crank rocker.*

The reader should verify that the same sequence of linkages can be generated using the assembly of Figure 2.4b. The nature of the mechanism depends only on the relation of the fixed link to s. With s fixed the linkage is a drag-link mechanism. With the opposite link fixed, the linkage is a double rocker. Fixing either of the other links gives a crank-rocker mechanism.

This can be applied to the three four-bar linkages introduced in Chapter 1 and shown in Figures 1.5–1.7. Table 2.1 gives the relative dimensions of the three systems, letting r_1 be unity. The first two are crank-rocker mechanisms, provided with stops so that the crank does not actually perform complete rotations.

Table 2.1 Three Four-Bar Linkages

Linkage	r_2	r_3	r_4	s	p	q	l	*Type*
Foot brake	0.162	0.986	0.204	0.162	0.204	0.986	1.000	Crank-rocker
Car window	0.026	0.041	1.000	0.026	0.041	1.000	1.000	Crank-rocker
Vise grip	0.787	0.320	0.507	0.320	0.507	0.787	1.000	Non-Grashof

The vise grip as given is a non-Grashof mechanism. Point d can be moved out far enough to make the mechanism into a Grashof mechanism. The mechanism would then be a double rocker, with the potential for the shortest link to rotate completely. The shortest link, however, is the handle and the pliers have stops to limit how far the handle can rotate.

SIX-BAR LINKAGES

The six-bar linkage with unit mobility has seven pins. Figure 2.6 shows a six-bar mechanism with six pins ($m = 3$) converted to one with seven pins by removing one link and connecting it across two of the remaining links, reducing the mobility to unity. The resulting mechanism has two links with three connections, links 1 and 3 in the example. These are called ternary links; the other links are called binary links. You should convince yourself that any six-bar linkage with unit mobility has exactly two ternary links.

The original linkage had a single closed loop. The modified linkage has two distinct, independent closed loops. This is a necessary consequence of reconnection. For the new linkage to be a "real" six-bar linkage, the new independent linkages must each have at least four links. A loop with only three links is immobile. There is a third, nonindependent outer loop. The three loops in Figure 2.6 are the inner loops, I: 1-2-3-5 and II: 1-5-3-4-6, and the outer loop III: 1-2-3-4-6.

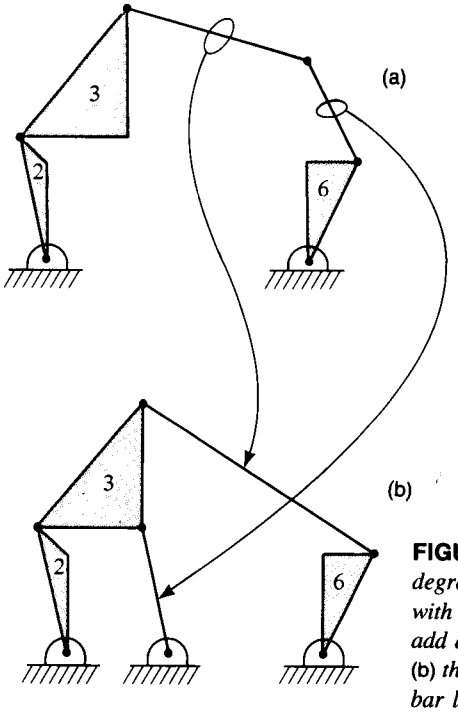

FIGURE 2.6 *A six-bar linkage with three degrees of freedom can be converted into one with one degree of freedom by reconnecting to add a joint:* (a) *the linkage before reconnection;* (b) *the reconnected system—a Stephenson III six-bar linkage.*

Distinct types of mechanisms in a system with two ternary and four binary links will be obtained, depending on whether the ternary links are adjacent. Other distinctions are kinematic inversions of one of the two basic types. The Watt mechanism has the two ternary links adjacent; the Stephenson has them separated. The mechanism in Figure 2.6 is a Stephenson six-bar linkage. The Watt linkage is further subdivided into Watt I, for which the ground link is binary, and Watt II, for which it is ternary. The Stephenson linkage has three realizations. Stephenson I uses one of the binary links separating the two ternary links as the ground link. The Stephenson II uses one of the other two binary links as ground, and the Stephenson III uses one of the ternary links as ground. Figure 2.6 shows a Stephenson III. Figure 2.7 shows all five six-bar linkages of unit mobility.

The various six-bar linkages have quite different degrees of complexity. This will be seen quantitatively when analysis and synthesis techniques for six-bar linkages are explored. For now, note that the Watt linkages are made up of two closed four-bar linkages. The Watt II is particularly simple. The follower (link 4) of the first four-bar linkage (links 1–4) is the crank of the second linkage (links 1 and 4–6). This is called a cascaded four-bar linkage and can be analyzed using the techniques to be developed for four-bar linkages. The Watt I is somewhat more complicated, although it is obvious that the position of links 4 and 5 can be found from geometry once the positions of links 3 and 6 are known. Those are just the coupler and follower of the first four-bar linkage. The difference in complication is that the second four-bar linkage in the Watt I has no ground link.

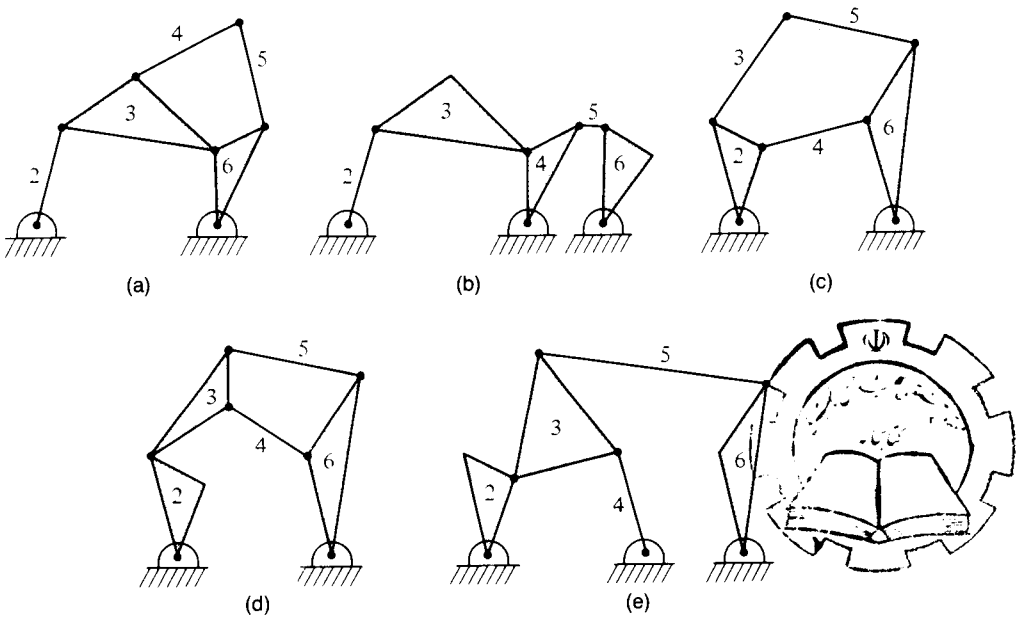

FIGURE 2.7 *The five kinematically distinct six-bar linkages:* (a) *the Watt I;* (b) *the Watt II;* (c) *the Stephenson I;* (d) *the Stephenson II;* (e) *the Stephenson III.*

The Stephenson linkages are made up of a four-bar and a five-bar linkage. In the Stephenson I and III linkages, the basic four-bar linkage is solvable separately, and the result of that solution provides the location of three of the five bars in the other (five-bar) linkage, so that the other two can be found simply. The Stephenson II is a basic five-bar linkage attached to a floating four-bar. The correct method of solution is not obvious and will be deferred until Chapter 5.

The process of kinematic inversion is general. It can be applied to six-bar linkages in the same way as it was to four-bar linkages. Figure 2.8 shows the six inversions (one for each distinct link) of the Watt I linkage shown in Figure 2.7a. Inversions 1, 2, 4, and 5 are Watt I linkages. The others are Watt II linkages.

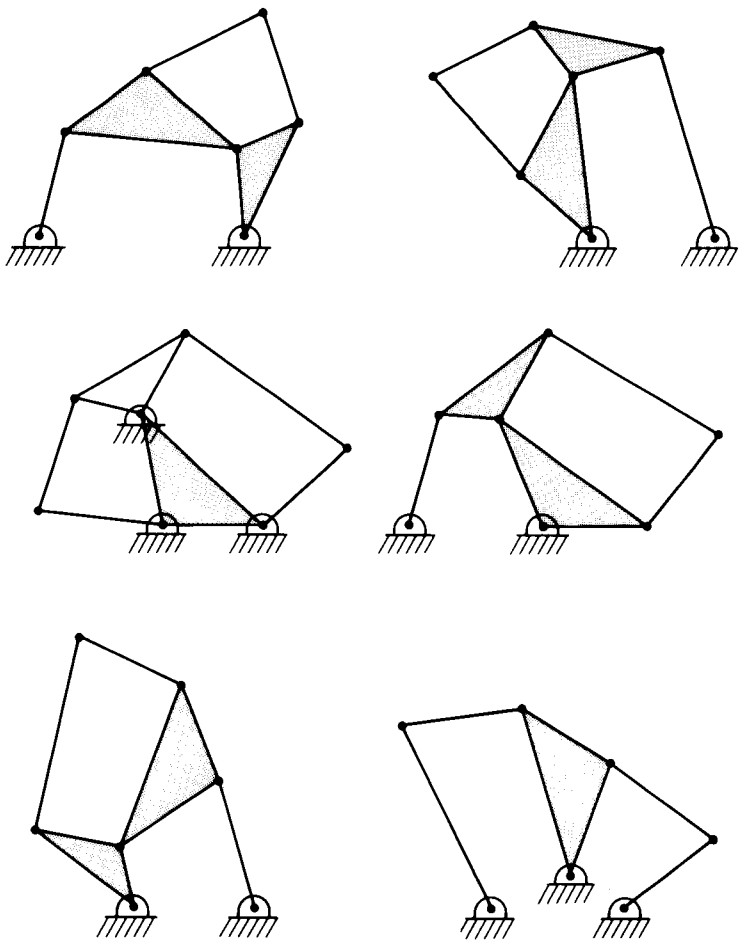

FIGURE 2.8 *The six inversions of a Watt I six-bar linkage.*

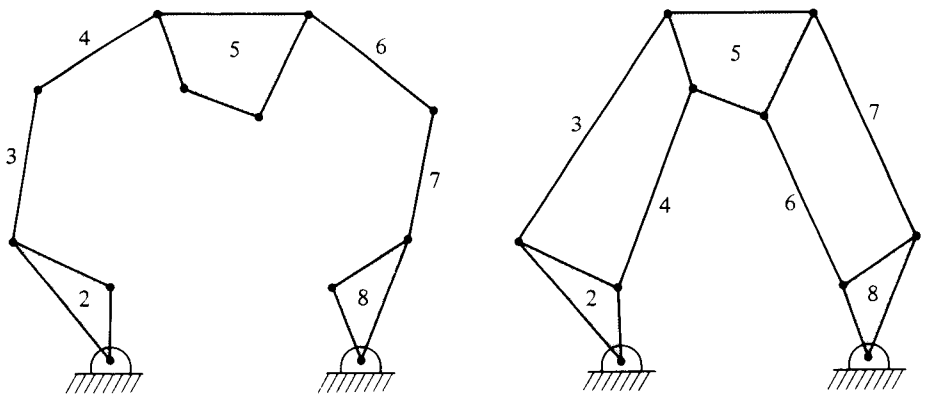

FIGURE 2.9 *An eight-bar linkage with five degrees of freedom can be converted into one with one degree of freedom by reconnecting to add two joints:* (a) *the linkage before reconnection;* (b) *the reconnected system.*

LINKAGES WITH MORE THAN SIX BARS

The reader interested in combinatorics and graph theory may find it amusing to investigate the various ways in which one can form eight-bar linkages of unit mobility. One case requires four ternary links and four binary links and is constructed in the same fashion that the $m = 3$ six-bar linkage is converted into the $m = 1$ six-bar linkage. Figure 2.9 shows the process. The resulting linkage has two four-bar sublinkages and one six-bar sublinkage. (In trying to construct additional examples, remember that all sublinkages must have at least four bars or a portion of the mechanism will be locked and the effective total number of bars reduced.)

A great deal of effort has been expended to answer the question of how many mechanisms of a given degree of freedom can be formed from a given number of links. A complete exploration of this is beyond the scope of this text, but some idea of the complexity of the problem is in order. Freudenstein and Dobrjanskyj (1964) developed a number of general relations, which they applied in detail to the question of eight-bar linkages of unit mobility, the case for which one example has been given. They introduce the concept of the *basic kinematic chain* (BKC), which is an ungrounded mechanism. This is equivalent to the reduced linkage used earlier. There are two distinct BKCs for the six-bar linkage of unit mobility, the Watt and the Stephenson. There are 16 eight-bar BKCs with unit mobility. Figure 2 of the Freudenstein and Dobrjanskyj paper shows these.

The two six-bar BKCs of unit mobility led to five distinct mechanisms. The 16 eight-bar BKCs of unit mobility lead to 71 distinct mechanisms! Woo (1967) demon-

strates that there are 230 ten-bar BKCs of unit mobility and shows all of them in diagrammatic form.

The focus of modern research in this area is the computerization of mechanism generation. This is beyond the scope of a basic course, but the interested reader can start with the thorough modern summary by Olson et al. (1985).

EXERCISES

1. For the four-bar linkages with dimensions (in mm) shown in the following table:

Link 1	*Link 2*	*Link 3*	*Link 4*
23	23	25	27
14	22	27	30
22	12	24	20
18	18	18	18

   a. Identify the Grashof linkages.
   b. For the Grashof linkages, find the link(s) that can rotate completely.
   c. For the linkages for which either link 2 and/or link 4 cannot rotate completely, find the angle limits.
   d. Draw all four linkages. If more than one assembly position is possible, draw all assembly positions.
   e. Classify (crank rocker, drag link, or double rocker) the four-bar linkages shown in Figures 1.5–1.7. Take the dimensions directly from the figures, and use 800 mm for the unmeasurable dimension in Figure 1.6.

2. Identify the independent loops in the mechanisms shown in Figure 2.7. How many bars in each? What is the formal mobility of each loop? How does the mobility of the linkage follow from that of the loop? (Hint: Think about the virtual assembly process introduced in Chapter 1.)

3. How many independent loops are there in the eight-bar linkage shown in the bottom half of Figure 2.9? Can you suggest a general rule for independent loops in a one-degree-of-freedom linkage? Can you prove it?

4. Show that the Stephenson II and Stephenson III linkages can be obtained from the Stephenson I by kinematic inversion. Identify the specific inversions by identifying which link in Figure 2.7c has been grounded to produce the other types.

5. Enumerate the types of eight-bar linkages, and classify their kinematic chains according to the types of links (quaternary, ternary, binary) they contain.

6. Draw the kinematic inversions of the eight-bar linkage shown in Figure 2.9.

7. The figure shows a plow mechanism. There are two hydraulic cylinder controls that function kinematically like sliders. Identify all links and joints, and give the degrees of freedom.

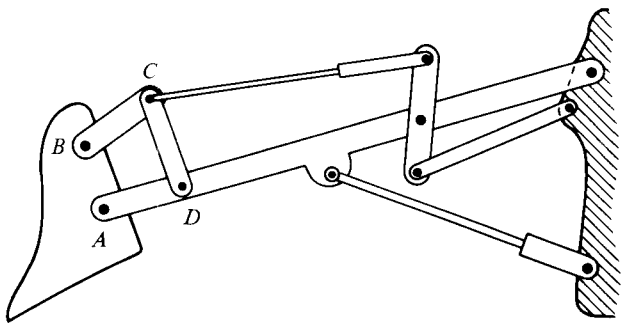

8. In the plow diagram, if AD is the frame link in a local four-bar linkage, and the dimensions are as follows: $AB = 13.5$ in., $BC = 14.75$ in., $CD = 19$ in., $DA = 16$ in. What kind of linkage is this?

9. What is the formal mobility of each of the following mechanisms?

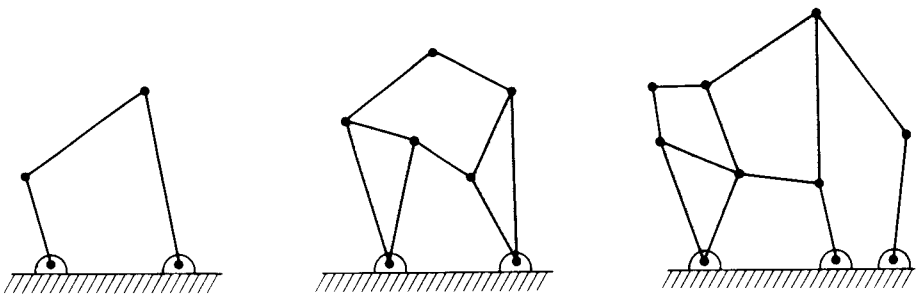

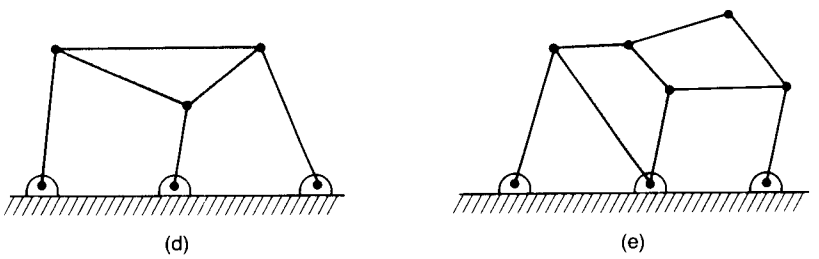

10. What is the mobility of the following mechanism?

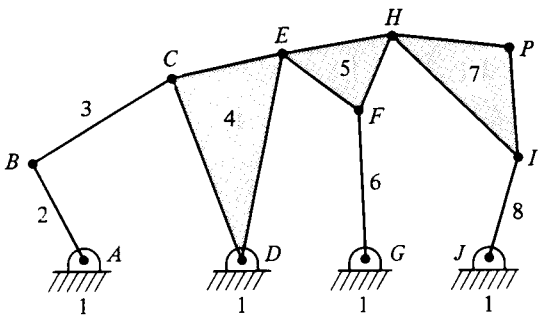

11. Identify the mechanism type of the four inversions of the kinematic chain for which the first inversion is $r_1 = 100$, $r_2 = 340$, $r_3 = 470$, and $r_4 = 340$.

PART II

Mathematical Preliminaries

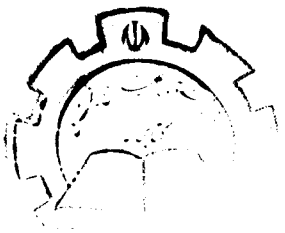

Chapter 3

Mechanisms, Coordinate Systems, and Vectors

THE FRAME OF REFERENCE

To analyze and synthesize mechanisms analytically, whether by hand or using the digital computer, it is necessary to be able to represent the position and orientation of links analytically. Eventually, I will use complex variables, which are ideally suited for planar mechanisms. Before introducing this novelty, I will briefly review analytic geometry and vector notation. The vector representation is more general than the complex variable representation. Spatial mechanisms cannot be analyzed using the complex variable techniques that form the backbone of this text. The reader should be aware that the third dimension is included only for completeness and for comparison to other general vector formulations. The book is otherwise restricted to two dimensions, and the reader who feels firmly in control of vector analysis can skim this chapter.

To describe the position or location of a point, there must be a frame of reference. This is obvious but often forgotten in simple everyday location tasks like map reading. Maps have a built-in, agreed-upon frame of reference—latitude and longitude (and height above sea level for a topographic map). For the description of a mechanism, it is necessary to construct a frame of reference, typically a Cartesian coordinate system. This is a six-degree-of-freedom task, three degrees of freedom to locate the origin and another three to specify the orientation of the axes. (These are the same six degrees of freedom that were subtracted from the calculation of the mobility of a spatial mechanism. The three orientation variables can be the Euler angles.)

Once a coordinate system (reference frame) has been defined, any point in space can be located uniquely by its distance from the origin (O) in the three mutually perpendicular directions defined by the coordinate frame. Figure 3.1 shows a Cartesian system and a point P. The coordinates of P are x_P, y_P, z_P. Let there be a second point Q with coordinates x_Q, y_Q, z_Q. Imagine a link connecting points P and Q. The link has an existence quite independent of the coordinate system. How can the description of the link be made independent as well?

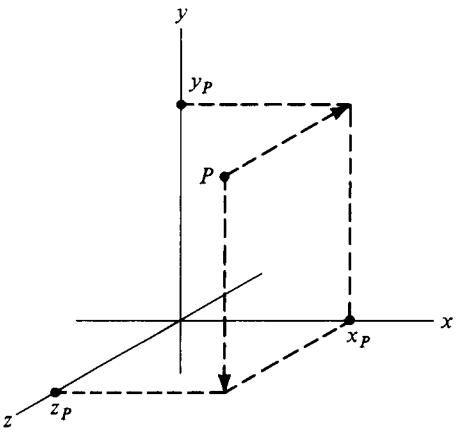

FIGURE 3.1 *A point* P *in a Cartesian coordinate system, showing the coordinates of the point,* x_P, y_P, z_P.

VECTOR ANALYSIS

A vector is a directed line segment. It has length and direction. In general, its location in space is not important. If a vector is moved through space without changing its length or orientation, it is unchanged just as a physical object is unchanged by its motion. Thus, a vector is a convenient mathematical abstraction of a link. The line connecting the origin to P can be made a vector most simply by drawing it and putting an arrowhead on the end at P, as in Figure 3.2. Call this the vector to P from O, and write it $\mathbf{R}_{PO}$. Figure 3.2 also shows the vector to Q from the origin and the vector to Q from P. The vector to Q from the origin should be the sum of the vector to P from the origin and the vector to Q from P. It is the role of the notation to make that work.

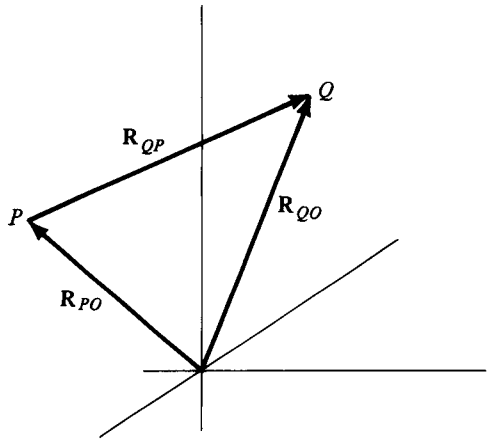

FIGURE 3.2 *Two points,* P *and* Q, *in a three-dimensional Cartesian frame, and their associated vectors* $\mathbf{R}_{PO}$, $\mathbf{R}_{QO}$ *and the difference vector* $\mathbf{R}_{QP}$.

Let $\mathbf{e}_x$, $\mathbf{e}_y$, $\mathbf{e}_z$ denote unit vectors in the x, y, and z directions. These can be visualized as arrows of unit length pointing in the positive x, y, and z directions. The vector to P from the origin can then be written as

$$\mathbf{R}_{PO} = x_P\mathbf{e}_x + y_P\mathbf{e}_y + z_P\mathbf{e}_z \tag{3.1}$$

and the vector to Q from the origin as

$$\mathbf{R}_{QO} = x_Q\mathbf{e}_x + y_Q\mathbf{e}_y + z_Q\mathbf{e}_z \tag{3.2}$$

The difference

$$\mathbf{R}_{QP} = \mathbf{R}_{QO} - \mathbf{R}_{PO} = (x_Q - x_P)\mathbf{e}_x + (y_Q - y_P)\mathbf{e}_y + (z_Q - z_P)\mathbf{e}_z \tag{3.3}$$

is the desired vector to Q from P.

Note some conventions that will be used for vector analysis. Vectors will be printed in boldface. The unit vectors will be denoted by **e** and will carry a single subscript denoting the direction. Other vectors will carry two subscripts with the letter denoting the "head" of the arrow before that denoting the "tail." This notation is quite cumbersome and, where it is possible without ambiguity, I will use a simpler notation, in which a vector is denoted by a single boldface unsubscripted letter and its components by the same letter in lightface with a single subscript:

$$\mathbf{A} = A_x\mathbf{e}_x + A_y\mathbf{e}_y + A_z\mathbf{e}_z \tag{3.4}$$

Addition and subtraction of vectors is easy and has been tacitly introduced. One adds and subtracts the components separately. Two separate products can be defined. (There is actually a third, but it has no use in kinematics and will be ignored here.) The first is the scalar, inner, or dot product. As its first name indicates, it is a scalar, formed by multiplying the pairs of components and adding the three products. The operator is symbolized by a dot:

$$\mathbf{A} \cdot \mathbf{B} = A_xB_x + A_yB_y + A_zB_z \tag{3.5}$$

The magnitude of $\mathbf{A} \cdot \mathbf{B}$ is equal to the length of **A** times the length of **B** times the cosine of the angle between the two vectors. From this it follows that the dot product of a vector with itself represents the square of the length of the vector. The dot product of two perpendicular vectors is zero. The dot product of two different unit vectors is zero and that of a unit vector with itself is unity.

The second is the vector, outer, or cross product. This produces a vector that is perpendicular to the two vectors from which it is formed. It points in the direction a right-hand thread screw would move when the first vector is turned into the second. This handedness means that the cross product does not commute: $\mathbf{A} \times \mathbf{B} \neq \mathbf{B} \times \mathbf{A}$. It is most easily formed using a determinant:

$$\mathbf{A} \times \mathbf{B} = \begin{vmatrix} \mathbf{e}_x \mathbf{e}_y \mathbf{e}_z \\ A_x A_y A_z \\ B_x B_y B_z \end{vmatrix} = (A_y B_z - A_z B_y)\mathbf{e}_x + (A_z B_x - A_x B_z)\mathbf{e}_y + (A_x B_y - A_y B_x)\mathbf{e}_z \tag{3.6}$$

The length of the cross product is the product of the two lengths multiplied by the sine of the (smaller) angle between them. The cross product of two parallel (or antiparallel) vectors is zero; therefore, the cross product of any vector with itself is zero. The unit vectors obey the following cyclical rules:

$$\begin{aligned} \mathbf{e}_x \times \mathbf{e}_y &= \mathbf{e}_z \\ \mathbf{e}_y \times \mathbf{e}_z &= \mathbf{e}_x \\ \mathbf{e}_z \times \mathbf{e}_x &= \mathbf{e}_y \end{aligned} \tag{3.7}$$

All this material is available in any good text in vector analysis or calculus (e.g., Greenspan and Benney 1973). I have included it here as review, to introduce consistent notation and to make this text self-contained.

MECHANISMS AS VECTOR CHAINS

A bar linkage can be represented vectorially by replacing each bar by one or more vectors. Analysis of a four-bar linkage requires only one vector per bar. Linkages with more bars will require more vectors per bar. It should be clear that a binary link is uniquely defined by one vector, a ternary by two, and so forth. More general mechanisms require more general formulations. A vector skeleton can be constructed for any mechanism by defining a set of vectors linking distinct joints in a way kinematically equivalent to the actual mechanism. Some of the vectors in such a set can change their length during the operation of the mechanism. Some examples will clarify this prescription.

Figure 3.3 shows a four-bar linkage and a vector skeleton that represents it. Each link, including the frame, has been replaced by a vector. Figure 3.4 shows a Stephenson III six-bar linkage (from Reuleaux), and a vector skeleton that represents it. The six-bar linkage has been represented by eight vectors. Each ternary link has been replaced by two vectors, necessary to depict the complete set of connections among the joints. Note that the choice of the extra vectors is not unique. Any two of the three sides of a ternary link will do. Note also that no new degrees of freedom have been introduced, as the vectors $\mathbf{R}_3'$ and $\mathbf{R}_1'$ are known when their unprimed versions are known. They represent different aspects of the same link.

Figure 3.5 shows an offset slider-crank mechanism, and one choice for a vector skeleton. Link 4, the slider, has vanished from the vector representation. There is no stationary vector in this diagram, and there is only one fixed point, the crank axle. This is the price one pays for the reduction to three vectors. It is too steep a price to pay.

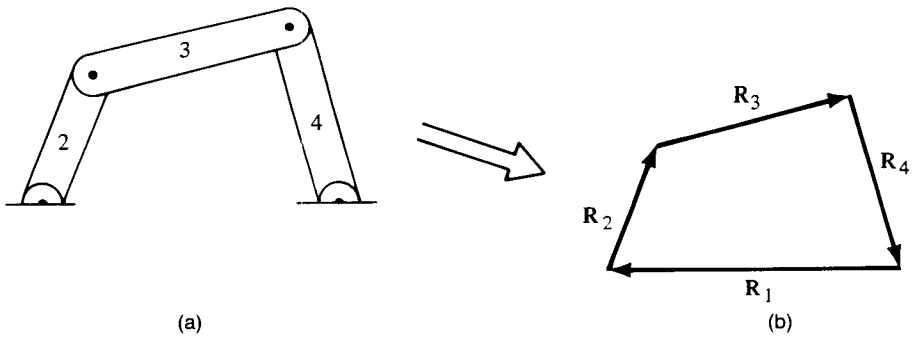

FIGURE 3.3 *Illustration of the conversion of a mechanism to a vector diagram:* (a) *the physical mechanism;* (b) *the corresponding vector diagram.*

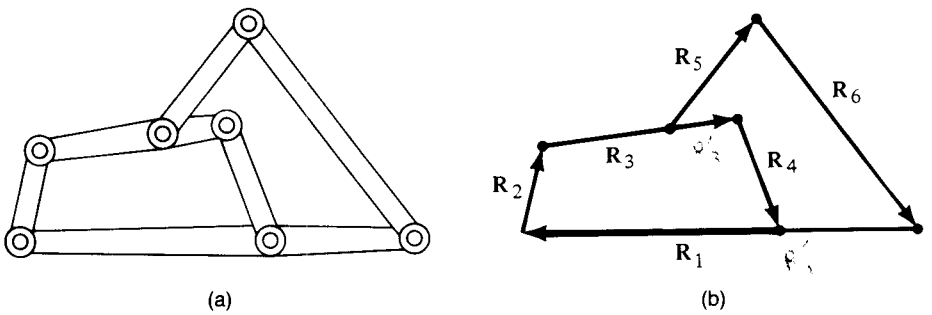

FIGURE 3.4 *Illustration of the conversion of a six-bar (Stephenson III) linkage to a vector diagram:* (a) *the physical linkage [after Reuleaux (1876)];* (b) *the vector diagram.*

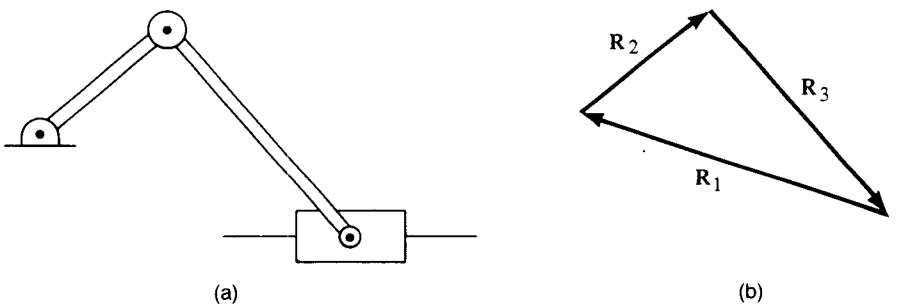

FIGURE 3.5 *Illustration of the conversion of a slider-crank mechanism to a vector diagram:* (a) *the physical mechanism;* (b) *the vector diagram.*

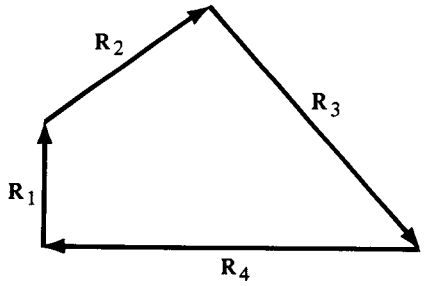

FIGURE 3.6 *A four-vector diagram of an offset slider-crank mechanism.*

A better choice is a four-vector representation. Figure 3.6 shows the four-vector representation. The new $\mathbf{R}_1$ is stationary, and it represents the frame in much the same way as $\mathbf{R}_1$ represents the frame in a four-bar linkage. $\mathbf{R}_4$ is variable, changing its length but not its direction. This representation helps unify the treatment of four-bar linkages and slider-crank mechanisms.

Figure 3.7 shows the vector skeleton for a cam follower system. Here all the information is in the cam vector $\mathbf{R}_2$, which points from the axle to the contact point. Cams will be considered in some detail in Chapter 7, after the necessary analytical machinery has been developed.

In the preceding representations, no mention has been made of the coordinate system. Vector representations are independent of the coordinate system. However, if one is to assign numbers to these vectors, say, for digital computation, it is necessary to choose a specific coordinate system. It is almost always most convenient to attach the coordinate system (reference frame) to the frame of the mechanism. This will be done throughout this text unless it is noted specifically. The origin is best placed at a fixed point, and in all the preceding examples, the joint connecting the frame to the

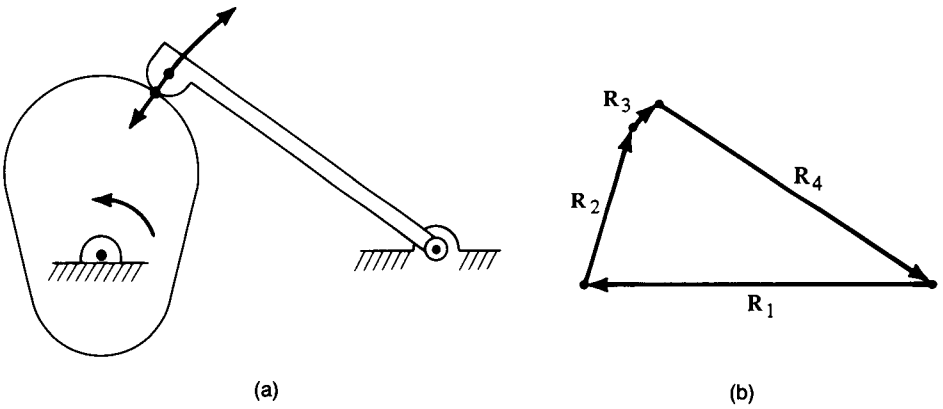

FIGURE 3.7 *Illustration of the conversion of a cam-follower pair to a four-vector diagram:* (a) *the physical mechanism;* (b) *the vector diagram.*

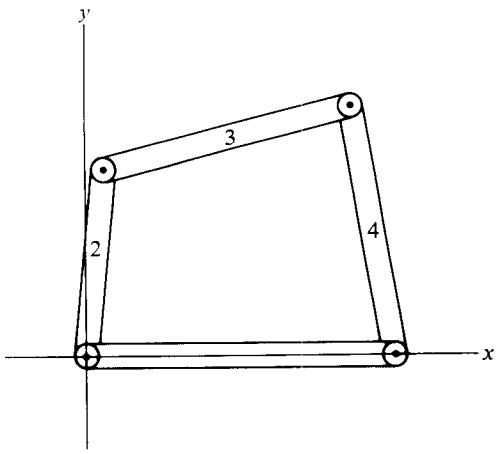

FIGURE 3.8 *A four-bar linkage in a two-dimensional Cartesian frame.*

crank is such a fixed point. For planar mechanisms, the z axis is taken perpendicular to the plane of the mechanism, so that that plane is the x-y plane. The x axis can be chosen in any convenient direction. It will typically be taken to be horizontal in this text. The y axis lies in the same plane, rotated $\pi/2$ in a counterclockwise direction from the x axis. Figure 3.8 shows a four-bar linkage with a conveniently chosen coordinate system.

The same sort of vector idealization can be constructed for the various planar mechanisms of Chapter 1. As an example of a four-bar linkage, take the vise-grip pliers shown in Figure 1.7. Figure 1.17c shows an abstraction of this mechanism. It can be made to look more like a standard four-bar linkage by drawing it as in Figure 3.9.

The sommelier's corkscrew, shown in Figures 1.3 and 1.15, can be seen in the standard slider-crank orientation as the vector skeleton of Figure 3.10.

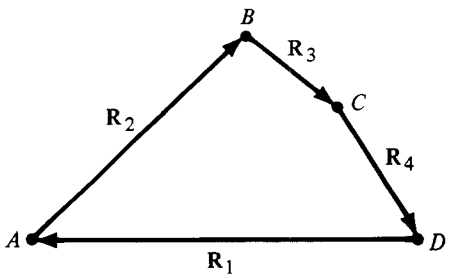

FIGURE 3.9 *The vector skeleton (diagram) for the locking pliers (rotated to put the frame link at the bottom of the diagram).*

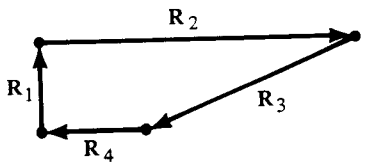

FIGURE 3.10 *The vector skeleton for the (reoriented) sommelier's corkscrew.*

EXERCISES

1. For the mechanism shown in Figure 1.4:
   a. Construct a vector skeleton with a suitably defined ground link.
   b. For each vector in the skeleton:
      Does its length change?
      Does its direction change?
   c. How are the answers to question b affected by the choice of ground link?
2. Repeat exercise 1 for the mechanism shown in Figure 1.5.
3. Repeat exercise 1 for the mechanism shown in Figure 1.6.
4. The mechanism shown in Figure 1.1 is not a planar mechanism, yet its useful motion is in a plane. Construct a vector skeleton for its useful motion. (Hint: Choose one of the tips as a fixed point, and include a vector joining the tips in the skeleton.)
5. Construct a planar vector skeleton for the pathological mechanism shown in Figure 1.2.

Chapter 4

Complex Variables

HISTORICAL ORIGINS

The geometry and behavior of planar mechanisms can be expressed entirely in terms of complex variables. This treatment is equivalent to the vector representation but is more compact and easily manipulated, ideally suited for digital computation, particularly using computer languages that support complex arithmetic. To use this representation, some understanding of complex numbers and facility in their manipulation are necessary. This section provides a self-contained discussion of complex variables at the level necessary for planar kinematics. There is a nice "philosophical" discussion in Courant and Robbins (1941).

Complex numbers arise naturally in the attempt to solve general polynomial equations. The fundamental theorem of algebra, first correctly proved by Gauss (Bell 1956), states that any polynomial expression of degree n can be factored into exactly n factors, that is, that

$$\begin{aligned} P_n(z) &= z^n + C_{n-1}z^{n-1} + \cdots + C_o \\ &= (z - \zeta_1)(z - \zeta_2) \ldots (z - \zeta_n) \end{aligned} \tag{4.1}$$

where z is a variable and $C_0, C_1, \ldots, C_{n-1}$ are constants. The n constants $\zeta_1, \zeta_2, \ldots, \zeta_n$ (not necessarily different) correspond to the roots of the nth-order equation obtained by setting the nth-degree polynomial equal to zero. Thus, an nth-degree equation has n roots (not necessarily distinct). Linear equations have one root, quadratic equations two roots, cubic equations three roots, and so on.

The student of today encounters complex numbers in algebra when the formula for the solution of quadratic equation is introduced. Recall that the formal solution of

$$az^2 + bz + c = 0$$

is

$$z = -\frac{b}{2a} \pm \frac{1}{2a}\{b^2 - 4ac\}^{1/2}$$

The quantity $b^2 - 4ac$ is called the discriminant, and one learns that there are no real solutions if the discriminant is negative. When the discriminant is negative, it can be written $b^2 - 4ac = (-1)(d^2)$, so that $\{b^2 - 4ac\}^{1/2} = \pm di$. Then, putting $-b/2a = x$, $d/2a = y$,

$$z = x \pm iy$$

is the solution for the negative discriminant.

The theorem is untrue if the roots are required to be real numbers. (Real numbers include both rational numbers, those expressible as a ratio of two integers, and irrational numbers, not so expressible, such as π and e, the base of the natural logarithms.) The simplest counterexample is $P_2(z) = z^2 + 1$ which, according to the theorem, must have two roots. Following what would be the usual operations of algebra leads formally to the two roots

$$\zeta_1 = \sqrt{-1}, \qquad \zeta_2 = -\sqrt{-1} \tag{4.2}$$

The $\sqrt{-1}$ has no meaning in the field of real numbers, so that one defines $i = \sqrt{-1}$ as the unit *imaginary number*. Any imaginary number can be represented as a magnitude times the unit imaginary number i. For example, the solution to

$$z^2 + 4 = 0$$

is $z = \pm 2i$.

A complex number has a real and imaginary component. The real component is a real number. The imaginary component can be written as a (real) magnitude times the unit imaginary number i, defined as the (positive) square root of -1. A complex constant will be written

$$c = a + ib$$

and a complex variable

$$z = x + iy$$

As is the normal practice in algebra, c will stand for a specific number, say, $3 + 4i$, and z for a variable. It is conventional to refer to a as the *real part* of c and to b as the *imaginary part* of c. In the same way, x is called the real part of z and y the imaginary part of z. Note that the imaginary part of a complex number is a real number, whereas the imaginary component of a complex number is an imaginary number.

It is useful to have operators that take the real and imaginary parts of a complex number. These will be symbolized by Re and Im, as in $x = \mathrm{Re}(z)$ and $y = \mathrm{Im}(z)$.

Note that the quadratic formula applies when a, b, and c are complex. Establishing the meaning of the formula is a little outside the mainstream of the text, but it provides a useful example of complex arithmetic, which will be used throughout the text. I will return to this once I have introduced the various arithmetic operations.

ARITHMETIC

The rules for complex arithmetic are simple. The sum of two complex numbers c_1 and c_2 is formed by adding the real and imaginary components separately, so that

$$c_1 + c_2 = (a_1 + a_2) + i(b_1 + b_2) \tag{4.3}$$

The multiplication rule can be deduced from the addition rule and the definition of i:

$$c_1 c_2 = a_1 a_2 - b_1 b_2 + i(a_1 b_2 + a_2 b_1) \tag{4.4}$$

Division follows from multiplication:

$$\frac{c_1}{c_2} = \frac{a_1 + ib_1}{a_2 + ib_2} = \frac{a_1 + ib_1}{a_2 + ib_2}\frac{a_2 - ib_2}{a_2 - ib_2}$$

$$= \frac{a_1 a_2 + b_1 b_2 - i(a_1 b_2 - a_2 b_1)}{a_2^2 + b_2^2} \tag{4.5}$$

The process of division illustrates a useful manipulation that will be used often. The denominator was multiplied by $a_2 - ib_2$, the original number with the sign of the imaginary part reversed. The number $a_2 - ib_2$ is called the *complex conjugate* of the original number $a_2 + ib_2$. The product of a number and its complex conjugate is a real positive number, equal to the sum of the squares of the real and imaginary parts of the number.

EXAMPLES OF COMPLEX ARITHMETIC

(1) Let

$$c_1 = 3 + 4i, \qquad c_2 = 2 - 7i$$

Then,

$$c_1 + c_2 = 3 + 2 + i(4 - 7) = 5 - 3i$$

$$c_1 c_2 = (3 + 4i)(2 - 7i)$$

$$= 6 + 28 + i(8 - 21) = 34 - 13i$$

$$\frac{c_1}{c_2} = \frac{3 + 4i}{2 - 7i} = \frac{(3 + 4i)(2 + 7i)}{(2 - 7i)(2 + 7i)}$$

$$= \frac{6 - 28 + i(8 + 21)}{4 + 49}$$

$$= \frac{-22}{53} + i\frac{29}{53}$$

(2) Let

$$c_3 = -2 + i, \qquad c_4 = 1 - 2i$$

Then,

$$c_3 + c_4 = -2 + 1 + i - 2i = -1 - i$$

$$c_3 c_4 = (-2 + i)(1 - 7i)$$
$$= -2 + 2 + i + 4i = 0 + 5i$$

$$\frac{c_3}{c_4} = \frac{2 + i}{1 - 2i} = \frac{(-2 + i)(1 + 2i)}{(1 - 2i)(1 + 2i)}$$

$$= \frac{-2 - 2 + i - 4i}{1 + 4}$$

$$= \frac{-4}{5} - i\frac{3}{5}$$

GRAPHICAL REPRESENTATION

The utility of complex numbers in planar kinematics comes from the geometrical representation, constructed independently by Wessel, Argand (who generally gets the credit, and for whom the representation is named), and Gauss (Courant and Robbins 1941). Note that the addition rule for complex numbers is the same as that for a two-dimensional vector if one identifies the real and imaginary parts of the complex number with the two orthogonal components of a two-dimensional vector. The common way to visualize this is on the Argand diagram, on which the real part of a complex number is plotted on the x axis of a Cartesian system and the imaginary part on the y axis. Figure 4.1 shows an Argand diagram with c_1, c_2, c_3, and c_4 depicted. Any complex variable z can be represented as a vector from the origin to the point (x,y), and any vector in the plane can be represented as a complex variable. The plane on which the Argand diagram is drawn is called the *complex plane.*

The correspondence can be written out if one lets $\mathbf{R}_1$, $\mathbf{R}_2$, $\mathbf{R}_3$, and $\mathbf{R}_4$ be vectors corresponding to the complex numbers c_1, c_2, c_3, and c_4:

$$\mathbf{R}_1 = 3\mathbf{e}_x + 4\mathbf{e}_y$$
$$\mathbf{R}_2 = 2\mathbf{e}_x - 7\mathbf{e}_y$$
$$\mathbf{R}_3 = -2\mathbf{e}_x + \mathbf{e}_y$$
$$\mathbf{R}_4 = \mathbf{e}_x - 2\mathbf{e}_y$$

Any complex number can be written as a two-dimensional Cartesian vector, and any two-dimensional Cartesian vector can be written as a complex number. The vector

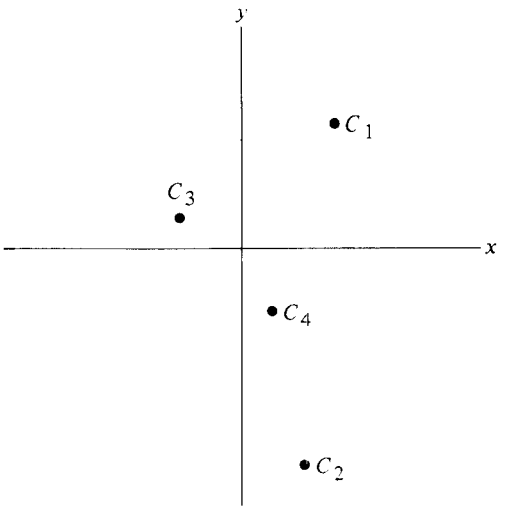

FIGURE 4.1 *The complex plane showing four points:* c_1, c_2, c_3, c_4.

skeletons introduced in Chapter 3 can be written as complex variable skeletons, and this will be done in Chapter 5 and in the rest of the text.

The diagram also provides a geometric interpretation for multiplication. First, consider the multiplication of a complex number by its complex conjugate. If z denotes a complex variable, it is conventional to denote its complex conjugate by z^*, and that convention will be followed here. Using this notation, and the arithmetic introduced earlier, the product

$$zz^* = x^2 + y^2 = r^2$$

is an expression of the Pythagorean Theorem. The product zz^* is the square of the length of a vector representing the complex variable z.

A point on the Argand diagram can be located by its Cartesian components, x and y. It can also be defined in terms of polar coordinates r and θ. The distance from the origin to the point is the *magnitude* r, and θ is a phase angle between the vector and the x axis, measured from the x axis in a counterclockwise direction. Note that the magnitude r is identical to the length of the equivalent vector and that θ is just the single Euler angle required to specify the direction of a line confined to a plane. In terms of that notation, one can write

$$z = r\{\cos\theta + i \sin\theta\} \tag{4.6}$$

using the conventional polar coordinates r and θ defined by

$$x = r\cos\theta, \qquad y = r\sin\theta \tag{4.7}$$

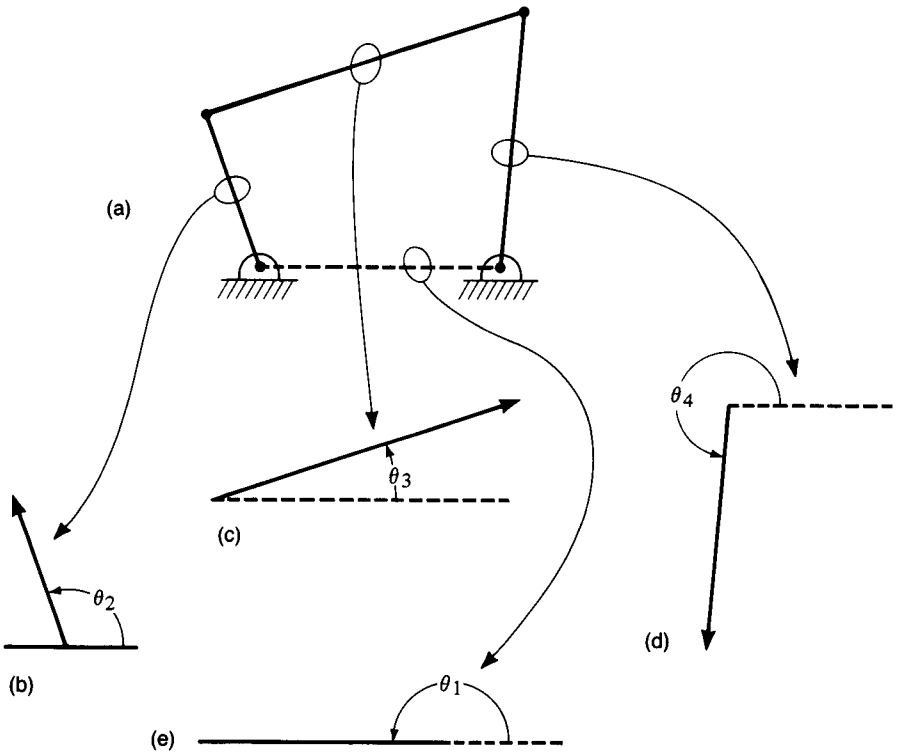

FIGURE 4.2 *Decomposition of a four-bar linkage into its constituent complex vectors:* (a) *the vector skeleton;* (b) *the crank;* (c) *the coupler;* (d) *the follower;* (e) *the ground (frame) link.*

A still more compact notation can be found by using the infinite series representation for the sine and cosine. Using these gives

$$\cos\theta + i\sin\theta = 1 - \frac{1}{2!}\theta^2 + \frac{1}{4!}\theta^4 + i\left\{\theta - \frac{1}{3!}\theta^3 + \frac{1}{5!}\theta^5 + \cdots\right\} \tag{4.8}$$

which can be seen to be equal to

$$1 + i\theta + \frac{1}{2!}(i\theta)^2 + \frac{1}{3!}(i\theta)^3 + \cdots + \frac{1}{n!}(i\theta)^n + \cdots \tag{4.9}$$

which is the series expansion of $e^{i\theta}$, so that a complex variable z can be written in the compact form $re^{i\theta}$. The polar components r and θ (called the magnitude and phase, respectively) can be obtained from the Cartesian components by inverting equations

(4.7). Unambiguous inversion of x and y to obtain r and θ will be important later. Note that r, being a length, is always positive and so can be determined unambiguously. The cosine and sine of the angle are given by the two Equations (4.7). Neither of these formulas can be inverted to find θ unambiguously by itself. The sine is symmetric with respect to the reflection across the y axis, and the cosine is symmetric with respect to reflection across the x axis. In equation form,

$$\begin{aligned} \sin(\pi - \theta) &= \sin\pi\cos\theta - \cos\pi\sin\theta = \sin\theta \\ \cos(2\pi - \theta) &= \cos 2\pi\cos\theta + \sin 2\pi\sin\theta = \cos\theta \end{aligned} \tag{4.10}$$

so that inverting either equation by itself does not provide a unique answer. The ambiguities must be resolved using the information from both equations to identify the appropriate quadrant. Note these operations in the following examples and in the algorithms constructed to solve kinematic problems.

Finally, note that $e^{i\theta}$ is the complex representation of a unit vector pointing at an angle θ measured counterclockwise from the x axis. Figure 4.2 shows all four links of a four-bar linkage as complex vectors, showing the radius r and the phase angle θ for each. Note that the angles are measured from the x axis.

EXAMPLES OF POLAR NOTATION

(1) $c_1 = 3 + 4i$

$$c_1 c_1^* = (3 + 4i)(3 - 4i) = 9 + 16 = 25$$

$$r_1 = 5$$

$$\tan^{-1}\theta_1 = \frac{4}{3}, \qquad \theta_1 = \begin{cases} 0.9273 \\ 4.0689 \end{cases}$$

and because

$$\sin\theta_1 = \frac{3}{5}, \qquad \cos\theta_1 = \frac{4}{5}$$

are both positive, θ_1 is in the first quadrant,

$$\theta_1 = 0.9273 \text{ rad}$$

(2) $c_2 = 2 - 7i$

$$c_2 c_2^* = (2 - 7i)(2 + 7i) = 4 + 49 = 53$$

$$r_2 = \sqrt{53} \approx 7.2801$$

$$\tan^{-1}\theta_2 = \frac{-7}{2}, \qquad \theta_2 = \begin{cases} 1.8491 \\ 4.9907 \end{cases}$$

Because

$$\sin \theta_2 < 0, \qquad \cos \theta_2 > 0$$

θ_2 lies in the fourth quadrant,

$$\theta_2 = 4.9907 \text{ rad}$$

(3) $c_3 = -2 + i$

$$c_3 c_3^* = (-2 + i)(-2 - i) = 4 + 1 = 5$$

$$r_3 = \sqrt{5} \approx 2.2361$$

$$\tan^{-1} \theta_3 = \frac{1}{-2}, \qquad \theta_3 = \begin{cases} 2.6779 \\ 5.8195 \end{cases}$$

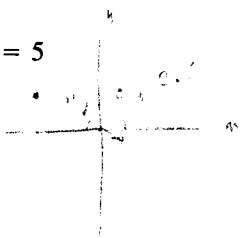

Because

$$\sin \theta_3 > 0, \qquad \cos \theta_3 < 0,$$

θ_3 lies in the second quadrant,

$$\theta_3 = 2.6779 \text{ rad}$$

(4) $c_4 = 1 - 2i$

$$c_4 c_4^* = (1 - 2i)(1 + 2i) = 5$$

$$r_4 = \sqrt{5} \approx 2.2361$$

$$\tan^{-1} \theta_4 = \frac{-2}{1}, \qquad \theta_4 = \begin{cases} 2.0344 \\ 5.1760 \end{cases}$$

Because

$$\sin \theta_4 < 0, \qquad \cos \theta_4 > 0$$

θ_4 is in the fourth quadrant,

$$\theta_4 = 5.1760 \text{ rad}$$

Because of the periodicity of the trigonometric functions, one can add or subtract as many multiples of 2π as one chooses to or from any θ without changing the value of the complex variable. (Those who have studied analytic functions will realize that things are not quite so simple, but my comment applies to planar kinematics.) To keep things manageable and to make the inverse functions single-valued, all angles will be supposed to lie on the half-open interval $[0,2\pi)$. That is, θ can take on any value from zero to 2π, including zero and excluding 2π.

The polar representation allows one to demonstrate additional geometric properties of multiplication. The product of two complex variables z_1 and z_2 can be written

$$z_1 z_2 = r_1 r_2 e^{i(\theta_1 + \theta_2)} \tag{4.11}$$

the magnitude of which is the product of the magnitudes of its factors and the phase of which is the sum of the phases. In the special case in which the magnitude of z_2 is unity, it is clear that multiplication is equivalent to rotation by θ_2 and that rotation of a vector can be represented by multiplication in the complex plane. This will be very useful in the analysis of mechanisms. Division can be written as the ratio of the magnitudes times the difference of the phases:

$$z_1/z_2 = r_1/r_2 \exp i(\theta_1 - \theta_2) \tag{4.12}$$

When $\theta = \pi/2$, $e^{i\theta} = \cos\theta + i \sin\theta = i$. When $\theta = 0$, $e^{i\theta} = \cos\theta + i \sin\theta = 1$. These are special unit vectors. It is useful to remember that, because $i = e^{i\pi/2}$, multiplication by i is equivalent to rotation by $\pi/2$ rad in the clockwise direction. The two complex numbers z and iz represent orthogonal vectors.

EXAMPLES OF POLAR MULTIPLICATION AND DIVISION

(1)

$$\begin{aligned} c_1 c_2 &= (5)(\sqrt{53}) \exp i(0.9273 + 4.9907) \\ &= 36.4005\{\cos(5.9180) + i \sin(5.9180)\} \\ &= 36.4005\{0.9341 - i0.3571\} \\ &= 34.0017 - 17.9986i \end{aligned}$$

(Note round-off error.)

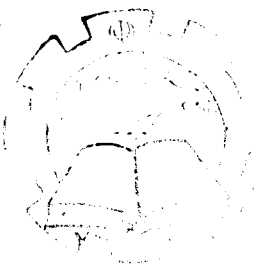

(2)

$$\begin{aligned} \frac{c_1}{c_2} &= \frac{5}{\sqrt{53}} \exp i(0.9273 - 4.9907) \\ &= 0.6868\{\cos(2.2198) + i \sin(2.2198)\} \\ &= 0.6868\{-0.6044 + i0.7967\} \\ &= -0.4151 + 0.5472i \\ &\approx \frac{-22}{53} + i\frac{29}{53} = -0.4151 + 0.5472i \end{aligned}$$

(Note that $\theta_1 - \theta_2 = -4.0634$, so that 2π was added to maintain the conventional range of θ.)

ROOTS AND THE QUADRATIC FORMULA

Although the need to take roots of complex numbers does not arise in kinematics, I include this procedure here for the sake of completeness, and to allow me to expand the quadratic formula. Consider the nth root of a complex number z. Call that root w. The relation between z and w can be written as $z = w^n$. That is, w is a number which, when raised to the nth power, gives z. In simpler terms, $w \cdot w \cdot w \cdot \cdot \cdot w = z$.

Multiplication has already been explained. One multiplies the magnitudes of the factors and adds their phases (angles). Thus, if r_w and θ_w denote the magnitude and phase of w, and r and θ the magnitude and phase of z,

$$r_w^n = r, \qquad r = \sqrt[n]{r_w} \tag{4.13a}$$

and

$$n\theta_w = \theta, \qquad \theta_w = \theta/n \tag{4.13b}$$

The first expression is unambiguous. The second leads to the multiple roots one expects because of the periodicity inherent in θ.

As noted earlier, z is unchanged if θ is increased or decreased by a multiple of 2π. Thus, I can rewrite the first of Equations (4.13b) as

$$n\theta_w = \theta + 2k\pi \tag{4.14}$$

where k is any integer. Division by n gives

$$\theta_w = \frac{\theta}{n} + 2\left(\frac{k}{n}\right)\pi \tag{4.15}$$

and n distinct values of θ_w can be obtained by setting $k = 1,2, \ldots, n-1$. These n distinct values of θ_w combine with the single unique value of r_w to give the n distinct nth roots of z.

All the arithmetic procedures just given can be exercised by indicating how one would write out the quadratic formula (4.2) in the case in which the coefficients a, b, and c are complex. Let

$$a = a_R + ia_I, \qquad b = b_R + ib_I, \qquad c = c_R + ic_I$$

where a_R, a_I, b_R, b_I, c_R, and c_I are real numbers, the real and imaginary parts of a, b, and c.

Begin by constructing the discriminant

$$4ac = 4(a_R + ia_I)(c_R + ic_I) = 4(a_Rc_R - a_Ic_I) + 4i(a_Rc_I + a_Ic_R)$$

$$\text{Re}\,(b^2 - 4ac) = b_R^2 - b_I^2 - 4(a_Rc_R - a_Ic_I) = d_R$$

$$\text{Im}\,(b^2 - 4ac) = 2b_Rb_I - 4(a_Rc_I - a_Ic_R) = d_I$$

To take the square root of the discriminant, it is necessary to convert to polar notation. Let r_d^2 denote the magnitude of the discriminant and $2\theta_d$ its phase:

$$r_d^2 = \left\{d_R^2 + d_I^2\right\}^{1/2}$$

$$\cos 2\theta_d = \frac{d_R}{r_d^2}, \qquad \sin 2\theta_d = \frac{d_I}{r_d^2}$$

and

$$\begin{aligned}\{d_R + id_I\}^{1/2} &= r_d \exp i\theta_d = r_d \cos \theta_d + ir_d \sin \theta_d \\ &= r_d \exp i(\theta_d + \pi) = -r_d \cos \theta_d - ir_d \sin \theta_d\end{aligned}$$

are the two square roots of the discriminant.

This can be combined to give

$$z = \frac{(-b_R \pm r_d \cos \theta_d) + i(-b_I \pm r_d \sin \theta_d)}{2(a_R + ia_I)}$$

Finally, the denominator can be rationalized and the results rearranged to give

$$\text{Re } (z) = \frac{(-b_R \pm r_d \cos \theta_d)a_R + (-b_I \pm r_d \sin \theta_d)a_I}{2(a_R^2 + a_I^2)}$$

$$\text{Im } (z) = \frac{-(-b_R \pm r_d \cos \theta_d)a_I + (-b_I \pm r_d \sin \theta_d)a_R}{2(a_R^2 + a_I^2)}$$

The reader will note that this result is not expressed in closed form in terms of the original variables. Such an expression would be remarkably clumsy and would require several notes to cover the various possibilities for θ_d. I have, however, outlined a procedure by which the values of z could be calculated. This procedure is an algorithm. The idea of an algorithm, the basis of all numerical computation, will be introduced formally in Chapter 5, providing a method of dealing with defined methods of calculation too complicated to be written out in formula form.

VECTOR OPERATIONS

Two further vector operations, the scalar, inner, or dot product and the vector, outer, or cross product, introduced in Chapter 3, will be important in the analysis of planar mechanisms. The scalar product is given by the product of the magnitudes of the vectors multiplied by the cosine of the angle between them. The vector product gives a vector; however, simplification is possible in a planar contact. Two vectors with a common point define a plane. For planar kinematics, this plane is the plane in which

the mechanism lies. For two vectors represented by complex numbers z_1 and z_2, the magnitudes are r_1 and r_2 and the angle between is the difference between the phases. The vector product is perpendicular to the plane and points in the direction a right-hand screw would travel when the first vector is rotated toward the second through the smaller available angle. More simply, it points "up" or "down"—out of or into the page. If up with respect to the complex plane is considered to be positive and down negative, then the vector product can be replaced by the signed scalar equal to the product of the magnitudes times the sine of the difference between the phases.

Both these scalars can be obtained from the real and imaginary parts of a single complex expression

$$z_1^* z_2 = r_1 r_2 \exp\left[i(\theta_2 - \theta_1)\right] = r_1 r_2 \{\cos(\theta_2 - \theta_1) + i \sin(\theta_2 - \theta_1)\} \tag{4.16}$$

The real part of this expression represents the scalar product, and the imaginary part represents the vector product of the vector represented by z_1 into that represented by z_2. [The scalar product is independent of the order; the sign of the vector product reflects whether the true three-dimensional vector points up (+) or down (−). The scalar product commutes; the vector product does not.] The equivalence can be expressed by the equation

$$z_1^* z_2 = \mathbf{R}_1 \cdot \mathbf{R}_2 + i\mathbf{e}_z \cdot (\mathbf{R}_1 \times \mathbf{R}_2) \tag{4.17a}$$

This can be inverted to give

$$\begin{aligned} \mathbf{R}_1 \cdot \mathbf{R}_2 &= \mathrm{Re}\,(z_1^* z_2) \\ \mathbf{e}_z \cdot (\mathbf{R}_1 \times \mathbf{R}_2) &= \mathrm{Im}\,(z_1^* z_2) \end{aligned} \tag{4.17b}$$

as an alternate connection between the vector and complex representations.

DIFFERENTIATION

It will be necessary to differentiate complex numbers when they are used to define mechanisms, in order to find the velocity and acceleration of the members of the mechanism. Differentiation is obvious and follows from what one already knows. The only thing necessary to remember is that i is a constant, so that the derivatives of i of any order with respect to anything are all zero. Thus,

$$\frac{dz}{dt} = \frac{dx}{dt} + i\left(\frac{dy}{dt}\right) \tag{4.18}$$

or

$$\frac{dz}{dt} = \left(\frac{dr}{dt}\right)e^{i\theta} + ri\left(\frac{d\theta}{dt}\right)e^{i\theta} = \left(\frac{dr}{dt} + ir\frac{d\theta}{dt}\right)e^{i\theta} \tag{4.19}$$

The reader should confirm that

$$\frac{d^2z}{dt^2} = \left[\frac{d^2r}{dt^2} + 2i\frac{dr}{dt}\frac{d\theta}{dt} - r\left(\frac{d\theta}{dt}\right)^2 + ir\frac{d^2\theta}{dt^2}\right]e^{i\theta} \tag{4.20}$$

EXERCISES

1. Add the following pairs of complex numbers and express the sums in polar notation:

   $3e^{i\pi} + 5e^{i\pi/3}$ $\qquad$ $7e^{12.66i} + 6e^{3.33i}$

   $2e^{0.72i} + 2e^{0.72i}$ $\qquad$ $e^{0i} + e^{i}$

   $3e^{0.68i} + 6e^{3.65i}$

2. Divide the following pairs of complex numbers, and express the results in Cartesian and polar notation:

   $(1 + i)/(3 - 7i)$ $\qquad$ $(6 + 3i)/(6 - 3i)$

   $(6 + i)/(3 + i)$ $\qquad$ $(4 - 12i)/(6i)$

   $(2 + 6i)/(1 - i)$

3. For the following vectors **a, b,** convert to complex notation and find $\mathbf{a} \cdot \mathbf{b}$, $\mathbf{a} \times \mathbf{b}$, $\mathbf{b} \times \mathbf{a}$ *in complex notation:*

a	**b**
$3\mathbf{e}_x + 7\mathbf{e}_y$	$\mathbf{e}_x - \mathbf{e}_y$
$2\mathbf{e}_x + 6\mathbf{e}_y$	$6\mathbf{e}_x - 2\mathbf{e}_y$
$\mathbf{e}_x$	$-3\mathbf{e}_x - 3\mathbf{e}_y$
$-\mathbf{e}_y$	$\mathbf{e}_x$
$\mathbf{e}_x + \mathbf{e}_y$	$3\mathbf{e}_x + 3\mathbf{e}_y$

4. Refer to text Figure 1.7. Let d be the origin, and let the positive x axis point from d to a. Find the four complex numbers representing the vise-grip links. Express in both Cartesian and polar forms.

5. What are the five distinct values of $(-7)^{1/5}$?

6. The complex variable z points in the direction defined by its phase θ. In what direction do dz/dt and d^2z/dt^2 point?

7. Write a set of subprograms, using the computer language of your choice, to add, subtract, multiply, and divide complex numbers, assuming no direct support from complex arithmetic. Denote complex variables to two-element arrays in the programs.

8. Write a computer program to calculate the quadratic formula for complex coefficients, assuming no support from complex arithmetic.

9. You know that $\mathbf{e}_z \times \mathbf{e}_x = \mathbf{e}_y$ and that $\mathbf{e}_z \times \mathbf{e}_y = -\mathbf{e}_x$. If the vector $\mathbf{a}$ corresponds to the complex number z, how would you write $\mathbf{e}_z \times \mathbf{a}$ using complex notation? The result should contain only z and other complex numbers in polar form.

PART III

Kinematics I: Analysis

Chapter 5

Position Analysis of Bar Linkages

THE LOOP-CLOSURE EQUATION FOR FOUR-LINK MECHANISMS

The basic elements of kinematic analysis and the substructure required for kinematic synthesis can be developed by an exploration of two important four-link mechanisms, the four-bar and the slider crank. Figure 5.1 shows a typical four-bar linkage, its vector skeleton, and its complex variable representation. Figure 5.2 shows the same sequence for a slider-crank mechanism. Note that the simplification to three links has not been made. Using four complex variables (not equivalent to the four links) allows a unified treatment of the two linkages in terms of general solutions to four complex-variable problems.

The fundamental relation from which this general approach is developed is the *loop-closure equation.* In terms of complex variables,

$$z_1 + z_2 + z_3 + z_4 = 0 \tag{5.1}$$

The statement is a tautology. It says that if one walks around a closed loop, one gets back to where one started. Equation (5.1), written in terms of complex variables, is complex and can be separated into two real equations by taking its real and imaginary parts. The loop-closure equation represents, compactly, two independent algebraic equations, and one would hope to be able to solve it for two unknowns. It is not a linear equation, however, so that there is no guarantee of a unique solution.

The variables in the loop-closure equation are the four link lengths r_1–r_4 and the four link angles θ_1–θ_4. For the four-bar linkage, the four lengths are known, and the choice of coordinate system has fixed $\theta_1 = \pi$. There remain three unknowns for the two equations. This is to be expected in a single-degree-of-freedom system and, thus, one independent variable needs to be specified. Usually, this is the crank angle θ_2. The slider crank has also been described by a four-vector skeleton. The unknowns are r_4, θ_2, and θ_3, reflecting that this is also a single-degree-of-freedom problem. One can specify θ_2 as for the four-bar linkage or, if the mechanism is to represent an internal combustion engine, r_4 could be specified.

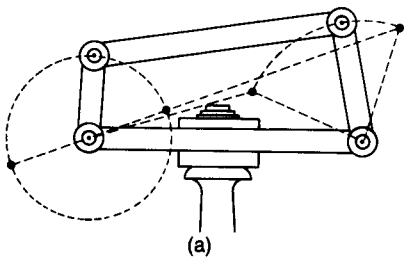

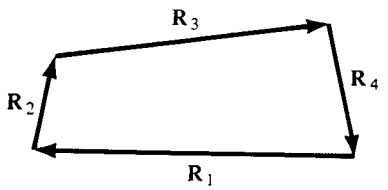

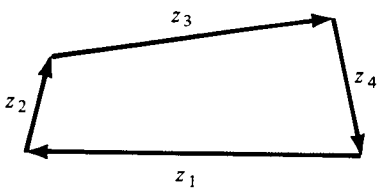

FIGURE 5.1 *Three stages in the abstraction of a four-bar linkage:* (a) *the physical linkage [after Reuleaux (1876)];* (b) *the vector skeleton;* (c) *the complex-variable representation.*

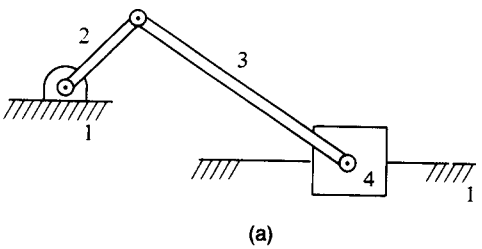

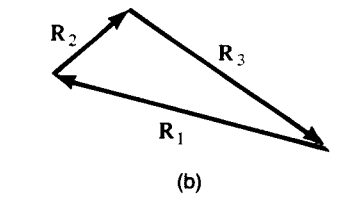

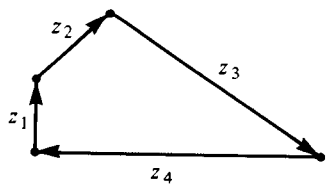

FIGURE 5.2 *Three stages in the abstraction of a slider-crank mechanism:* (a) *the physical linkage;* (b) *the vector skeleton;* (c) *the complex-variable representation.*

These two simple model problems demand a solution of the loop-closure equation for either two angles or one length and one angle. For the sake of completeness, the solution for two lengths will also be given. In all cases, it will be supposed that z_1 and z_2 are known.

DIRECT METHODS OF SOLUTION

Case I: Two Lengths Unknown

Let r_3 and r_4 be unknown. Write the loop-closure equation in the form

$$r_1 e^{i\theta_1} + r_2 e^{i\theta_2} + r_3 e^{i\theta_3} + r_4 e^{i\theta_4} = 0 \tag{5.2}$$

Multiply the loop-closure equation by $e^{-i\theta_3}$, giving

$$r_1 e^{i(\theta_1 - \theta_3)} + r_2 e^{i(\theta_2 - \theta_3)} + r_3 + r_4 e^{i(\theta_4 - \theta_3)} = 0 \tag{5.3}$$

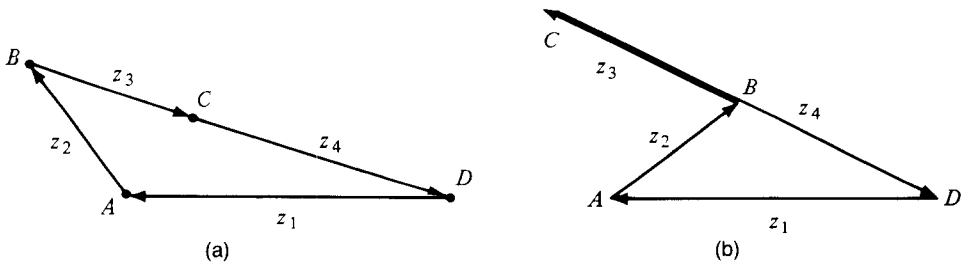

FIGURE 5.3 *The two ambiguous positions of the coupler and follower of a four-bar linkage:* (a) z_3 *and* z_4 *parallel;* (b) z_3 *and* z_4 *antiparallel.*

Taking the imaginary part of this equation eliminates r_3, giving a simple equation for r_4:

$$r_4 \sin(\theta_4 - \theta_3) + r_2 \sin(\theta_2 - \theta_3) + r_1 \sin(\theta_1 - \theta_3) = 0 \tag{5.4}$$

Repeating the process using $e^{-i\theta_4}$ leads to a similar expression for r_3:

$$r_3 \sin(\theta_3 - \theta_4) + r_2 \sin(\theta_2 - \theta_4) + r_1 \sin(\theta_1 - \theta_4) = 0 \tag{5.5}$$

These expressions break down when $\sin(\theta_3 - \theta_4) = 0$. Figure 5.3 shows the two cases for which this can take place, when z_3 and z_4 are parallel or antiparallel. In both cases, the real part of Equation (5.3) gives the distance between points B and D, $r_3 + r_4$ when $\theta_4 = \theta_3$ and $r_4 - r_3$ when $\theta_4 = \theta_3 \pm \pi$.

The case of two unknown lengths is easy, easier than it appears in the analysis just demonstrated. The loop-closure equations (the real and imaginary parts of the complex loop-closure equations) are *linear* in the unknowns r_3 and r_4. I have gone through the apparent "tricks" because I will need them for the other cases. I can obtain the same result simply by writing the real and imaginary parts of Equation (5.2). These are two linear equations for r_3 and r_4, and they can be solved easily. In matrix form, the two real equations are:

$$\begin{Bmatrix} \cos\theta_3 & \cos\theta_4 \\ \sin\theta_3 & \sin\theta_4 \end{Bmatrix} \begin{Bmatrix} r_3 \\ r_4 \end{Bmatrix} = - \begin{Bmatrix} r_1 \cos\theta_1 + r_2 \cos\theta_2 \\ r_1 \sin\theta_1 + r_2 \sin\theta_2 \end{Bmatrix} \tag{5.6}$$

These can be solved to give

$$\begin{Bmatrix} r_3 \\ r_4 \end{Bmatrix} = - \frac{1}{\sin(\theta_4 - \theta_3)} \begin{bmatrix} \sin\theta_4 & -\cos\theta_4 \\ -\sin\theta_3 & \cos\theta_3 \end{bmatrix} \begin{Bmatrix} r_1 \cos\theta_1 + r_2 \cos\theta_2 \\ r_1 \sin\theta_1 + r_2 \sin\theta_2 \end{Bmatrix} \tag{5.7}$$

which can be seen to be the same as Equations (5.4) and (5.5), and the singularity at $\theta_3 = \theta_4$ is seen to be a vanishing determinant in a pair of linear equations. [Recall that $\cos\theta_3 \sin\theta_4 - \sin\theta_3 \cos\theta_4 = \sin(\theta_4 - \theta_3)$.]

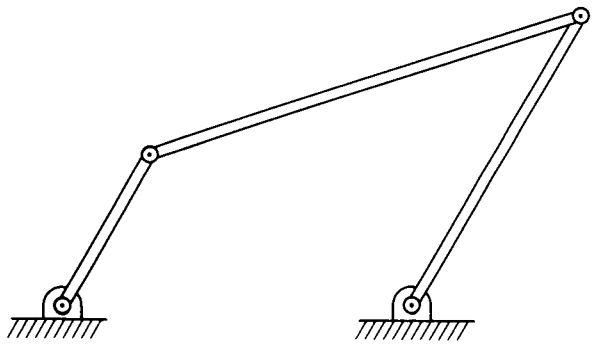

FIGURE 5.4 *A sketch of the linkage found in Example 5.1.*

EXAMPLE 5.1

Let

$$r_1 = 4, \qquad r_2 = 2$$

$$\theta_1 = \pi, \qquad \theta_2 = \pi/3, \qquad \theta_3 = \pi/10, \qquad \theta_4 = 4\pi/3$$

then

$$r_4 = -\left\{2 \sin\left(\frac{\pi}{3} - \frac{\pi}{10}\right) + 4 \sin\left(\pi - \frac{\pi}{10}\right)\right\} \Big/ \sin\left(\frac{4\pi}{3} - \frac{\pi}{10}\right)$$

$$r_4 = -\frac{1.3383 + 1.2361}{(-0.6691)} = 3.8476$$

and

$$r_3 = -\left\{2 \sin\left(\frac{\pi}{3} - \frac{4\pi}{3}\right) + 4 \sin\left(\pi - \frac{4\pi}{3}\right)\right\} \Big/ \sin\left(\frac{\pi}{10} - \frac{4\pi}{3}\right)$$

$$r_3 = -\frac{-3.4641}{0.6691} = 5.1773 \tag{5.8}$$

Figure 5.4 shows the calculated linkage.

Case II: One Length and One Angle Unknown

IIa: Both on the Same Link

This case is trivial. Let r_3 and θ_3 be the unknowns. This is equivalent to z_3 being unknown, and that can be found directly from the loop-closure equation

$$z_3 = -(z_1 + z_2 + z_4)$$

IIb: r_4 and θ_3 Unknown

Multiplication by $e^{-i\theta_4}$, followed by taking the imaginary part, eliminates the unknown length r_4. This gives an equation for the sine of the difference between θ_3 and θ_4:

$$r_3 \sin(\theta_3 - \theta_4) = -r_2 \sin(\theta_2 - \theta_4) - r_1 \sin(\theta_1 - \theta_4) \tag{5.9}$$

The sine of an angle does not determine that angle uniquely, even when angles are restricted to between zero and 2π. For $\sin\theta > 0$, there are two possible values of θ, symmetric with respect to $\theta = \pi/2$. For $\sin\theta < 0$, there are also two values, symmetric with respect to $\theta = 3\pi/2$. Further information, in the form of the sign of $\cos\theta$, is needed to resolve this ambiguity.

The problem is further complicated by the mechanics of taking inverse trigonometric functions. Scientific calculators typically can invert all the trigonometric (and hyperbolic) functions. Many computer languages support only the inverse tangent. The programmer is expected to make use of simple trigonometric identities to generate the other functions. This will be left as an exercise for the reader.

For the sake of convenience, let $\sin(\theta_3 - \theta_4) = \arg$, arg being the right-hand side of Equation (5.9) divided by r_3. Multiply the loop-closure equation by $e^{-i\theta_3}$, and take the imaginary part. Then,

$$r_4 \arg = r_2 \sin(\theta_2 - \theta_3) + r_1 \sin(\theta_1 - \theta_3) \tag{5.10}$$

Now,

$$\theta_2 - \theta_3 = \theta_2 + (-\theta_4 + \theta_4) - \theta_3 = \theta_2 - \theta_4 - (\theta_3 - \theta_4)$$

and

$$\theta_1 - \theta_3 = (\theta_1 - \theta_4) - (\theta_3 - \theta_4)$$

so that the sines on the right-hand side can be written out, as, for example,

$$\begin{aligned}\sin(\theta_2 - \theta_3) &= \sin[\theta_2 - \theta_4 - (\theta_3 - \theta_4)] \\ &= \sin(\theta_2 - \theta_4)\cos(\theta_3 - \theta_4) - \cos(\theta_2 - \theta_4)\sin(\theta_3 - \theta_4)\end{aligned} \tag{5.11}$$

If $\sin(\theta_3 - \theta_4) = \arg$, then $\cos(\theta_3 - \theta_4) = \pm[1 - (\arg)^2]^{1/2}$ and a series of substitutions leads to an ambiguous expression for r_4:

$$\begin{aligned}r_4 = &-r_1 \cos(\theta_1 - \theta_4) - r_2 \cos(\theta_2 - \theta_4) \\ &\pm [r_1 \sin(\theta_1 - \theta_4) + r_2 \sin(\theta_2 - \theta_4)](1 - \arg^2)^{1/2}/\arg\end{aligned} \tag{5.12}$$

and, because r_4 must be positive, a unique choice of sign can be made. At this point, without inverting the trigonometric functions, both $\sin(\theta_3 - \theta_4)$ and $\cos(\theta_3 - \theta_4)$ are known, so that $\theta_3 - \theta_4$ is specified uniquely (in the interval zero to 2π).

EXAMPLE 5.2

Let

$$r_1 = 4, \quad r_2 = 2, \quad r_3 = 5.1773$$

$$\theta_1 = \pi, \quad \theta_2 = \pi/3, \quad \theta_4 = 4\pi/3$$

then

$$\theta_2 - \theta_4 = -\pi; \quad \sin(\theta_2 - \theta_4) = 0, \quad \cos(\theta_2 - \theta_4) = -1$$

$$\theta_1 - \theta_4 = -\pi/3; \quad \sin(\theta_1 - \theta_4) = -\sqrt{3}/2, \quad \cos(\theta_1 - \theta_4) = 0.5$$

and

$$5.1773 \sin(\theta_3 - \theta_4) = 2\sqrt{3}$$

$$\sin(\theta_3 - \theta_4) = 0.6691 = \arg$$

$$\theta_3 - \theta_4 = \begin{cases} 0.7330 \\ 2.4086 \end{cases} \tag{5.13a}$$

$$r_4 = 4(1/2) + 2(-1)$$

$$\pm [4(-\sqrt{3}/2 + 2(0)][1 - (0.6691)^2]^{1/2}/1.6691 \tag{5.13b}$$

$$= 0 \pm (-3.8476)$$

$$r_4 = 3.8476 \tag{5.14}$$

The lower sign is correct, so that $\sin(\theta_3 - \theta_4) > 0$ and $\cos(\theta_3 - \theta_4) < 0$, and $(\theta_3 - \theta_4)$ is in the second quadrant. Thus,

$$\theta_3 = 6.5974 \rightarrow 0.3142 \quad (=\pi/10)$$

Case III: Two Angles Unknown

Let θ_3 and θ_4 be the unknown angles. Taking the loop-closure equation (5.2)

$$r_1 e^{i\theta_1} + r_2 e^{i\theta_2} + r_3 e^{i\theta_3} + r_4 e^{i\theta_4} = 0 \tag{5.15}$$

and combining the first two terms to simplify it gives

$$r_T e^{i\theta_T} + r_3 e^{i\theta_3} + r_4 e^{i\theta_4} = 0 \tag{5.16}$$

where the subscript T indicates that $z_T = r_T e^{i\theta_T} = z_1 + z_2$. (These can be found directly in a system using complex variables. A method without using complex vari-

ables will be demonstrated in Example 5.3. It is easy to implement in a computer language that does not support complex arithmetic.) Rearranging the simplified loop-closure equation to isolate z_4,

$$r_T e^{i\theta_T} + r_3 e^{i\theta_3} = -r_4 e^{i\theta_4} \tag{5.17}$$

and multiplying each side by its complex conjugate gives

$$r_T^2 + r_3^2 + 2r_T r_3 \cos(\theta_3 - \theta_T) = r_4^2 \tag{5.18}$$

where the identity

$$e^{i\theta} + e^{-i\theta} = 2\cos\theta \tag{5.19}$$

was used. Equation (5.18) defines $\cos(\theta_3 - \theta_T)$, and repeating the derivation or interchanging 3 and 4 gives a similar relation for $\cos(\theta_4 - \theta_T)$:

$$r_T^2 + r_4^2 + 2r_T r_4 \cos(\theta_4 - \theta_T) = r_3^2 \tag{5.20}$$

Equations (5.18) and (5.20) can be recognized as the law of cosines when suitably rewritten; for example,

$$r_T^2 + r_4^2 - 2r_T r_4 \cos(\theta_4 - \theta_T \pm \pi) = r_3^2$$

Both relations have the ambiguity associated with the inverse cosine. This apparently suggests the existence of four solutions, two each for $\theta_3 - \theta_T$ and $\theta_4 - \theta_T$. These cannot be combined arbitrarily, however. To show this, multiply Equation (5.17) by $e^{-i\theta_T}$, and take the imaginary part. This gives

$$r_3 \sin(\theta_3 - \theta_T) + r_4 \sin(\theta_4 - \theta_T) = 0 \tag{5.21}$$

which shows that $\sin(\theta_3 - \theta_T)$ and $\sin(\theta_4 - \theta_T)$ must have opposite signs. The two sets of solutions represent a reflection of the third and fourth links across the line z_T. To derive them, I will assume that the inverse cosine is available and let

$$\arg_3 = \{r_4^2 - r_T^2 - r_3^2\}/(2r_T r_3) \tag{5.22a}$$

$$\arg_4 = \{r_3^2 - r_T^2 - r_4^2\}/(2r_T r_4) \tag{5.22b}$$

The inverse cosine is used to find $C_j = \cos^{-1}(\arg_j)$. Under the usual inversion schemes, $C_j \in [0,\pi]$, and the two valid pairs for θ_3 and θ_4 are

$$\theta_3 = \theta_T + C_3, \qquad \theta_4 = \theta_T + 2\pi - C_4 \tag{5.23a}$$

$$\theta_3 = \theta_T + 2\pi - C_3, \qquad \theta_4 = \theta_T + C_4 \tag{5.23b}$$

EXAMPLE 5.3

Let

$$r_1 = 4, \quad r_2 = 2, \quad r_3 = 5.1777, \quad r_4 = 3.8476$$

$$\theta_1 = \pi, \quad \theta_2 = \pi/3$$

then

$$z_T = z_1 + z_2 = 3.4641 e^{i(2.6180)}$$

(This is a direct calculation using a hand calculator with complex arithmetic. Without complex arithmetic, this proceeds from the law of cosines. First,

$$r_T^2 = r_1^2 + r_2^2 + 2r_1 r_2 \cos(\theta_1 - \theta_2)$$

$$= 3.4641$$

and then

$$\cos \theta_T = \frac{r_1 \cos \theta_1 + r_2 \cos \theta_2}{r_T} = -0.8660 \rightarrow \theta_T = \begin{cases} 2.6180 \\ 3.6652 \end{cases}$$

$$\sin \theta_T = \frac{r_1 \sin \theta_1 + r_2 \sin \theta_2}{r_T} = -0.5000 \rightarrow \theta_T = \begin{cases} 0.5236 \\ 2.6180 \end{cases}$$

and the common value is 2.6180, in agreement with the direct calculation.)

$$\arg_3 = -0.6691 \rightarrow C_3 = 2.3038$$

$$\arg_4 = 0 \rightarrow C_4 = 1.5708 \quad (\pi/2)$$

so that

$$\theta_3 = 6.5974 \rightarrow 0.3142, \quad \theta_4 = 4.1888$$

or

$$\theta_3 = 4.9218, \quad \theta_4 = 7.3304 \rightarrow 1.0472$$

Figure 5.5 shows the upper set in solid lines and the lower in dashed lines.

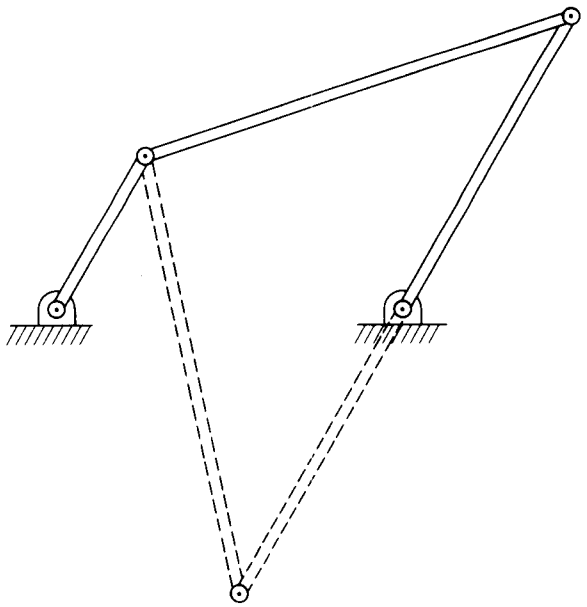

FIGURE 5.5 *A sketch of the two solutions to Example 5.3.*

ALGORITHMS FOR COMPUTATION

Most problems in kinematics cannot be reduced to a single formula, yet well-defined procedures for generating solutions are possible. Such procedures are called algorithms, and digital computers are ideally suited to following algorithms. Indeed, computer programs are sets of algorithms linked by control statements.

Specific computer programs, in one language or another, do not belong in this text. The important issue is the idea of computation, the following of a procedure, or *algorithm,* which leads reliably to the correct answer. I will use "generic" programs written in a language resembling computer languages but without the complicated syntax requirements or, I hope, the use of unclear words. The computer-literate student should be able to construct actual programs in the language of choice from the models here and later in the text. The five programs that follow are two simple complex-variable manipulation codes, followed by the formalization of the procedures outlined for four-link position analysis.

PROGRAM 5.1: ADDITION OF TWO COMPLEX NUMBERS

enter $(x_1, y_1 \text{ and } x_2, y_2)$;

$x_3 = x_1 + x_2; \quad y_3 = y_1 + y_2$

print (x_3, y_3);

PROGRAM 5.2: ADDITION OF TWO COMPLEX NUMBERS IN POLAR FORM

enter $(r_1, \theta_1 \text{ and } r_2, \theta_2)$.

$r_T = \text{sqrt}\{r_1^2 + r_2^2 + 2r_1r_2\cos(\theta_1 - \theta_2)\}$;

$c_T = [r_1\cos\theta_1 + r_2\cos\theta_2]/r_T$;

$s_T = [r_1\sin\theta_1 + r_2\sin\theta_2]/r_T$;

$\theta_{Ts1} = \sin^{-1}s_T$; $\quad \theta_{Ts2} = \pi - \sin^{-1}s_T$;

$\theta_{Tc1} = \cos^{-1}c_T$; $\quad \theta_{Tc1} = 2\pi - \cos^{-1}c_T$;

if $\theta_{Tc1} = \theta_{Ts1}$ **then** $\theta_T = \theta_{Tc1}$;

if $\theta_{Tc1} = \theta_{Ts2}$ **then** $\theta_T = \theta_{Tc1}$;

if $\theta_{Tc2} = \theta_{Ts1}$ **then** $\theta_T = \theta_{Tc2}$;

if $\theta_{Tc2} = \theta_{Ts2}$ **then** $\theta_T = \theta_{Tc2}$;

print (r_T, θ_T);

PROGRAM 5.3: FOUR-BAR ANALYSIS, TWO LINK LENGTHS UNKNOWN

enter $(r_1, r_2, \theta_1, \theta_2, \theta_3, \theta_4)$;

$s_{43} = \sin(\theta_4 - \theta_3)$; $\quad s_{23} = \sin(\theta_2 - \theta_3)$;

$s_{13} = \sin(\theta_1 - \theta_3)$; $\quad s_{14} = \sin(\theta_1 - \theta_4)$;

$s_{24} = \sin(\theta_2 - \theta_4)$;

$r_3 = +[r_2s_{24} + r_1s_{14}]/s_{43}$;

$r_4 = -[r_2s_{23} + r_1s_{13}]/s_{43}$;

print (r_3, r_4);

PROGRAM 5.4: FOUR-BAR ANALYSIS, ONE LENGTH AND ONE ANGLE UNKNOWN

enter $(r_1, r_2, r_3, \theta_1, \theta_2, \theta_4)$;

$s_{14} = \sin(\theta_1 - \theta_4)$; $\quad s_{24} = \sin(\theta_2 - \theta_4)$;

$s_{34} = -[r_2s_{24} + r_1s_{14}]/r_3$;

$c_{14} = \cos(\theta_1 - \theta_4)$; $\quad c_{24} = \cos(\theta_2 - \theta_4)$;

$c_{34} = [1 - s_{34}^2]^{1/2}$;

$r_A = -r_1c_{14} - r_2c_{24} - r_3c_{34}$;

$r_B = -r_1c_{14} - r_2c_{24} + r_3c_{34}$;

if	$r_A \geq 0$	**then**	$r_4 = r_A$;
if	$r_B \geq 0$	**then**	$r_4 = r_B$ and $c_{34} = -c_{34}$;
if	$s_{34} \geq 0$	**then**	$\theta_3 = \theta_4 + \cos^{-1}(c_{34})$;
if	$s_{34} \leq 0$	**then**	$\theta_3 = \theta_4 + 2\pi - \cos^{-1}(c_{34})$;
if	$\theta_3 < 0$	**put**	$\theta_3 = \theta_3 + 2\pi$; **repeat**;
if	$\theta_3 > 2\pi$	**put**	$\theta_3 = \theta_3 - 2\pi$; **repeat**;
print	(r_4, θ_3);		

PROGRAM 5.5: FOUR-BAR ANALYSIS, TWO ANGLES UNKNOWN

enter $(r_1, r_2, r_3, r_4, \theta_1, \theta_2)$;

$z_1 = r_1 e^{i\theta_1}$; $z_2 = r_2 e^{i\theta_2}$; $z = z_1 + z_2$;

$r_T = \text{sqrt}\{zz^*\}$; $\theta_T = \text{Im}\{\log[z/r]\}$;

$c_3 = \{r_4^2 - r_T^2 - r_3^2\}/(2r_T r_3)$;

$c_4 = \{r_3^2 - r_T^2 - r_4^2\}/(2r_T r_4)$;

$\theta_{3A} = \cos^{-1} c_3 + \theta_T$; $\theta_{4A} = 2\pi - \cos^{-1} c_4 + \theta_T$;

$\theta_{3B} = 2\pi - \cos^{-1} c_3 + \theta_T$; $\theta_{4B} = \cos^{-1} c_4 + \theta_T$;

print $(\theta_{3A}, \theta_{4A}$ and $\theta_{3B}, \theta_{4B};)$

Note that this program assumes that the machine is capable of working directly with complex variables. If this is not the case, one can insert the second program in the appropriate spot in the program.

COUPLER CURVES

The motion of any rigid body can be decomposed into a rotation and a translation. In planar kinematics, these motions give the three degrees of freedom discussed earlier. If a link in a bar linkage is pinned to the frame, that link cannot translate with respect to the frame. Such a link rotates, and any point on such a link traces a circular arc in the plane. Other links in a bar linkage rotate about a point that is translating. Points on such a link trace closed noncircular curves. These curves are called *coupler curves.* The archetypal coupler curve is that traced by an arbitrary point on the coupler of a four-bar linkage. These have been studied exhaustively. A catalog of coupler curves has been published by Hrones and Nelson (1951).

The problem of designing a linkage to generate a specified motion, called *synthesis,* and discussed in detail in Chapters 8 and 9, is linked to the problem of coupler curves. It is useful to discuss coupler curves from an analytic viewpoint before moving on to study their synthesis.

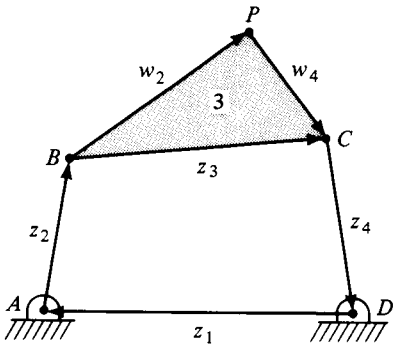

FIGURE 5.6 *A sketch of a four-bar linkage showing the variables necessary for the analysis and synthesis of coupler curves. Note that* w_2 *and* w_4 *always bear a fixed relation to the basic coupler variable* z_3.

Figure 5.6 shows a four-bar linkage with an arbitrary point P attached to the coupler. Two additional vectors have been added to the usual four-bar linkage diagram. These vectors, w_2 and w_4, are attached to the coupler, denoted in complex variable space, as usual, by z_3. Because w_2 and w_4 are attached to the coupler, they are proportional to z_3. The proportionality constant is complex, representing both a change in length and a rotation. During the motion of the linkage, the position of P (with respect to the crank origin, say) can be represented by either of two sums: $z_2 + w_2$ or $-(z_1 + z_4 + w_4)$. Either of these can be generated trivially once the position of z_3 has been found, using Program 5.5. To trace coupler curves, one need merely add a step that gives w_2 in terms of z_3 and then a step that traces out the sum $z_2 + w_2$.

The two sums $z_2 + w_2$ and $-(z_4 + w_4)$ are called *dyads.* The first is the *left-hand dyad* and the second is the *right-hand dyad.* Either dyad traces out the coupler curve, and use will be made of this and of this language in Chapter 7, when synthesis is approached systematically. Note that the standard dyad notation omits the frame link.

Program 5.6 will calculate coupler curves. In this program, q_3 is a complex number such that $w_2 = q_3 z_3$.

PROGRAM 5.6: COUPLER CURVES

enter $(r_1, r_2, r_3, r_4, \theta_1)$
enter (q_3)
enter $(\theta_2, \Delta\theta_2)$
$n = 0$
begin loop
$n = n + 1$
call program 5.5$(r_1, r_2, r_3, r_4, \theta_1, \theta_2, \theta_3, \theta_4)$
$z_3 = r_3 \exp(i\theta_3)$
$w_2 = q_3 z_3$
$x_p = \mathrm{Re}(w_2); \quad y_p = \mathrm{Im}(w_2)$

print (θ_2, x_p, y_p)
if $n\Delta\theta_2 > 2\pi$ **goto end**
$\theta_2 = \theta_2 + \Delta\theta_2$
repeat the loop
end

A coupler curve is typically generated by a Grashof linkage for which the crank can make a complete rotation. As an example, consider the crank-rocker mechanism abstracted from the motorcycle foot brake, for which

$$r_2 = 0.162, \quad r_3 = 0.986, \quad r_4 = 0.204$$

in dimensionless units, and look at the motion of different points on the coupler, link 3, as the crank makes a complete rotation. Figure 5.7a shows the mechanism redrawn in its standard position (a redrawing of Figure 1.17a). Figure 5.7b shows it redrawn once again in a reassembled position, more like the crank-rocker mechanisms shown earlier. Figure 5.7c shows a number of linkage positions. Four coupler points, P_1, P_2, P_3, and P_4, are shown. These lie on the line joining B and C, so that all the w_2 vectors are parallel to z_3:

$$(w_2)_1 = 0.1z_3, \quad (w_2)_2 = 0.25z_3, \quad (w_2)_3 = 0.5z_3, \quad (w_2)_4 = 0.9z_3$$

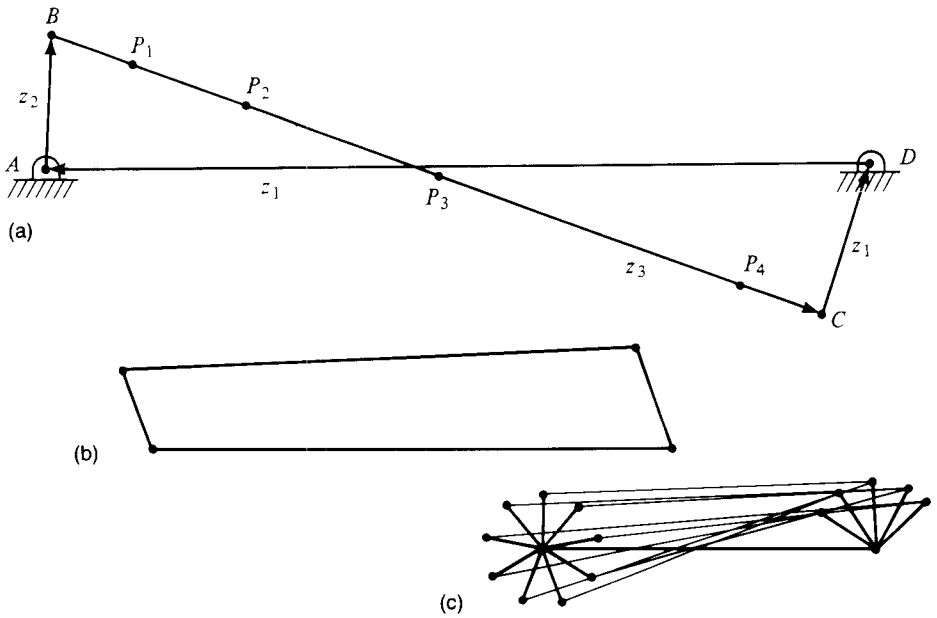

FIGURE 5.7 *The behavior of a mechanism based on the motorcycle foot brake of Chapter 1:* (a) *abstraction of the mechanism, showing four coupler points* P_1 *through* P_4*;* (b) *the mechanism reassembled in a standard crank-rocker orientation;* (c) *the mechanism in several positions throughout its cycle.*

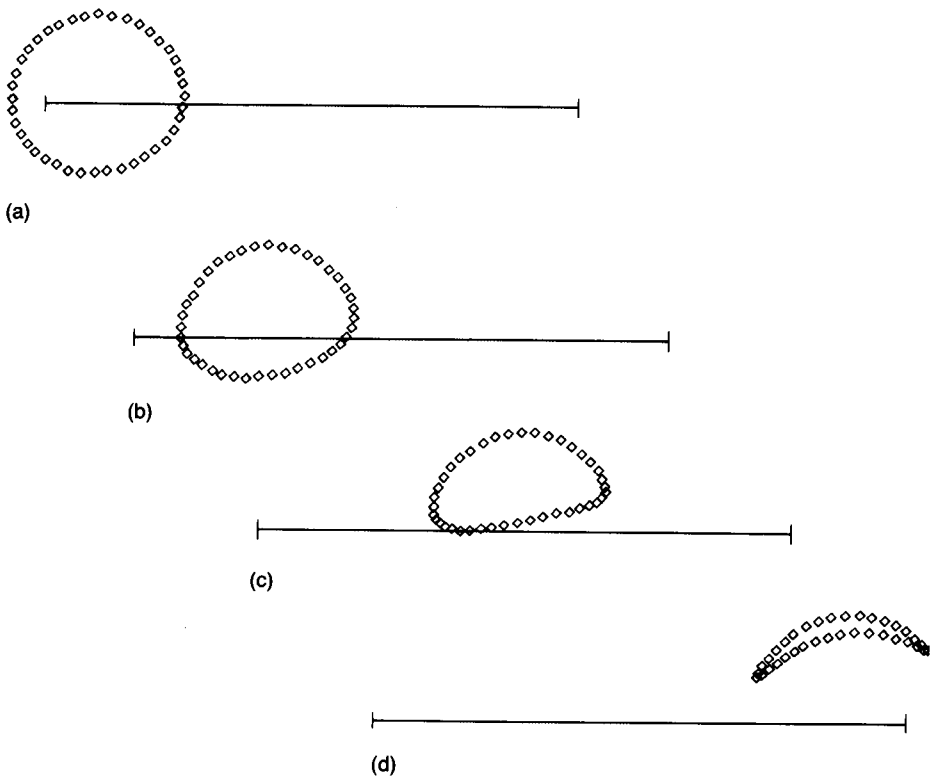

FIGURE 5.8 *Coupler curves for the linkage shown in Figure 5.7b:* (a) *the coupler curve corresponding to* P_1; (b) *the coupler curve corresponding to* P_2; (c) *the coupler curve corresponding to* P_3; (d) *the coupler curve corresponding to* P_4.

Figures 5.8a–5.8d show the four coupler curves, calculated using a specific realization of Program 5.6. The results are in agreement with intuition. When the coupler point is near the crank, its motion is nearly circular, nearly the motion of the crank. At the other end, the motion of the coupler point is nearly an arc, nearly the motion of the follower. In between, the motion is in between. All these are simple closed curves, and synthesized coupler curves for four-bar linkages will always be simple closed curves. For fancier curves, fancier linkages are necessary. I will look briefly at coupler curves for six-bar linkages later in this chapter. This will require a more general approach than that taken to date, an approach based on indirect, iterative solution methods, described in the next section.

INDIRECT METHODS OF SOLUTION

The examples and techniques presented so far are somewhat unrealistic and limited. Only four-link mechanisms have been analyzed. The analysis has been direct and

sufficiently compact to be addressed by hand calculation. Practical problems are not so simple. Practical problems are solved using commercial software packages. However, while no carpenter need be able to manufacture a saw, no good carpenter fails to understand saws. One need not be able to manufacture the tools of one's trade, but one must understand them.

This is not the place to dissect commercial code, even if that were possible. It is however, the place in which some of the fundamental mathematics and numerical analysis that form the bases of these codes should be presented. To that end, I include material more commonly found in textbooks on numerical analysis, so that these tools can be understood.

For practical complicated problems, exact direct solutions are either impossible or impossibly lengthy. It is easier to proceed by a method of successive approximations. One of the most common of these is based on the Newton–Raphson scheme for finding approximations to the zeros of a function. For a thorough discussion of the method, the reader is referred to any good numerical analysis text, such as that by Carnahan et al. (1969). The discussion here is compact but self-contained.

Consider a function F for which it is desired to find X such that $F(X) = 0$. Imagine that an approximate value of X, say X_0, is available. (Typically, one guesses this value using whatever knowledge of the function is available. For linkages, where several angles must be guessed, a rough sketch may be helpful.) Then $F(X_0)$ is in some sense small, near zero, and $X_0 - X$ is also small. Let the true value of $X = X_0 + \Delta X$. *If* X_0 is a good guess, the magnitude of ΔX will be small compared to that of X_0. The function $F(X)$ that is to vanish can be written in terms of a Taylor series valid in a neighborhood of X_0

$$F(X_0 + \Delta X) = 0 = F(X_0) + \frac{dF(X_0)}{dX}\Delta X + \text{higher-order terms} \tag{5.24}$$

This equation can be "solved" for ΔX, giving an approximate correction term

$$\Delta X = -F(X_0)\left(\frac{dF(X_0)}{dX}\right)^{-1} \tag{5.25}$$

Adding this to X_0 gives an improved estimate for the root, X_1. The process can then be repeated indefinitely. If the successive corrections approach zero, this method will *converge* to the correct value of X. The general step, amenable to computation, can be written

$$X_{n+1} = X_n - \frac{F(X_n)}{F'(X_n)} \tag{5.26}$$

where the prime has been introduced to denote derivative with respect to argument. Equation (5.26) is an algorithm. It can be followed more easily in pseudocode, and Program 5.7 is a representation of this algorithm in pseudocode. The functions $f(x)$ and $f'(x)$ are auxiliary functions that need to be supplied to the main program.

PROGRAM 5.7: (ONE-DIMENSIONAL) NEWTON–RAPHSON ROOT FINDER

```
function f(x)
function f'(x)
guess (x)
begin loop
        delta = −f(x)/f'(x)
        if |delta| < limit goto end
        x = x + delta
        repeat loop
end
```

This scheme will not always work. It requires a sufficiently good initial guess; the value of X_0 must be close enough to the correct result. A clearly unworkable initial guess is one for which the derivative vanishes, making the iteration routine singular. A complete discussion is out of place here. The interested reader is referred to the text by Carnahan et al. cited earlier.

As an example, consider the function $x^2 - 11x + 28$, which has the two roots 4 and 7. The iteration relation is

$$X_{n+1} = X_n - [X_n^2 - 11X_n + 28]/[2X_n - 11] \tag{5.27}$$

and two sequences are:

5,3.0000, 3.8000, 3.9882, 4.0000, . . .

6,8.0000, 7.2000, 7.0118, 7.0000, . . .

both displaying rapid convergence.

To apply these ideas to the linkage problems in this chapter and to the more complicated linkage problems that will arise, it is necessary to extend this to more than one independent variable. It happens that the two-variable case contains all the essentials of the n-variable case, and so I will explore the two-variable case in some detail. I will then construct the routines necessary to solve the three nontrivial cases explored in this chapter.

If there are two variables to be determined, there must be two relations that these variables satisfy. Thus, the problem to which a solution is sought can be written

$$\begin{aligned} F_1(x_1, x_2) &= 0 \\ F_2(x_1, x_2) &= 0 \end{aligned} \tag{5.28}$$

Again, an initial guess is required to get the problem started. Let that guess be X_1, X_2, and let

$$x_1 = X_1 + \delta_1, \qquad x_2 = X_2 + \delta_2 \tag{5.29}$$

Both F_1 and F_2 can be expanded in a two-variable Taylor series, and the same smallness hypotheses can be made concerning δ_1 and δ_2. Thus,

$$\begin{Bmatrix} F_{1,1} & F_{1,2} \\ F_{2,1} & F_{2,2} \end{Bmatrix} \begin{Bmatrix} \delta_1 \\ \delta_2 \end{Bmatrix} = - \begin{Bmatrix} F_1 \\ F_2 \end{Bmatrix} \tag{5.30}$$

where the comma subscript notation denotes the partial derivative, That is,

$$F_{i,j} = \frac{\partial F_i}{\partial x_j} \tag{5.31}$$

Equation (5.30) can be inverted to find the δs, provided that the Jacobean

$$J = F_{1,1}F_{2,2} - F_{1,2}F_{2,1} \tag{5.32}$$

is not equal to zero. That result is

$$\begin{Bmatrix} \delta_1 \\ \delta_2 \end{Bmatrix} = \frac{-1}{J} \begin{Bmatrix} F_{2,2} & -F_{1,2} \\ -F_{2,1} & F_{1,1} \end{Bmatrix} \begin{Bmatrix} F_1 \\ F_2 \end{Bmatrix} \tag{5.33}$$

An iteration routine can be constructed using this. The general step is

$$\begin{aligned} (X_1)_{n+1} &= (X_1)_n + (\delta_1)_n \\ (X_2)_{n+1} &= (X_2)_n + (\delta_2)_n \end{aligned} \tag{5.34}$$

with the δs calculated from Equation (5.33).

For the simple four-link mechanism problems that we have solved exactly here, the same pair of equations serve for F_1 and F_2: the real and imaginary parts of Equation (5.2). For case 1, let $x_1 = r_3$ and $x_2 = r_4$, so that the matrix elements are

$$\begin{aligned} F_{1,1} &= \cos\theta_3, \qquad F_{1,2} = \cos\theta_4 \\ F_{2,1} &= \sin\theta_3, \qquad F_{2,2} = \sin\theta_4 \end{aligned} \tag{5.35}$$

and the Jacobean is $J = \sin(\theta_4 - \theta_3)$.

For the nontrivial second case, case IIb, let $x_1 = r_4$ and $x_2 = \theta_3$. The matrix elements become

$$\begin{aligned} F_{1,1} &= \cos\theta_4, \qquad F_{1,2} = -r_3 \cos\theta_3 \\ F_{2,1} &= \sin\theta_4, \qquad F_{2,2} = r_3 \sin\theta_3 \end{aligned} \tag{5.36}$$

and the Jacobean becomes $J = r_3 \cos(\theta_4 - \theta_3)$. Finally, for case III, let $x_1 = \theta_3$ and $x_2 = \theta_4$, making the matrix elements

$$F_{1,1} = -r_3 \sin \theta_3, \qquad F_{1,2} = -r_4 \sin \theta_4$$

$$F_{2,1} = r_3 \cos \theta_3, \qquad F_{2,2} = r_4 \cos \theta_4 \tag{5.37}$$

and the Jacobean, $J = r_3 r_4 \sin(\theta_4 - \theta_3)$.

It is interesting to compare the program necessary to do one of these with the corresponding code for the direct solution. The hardest code for direct solution is that for two angles, case III. The following code will do that in a Newton–Raphson sense.

PROGRAM 5.8: FOUR-BAR ANALYSIS, TWO ANGLES UNKNOWN

```
enter      (r1, r2, r3, r4, θ1, θ2);
guess      θ3, θ4;
begin loop
           J = r3r4 sin(θ4 − θ3);
           if J = 0 goto end

           D3 = −r4[r1 cos(θ4 − θ1) + r2 cos(θ4 − θ2)
                + r3 cos(θ4 − θ3) + r4]/J;

           D4 = r3[r1 cos(θ3 − θ1) + r2 cos(θ3 − θ2)
                + r3 + r4 cos(θ3 − θ4)]/J;

           if |D3| < limit and |D4| < limit goto end
           θ3 = θ3 + D3;
           θ4 = θ4 + D4;
           repeat the loop
           end;
```

The Newton–Raphson technique is no more restricted to two unknowns than it is to one. Mechanisms of any degree of complexity can be analyzed. To illustrate this, I will run through the analysis of the six-bar Stephenson II linkage shown in Figure 2.7d. I chose this as the "most difficult" six-bar linkage, most difficult in the sense that its grounded loop is a five-bar linkage, and the techniques developed for four-bar linkages cannot be applied automatically. Note also that once there are more than two constraints, the "trick" of solving the two equations defining the corrections symbol-

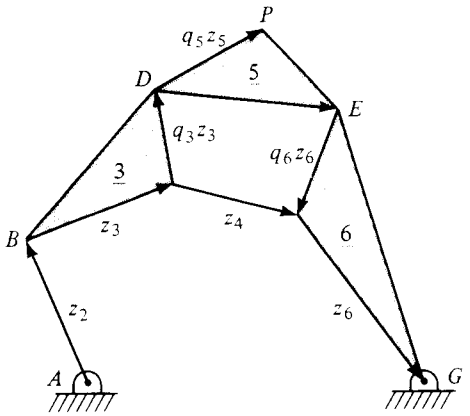

FIGURE 5.9 *Definition sketch for a Stephenson II linkage. The complex numbers* q_3, q_5, *and* q_6 *are constants (see text).*

ically is no longer available. The set of equations determining the correction vector must be solved anew at each iteration.

Begin by redrawing the skeleton of the linkage in Figure 5.9. Instead of one complex loop-closure equation leading to two real constraint equations, there are two independent complex loop-closure equations leading to four real constraint equations. One choice of two independent equations is

$$z_1 + z_2 + z_3 + z_4 + z_6 = 0 \tag{5.38a}$$

$$q_3 z_3 + z_5 + q_6 z_6 - z_4 = 0 \tag{5.38b}$$

where $q_3 = a_3 \exp(i\alpha_3)$ and $q_6 = a_6 \exp(i\alpha_6)$ are the two complex constants relating different edges of links 3 and 6, as shown in Figure 5.9.

As in the four-bar example, all the lengths are specified, as is the frame angle ($=\pi$). Both q_3 and q_6 are consequences of the linkage geometry, hence known and constant. Unknown are the remaining five angles—five unknowns to be determined from four equations. Again, it is convenient to suppose that the crank angle is given and to determine the four remaining angles as a function of the crank angle.

The four real constraint equations are

$$\begin{aligned}
F_1 &= -r_1 + r_2 \cos\theta_2 + r_3 \cos\theta_3 + r_4 \cos\theta_4 + r_6 \cos\theta_6 = 0 \\
F_2 &= r_2 \sin\theta_2 + r_3 \sin\theta_3 + r_4 \sin\theta_4 + r_6 \sin\theta_6 = 0 \\
F_3 &= a_3 r_3 \cos(\theta_3 + \alpha_3) + r_5 \cos\theta_5 + a_6 r_6 \cos(\theta_6 + \alpha_6) - r_4 \cos\theta_4 = 0 \\
F_4 &= a_3 r_3 \sin(\theta_3 + \alpha_3) + r_5 \sin\theta_5 + a_6 r_6 \sin(\theta_6 + \alpha_6) - r_4 \sin\theta_4 = 0
\end{aligned} \tag{5.39}$$

Each constraint equation can be replaced by its Taylor series expansion

$$F_j(\theta_3, \theta_4, \theta_5, \theta_6) = 0 = F_j(\hat{\theta}_3, \hat{\theta}_4, \hat{\theta}_5, \hat{\theta}_6) + \delta\theta_3 \frac{\partial F_j}{\partial \theta_3} + \delta\theta_4 \frac{\partial F_j}{\partial \theta_4} + \delta\theta_5 \frac{\partial F_j}{\partial \theta_5} + \delta\theta_6 \frac{\partial F_j}{\partial \theta_6} + \cdots \tag{5.40}$$

where the caret denotes the initial and subsequent guesses. Each Taylor series is truncated at the two-term level shown earlier, leaving a set of four coupled linear algebraic equations for the correction terms. These are most conveniently written in matrix form as

$$\begin{Bmatrix} F_{1,3} & F_{1,4} & F_{1,5} & F_{1,6} \\ F_{2,3} & F_{2,4} & F_{2,5} & F_{2,6} \\ F_{3,3} & F_{3,4} & F_{3,5} & F_{3,6} \\ F_{4,3} & F_{4,4} & F_{4,5} & F_{4,6} \end{Bmatrix} \begin{Bmatrix} \delta\theta_3 \\ \delta\theta_4 \\ \delta\theta_5 \\ \delta\theta_6 \end{Bmatrix} = - \begin{Bmatrix} F_1 \\ F_2 \\ F_3 \\ F_4 \end{Bmatrix} \tag{5.41}$$

where the comma subscript notation is as defined in Equation (5.31), and the coefficients for the Taylor series matrix are

$$\begin{aligned} F_{1,3} &= -r_3 \sin\theta_3, \quad F_{1,4} = -r_4 \sin\theta_4, \quad F_{1,5} = 0, \quad F_{1,6} = -r_6 \sin\theta_6 \\ F_{2,3} &= r_3 \cos\theta_3, \quad F_{2,4} = r_4 \cos\theta_4, \quad F_{2,5} = 0, \quad F_{2,6} = r_6 \cos\theta_6 \\ F_{3,3} &= -a_3 r_3 \sin(\theta_3 + \alpha_3), \quad F_{3,4} = r_4 \sin\theta_4 \\ F_{3,5} &= -r_5 \sin\theta_5, \quad F_{3,6} = -a_6 r_6 \sin(\theta_6 + \alpha_6) \\ F_{4,3} &= a_3 r_3 \cos(\theta_3 + \alpha_3), \quad F_{4,4} = r_4 \cos\theta_4 \\ F_{4,5} &= r_5 \cos\theta_5, \quad F_{4,6} = -a_6 r_6 \cos(\theta_6 + \alpha_6) \end{aligned} \tag{5.42}$$

The matrix equation (5.41) is the six-bar equivalent of Equation (5.30). Its inversion is not so simple, and it is not convenient to construct an algebraic representation for the correction terms. The iteration scheme will be as follows:

1. Make an initial guess.
2. Evaluate the matrix elements on the left-hand side of Equations (5.36), and the vector elements on the right-hand side of Equation (5.41).
3. Solve Equation (5.41) numerically.
4. If all four correction terms are not sufficiently small, update the guesses for the angles, and repeat the process.

The third step is time-consuming. In practice, one would use a commercial code to solve the matrix equation. Students who wish to implement their own programs

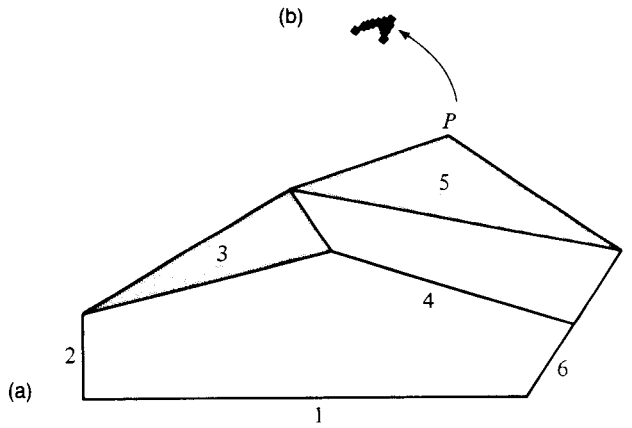

FIGURE 5.10 *The coupler curve for a six-bar linkage:* (a) *the linkage* $r_1 = 300$, $r_2 = 60$, $r_3 = 173.1$, $r_4 = 173.1$, $r_5 = 231.6$, $r_6 = 60$; (b) *motion of point* P.

should take a look at the routines in Press et al. (1986). The following example makes use of these routines.

Figure 5.10a shows a Stephenson II linkage, and Figure 5.10b shows the motion of point P while the crank moves between zero and 90°. The crank is not free to make a complete rotation. If one wanted to drive this with a rotating prime mover, it would be necessary to add a crank-rocker mechanism driving the crank of the six-bar system. The result would be an eight-bar linkage containing four ternary links (the frame and link 2 of the six-bar linkage are now ternary) and four binary links: the new crank and coupler and links 4 and 5 of the original six-bar linkage.

While the Press et al. code is excellent, and well described in that text, it is useful to have a short discussion of the solution of matrix equations in this text, particularly since this method is extendable to larger systems. The analysis of a six-bar linkage requires the solution of a fourth-order system; that of an eight-bar linkage requires the solution of a sixth-order system; that of a ten-bar linkage requires the solution of an eighth-order system, and so forth. The situation is much more complicated for synthesis, which will be discussed in Chapters 8 and 9.

In general, imagine that there are n variables and n relations containing these variables—n constraints. The matrix equation for the general correction vector δ can be written

$$\{F_{ij}\}\ \{\delta_i\} = -\{F_j\} \tag{5.43}$$

where $\{F_{ij}\}$ is an $n \times n$ matrix and $\{\delta_i\}$ and $\{F_j\}$ are $1 \times n$ matrices (column vectors). The obvious extension of the iteration scheme given by Equation (5.32) is

$$\{X_i\}_{n+1} = \{X_i\}_n + \{\delta_i\}_n \tag{5.44}$$

where all the terms are column vectors. The solution of the linear equation (5.43) can be time-consuming for large systems. For matrices for which most of the elements are nonzero, the method of choice is Gaussian elimination, discussed as follows.

Gaussian elimination is the name given to the systematic triangularization of the matrix of the coefficients of a set of linear equations and to the necessary simultaneous modification of the "right-hand side." The discussion here owes much to that in Strang (1986). That reference should be read in parallel with the Press et al. reference already given.

Consider as an example the general matrix problem typified by Equation (5.43). In the interest of neatness, let the matrix $\{F_{ij}\}$ be replaced by A, and denote the elements of A by a_{ij}. Similarly, replace the correction vector by x, with elements x_j, and the function matrix $-\{F_i\}$ by b, with elements b_i, so that the equation to be solved is simply

$$Ax = b \tag{5.45}$$

Written out in "longhand," this is

$$\begin{Bmatrix} a_{11} & a_{12} & \cdots & a_{1n} \\ a_{21} & a_{22} & \cdots & a_{2n} \\ \cdot & & & \\ & & & \\ \cdot & & \cdot & \\ a_{n1} & a_{n2} & \cdots & a_{nn} \end{Bmatrix} \begin{Bmatrix} x_1 \\ x_2 \\ \cdot \\ \cdot \\ \cdot \\ x_n \end{Bmatrix} = \begin{Bmatrix} b_1 \\ b_2 \\ \cdot \\ \cdot \\ \cdot \\ b_n \end{Bmatrix} \tag{5.46}$$

How can this be solved?

First, consider the following specific example:

$$8x_1 + 4x_2 + 4x_3 + 2x_4 = 1 \tag{5.47a}$$

$$6x_1 + x_2 + 3x_3 + 5x_4 = 2 \tag{5.47b}$$

$$x_1 + 4x_3 + 7x_4 = 3 \tag{5.47c}$$

$$2x_1 + 2x_2 + 3x_3 + 6x_4 = 4 \tag{5.47d}$$

I can eliminate x_1 from Equations (5.47b)–(5.47d) in the following way:

1. Multiply Equation (5.47a) by 6/8 and subtract from Equation (5.47b).
2. Multiply Equation (5.47a) by 1/8 and subtract from Equation (5.47c).
3. Multiply Equation (5.47a) by 2/8 and subtract from Equation (5.47d).

The set of equations (5.47) is now:

$$
\begin{aligned}
8x_1 + 4x_2 + 4x_3 + 2x_4 &= 1 && (5.48a)\\
-2x_2 + (7/2)x_4 &= 5/4 && (5.48b)\\
-(1/2)x_2 + (7/2)x_3 + (27/4)x_4 &= 23/8 && (5.48c)\\
x_2 + 2x_3 + (1/2)x_4 &= 15/4 && (5.48d)
\end{aligned}
$$

and I can eliminate x_2 from Equation (5.48c) and (5.48d) in a similar fashion:

1. Multiply Equation (5.48b) by (1/2)/2 and subtract from Equation (5.48c).
2. Multiply Equation (5.48b) by $1/(-2)$ and subtract from Equation (5.48d).

These operations reduce the set (5.48) to a still simpler set:

$$
\begin{aligned}
8x_1 + 4x_2 + 4x_3 + 2x_4 &= 1 && (5.49a)\\
-2x_2 + (7/2)x_4 &= 5/4 && (5.49b)\\
(7/2)x_3 + (47/8)x_4 &= 41/16 && (5.49c)\\
2x_3 + (29/4)x_4 &= 35/8 && (5.49d)
\end{aligned}
$$

which can be reduced to a still simpler set in the single operation: multiply Equation (5.49c) by 2/(7/2) and subtract from Equation (5.49d). The final equations to be solved are:

$$
\begin{aligned}
8x_1 + 4x_2 + 4x_3 + 2x_4 &= 1 && (5.50a)\\
-2x_2 + (7/2)x_4 &= 5/4 && (5.50b)\\
(7/2)x_3 + (47/8)x_4 &= 41/16 && (5.50c)\\
(109/28)x_4 &= 163/56 && (5.50d)
\end{aligned}
$$

and these can be solved directly from the bottom up:

$$
\begin{aligned}
x_4 &= 163/56 \cdot 28/109 = 0.7477\\
x_3 &= (2/7)[41/56 - (47/8)x_4] = -0.5229\\
x_2 &= -(1/2)[5/4 - (7/2)x_4] = 0.6835\\
x_1 &= (1/8)[1-(1/4)x_4 - (1/2)x_3 - (1/2)x_2] = -0.1422 \qquad (5.51)
\end{aligned}
$$

(This result should be checked by substituting it back into the original set.)

The general situation can be handled in the context of matrix operations. While the derivation proceeds, remember the steps in the example just worked, in which no matrix operations were performed. In this derivation, a number of small possible difficulties will be ignored. In particular, there will be a lot of division, and I will assume

all divisors to be nonzero. When it comes time to write programs to perform these operations, the question of zero divisors will have to be faced.

As already seen, the idea of Gaussian elimination is to eliminate x_1 from the second linear equation represented by the matrix equation, then to eliminate x_1 and x_2 from the third equation, and to continue this process until the ith equation has zero coefficients for $x_1, x_2, \ldots, x_{i-1}$ and the modified matrix is *triangular*, that is, all the elements below the main diagonal are zero. Once this is done, the solution for x is immediate. I will now outline how this is done in general.

First, I will use := to denote the sort of = that is used in computer programming. In ordinary arithmetic, $x = x + 3$ is nonsense. In programming, this means to add 3 to the number at the address indicated by x, and store the result at that address. This is usually understood, but I want to emphasize that difference in this section.

The elimination proceeds by subtracting a multiple of the first row from each of the other rows in turn. The multipliers are chosen such that the leading term of each succeeding row is zero, that is,

$$
\begin{aligned}
l_{21} &:= a_{21}/a_{11},\ a_{21} = 0\\
a_{22} &:= a_{22} - l_{21}a_{12},\ a_{23} := a_{23} - l_{21}a_{13}, \ldots, a_{2n} := a_{2n} - l_{21}a_{1n}\\
b_2 &:= b_2 - l_{21}b_1;\\
l_{31} &:= a_{31}/a_{11},\ a_{31} = 0\\
a_{32} &:= a_{32} - l_{31}a_{12},\ a_{33} := a_{33} - l_{31}a_{13}, \ldots, a_{3n} := a_{3n} - l_{31}a_{1n}\\
b_3 &:= b_3 - l_{31}b_1;\\
&\ \ \vdots\\
l_{n1} &:= a_{n1}/a_{11},\ a_{n1} = 0\\
a_{n2} &:= a_{n2} - l_{n1}a_{12},\ a_{n3} := a_{n3} - l_{n1}a_{13}, \ldots, a_{nn} := a_{nn} - l_{n1}a_{1n}\\
b_n &:= b_n - l_{n1}b_1
\end{aligned}
$$

This operation is then repeated to eliminate the second coefficient from the third through nth equations, as

$$
\begin{aligned}
l_{32} &:= a_{32}/a_{22},\ a_{32} = 0\\
a_{33} &:= a_{33} - l_{32}a_{23},\ a_{34} := a_{34} - l_{32}a_{24}, \ldots, a_{3n} := a_{3n} - l_{32}a_{2n}\\
b_3 &:= b_3 - l_{32}b_2;\\
l_{42} &:= a_{42}/a_{22},\ a_{42} = 0\\
a_{43} &:= a_{43} - l_{42}a_{23},\ a_4 := a_{44} - l_{42}a_{24}, \ldots, a_{4n} := a_{4n} - l_{42}a_{2n}\\
b_4 &:= b_4 - l_{42}b_2;
\end{aligned}
$$

$$l_{n2} := a_{n2}/a_{22},\ a_{n2} = 0$$

$$a_{n3} := a_{n3} - l_{n2}a_{23},\ a_{n4} := a_{n4} - l_{n2}a_{24},\ \ldots,\ a_{nn} := a_{nn} - l_{n2}a_{2n}$$

$$b_n := b_n - l_{n2}b_2$$

At the end of this procedure, one has an upper triangular matrix U and a new right-hand side vector c, so that the original equation can be replaced by the simpler equation $Ux = c$.

This whole ritual can be compacted into a pair of nested loops. Before going on to that, and demonstrating some other interesting properties of U, I will work two examples to illustrate the process. I will start by showing how the 2×2 works symbolically, deriving a cute, quick inversion formula for 2×2 systems in the process. *Note that this works only for 2×2 systems.* To that end, consider the equations

$$\begin{bmatrix} a_{11} & a_{12} \\ a_{21} & a_{22} \end{bmatrix} \begin{bmatrix} x_1 \\ x_2 \end{bmatrix} = \begin{bmatrix} b_1 \\ b_2 \end{bmatrix} \tag{5.52}$$

After the first step, these become

$$\begin{bmatrix} a_{11} & a_{12} \\ 0 & a_{22} - a_{21} \cdot a_{12}/a_{11} \end{bmatrix} \begin{bmatrix} x_1 \\ x_2 \end{bmatrix} = \begin{bmatrix} b_1 \\ b_2 - a_{21} \cdot b_1/a_{11} \end{bmatrix} \tag{5.53}$$

and

$$\begin{aligned} x_2 &= [b_2 - a_{21} \cdot b_1/a_{11}]/[a_{22} - a_{21} \cdot a_{12}/a_{11}] \\ &= [a_{11}b_2 - a_{21}b_1]/[a_{11}a_{22} - a_{12}a_{21}] \end{aligned} \tag{5.54}$$

and

$$x_1 = [a_{22}b_1 - a_{12}b_2]/[a_{11}a_{22} - a_{12}a_{21}] \tag{5.55}$$

which is equivalent to

$$\begin{bmatrix} x_1 \\ x_2 \end{bmatrix} = \frac{1}{J} \begin{bmatrix} a_{22} & -a_{12} \\ -a_{21} & a_{11} \end{bmatrix} \begin{bmatrix} b_1 \\ b_2 \end{bmatrix} \tag{5.56}$$

where $J = [a_{11}a_{22} - a_{12}a_{21}]$ is the determinant of the original matrix. The quick ritual that shows up in Equation (5.56) is

1. Swap the terms on the main diagonal.
2. Change the signs of the other two terms.
3. Put the resulting matrix on the right-hand side.
4. Divide by the determinant.

It is important to remember that this is valid only for 2×2 systems.

To make the abstract connection clearer, solve the set of equations given in Equations (5.47) using the matrix operations.

EXAMPLE 5.4
A 4 × 4 MATRIX EQUATION BY GAUSSIAN ELIMINATION

Consider the matrix equation

$$\begin{Bmatrix} 8 & 4 & 4 & 2 \\ 0 & -2 & 0 & 7/2 \\ 0 & -1/2 & 7/2 & 27/4 \\ 0 & 1 & 2 & 11/2 \end{Bmatrix} \begin{Bmatrix} x_1 \\ x_2 \\ x_3 \\ x_4 \end{Bmatrix} = \begin{Bmatrix} 1 \\ 5/4 \\ 23/8 \\ 15/4 \end{Bmatrix} \tag{5.57}$$

The multipliers l_{i1} are

$$l_{21} = 3/4, \quad l_{31} = 1/8, \quad l_{41} = 1/4 \tag{5.58}$$

and the reduced matrix equation is

$$\begin{Bmatrix} 8 & 4 & 4 & 2 \\ 0 & -2 & 0 & 7/2 \\ 0 & -1/2 & 7/2 & 27/4 \\ 0 & 1 & 2 & 11/2 \end{Bmatrix} \begin{Bmatrix} x_1 \\ x_2 \\ x_3 \\ x_4 \end{Bmatrix} = \begin{Bmatrix} 1 \\ 5/4 \\ 23/8 \\ 15/4 \end{Bmatrix} \tag{5.59}$$

The next set of multipliers is

$$l_{32} = 1/4, \quad l_{42} = -1/2 \tag{5.60}$$

and the matrix equation reduces by 1 again, to

$$\begin{Bmatrix} 8 & 4 & 4 & 2 \\ 0 & -2 & 0 & 7/2 \\ 0 & 0 & 7/2 & 47/8 \\ 0 & 0 & 2 & 29/4 \end{Bmatrix} \begin{Bmatrix} x_1 \\ x_2 \\ x_3 \\ x_4 \end{Bmatrix} = \begin{Bmatrix} 1 \\ 5/4 \\ 41/16 \\ 35/8 \end{Bmatrix} \tag{5.61}$$

Finally, $l_{43} = 4/7$, and the triangular matrix equation $Ux = c$ is

$$\begin{Bmatrix} 8 & 4 & 4 & 2 \\ 0 & -2 & 0 & 7/2 \\ 0 & 0 & 7/2 & 47/8 \\ 0 & 0 & 0 & 109/28 \end{Bmatrix} \begin{Bmatrix} x_1 \\ x_2 \\ x_3 \\ x_4 \end{Bmatrix} = \begin{Bmatrix} 1 \\ 5/4 \\ 41/16 \\ 163/56 \end{Bmatrix} \tag{5.62}$$

which can be solved directly from the bottom up:

$$\begin{aligned} x_4 &= (163/56)(28/109) = 0.7477 \\ x_3 &= (2/7)[41/56 - (47/8)x_4] = -0.5229 \\ x_2 &= -(1/2)[5/4 - (7/2)x_4] = 0.6835 \\ x_1 &= (1/8)[1 - x_4/4 - x_3/2 - x_2/2] = -0.1422 \end{aligned} \tag{5.63}$$

This result should be checked by substitution back into the original matrix

$$\begin{Bmatrix} 8 & 4 & 4 & 2 \\ 6 & 1 & 3 & 3 \\ 1 & 0 & 4 & 7 \\ 2 & 2 & 3 & 6 \end{Bmatrix} \begin{Bmatrix} -0.1422 \\ 0.6835 \\ -0.5229 \\ 0.7477 \end{Bmatrix} = \begin{Bmatrix} 1.0000 \\ 2.0000 \\ 3.0000 \\ 4.0000 \end{Bmatrix} \tag{5.64}$$

Note that the operations on the matrix and the operations on the right-hand side can be done independently. This is useful when one wants several solutions to the same linear system for different forcing vectors b. The operations on the matrix need be performed only once. This can be accomplished as follows.

Form the matrix L. The elements of the main diagonal of L are all ones. All the terms above the main diagonal are zero. The terms below the main diagonal are given by l_{ij}, the multipliers found at each stage of the reduction. It is a remarkable fact that the original matrix A is the product of L and U: $A = LU$. A *factorization* of the matrix has been performed. This factorization is called the *LU decomposition.*

One more fact emerges. The original problem was $Ax = b$, and the reduced problem is $Ux = c$. Multiplying the latter expression by L produces the following sequence:

$$Ux = c$$

$$LUx = Lc$$

$$LUx = Ax = Lc = b \tag{5.65}$$

so that c is determined by solving the matrix equation $Lc = b$. L is a triangular matrix, so that the solution is direct. The reduction ritual converts A to U and, at the same time, creates the lower diagonal matrix L. The original problem is reduced to two simpler problems:

$$Ux = c$$

$$Lc = b \tag{5.66}$$

Thus, once U has been determined, the system of equations represented by $Ax = b$ can be solved for any b by:

1. Finding c from $Lc = b$.
2. Finding x from $Ux = c$.

EXERCISES

1. Find r_3 and r_4 from Equations (5.4) and (5.5). Multiply the matrices in Equation (5.5a) to find explicit expressions for r_3 and r_4. Show that these are the same as the expressions found from Equations (5.4) and (5.5). (Hint: Use trigonometric identities.)
2. For the four-bar linkage defined by $r_1 = 10$, $r_2 = 3$, $r_3 = 7$, $r_4 = 8$:
   a. Sketch the linkage for $\theta_2 = \pi/2$ (assuming θ_3 in the first quadrant).
   b. Find θ_3 and θ_4 using the closed-form complex-variable algorithm.
   c. Find θ_3 and θ_4 for $\theta_2 = 1.55$ using the Newton–Raphson method with the starting guess taken from 2.
   d. Write a general Newton–Raphson code in a language of your choice to solve the four-bar analysis problem. Use this to trace the location of point C throughout the cycle as θ_2 runs from 0 to 2π.
3. In the first diagram, the variable $z_3' = 0.8e^{0.8i}z_3$. Find the position of point P at $\theta_2 = 0$, $\pi/3$, $\pi/2$, π, and $7\pi/3$:

$$r_1 = 5.43, \quad r_2 = 3, \quad r_3 = 5, \quad r_4 = 5$$

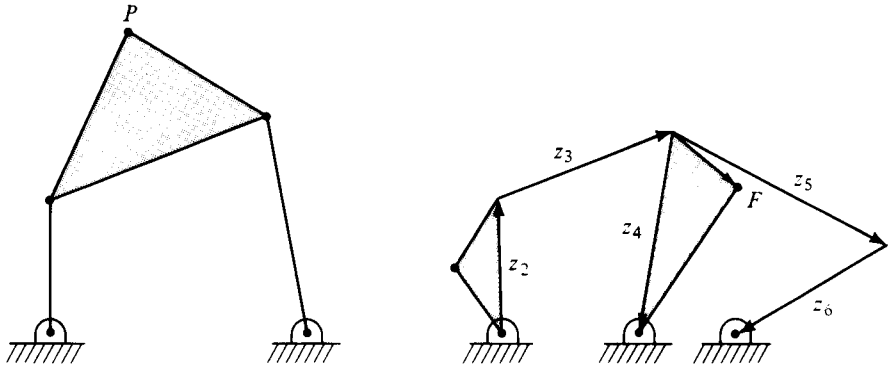

4. Find the position of point F in the second diagram when $\theta_2 = 2\pi/3$:

$$r_1 = 10, \quad r_2 = 6, \quad r_3 = 8, \quad r_4 = 9, \quad r_5 = 10.61, \quad r_6 = 7.78$$

$$z_2' = 0.6e^{0.6i}z_2, \quad z_4' = 0.4e^{1.04i}z_4$$

✓ 5. Draw the path of point P at 20° intervals in θ_2 for

$$\alpha = 20, 60, 75, 105°$$

(This is a total of $18 \times 4 = 72$ position locations.)

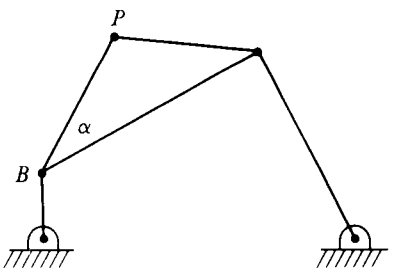

$r_1 = 10, r_2 = 2, r_3 = 8, r_4 = 7, |BP| = 5$

6. Add a four-bar linkage to drive the crank of the six-bar linkage shown in Figure 5.10 to drive link 2 back and forth between 0 and $\pi/2$ when the four-bar crank makes a complete circle. Timing and the choice of the ground link are free.

7. Identify the interior loops in each mechanism. How many links are in each loop?

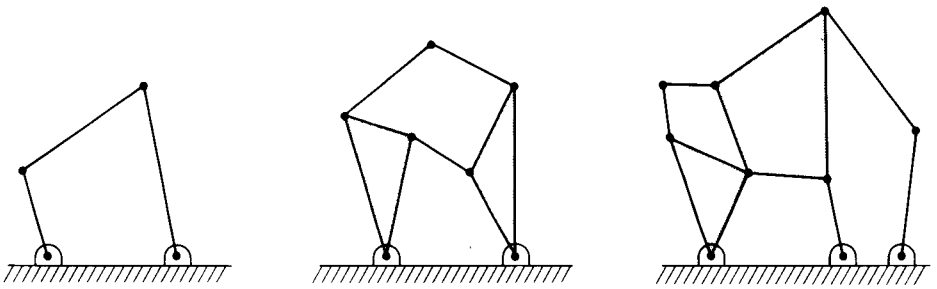

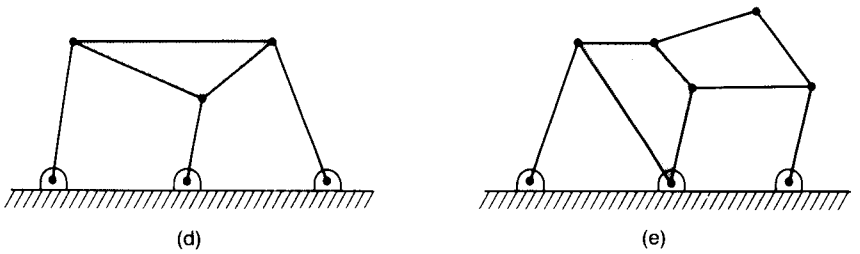

8. Assume that you can solve a four-bar linkage. Outline the procedure you would use to solve the linkage shown in part b of the sketch.

√ 9. Write a complete set of loop-closure equations for the following mechanism. Be sure to define all the vectors necessary, and sketch them clearly.

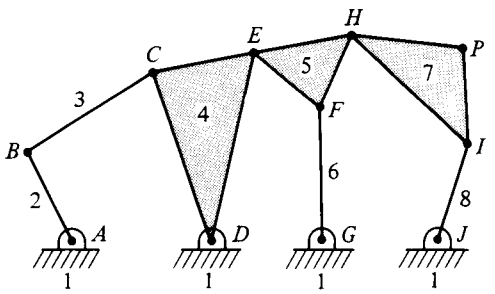

10. Using the answer to the previous exercise, describe how you would calculate a coupler curve for P as a function of θ_2.

√ 11. In which direction should the crank turn to make the timing ratio greater than unity?

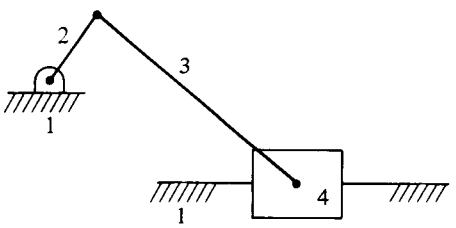

12. If the stroke length is to be 100 mm, what is the maximum length of the crank?

13. If the stroke length is to be 100 mm, what is the maximum length of the coupler?

14. Find the crank angle limits (if any) for the following linkage and all its inversions: $r_1 = 100$, $r_2 = 340$, $r_3 = 470$, and $r_4 = 340$. Draw the linkage in several positions between the two limits, or throughout a complete cycle if there are no limits.

Chapter 6

Velocity and Acceleration of Bar Linkages

Every point on a given link shares its motion and will have a velocity and acceleration expressible in terms of the rates of change of the link angles θ_2, θ_3, and θ_4. (For a slider crank, the variables are, of course, θ_2, θ_3, and r_4.) To find these, it is necessary only to express an arbitrary point P on a given link in terms of the basic link vector z_j. Let the position with respect to A (see Figure 6.1) of a point P on link j be written $(z_P)_j$. Because point P is attached to link j, $(z_P)_j$ can be expressed in terms of the fundamental link variables z_j.

For P on link 2,

$$(z_P)_2 = q_2 z_2 \tag{6.1}$$

For P on link 3,

$$(z_P)_3 = z_2 + q_3 z_3 \tag{6.2a}$$

For P on link 4,

$$(z_P)_4 = z_2 + z_3 + q_4 z_4 \tag{6.3}$$

In these equations, each q_j is a complex constant representing the amount that z_j must be rotated and stretched to point from its base joint to point P. As in the preceding chapter, the q will have the form

$$q_j = a_j \exp(i\theta_j)$$

The notation here is general in that points attached to any link can be written in a uniform notation. The reader will note that the special dyad notation for coupler points could have been used. For example,

$$(z_P)_3 = z_2 + w_2 \tag{6.2b}$$

$$= z_2 + z_3 - w_4 \tag{6.2c}$$

I have introduced the q_j notation as a more general one.

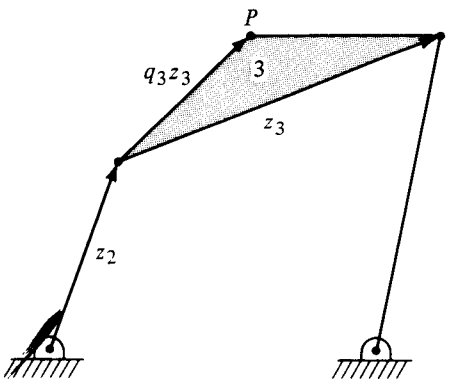

FIGURE 6.1 *A four-bar linkage illustrating an alternate notation for the complex representation of the coupler point* P, z_P.

Figure 6.1 shows a four-bar linkage with the point P on link 3. As drawn,

$$z_1 = -5$$

$$z_2 = 3.1623 \exp(1.2490i) = 1 + 3i$$

$$z_3 = 5.3852 \exp(0.3605i) = 5 + 2i$$

$$z_4 = 5.0990 \exp(4.5150i) = -1 - 5i$$

and one can see that

$$z_P = 5.8310 \exp(1.0304i) = 3 + 5i$$

and

$$q_3 z_3 = 2.8284 \exp(0.7854i) = 2 + 2i$$

Complex division gives

$$q_3 = \frac{q_3 z_3}{z_3} = \frac{2.8284}{5.3852} \exp(0.4049i)$$

$$= 0.5252 \exp(0.4049i)$$

Note that the q_j are constants of the mechanism, independent of its position, and that the velocity and acceleration of the points $(z_P)_j$ can be obtained by differentiation and will involve the first two derivatives of the link angles θ_j.

It is worth reminding the reader that z_4 points down and to the left. The angle 4.5150 lies in the fourth quadrant.

CALCULATION OF VELOCITY AND ACCELERATION

The complete loop-closure equation may be written

$$\sum_j z_j = 0 \tag{6.4}$$

Differentiating, noting that z_1 is a constant, and using ω_j to denote the rate of change of the angle θ_j, leads to

$$i\omega_2 z_2 + i\omega_3 z_3 + i\omega_4 z_4 = 0 \tag{6.5}$$

where it is usual to suppose that ω_2 is given. Dividing by i, multiplying by z_4^*, and taking the imaginary part gives

$$\omega_3 = -\{\mathrm{Im}[z_4^* z_2]/\mathrm{Im}[z_4^* z_3]\}\omega_2 \tag{6.6}$$

and a similar analysis [or the interchange of 3 and 4 in Equation (6.6)] gives the expression for

$$\omega_4 = -\{\mathrm{Im}[z_3^* z_2]/\mathrm{Im}[z_3^* z_4]\}\omega_2 \tag{6.7}$$

Note that ω_3 and ω_4 are formally infinite when $\mathrm{Im}(z_3^* z_4) = 0$. This factor vanishes when z_3 and z_4 are aligned. This special orientation of a four-bar linkage will be discussed further in Chapter 10, when the forces and torques required to make actual linkages move are considered. A second differentiation gives an equation from which the rates of change of ω_j can be determined:

$$[i\dot{\omega}_2 - \omega_2^2]z_2 + [i\dot{\omega}_3 - \omega_3^2]z_3 + [i\dot{\omega}_4 - \omega_4^2]z_4 = 0 \tag{6.8}$$

The only unknowns in Equation (6.8) are the two rates of change of ω_3 and ω_4. Thus, the techniques used to derive Equations (6.6) and (6.7) can be applied again to eliminate each one in turn. Multiplication by z_4^* makes the coefficient of $\dot{\omega}_4$ purely imaginary. Taking the real part of the equation thus eliminates $\dot{\omega}_4$. Noting that $\mathrm{Re}(iz) = -\mathrm{Im}(z)$ and simplifying gives

$$\begin{aligned}\mathrm{Im}(z_4^* z_3)\dot{\omega}_3 = {} & -\mathrm{Im}(z_4^* z_2)\dot{\omega}_2 - \mathrm{Re}(z_4^* z_2)\omega_2^2 \\ & -\mathrm{Re}(z_4^* z_3)\omega_3^2 - z_4^* z_4 \omega_4^2\end{aligned} \tag{6.9}$$

The result for $\dot{\omega}_4$ is obtained by interchanging the subscripts 3 and 4:

$$\mathrm{Im}[z_3^* z_4]\dot{\omega}_4 = -\mathrm{Im}[z_3^* z_2]\dot{\omega}_2 - \mathrm{Re}[z_3^* z_2]\omega_2^2 - \mathrm{Re}[z_3^* z_4]\omega_4^2 - z_3^* z_3 \omega_3^2 \tag{6.10}$$

These can be used to write the velocity v_{jP} and acceleration a_{jP} by differentiating expressions (6.1)–(6.3) and substituting for the ω_j and their derivatives. That result is

$$v_{2P} = i\omega_2 q_2 z_2 \tag{6.11a}$$

$$v_{3P} = i\omega_2 z_2 + i\omega_3 q_3 z_3 \tag{6.11b}$$

$$v_{4P} = i\omega_2 z_2 + i\omega_3 z_3 + i\omega_4 q_4 z_4 \tag{6.11c}$$

for the velocities and

$$a_{2P} = [i\dot{\omega}_2 - \omega_2^2]q_2 z_2 \tag{6.12a}$$

$$a_{3P} = [i\dot{\omega}_2 - \omega_2^2]z_2 + [i\dot{\omega}_3 - \omega_3^2]q_3 z_3 \tag{6.12b}$$

$$a_{4P} = [i\dot{\omega}_2 - \omega_2^2]z_2 + [i\dot{\omega}_3 - \omega_3^2]z_3 + [i\dot{\omega}_4 - \omega_4^2]q_4 z_4 \tag{6.12c}$$

for the accelerations.

These formulas are ideally suited to the construction of an algorithmic solution sequence. The input to such a sequence would be the position of the mechanism, z_1, z_2, z_3, and z_4, q_2, q_3, and q_4, and ω_2 and $\dot{\omega}_2$. The first calculation is of ω_3 and ω_4. These are used to find $\dot{\omega}_3$ and $\dot{\omega}_4$, and then the complex velocities and accelerations follow immediately.

EXAMPLE 6.1

Let $\omega_2 = -0.5$ rad/s, $\dot{\omega}_2 = 0$, and use the mechanism shown in Figure 6.1 with the dimensions given in centimeters. The object is to find the velocity and acceleration of P.

Begin by finding ω_3 and ω_4:

$$\omega_3 = -\frac{\text{Im}\{(5.0990)(3.1623)\exp[(-4.5150 + 1.2490)i]\}}{\text{Im}\{(15.0990)(5.3852)\exp[(-4.5150 + 0.3805)i]\}}(-0.5)$$

$$= -\frac{3.1623}{5.3852}\frac{0.1241}{0.8376}(-0.5)$$

$$= +0.0435 \text{ rad/s}$$

$$\omega_4 = -\frac{\text{Im}\{(5.3852)(3.1623)\exp[(-0.3805 + 1.2490)i]\}}{\text{Im}\{(5.3852)(5.0990)\exp[(-0.3805 + 4.5150)i]\}}(-0.5)$$

$$= -\frac{3.1623}{5.0990}\frac{0.7634}{(-0.8376)}(-0.5)$$

$$= -0.2826 \text{ rad/s}$$

Intermediate calculations required for $\dot{\omega}_3$ and $\dot{\omega}_4$ are

$$z_4{}^*z_3 = (5.0990)(5.3852)\exp[(-4.5150 + 0.3805)i]$$

$$\mathrm{Re}(z_4{}^*z_3) = -14.9997, \qquad \mathrm{Im}(z_4{}^*z_3) = 23.0003$$

$$z_4{}^*z_2 = (5.0990)(3.1623)\exp[(-4.5150 + 1.2490)i]$$

$$\mathrm{Re}(z_4{}^*z_2) = -15.9999, \qquad \mathrm{Im}(z_4{}^*z_2) = 2.0008$$

$$z_3{}^*z_2 = (5.3852)(3.1623)\exp[(-0.3805 + 1.2490)i]$$

$$\mathrm{Re}(z_3{}^*z_2) = 11.0007, \qquad \mathrm{Im}(z_3{}^*z_2) = 12.9997$$

and, of course,

$$\mathrm{Re}(z_3{}^*z_4) = -14.9997, \qquad \mathrm{Im}(z_3{}^*z_4) = -23.0003$$

Substituting these values gives the angular accelerations of links 3 and 4:

$$\dot{\omega}_3 = \frac{15.9999}{23.0003}(0.5)^2 + \frac{14.9997}{23.0003}(0.0435)^2 - \frac{(5.0990)^2}{23.0003}(-0.2826)^2$$

$$= 0.1739 + 0.0012 - 0.0903 = 0.0848 \text{ rad/s}^2 \tag{6.13}$$

$$\dot{\omega}_4 = \frac{-11.0007}{-23.0003}(0.5)^2 + \frac{14.9997}{-23.0003}(-0.2826)^2 + \frac{-(5.3852)^2}{-23.0003}(0.0435)^2$$

$$= 0.1196 - 0.0521 + 0.0024 = 0.0699 \text{ rad/s}^2 \tag{6.14}$$

and it is a simple matter to complete the calculation

$$v_{3P} = i(-0.5)(3.1623)\exp(1.2490i) + i(0.0435)(2.8284)\exp(0.7854i)$$

$$= 1.5 - 0.5i - 0.0870 + 0.0870i$$

$$= 1.4130 - 0.4130i = 1.4721\exp(5.9988i) \text{ cm/s} \tag{6.15}$$

and

$$a_{3P} = -(-0.5)^2(3.1623)\exp(1.2490i)$$

$$\times [0.0848i - (0.0435)^2](2.8284)\exp(0.7854i)$$

$$= -0.25 - 0.75i - 0.1696 + 0.1696i - 0.0038 - 0.0038i$$

$$= -0.4234 - 0.5842i = 0.7215\exp(4.0852i) \text{ cm/s}^2 \tag{6.16}$$

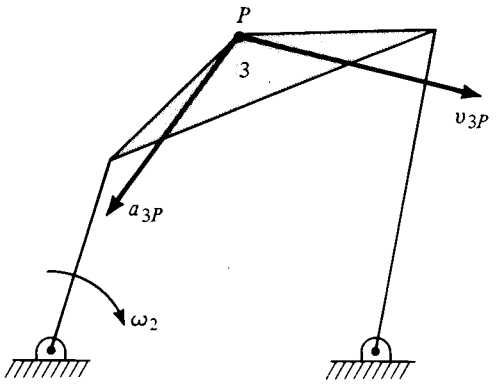

FIGURE 6.2 *Velocity and acceleration vectors* v_{3P} *and* a_{3P} *for the coupler point of the linkage shown in Figure 6.1, assuming counterclockwise rotation of the crank, as shown.*

Figure 6.2 shows the mechanism with the velocity and acceleration of point P superposed.

THE PHYSICAL NATURE OF VELOCITY AND ACCELERATION

The velocity of one point with respect to another can be decomposed into a component parallel to the vector joining the points and one perpendicular to that vector, as well as, of course, the usual Cartesian decomposition. The acceleration can also be decomposed. Equations (6.15) and (6.16) give the Cartesian decomposition. In kinematic applications, the parallel–perpendicular decomposition has more physical significance and can be linked to what you have already learned in elementary dynamics.

Consider first a single link rotating steadily about a fixed point. The complex representation of this can be written as $z = re^{i\omega t}$, where I have written ωt for θ. In this simplest case, ω is constant, so that v_P and a_P are at right angles to each other, v_P at right angles to z, pointing in the direction of rotation, and a_P antiparallel to z, pointing back at the origin. This simple system is depicted in Figure 6.3. This center-directed radial acceleration is just the usual centripetal acceleration.

If the system is complicated by allowing ω to vary with time, then the direction of acceleration (but not of velocity) changes. Taking the second derivative of z in this more complicated case gives

$$a = [i\omega - \omega^2]z \tag{6.17}$$

[Compare this equation to Equation (6.12a).] The second term is antiparallel to z and is the centripetal component of the acceleration. The first term is new and represents a change in v parallel to v, perpendicular to z. This is usually referred to in kinematics as the *tangential acceleration.*

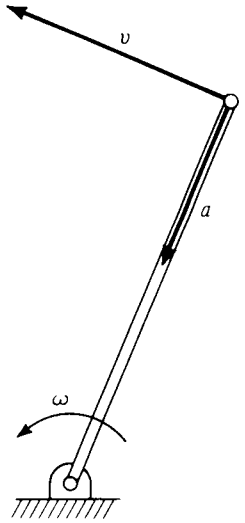

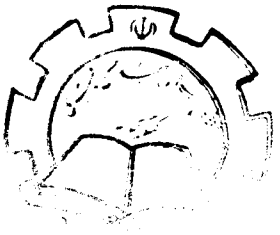

FIGURE 6.3 *Velocity and acceleration of a simple grounded link, say, a crank or a follower.*

Each link of a mechanism is a rigid body (in the approximations with which kinematics is concerned). Thus, the motion of one point with respect to another can only be a rotation. The velocity of one point with respect to another is always perpendicular to the line joining the points, as in the simple example just discussed. The rotation need not be constant, so that the local relative acceleration need not be purely centripetal, as shown in Example 6.1.

The motion of an arbitrary point on a link can then be viewed as the sum of the motion of the point with respect to some point on that link, usually one of the joints, and the motion of the reference point. This decomposition is natural in the complex-variable formulation, as can be seen by examining Equations (6.11) and (6.12). These equations show what is meant by taking the sum. In the velocity expressions, the last terms on the right-hand sides represent the rotation of P with respect to one of the joints of the link. Each additional expression represents the motion of one joint with respect to the previous joint. The chain closes with the ground pivot joint A, the reference point for the analysis. In Equation (6.11a), there is simple rotation of link 2 around joint A. In Equation (6.11b), the first term is the rotation of B around A, and the second that of P around B. In Equation (6.11c), the first term is B around A; the second, C, around B; and the third, P, around C.

The accelerations can be similarly decomposed. In Equation (6.12a), the two parts of the acceleration are the tangential and centripetal acceleration of P around A, the basic link 2 rotation. Equation (6.12b) has the two components of acceleration of B around A, followed by the two components of P around B. Finally, Equation (6.12c) shows the components of acceleration of B around A, C around B, and P around C.

It is of some interest to reexamine Equations (6.15) and (6.16) from this point of view. In Equation (6.15), the term $1.5\text{-}0.5i$ represents the motion of B with respect to A, and the term $-0.0970 + 0.0870i$ represents motion of P around B. Note that this

is perpendicular to $q_3 z_3$, the line from B to P, as it must be. Equation (6.16) gives the accelerations. The term $-0.25 - 0.75i$ is the centripetal acceleration of link 2, which has no tangential acceleration because ω is constant. The terms $-0.1696 + 0.1696i$ and $-0.0038 - 0.0038i$ represent the tangential and centripetal accelerations, respectively, of P with respect to B.

The process of calculating velocities and accelerations can obviously be put in the form of a pseudocode algorithm. Program 6.1 is such a code, using a position analysis code such as Program 5.8 to find the angles.

PROGRAM 6.1: FOUR-BAR VELOCITY AND ACCELERATION

enter $(r_1, r_2, r_3, r_4, \theta_1, \theta_2, \omega_2, \dot{\omega}_2)$

find angles $(r_1, r_2, r_3, r_4, \theta_1, \theta_2, \theta_3, \theta_4)$

$$\omega_3 = -\text{Im}\{z_4^* z_2\}/\text{Im}\{z_4^* z_3\}\,\omega_2$$

$$\omega_4 = \text{Im}\{z_3^* z_2\}/\text{Im}\{z_3^* z_4\}\,\omega_2 \ldots$$

$$\text{temp}_3 = -\text{Im}\{z_4^* z_2\}\dot{\omega}_2 - \text{Re}\{z_4^* z_2\}\omega_2^2 - \text{Im}\{z_4^* z_3\}\omega_3^2 - z_4^* z_4 \omega_4^2$$

$$\text{temp}_4 = -\text{Im}\{z_3^* z_2\}\dot{\omega}_2 - \text{Re}\{z_3^* z_2\}\omega_2^2 - \text{Im}\{z_3^* z_4\}\omega_4^2 - z_3^* z_3 \omega_3^2$$

$$\dot{\omega}_3 = \text{temp}_3/\text{Im}\{z_4^* z_3\}$$

$$\dot{\omega}_4 = \text{temp}_4/\text{Im}\{z_3^* z_4\}$$

$$\dot{z}_2 = i\omega_2 z_2; \quad \dot{z}_3 = i\omega_3 z_3; \quad \dot{z}_4 = i\omega_4 z_4$$

$$\ddot{z}_2 = (i\dot{\omega}_2 - \omega_2^2) z_2; \quad \ddot{z}_3 = (i\dot{\omega}_3 - \omega_3^2) z_3; \quad \ddot{z}_4 = (i\dot{\omega}_4 - \omega_4^2) z_4;$$

end

Figure 6.4 shows an example of how the velocity and acceleration change during the motion of a coupler point. The linkage has relative dimensions

$$r_1 = 110, \quad r_2 = 60, \quad r_3 = 100 = r_4$$
$$a_3 = 0.8, \quad \alpha_3 = 45.8°$$

The first part of the figure (Figure 6.4a) shows the linkage in its upright position, with the crank angle at 90° and the coupler curve traced out by one complete rotation of the crank in the counterclockwise direction. The points are drawn at equal intervals. The coupler point moves slowly where the curvature is high and more rapidly where

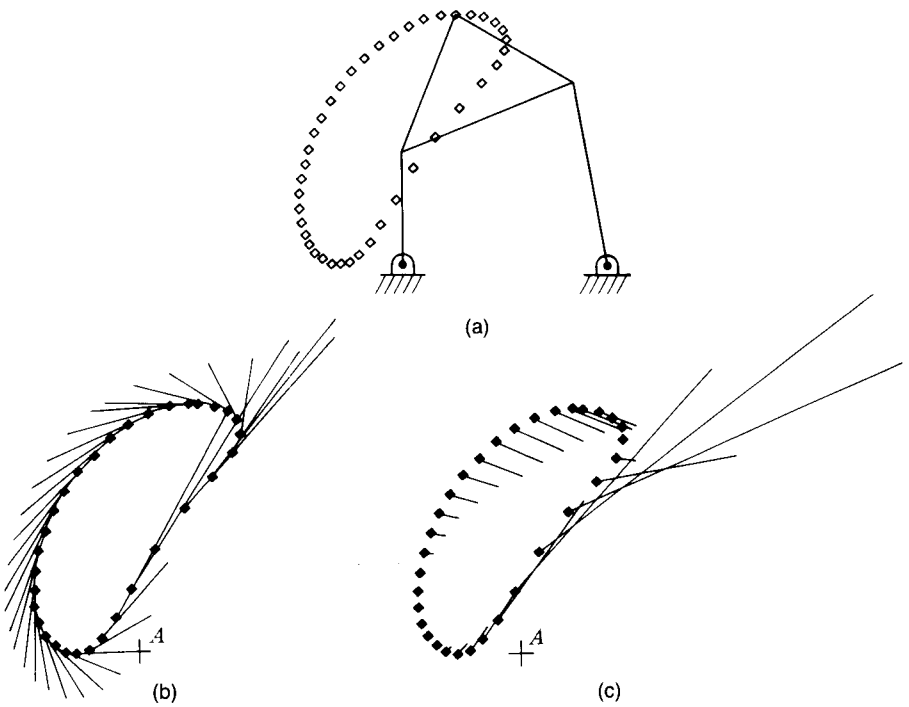

FIGURE 6.4 *The motion, velocity, and acceleration of the coupler point of a four-bar linkage:* (a) *the linkage and its coupler curve;* (b) *the coupler curve with velocity vectors;* (c) *the coupler curve with acceleration vectors. The dimensions of the linkage are* $r_1 = 110$, $r_2 = 60$, $r_3 = 100$, $r_4 = 100$.

the curvature is small. The second and third parts of the figure (Figures 6.4b and 6.4c) show the same coupler curve, with arrows indicating the relative magnitude and direction of the velocity and acceleration of the coupler point, respectively.

The velocity is tangent to the curve. The acceleration is centripetal during most of the cycle. There is a significant positive tangential component of acceleration on the nearly straight path segment running up the right-hand side, and a significant negative tangential component as the point passes over the upper corner in a counterclockwise sense.

VELOCITY AND ACCELERATION ANALYSIS OF SIX-BAR AND HIGHER LINKAGES

The technique for finding the velocity and acceleration for four-bar linkages can be extended easily to linkages of an arbitrary number of bars. For a six-bar linkage, there are two independent loop-closure equations; for an eight-bar, three, and so on, as has been shown. The velocity and acceleration of each link can be related to that of the

crank by successive differentiations, just as for the four-bar linkage. For example, the Stephenson II six-bar linkage has the two loop-closure equations given in the last chapter, Equations (5.38). These are

$$z_1 + z_2 + z_3 + z_4 + z_6 = 0$$
$$q_3 z_3 + z_5 + q_6 z_6 - z_4 = 0$$

Differentiating each once gives a pair of (complex) equations for the angular velocities,

$$\omega_2 z_2 + \omega_3 z_3 + \omega_4 z_4 + \omega_6 z_6 = 0$$
$$\omega_3 q_3 z_3 + \omega_5 z_5 + \omega_6 q_6 z_6 - \omega_4 z_4 = 0$$

and differentiating once again gives a set of equations for the angular accelerations,

$$(\omega_2^2 - i\dot{\omega}_2)z_2 + (\omega_3^2 - i\dot{\omega}_3)z_3 + (\omega_4^2 - i\dot{\omega}_4)z_4 + (\omega_6^2 - i\dot{\omega}_6)z_6 = 0$$
$$(\omega_3^2 - i\dot{\omega}_3)q_3 z_3 + (\omega_5^2 - i\dot{\omega}_5)z_5 + (\omega_6^2 - i\dot{\omega}_6)q_6 z_6 - (\omega_4^2 - i\dot{\omega}_4)z_4 = 0$$

The simple trick used to isolate the individual angular velocities and angular accelerations for the four-bar linkage does not apply here. The entire linear system must be solved simultaneously. This is simple enough if an algebraic equations solver is available, presumably one based on the techniques explored at the end of the preceding chapter. The four velocity equations determining the angular velocities in terms of the crank rotation rate are

$$r_3 \cos\theta_3 \omega_3 + r_4 \cos\theta_4 \omega_4 + r_6 \cos\theta_6 \omega_6 = -r_2 \cos\theta_2 \omega_2$$
$$r_3 \sin\theta_3 \omega_3 + r_4 \sin\theta_4 \omega_4 + r_6 \sin\theta_6 \omega_6 = -r_2 \sin\theta_2 \omega_2$$
$$a_3 r_3 \cos(\theta_3 + \alpha_3)\omega_3 - r_4 \cos\theta_4 \omega_4 + r_5 \cos\theta_5 \omega_5 + a_6 r_6 \cos(\theta_6 + \alpha_6)\omega_6 = 0$$
$$a_3 r_3 \sin(\theta_3 + \alpha_3)\omega_3 - r_4 \sin\theta_4 \omega_4 + r_5 \sin\theta_5 \omega_5 + a_6 r_6 \sin(\theta_6 + \alpha_6)\omega_6 = 0$$

A similar set can be written down for the angular accelerations. This is left as a homework problem. Either set is a set of linear algebraic equations, nonsingular for almost all orientations of the linkage, that can be solved straightforwardly using numerical techniques, such as the codes given in any modern numerical analysis book. The reader should remember that the position problem needs to be solved for each velocity problem, using, for six-bar and higher linkages, one of the indirect, successive approximation methods.

VELOCITY ANALYSIS OF SINGULAR MECHANISMS

There are other ways of analyzing mobility than those explained in Chapter 1. A mobile mechanism can move, can have velocities. That fact provides an alternate method of analysis.

Consider a simple n-bar linkage with n revolute joints. The loop-closure equation can be written

$$z_1 + z_2 + \cdots + z_n = 0 \tag{6.18}$$

If z_1 is the frame link, the first derivative of the loop-closure equation with respect to time is

$$i\dot{\theta}_2 z_2 + \cdots + i\dot{\theta}_n z_n = 0 \tag{6.19}$$

One solution to Equation (6.19) is that all the $\dot{\theta}_j$ vanish. The mobility is equal to the number of other solutions that can exist.

Equation (6.19) represents two homogeneous real equations in $n - 1$ unknowns. In general, if $n \leq 3$, there are no nonzero sets and, if $n > 3$, one can choose $n - 3$ velocities arbitrarily. The mobility for this simple situation is $n - 3$, in agreement with the Kutzbach criterion, Equation (1.3),

$$m = 3(n - 1) - 2j_1 = 3(n - 1) - 2n = n - 3 \tag{6.20}$$

For more complicated situations, it is necessary to differentiate all the independent loop-closure equations. If there are k independent loops, this will produce $2k$ equations in $n - 1$ unknowns. If $(n - 1) > 2k$, then $2k + 1 - n$ unknowns can be chosen arbitrarily, and the mobility is $2k + 1 - n$.

This same technique can be used to assess apparently immobile mechanisms such as that shown in Figure 1.10f. Figure 6.5 shows a more general version of the linkage. Two independent loop-closure equations are

$$z_1 + z_2 + z_3 + z_4 = 0 \tag{6.21a}$$

$$-z_4 + z_5 + z_6 + z_7 = 0 \tag{6.21b}$$

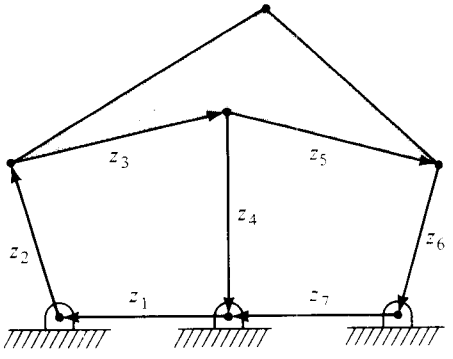

FIGURE 6.5 *A five-bar (z_3 and z_5 are part of the same link, as are z_1 and z_7) linkage with six joints. This is formally immobile (3(5 − 1) − 2(6) = 0) and potentially pathological.*

Differentiating these gives

$$i\dot{\theta}_2 z_2 + i\dot{\theta}_3 z_3 + i\dot{\theta}_4 z_4 = 0 \tag{6.22a}$$

$$-i\dot{\theta}_4 z_4 + i\dot{\theta}_3 z_5 + i\dot{\theta}_6 z_6 = 0 \tag{6.22b}$$

using the fact that $\dot{\theta}_5 = \dot{\theta}_3$ because z_3 and z_5 are attached to the same link and will rotate together.

Equation (6.22) can be rewritten in matrix form

$$\begin{Bmatrix} r_2 \cos\theta_2 & r_3 \cos\theta_3 & r_4 \cos\theta_4 & 0 \\ r_2 \sin\theta_2 & r_3 \sin\theta_3 & r_4 \sin\theta_4 & 0 \\ 0 & r_5 \cos(\theta_3 r_4) & -r_4 \cos\theta_4 & r_6 \cos\theta_6 \\ 0 & r_5 \sin(\theta_2 r_4) & -r_4 \sin\theta_4 & r_6 \sin\theta_6 \end{Bmatrix} \begin{Bmatrix} \dot{\theta}_2 \\ \dot{\theta}_3 \\ \dot{\theta}_4 \\ \dot{\theta}_6 \end{Bmatrix} = 0 \tag{6.23}$$

and this set will have a nontrivial (not all $\dot{\theta}$s $= 0$) solution only if the determinant vanishes. That determinant can be written

$$D = r_2 r_4 r_6 [r_3 \sin(\theta_4 - \theta_6) \sin(\theta_3 - \theta_2) + r_5 \sin(\theta_3 + \phi - \theta_6) \sin(\theta_4 - \theta_2)] \tag{6.24}$$

where $\theta_5 = \theta_3 + \phi$, ϕ constant.

If $\theta_2 = \theta_4 = \theta_6$, the determinant vanishes. However, unless $\phi = 0$, this is only a local vanishing, and the system is not truly mobile. Other local mobility conditions also exist.

EXERCISES

1. A well-designed slider-crank mechanism has the following relations among its links:

$$0 \leq r_1 \leq r_3 - r_2$$

(For definitions, see the sketch.)

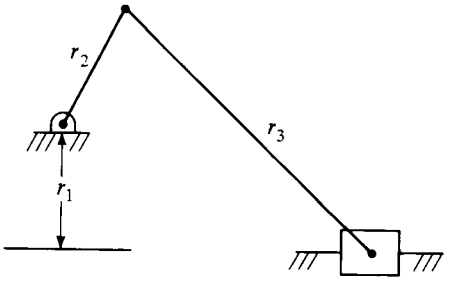

Show that

$$\sin \theta_3 = -[r_1 + r_2 \sin \theta_2]/r_3$$

$$r_4 = r_2 \cos \theta_2 + r_3[1 - \sin^2 \theta_3]^{1/2}$$

2. Using these, write a program to find θ_3 and r_4 for the general well-designed slider crank.
3. If $\dot{\theta}_2 = \omega t$, find dr_4/dt.
4. At what value(s) of θ_2 is dr_4/dt
   a. maximum?
   b. minimum?
   c. zero?
5. What is the stroke length, that is, the difference between the largest and smallest values of r_4?
6. For the slider crank in the figure, write the outline of a computer program to find the velocity and acceleration of the slider, assumed to have a mass m. The outline will be a list of procedures, with an explanation of what each does. Give each procedure an argument list, and identify which are inputs and which are outputs. No pseudocode is required, but enough detail should be given to make the operation clear.

Chapter 7

Higher Pairs: Analysis of Gears and Cams

WHEELS AND GEARS

The higher pairs are characterized by line or point contact rather than surface contact. Higher pairs include wheels, gears, cams, chains, belts, and fluids. This chapter discusses the behavior of (spur) gears and wheels and provides an introduction to the behavior of cams. The discussion is limited to *spur gears,* gears that behave like wheels that turn without slipping in their *pitch circles.* This limitation is consistent with the limitation of the text to planar kinematics. Closely related to spur gears are parallel helical gears and noncircular gears. The most common example of the latter is the drive gear (chain wheel) in many modern bicycles. These can be analyzed by combining the techniques introduced here for spur gears with the noncircular analysis introduced for cam motion.

Gear design involves tooth shape, selection of materials, and many other nonkinematic considerations. Any standard textbook on machine design (e.g., Shigley 1977) provides a useful introduction to these problems, which are dealt with in specialized books on gear design. The essential kinematic feature of gears is that they can be idealized as wheels that contact without slipping. There is no kinematic distinction between wheels and gears. Figure 7.1 is a sketch of a portion of a spur gear showing three teeth. I have labeled three radii. The two important kinematic radii are R, the outer radius of the gear, and r_p, the radius of the *pitch circle.* The latter is the radius of the equivalent wheel. R is the maximum radius of the gear and needs to be taken into account in designing clearance.

For the purpose of kinematic analysis, I will idealize gears as wheels rolling without slipping on their pitch circles. Systems of gears will be limited to planar gear trains, for which the rotation axes of all gears are parallel. I will consider standard and planetary gear trains, including the simple limit of the rack-and-pinion system. The latter is also the limit that gives the kinematics of a wheel rolling on the ground without slipping. Phenomena associated with real teeth, such as tooth slippage, contact, wear, and chatter, will be neglected. Inasmuch as wheels and gears are kinematically equivalent, I will not always distinguish between them, using the word that is more appropriate

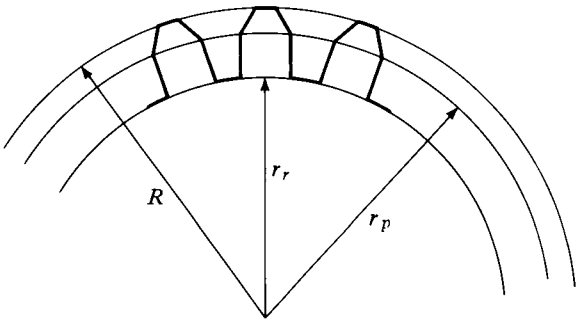

FIGURE 7.1 *Sketch of a portion of a spur gear, showing three teeth and the outer radius* R, *the root radius* r_r, *and the pitch circle radius* r_p.

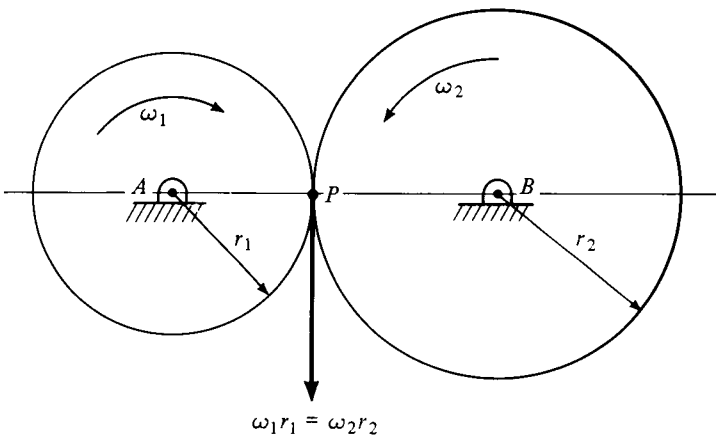

FIGURE 7.2 *Two rollers in contact at point* P.

for the situation I am discussing at the time. I will refer to either as a *roller* when I wish to emphasize the generality of the discussion.

The Basic Roller Pair

Rollers are used to transform rotary motion. Consider two rollers of radii $r_1 \leq r_2$, touching at a line contact, as shown in Figure 7.2. (In the particular case of gears, it is common to call the smaller gear the *pinion* and the larger the *gear*.) The use of r for radius will be seen to be consistent with the use of r as the magnitude of the complex variable z.

Any roller has one degree of freedom; it can rotate about its axle. The axles are supposed to be fixed in some way that makes the center-to-center distance between the

two rollers constant. If there is no friction at the contact point (no teeth on the gear), the rollers can slip, the system is unconstrained, and it has two degrees of freedom. If there is no slippage, the case of interest, the system is constrained. It has one degree of freedom: the rotation of one roller is completely determined by that of the other.

Slip is relative tangential velocity. The velocity of the material points on the rollers is everywhere tangent to the pitch circle. (This is kinematically indistinguishable from the motion of a single bar rotating about its pin, discussed in Chapter 6.) If there is to be no slip, the tangential velocity of the two rollers at the point of contact must be the same. In the figure, the tangential velocity is directed down for both rollers and is of magnitude ωr. I will use ω to denote rotation rate (in rad/s when dimensional) and r to denote radius of the (pitch) circle. Unsubscripted variables are general; when I wish to specify a specific roller, I will add numerical subscripts.

The relation between the rotation rates of the two rollers can be determined by equating the magnitudes of the tangential velocities:

$$\omega_1 r_1 = \omega_2 r_2 \tag{7.1}$$

Notice, however, that the *direction* of rotation changes. The left-hand roller rotates in a clockwise sense and the right-hand roller in a counterclockwise sense. This simple formulation, useful for getting started in understanding the motion of rollers, requires one to keep track of the direction of rotation independently. To keep track of magnitude and direction simultaneously requires a vector formulation, which can be transformed into the complex-variable formulation used in the rest of this text. This can be done using loop-closure equations and velocity analysis.

Recall that the velocity vector $\mathbf{v}$ of a point P that is defined by a position vector $\mathbf{r}$ from any point on the axis of rotation ω is given (in three dimensions) by $\boldsymbol{\omega} \times \mathbf{r}$. The vector $\boldsymbol{\omega}$ is parallel to the rotation axis, and its direction is such that positive ω (the magnitude of $\boldsymbol{\omega}$) gives counterclockwise rotation. For planar kinematics, all rotation vectors are perpendicular to the plane, parallel to $\mathbf{e}_z$. Positive rotation rotates a position vector counterclockwise by $\pi/2$, and negative rotation clockwise by $\pi/2$. If the complex variable z now denotes the position vector to the contact point, rotation by $\pi/2$ is equivalent to multiplication of the complex vector by $e^{i\pi/2}$, and the velocity of any point on a roller can be represented in complex form by

$$v = \omega e^{i\pi/2} z = i\omega z \tag{7.2}$$

The sign of ω determines the direction of rotation. The vector z represents the instantaneous position of some fixed line scribed on the roller.

In Chapter 6, it was shown that simple rotation can be represented in complex notation by letting $\theta = \omega t$. Then, simple differentiation gives the same result as the argument leading to Equation (7.2). It is desirable to extend this to the case of roller pairs (and then to gear trains), but some additional preparation is necessary.

As the rollers shown in Figure 7.2 spin, the contact point P does not move. The linkage variables do move, and differentiating the linkage variables gives the velocity

of the tip of the linkage variable *at the tip of the linkage variable.* Because the linkage variable is rigidly attached to the roller and because the motion is purely circular, the tangential speed of every point on the pitch circle is the same, and no harm is done by ignoring the fact that the speed is calculated at some point other than the contact point. The velocity is not the same because the tangential direction is different at different points on the roller. This means that the analyst must keep mental track of what is being done and cannot automate the calculations. This can lead to error. It is therefore necessary to understand how to take time derivatives at a point fixed in space when the underlying link is moving. This is accomplished by taking the *convective derivative,* the rate of change of position of a material point that is, at any given instant, at a specified point P in space, not necessarily attached to the material. Alternatively, the absolute material velocity can be calculated for an arbitrary point on the link in question, and then the arbitrary point can be placed in coincidence with point P where the velocity is to be matched. The latter method is easier to understand and will be adopted here.

Figure 7.3 is a redrawing of Figure 7.2 with the addition of three complex vectors representing the two rollers and the frame. I show the variables as attached to the wheels. When $t = 0$, the linkage vectors point to the right. The acute angles between the horizontal and z_2 and z_3 are $\omega_2 t$ and $\omega_3 t$, respectively. Note that, as drawn, $\omega_2 < 0$ and $\omega_3 > 0$. Let the initial ($t = 0$) position be denoted by an (additional) zero subscript.

$$z_2 = z_{20}e^{i\omega_2 t} = r_2 e^{i\omega_2 t}, \qquad z_3 = z_{30}e^{i\omega_3 t} = r_3 e^{i\omega_3 t} = 0 \tag{7.3}$$

A loop-closure equation can be constructed exactly as for bar linkages. However, the "joints" are defined by the geometry, not by the physical objects. The joints are not attached to their respective rollers. The loop-closure equation is the very simple relation among the zero linkage variables,

$$z_1 + z_{20} - z_{30} = 0 \tag{7.4}$$

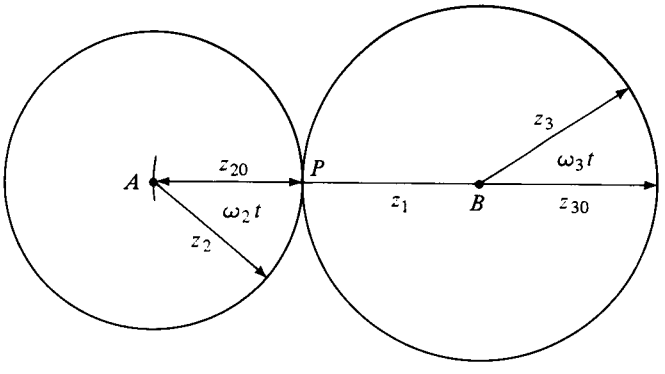

FIGURE 7.3 *Two rollers in contact at point* P, *showing complex vectors attached to the two rollers.*

Velocities can be found, not by differentiating the loop-closure equation [every term in Equation (7.5) is a constant], but by finding the velocity of the material point instantaneously at P from the point of view of link 2, and then from the point of view of link 3, and then equating these two. The rotation of link 2 is given by $i\omega_2 z_2$ and that for link 3 (in general) by

$$-i\omega_1 z_1 + i\omega_3 z_3 \tag{7.5}$$

where z_1 denotes a frame vector pointing from B to A, and ω_1 its possible rotation rate, here zero. The two velocities must be equal when $z_2 = z_{20}$ and $z_3 = -z_{30}$, leading to

$$i\omega_2 z_{20} = -i\omega_3 z_{30} \rightarrow i\omega_2 r_2 = -i\omega_3 r_3 \tag{7.6}$$

The complex-variable/vector approach makes it unnecessary to distinguish between exterior contact, as in Figure 7.2, or interior contact, shown in Figure 7.4. In the latter case, the rotation direction of the two rollers will be the same, both positive as drawn in the figure. This can be deduced directly, following the procedures just introduced:

$$-i\omega_2 z_{20} = -i\omega_3 z_{30} \rightarrow i\omega_2 r_2 = i\omega_3 r_3 \tag{7.7}$$

It is instructive for the reader to work out the directions of the vectors in Equation (7.7) in conjunction with Figure 7.4. (See Exercise 1 at the end of the chapter.)

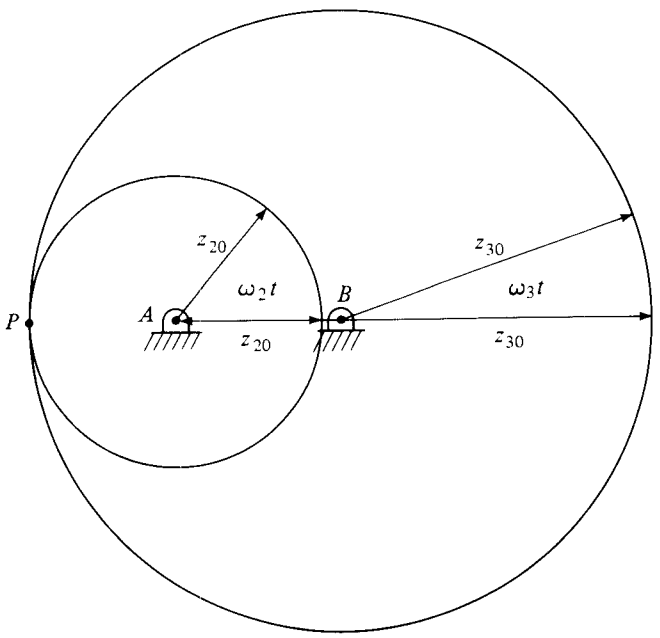

FIGURE 7.4 *Two rollers in contact at point* P. *Link 2 is inside link 3.*

Gear Trains

Real systems of gears use more than two gears (or one gear pair). Fortunately, the complex-variable approach makes it relatively easy to construct the appropriate equations for systems of gears, or *gear trains*. Figure 7.5a shows a train of five rollers. A loop-closure equation can be written for the entire system. This is useful as an exercise in understanding the behavior of the linkage variables z_j, although the analysis is best done one pair at a time by writing the material velocity at each contact point in terms of the two gears that meet at that point. An overall loop-closure equation is

$$\begin{aligned} & r_2 \exp i\theta_2 + r_3 \exp i\theta_2 \\ & r_3 \exp i\theta_3 + r_4 \exp i\theta_3 \\ & r_4 \exp i\theta_4 + r_5 \exp i\theta_4 \\ & r_5 \exp i\theta_5 + r_6 \exp i\theta_5 \\ & \qquad + \quad z_1 \quad = 0 \end{aligned} \tag{7.8}$$

This form of the loop-closure equation assumes that each link variable points to the axle of the next roller at $t = 0$. I introduce angles θ_j for each link. These represent phase angles, as it were. Each θ_j points from the axle of the jth link to the axle of the $(j + 1)$th link. Thus,

$$z_{j0} = r_j e^{i\theta_j}$$

Figure 7.5b shows a close-up view of the second roller, link 3, for $\omega_3 > 0$, to clarify the various angles introduced. Each line of Equation (7.8) represents a link variable that connects two axles. The first line connects A to B; the second, B to C; the third, C to D; and the fourth, D to E. The vector z_1, the frame, connects E back to A.

The absolute velocity of each link is then the rate of change of the appropriate base vector

for link 3: $\left(1 + \frac{r_3}{r_2}\right) z_{20}$

for link 4: $\left(1 + \frac{r_3}{r_2}\right) z_{20} + \left(1 + \frac{r_4}{r_3}\right) z_{30}$

for link 5: $\left(1 + \frac{r_3}{r_2}\right) z_{20} + \left(1 + \frac{r_4}{r_3}\right) z_{30} + \left(1 + \frac{r_5}{r_4}\right) z_{40}$

for link 6: $\left(1 + \frac{r_3}{r_2}\right) z_{20} + \left(1 + \frac{r_4}{r_3}\right) z_{30} + \left(1 + \frac{r_5}{r_4}\right) z_{40} + \left(1 + \frac{r_6}{r_5}\right) z_{50}$

plus the relative motion of each with respect to its axle. The first roller, link 2, has a zero base vector since the origin of the system has been chosen at A, the axle of

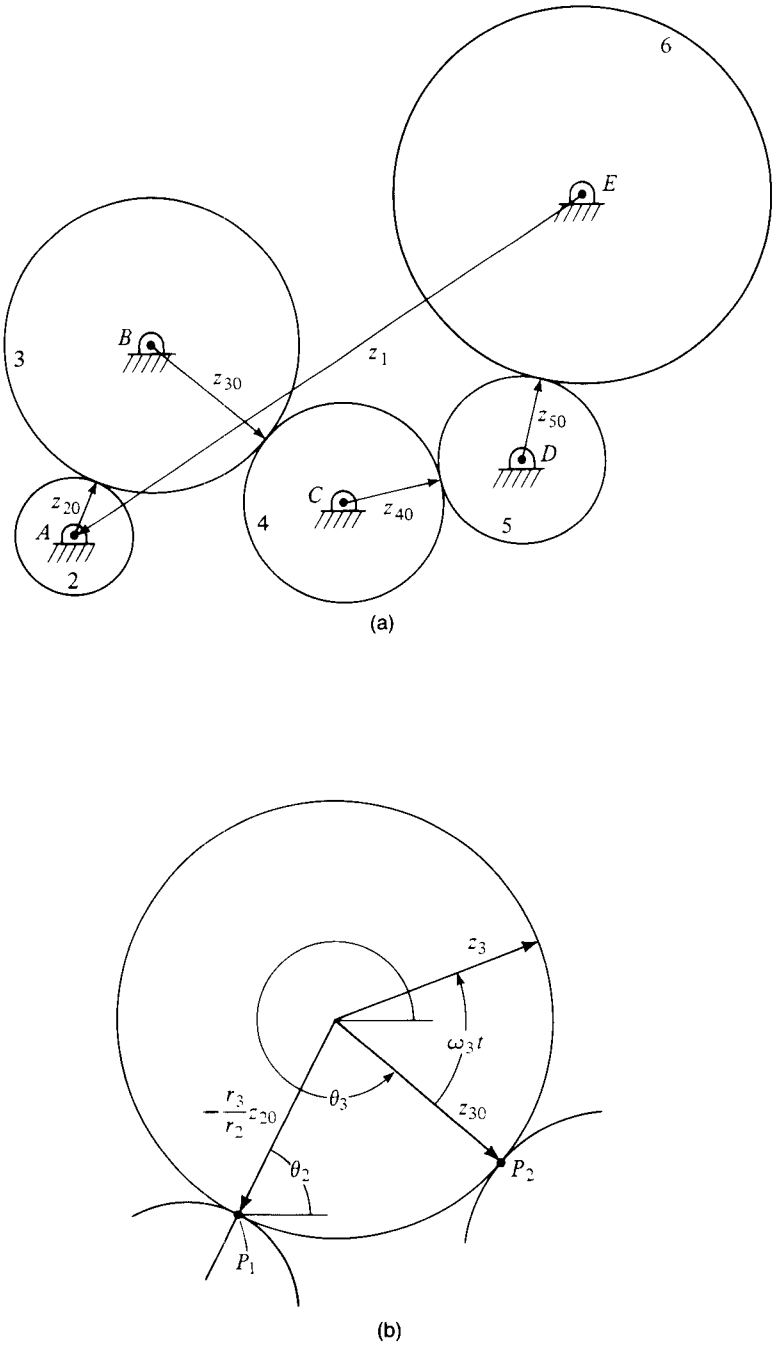

FIGURE 7.5 *A five-gear train of spur gears, showing the complex link vectors in their initial positions:* (a) *the complete gear train;* (b) *a close-up of the third link. Link 1 is the frame link connecting points* E *and* A.

link 2. All the axles are fixed, the derivatives of all base vectors vanish, and the velocity of each roller is rotation about its own axle—$i\omega_j z_j$. The (tangential) velocities must be equal at the four contact points defined by $z_2 = z_{20}$, $z_3 = z_{30}$, $z_4 = z_{40}$, $z_5 = z_{50}$, and

$$z_3 = -\frac{r_3}{r_2} z_{20}, \quad z_4 = -\frac{r_4}{r_3} z_{30}, \quad z_5 = -\frac{r_5}{r_4} z_{40}, \quad z_6 = -\frac{r_6}{r_5} z_{50} \tag{7.9}$$

Making this substitution leads to four equations relating the five rotation rates:

$$\begin{aligned} -\omega_2 r_2 + \omega_3 r_3 &= 0 \\ -\omega_3 r_3 + \omega_4 r_4 &= 0 \\ -\omega_4 r_4 + \omega_5 r_5 &= 0 \\ -\omega_5 r_5 + \omega_6 r_6 &= 0 \end{aligned} \tag{7.10}$$

Thus, knowledge of the geometry and any one rotation rate is sufficient to determine all the other rotation rates, as is to be expected in a one-degree-of-freedom system.

EXAMPLE 7.1

In Figure 7.5a, let $r_j = 9, 32, 14, 7, 20$ mm for $j = 2, 3, 4, 5, 6$, and let $\omega_2 = 1.2$ rad/s. (By writing this as a positive number, I imply counterclockwise rotation.) Direct substitution in Equations (7.10) gives the other four rotations as 0.3375, −0.7714, 1.5429, −0.5400 rad/s, respectively.

It is instructive to examine the *kinematic inversion* of gear trains. This will lead naturally to the discussion of *planetary* gear systems. Begin by considering the simple system shown in Figure 7.2. This is redrawn in Figures 7.6a–c. In the new figure, the frame link has been replaced by an arm, link 1, that is free to move. The three possible inversions are generated in the same way that bar linkages are inverted: by fixing in turn each of the links. Figure 7.6a shows the arm fixed. This is identical to the simple system shown in Figure 7.2. Figures 7.6b and 7.6c show the two inversions obtained by grounding links 2 and 3, respectively. These are comparable situations, and I will analyze the first one here, leaving the second for the Exercise section.

Figure 7.7 shows an expanded view of the second inversion, for which link 2 is grounded. Now z_P is a function of time,

$$z_P = r_2 \exp i\omega_1 t$$

but, as I deal with the absolute velocities of the links, this does not present a difficulty. The absolute velocity of any point on link 3 is given by $-i\omega_1 z_1 + i\omega_3 z_3$ (recall that z_1 points from B to A), and this must vanish when

$$z_3 = \frac{r_3}{r_1} z_1 \rightarrow i\left(\omega_1 - \frac{r_3}{r_1}\omega_3\right) z_1 \tag{7.11}$$

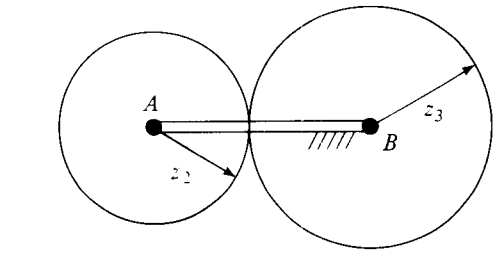

(a)

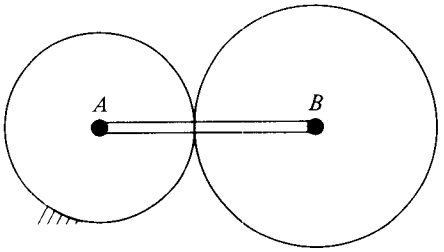

(b)

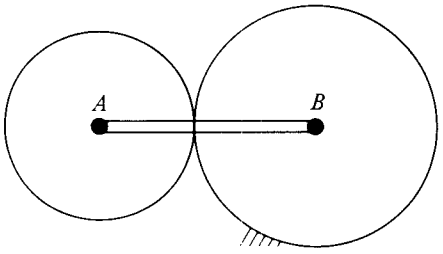

(c)

FIGURE 7.6 *Three inversions of the two-gear train:* (a) *arm grounded, as in Figure 7.2;* (b) *link 2 grounded;* (c) *link 3 grounded.*

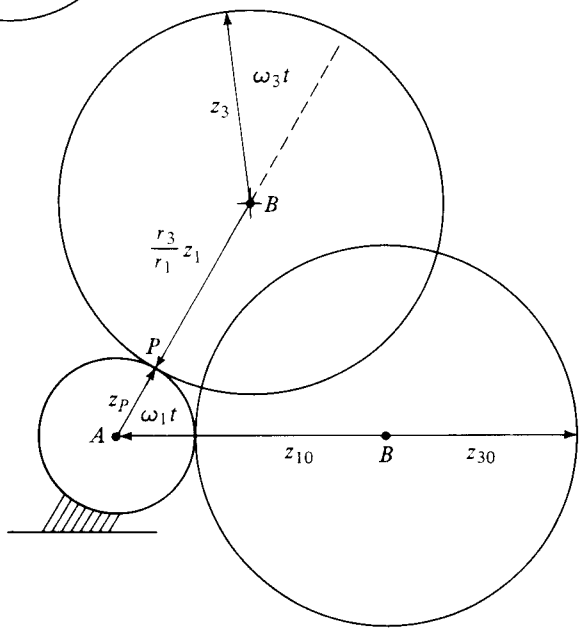

FIGURE 7.7 *Detailed picture of the second inversion, that shown in Figure 7.6b.*

Links 1 and 3 rotate in the same direction. The rotation of link 3 in the new frame is different from that in the old frame. [It may be helpful to compare this discussion with that in Erdman and Sandor (1984).]

The system shown in Figure 7.7 is the simplest example of a planetary gear train. The central gear 2 is called the sun gear, and gear 3 is the planet gear. More complex arrangements are, of course, possible. Several examples are given in Chironis's compendium of mechanisms (1965). Additional examples will be explored later but, first, it is interesting to look at one limiting case of the simple planetary system, the case for which r_1 (and r_2) tends to infinity and ω_1 tends to zero in such a way as to leave the product $\omega_1 r_1 = v_1$ constant.

Figure 7.8a shows the limiting case for a grounded link 2. The analysis given earlier is easily transformed. First, the absolute velocity of link 3 remains $-i\omega_1 z_1 + i\omega_3 z_3$ because the limiting process preserves the product $\omega_1 r_1 = v_1$. This must still vanish at $z_3 = -(r_3/r_1)z_1$, leading directly to Equation (7.11). This can be rewritten in a slightly different form to make clear the limiting process,

$$i(\omega_1 r_1 - r_3\omega_3)\exp(i\omega_1 t) = 0 \rightarrow v_1 = \omega_3 r_3 \tag{7.12}$$

so that the rotation rate of a wheel of radius r whose axle is translating at v is $\omega = v/r$. Conversely, if a wheel is turning at ω without slip, the translational velocity of its axle is ωr.

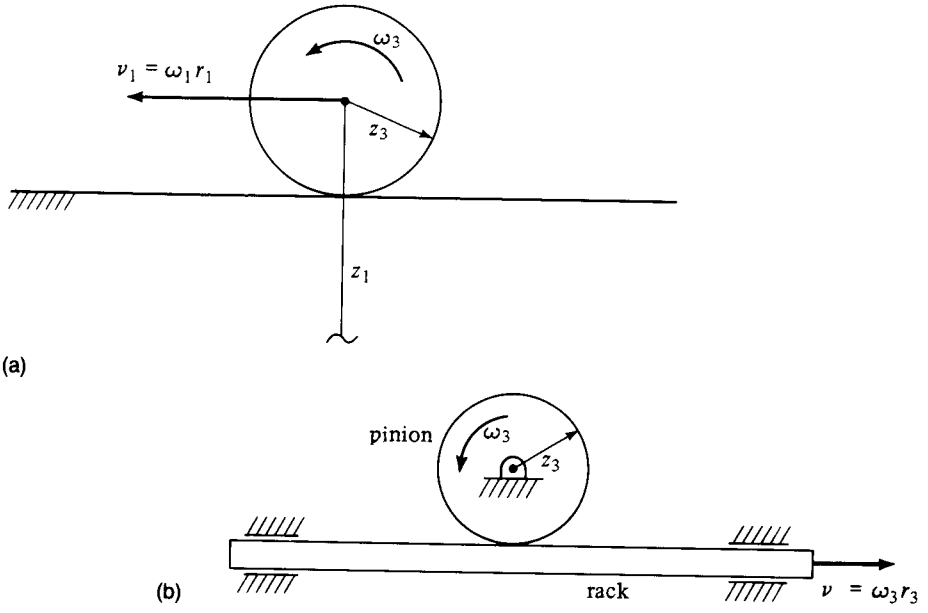

FIGURE 7.8 *Limiting cases of the two roller train:* (a) *the wheel rolling without slip;* (b) *the rack-and-pinion system.*

Fixing the axle of the small roller gives a rack-and-pinion arrangement. The small roller is the pinion, and the infinite roller is the rack. The rotation of the pinion is converted to linear motion of the rack. This is a commonly used automobile steering linkage. It is an inversion of the wheel rolling without slip. This can be made clear by a short argument illustrated by Figure 7.8b. Fixing the axle of the pinion is equivalent to grounding link 1. The speed of the rack is $\omega_3 r_3$, positive (to the right) when ω_3 is positive. The travel of the rack is obtained by integrating the expression for velocity. Thus, the rack travels $2\pi r_3$ for each full revolution of the pinion.

In a modern automobile, the number of turns of the pinion need not be the same as the number of turns of the steering wheel. There is a steering gear box, with or without power assist, between the steering wheel and the pinion. This is used to reconcile considerations of convenience to the driver with those relating to maneuverability of the vehicle and the strength of the pinion and rack.

The central feature of a planetary gear system is that the axle of at least one planet gear rotates around the sun gear. The sun gear itself may rotate. It was fixed in the example given, but requiring the rotation rate of the sun gear to be zero is just a special case of specifying that rotation rate. A general planetary gear train requires two inputs. One of them is frequently to fix one gear, sometimes the sun, sometimes the external *ring gear.*

Figure 7.9 shows a sketch of a three-gear planetary gear train. Links 1 and 4 (the ring gear) are coaxial, and link 2 (the sun gear) is fixed. As link 1 rotates, it carries

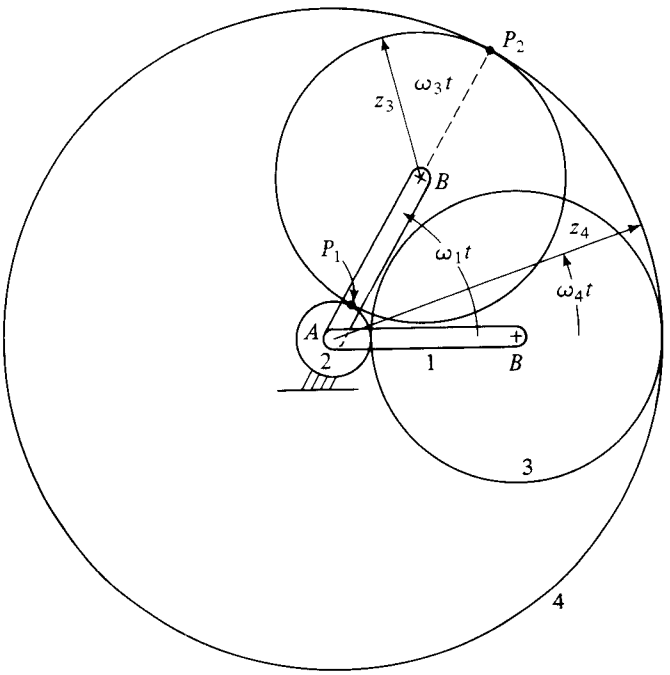

FIGURE 7.9 *A three-gear (four-link) planetary gear train with the sun gear (link 2) grounded.*

link 3 with it. Two positions are shown. The absolute motion of the four links in terms of their linkage variables and rotation rates are, for links 1–4, respectively, $i\omega_1 z_1$, 0, $i\omega_1 z_1 + i\omega_3 z_3$, and $i\omega_4 z_4$.

Figure 7.9 shows $\omega_1 > 0$. There are no-slip conditions at P_1 and P_2, and these points are defined by

$$P_1\colon z_3 = -\frac{r_3}{r_1} z_1, \qquad z_2 = \frac{r_2}{r_1} z_1$$

$$P_2\colon z_4 = \frac{r_4}{r_1} z_1, \qquad z_3 = \frac{r_3}{r_1} z_1$$

where z_1 has been taken to point from A to B. The rotation of the bar, link 1, will be taken to be ω_1. Application of the no-slip conditions leads to

$$i\omega_1 z_1 + i\omega_3 z_3 = i\left(\omega_1 - \frac{r_3}{r_1}\omega_3\right) z_1 = 0 \rightarrow \omega_1 = \frac{r_3}{r_1}\omega_3$$

$$i\omega_1 z_1 + i\omega_3 z_3 = i\left(\omega_1 + \frac{r_3}{r_1}\omega_3\right) z_1 = i\omega_4 z_4 = i\omega_4 \frac{r_4}{r_1} z_1 \tag{7.13}$$

$$\rightarrow \omega_1 + \frac{r_3}{r_1}\omega_3 = \frac{r_4}{r_1}\omega_4$$

EXAMPLE 7.2

Let $r_2 = 3$ in. and $r_3 = 6$ in. for the system shown in Figure 7.9. Geometry demands that $r_1 = 9$ in. and $r_4 = 15$ in. Let the arm, link 1, be driven at 3 rad/s. Substitution into the set (7.13) gives, in turn,

$$\omega_3 = \frac{9}{6}(3) = 4.5 \text{ rad/s}$$

$$\omega_4 = \frac{9}{15}\left(3 + \frac{6}{9}(4.5)\right) = 3.6 \text{ rad/s}$$

EXAMPLE 7.3

Consider an inversion of the simple planetary system shown in Figure 7.9. Ground the ring gear, link 4, and let the sun gear be free to rotate. Find the rotation rates of links 2 and 3 given the rotation rate of link 1.

First, list the absolute velocities of the four links: $i\omega_1 z_1$, $i\omega_2 z_2$, $i\omega_1 z_1 + i\omega_3 z_3$, and 0, for links 1–4, respectively. The two points at which the slip conditions must be applied are the same, and the equations necessary to solve for the rotations are

$$i\omega_1 z_1 + i\omega_3 z_3 = i\left(\omega_1 - \frac{r_3}{r_1}\omega_3\right)z_1 = i\omega_2 z_2 = \omega_2 \frac{r_2}{r_1} z_1 \rightarrow \omega_1 - \frac{r_3}{r_1}\omega_3 = \frac{r_2}{r_1}\omega_2$$

$$i\omega_1 z_1 + i\omega_3 z_3 = i\left(\omega_1 + \frac{r_3}{r_1}\omega_3\right)z_1 = 0 \rightarrow \omega_1 + \frac{r_3}{r_1}\omega_3 = 0 \tag{7.14}$$

Using the same numerical data as in Example 7.2 gives

$$\omega_3 = -\frac{9}{6}(3) = -4.5 \text{ rad/s}$$

$$\omega_2 = \frac{9}{3}\left(3 - \frac{6}{9}(-4.5)\right) = 18 \text{ rad/s}$$

Note that this arrangement reverses the direction of rotation of link 3.

EXAMPLE 7.4

Figure 7.10 shows a slightly more complicated planetary system. Links 1, 2, and 5 are coaxial. Link 5 is grounded. Links 3 and 4 are pinned to link 1. The rotation of link 1 drags links 3 and 4 with it. The problem is to find the relations among the rotation rates. As above, begin by listing the absolute velocity of each link: $i\omega_1 z_1$, $i\omega_2 z_2$, $i\omega_1[(r_3 + r_2)/r_1]z_1 + i\omega_3 z_3$, $i\omega_1 z_1 + i\omega_4 z_4$, and 0 for links 1–5, respectively.

There are three contact points, defined by

$$P_1\colon z_3 = -\frac{r_3}{r_1}z_1, \qquad z_2 = \frac{r_2}{r_1}z_1$$

$$P_2\colon z_4 = -\frac{r_4}{r_1}z_1, \qquad z_3 = \frac{r_3}{r_1}z_1$$

$$P_3\colon z_4 = \frac{r_4}{r_1}z_1, \qquad z_5 = \frac{r_5}{r_1}z_1$$

At P_1, links 2 and 3 must corotate. Equating the absolute velocities of the two links, substituting for z_2 and z_3 to locate the point P_1 and, finally, simplifying give one equation relating to ω_1, ω_2, and ω_3. The sequence of operations is

$$i\omega_2 z_2 = i\omega_1 \frac{r_3 + r_2}{r_1} z_1 + i\omega_3 z_3$$

$$i\omega_2 \frac{r_2}{r_1} z_1 = i\omega_1 \frac{r_3 + r_2}{r_1} z_1 - i\omega_3 \frac{r_3}{r_1} z_1 \tag{7.15}$$

$$\omega_2 \frac{r_2}{r_1} + \omega_3 \frac{r_3}{r_1} = \omega_1 \frac{r_3 + r_2}{r_1}$$

I leave it to the reader to follow the same procedures and show that the other two equations relating to rotation rates are

$$\omega_3 \frac{r_3}{r_1} + \omega_4 \frac{r_4}{r_1} = \omega_1 \frac{r_3 + r_4}{r_1}$$
$$\omega_4 \frac{r_4}{r_1} = -\omega_1 \tag{7.16}$$

If the system is driven by the sun gear rotating at 4 rpm (0.419 rad/s) and the link lengths are 11, 2, 4, 1, and 12 cm, respectively, the other rotation rates can be found by solving the set of algebraic equations

$$\begin{Bmatrix} 6 & -4 & 0 \\ 5 & -4 & -1 \\ 11 & 0 & +1 \end{Bmatrix} \begin{pmatrix} \omega_1 \\ \omega_3 \\ \omega_4 \end{pmatrix} = \begin{pmatrix} 2\omega_2 \\ 0 \\ 0 \end{pmatrix} \tag{7.17}$$

The reader can easily verify that the final result is: $\omega_1 = 0.667$ rpm, $\omega_3 = -1.000$ rpm, and $\omega_4 = 7.333$ rpm.

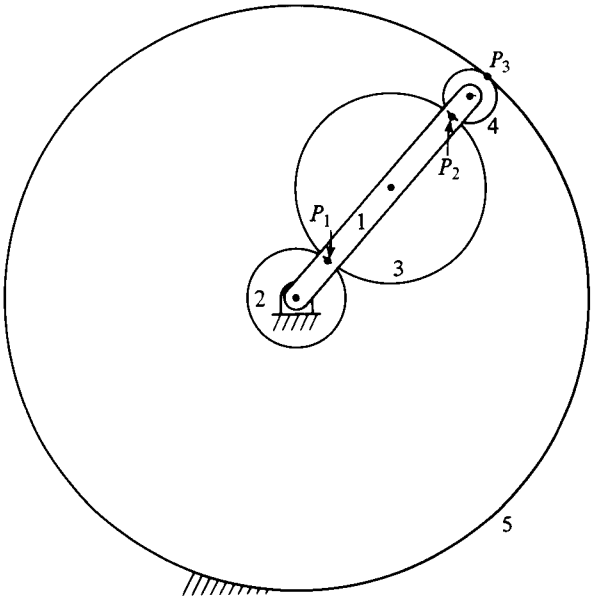

FIGURE 7.10 *A four-gear (five-link) planetary gear train with the outer-ring gear grounded.*

CAMS

Strictly speaking, one should talk of *cam pairs,* a pair consisting of an *eccentric* and a *follower.* In common usage, and in this book, the eccentric is called the *cam.* As with other kinematic elements, cam pairs also include mechanisms that produce three-dimensional motion. This introduction to the analysis of cam pairs will be restricted to what are called *disk cams*, rotating eccentrics that cause motion of a follower. These are the kind of cams that are used in modern overhead-cam internal combustion engines. An eccentric disk cam attached to the cam shaft drives the motion of each valve stem, opening and closing the intake and exhaust valves. A double overhead-cam system will have two cam shafts, one to operate intake valves and the other to operate exhaust valves.

The systematic analysis of cam pairs is of fairly recent origin. Reuleaux barely mentions cams, and those he does are not the ones the modern engineer would think of first.

Figure 7.11 shows a cam pair with a translating offset roller follower. It introduces some standard cam nomenclature and some notation to be used later. A *translating* follower means that the follower moves in a straight line, restrained by a guide. A pivoting follower is called an *oscillating follower.* The line of motion of the *offset* follower does not pass through the rotation axis of the cam; that of a *centered* follower does. The *trace point* is a fixed point on the follower, the motion of which is to be

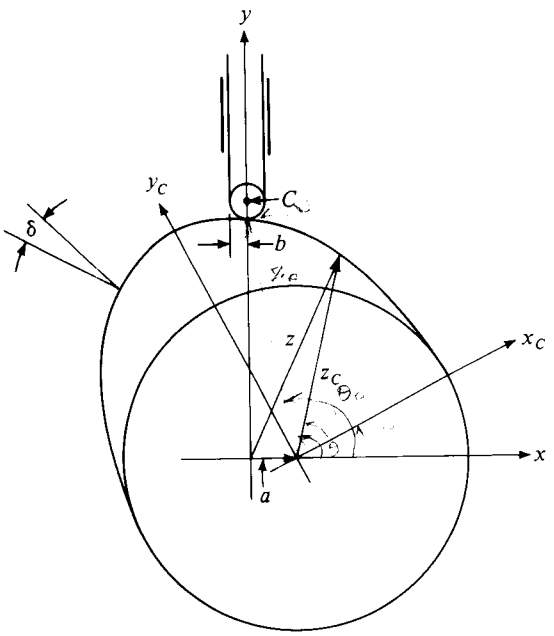

FIGURE 7.11 *Definition sketch for a translating roller follower cam pair.*

found in an analysis problem and specified in a synthesis problem. For a roller follower, the rotation axis C of the roller is appropriate. The projection of the shape of the cam onto the plane, the curves plotted in Figures 7.14, 7.16, and 7.18–7.20, is called the *cam profile.* The *pressure angle* δ is the angle between the normal to the cam profile and the line drawn through the cam axis.

The cam shown in Figure 7.11 has as a section of its profile a segment of a circle centered on the rotation axis. When that section is under the follower, it will not move; that is, it *dwells.* For the cam shown, the output dwells over more than half the rotation period of the cam. This cam is very nearly a circle with a single *lobe,* one region where the cam profile projects beyond the *minimum circle.* The latter is the largest circle centered on the rotation axis that can be drawn inside the cam profile.

Two coordinate systems (at least) are required to describe the behavior of a cam pair. One is attached to the rotating cam (the cam), and the other is fixed in space. Some authors (e.g., Chakraborty and Dhande 1977) introduce a third system attached to the follower, but that will not be necessary in this text. I show the two systems in Figure 7.11: the cam-fixed system (x_C, y_C) and the space-fixed system (x,y). The cam-fixed system has its origin at the rotation axis of the cam. The cam shown is symmetric, and I have taken the y_C axis to pass through the "highest" point on the lobe. The cylindrical coordinate system fixed in the cam frame is (ρ,ϕ), so that the cam profile is defined by $\rho = \rho(\phi)$, where the angle ϕ is measured counterclockwise from the x_C axis. The complex material vector from this axis to any point on the cam is given by

$$z_C = \rho(\phi) \exp(i\phi) \tag{7.18}$$

in the cam frame of reference.

The two systems have the same orientation at $t = 0$. During rotation of the cam, the angle between the x_C and x axes is ωt. The vector z, representing the location of a point on the cam profile with respect to the space-fixed system is, by inspection (use the parallelogram rule for adding vectors),

$$z = a + z_C = a + \rho(\theta - \omega t) \exp(i\theta) \tag{7.19}$$

where I have evaluated z_C at an arbitrary point in the space-fixed system, designated by the space-fixed angle θ. In particular, the vector to the contact point P can be written in the two systems as

$$\begin{aligned} z_{CP} &= \rho(\theta_P - \omega t) \exp(i\theta_P - \omega t) \\ z_P &= a + \rho(\theta_P - \omega t) \exp(i\theta_P) \end{aligned} \tag{7.20}$$

Note that the contact point is not necessarily on the line of motion. This is a key difficulty of cam analysis and synthesis. The angle θ, hence ϕ and $\rho(\phi)$, are all unknown. As the radius of the roller decreases, the contact point approaches the line of motion. The limit is the knife-edge follower. Such a follower is not practical, primarily because wear would quickly dull the knifelike edge. It is convenient for analysis, however, and, in many systems, the approximation introduced by assuming a knife-edge follower is a good one.

Methods of analysis, for finding θ, ϕ, and ρ as functions of time include the work of Raven (1959), who reduced general cam-pair *syntheses* to exercises in complex-variable arithmetic. An alternative vector approach is given in Chapter 2 of Chakraborty and Dhande's monograph (1977), which is an excellent treatise on the kinematics of cams. It covers many applications beyond the scope of this text, including three-dimensional cam pairs. A third method of analysis, more in keeping with the techniques used elsewhere in this book, will be introduced subsequently.

The Translating Roller Follower

The illustrations so far have shown translating roller followers. I will begin with a discussion of these and then look at oscillating followers. Translating flat followers can be analyzed using the methods explored for roller followers. This is relegated to the Exercise section.

Before examining the general case, it is instructive to look at the simplest case: that for which there is no offset and for which the roller radius is small enough to be approximated as a knife-edge follower. Such a situation is illustrated in Figure 7.12. In this case, $\theta = \pi/2$, so that $\phi = \pi/2 - \omega t$. As drawn, $\omega t < 0$. The vector to point P is given in the space-fixed system as

$$z_P = \rho(\pi/2 - \omega t) \exp(i\pi/2) = i\rho(\pi/2 - \omega t) \tag{7.21}$$

and the position of the trace point, the axis of the roller, is given by $x = 0$ and

$$y = h = r_3 + \rho(\pi/2 - \omega t) \tag{7.22}$$

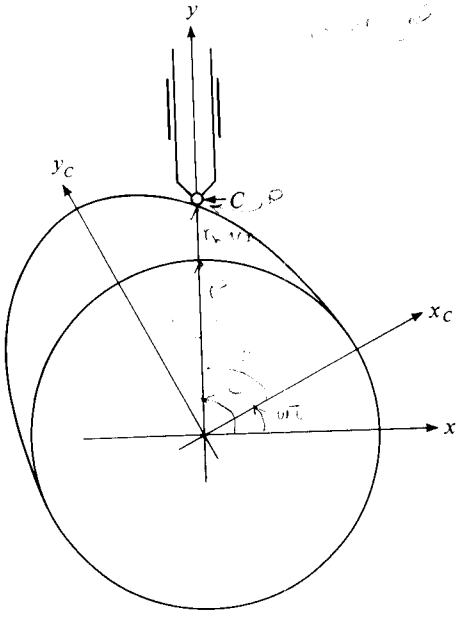

FIGURE 7.12 *The centered translating roller follower with vanishingly small* r_3.

The velocity and acceleration of the follower are then given by direct differentiation of Equation (7.22):

$$\begin{aligned} v_C &= \dot{h} = -\omega\rho'(\pi/2 - \omega t) \\ a_C &= \ddot{h} = \omega^2\rho''(\pi/2 - \omega t) \end{aligned} \tag{7.23}$$

where the dot denotes differentiation with respect to time and the prime differentiation with respect to argument.

General position analysis for both r_3 and a nonzero can be addressed using complex variables and the loop-closure equation. This leads to a complex transcendental equation for the position of the contact point. This equation can be solved using any of the numerical methods of successive approximation. I will give a program using the Newton–Raphson technique introduced in Chapter 5.

Figure 7.13 is a schematic redrawing of Figure 7.11, with complex vectors needed to find a loop-closure equation given. For any fixed moment in time, the loop-closure equation is

$$a + \rho(\phi)e^{i\theta} - r_3 e^{i\theta_3} - ih = 0 \tag{7.24}$$

The two angles θ and θ_3 are connected by the cam profile. The radius vector of a circle tangent to any curve is perpendicular to the curve at the point of tangency. The radius vector, here z_3, is (anti)parallel to the (outward) normal. The normal vector to any point on the cam profile can be calculated directly from the equation of the cam profile,

$$f = \rho - \rho(\phi) = 0 \tag{7.25}$$

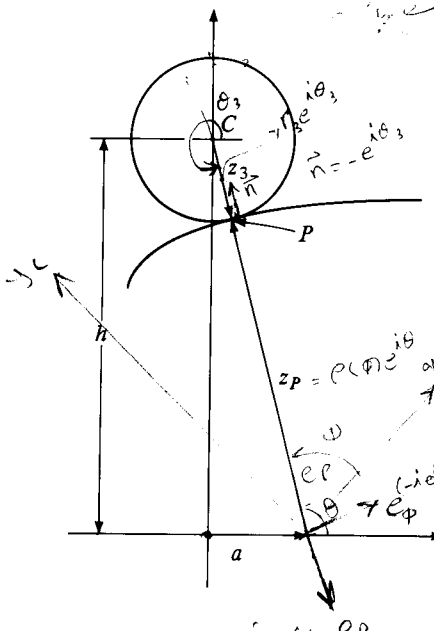

FIGURE 7.13 *A set of vectors appropriate for analyzing the offset translating roller follower cam pair.*

The gradient of the profile is normal to the profile. Dividing by the magnitude of the gradient gives the unit normal

$$\hat{\mathbf{n}} = \frac{\mathbf{e}_\rho}{\sqrt{1 + \rho'^2}} - \frac{\rho' \mathbf{e}_\phi}{\sqrt{1 + \rho'^2}} = -e^{i\theta_3} = n$$

$$n = e^{i\theta_n} = \frac{i\rho' - 1}{\sqrt{1 + \rho'^2}} e^{i\theta} \tag{7.26}$$

Recall that the complex representations of the two unit vectors are $e^{i\theta}$ and $ie^{i\theta}$, respectively. These have been used to write the complex unit normal $\hat{\mathbf{n}}$. The loop-closure equation can then be written in terms of the two unknowns θ and h as

$$a + \left(\rho + r_3 \frac{i\rho' - 1}{\sqrt{1 + \rho'^2}}\right) e^{i\theta} - ih = 0 \tag{7.27}$$

where the radius vector ρ and its derivative are to be evaluated at $\phi = \theta - \omega t$. Taking the real part of this equation eliminates h and leaves a single transcendental equation for θ:

$$(a + \rho \cos\theta)\sqrt{1 + \rho'^2} + r_3(\cos\theta - \rho' \sin\theta) = F(\theta) = 0 \tag{7.28}$$

where, again, the radius and its derivative are to be evaluated at $\theta - \omega t$.

This equation can be solved approximately by assuming that

$$\begin{aligned} \rho(\phi) &= r_b + \delta(\phi) \\ \theta &= \theta_0 + \delta\theta \end{aligned} \tag{7.29}$$

where $\cos\theta_0 = -a/r_b$, r_b denotes the radius of the minimum circle (any other "typical" radius of the cam can be used), and r_3, as before, denotes the radius of the roller. Substitution of this approximation into Equation (7.28) and linearizing will produce an equation for $\delta\theta$ in terms of $\delta(\phi)$.

$$\delta\theta = \frac{r_3}{r_p}\frac{d\delta}{d\phi} + \frac{a\delta}{r_p^2}\csc\theta_0 \tag{7.30}$$

Alternatively, Equation (7.28) can also be solved numerically using the Newton–Raphson techniques introduced in Chapter 5. This method is productive and relatively fast and robust. The following program works this for cams for which an analytic expression for the cam profile can be written. Profiles of the form

$$\rho(\phi) = r_b + r_h g(\phi) \tag{7.31}$$

where r_b denotes the minimum radius of the cam, r_h the maximum height from the minimum radius, and $g(\phi)$ a periodic function of maximum amplitude unity, are implicitly used in the program. Other two-parameter families are possible, of course. One will appear in the Exercise section at the end of the chapter.

PROGRAM 7.1: CAM ANALYSIS

```
function rho  (r_b, r_h, φ)
function rho1  (r_b, r_h, φ)
function rho2  (r_b, r_h, φ)

function F  (θ, a, ωt)
        φ = θ − ωt
        Δ = sqrt(rho(φ)*rho(φ) + rho1(φ)*rho1(φ))
        x1 = a + rho1(φ)*cos(θ)
        x2 = r3*(rho(φ)*cos(θ) − rho1(φ)*sin(θ))
        F = x1*Δ + x2
        end

function F1  (θ, a, ωt)
        φ = θ − ωt
        Δ = sqrt(rho(φ)*rho(φ) + rho1(φ)*rho1(φ))
        x1 =rho1(φ)*cos(θ) − rho(φ)*sin(θ)
        x2 = (a + rho1(φ)*cos(θ))*(rho1(φ) + rho2(φ))
        x3 = r3*(−rho(φ)*sin(θ) + rho2(φ)*sin(θ) + 2rho1(φ)*cos(θ))
        F1 = x1*Δ + x2/Δ + x3
        end

enter   (a, r_b, r_h, w, t_0, dt, nt)
for j = 0 to nt do
        t = t_0 + j*dt
        dθ = 1
        θ = cos^-1(−a/(r_b + r_3))
        while |dθ| > limit do
                dθ = −F(θ)/F1(θ)
                θ = θ + dθ
                repeat the loop
```

repeat the loop

write results

end

To use Program 7.1, the user must supply the three functions **rho**, **rho1**, and **rho2**. These are each two parameter (r_b, r_h) analytic expressions, respectively, for the radius as a function of the angle ϕ and its first two derivatives with respect to ϕ. The functions **F** and **F1** represent Equation (7.28) and its derivative with respect to θ. The initial guess for θ is the correct value when $\rho = r_b$.

Behavior of a One-Lobe Cam

To explore the behavior of cams, consider the behavior of a simple one-lobe cam, for which the cam profile can be written

$$\rho(\phi) = r_b + r_h \sin^4 \phi \tag{7.32}$$

The two parameters r_b and r_h are in themselves not important. Their ratio and, indeed, the ratios of r_3 and a to r_b are the important geometric parameters. If two cams are geometrically similar, their kinematic behavior will be the same. I will choose 10 as an arbitrary magnitude of r_b and will scale all the other geometric parameters as 10 times the relevant ratio. The figures in this section are all based on the same scaling. Where minimum circles are shown, their diameters are 20 in the dimensionless system appropriate for understanding kinematic relationships.

Figure 7.14a shows such a one-lobed cam (rotated 90° to the right so that it will fit better on the page) and the behavior of the trace point as a function of time during one rotation, assuming a translating roller follower of radius 2 and zero offset. The circle in the figure is the minimum circle, of radius 10. The maximum height of the lobe is 5; that is, $r_h = 5$. As is easily seen, the output dwells over half the cam cycle.

Figure 7.15 shows the cam, set vertically, with follower rollers of $r_3 = 1, 2, 5,$ and 10. Figure 7.16 shows the output curves for the new cases, $r_3 = 1, 5,$ and 10, reading from the top to the bottom. There is very little difference in the nondwelling part of the response. The absolute value of the height increases with the size of r_3.

Figure 7.17 shows a set of rollers, all of radius 2, at offsets $a = 0, 2, 5,$ and 10. Figure 7.18 shows the output curves for the nonzero offset cases. A nonzero offset leads to asymmetric follower output, increasing with the size of the offset. The differential lift also increases with offset. Although forces on the cam and follower are not discussed in this book, it is worth noting that the force between the cam and its follower acts, in the absence of significant friction, along the perpendicular. This means that for followers with extreme offset, such as the system shown with $a = 10$, the force on the follower is often nearly perpendicular to the line of motion of the cam. This is bad design, putting a large force on the cam and on the follower guides.

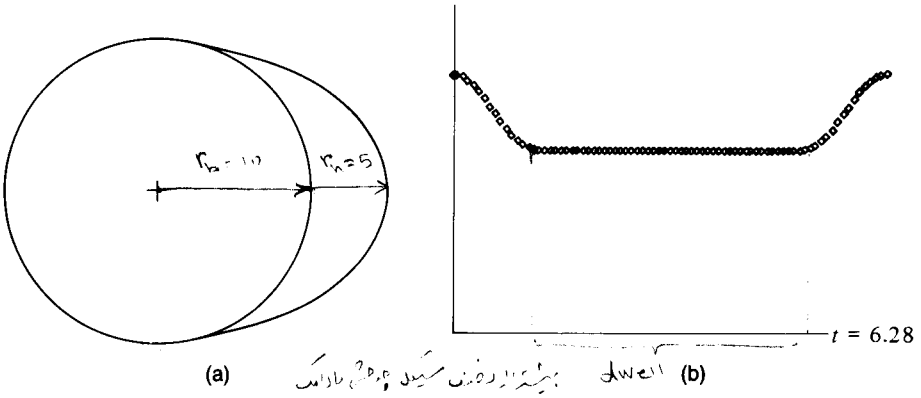

FIGURE 7.14 *The one-lobe cam pair:* (a) *the eccentric, rotated 90° from its zero position;* (b) *trace point height as a function of cam angle for one rotation.*

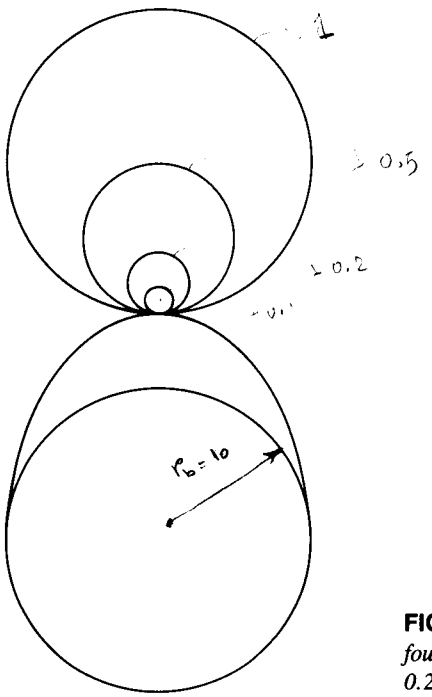

FIGURE 7.15 *The one-lobe cam with four centered follower rollers:* r_3/r_b = *0.1, 0.2, 0.5, and 1.0.*

A Four-Lobe Cam

Cams with more than one lobe are also possible. Until recently, most automobiles had distributors. The central element of a distributor is a cam with as many lobes as the car has cylinders. When the lobe is under the follower, the electrical connection between the coil and the spark plugs is broken, and the coil can "charge." When the

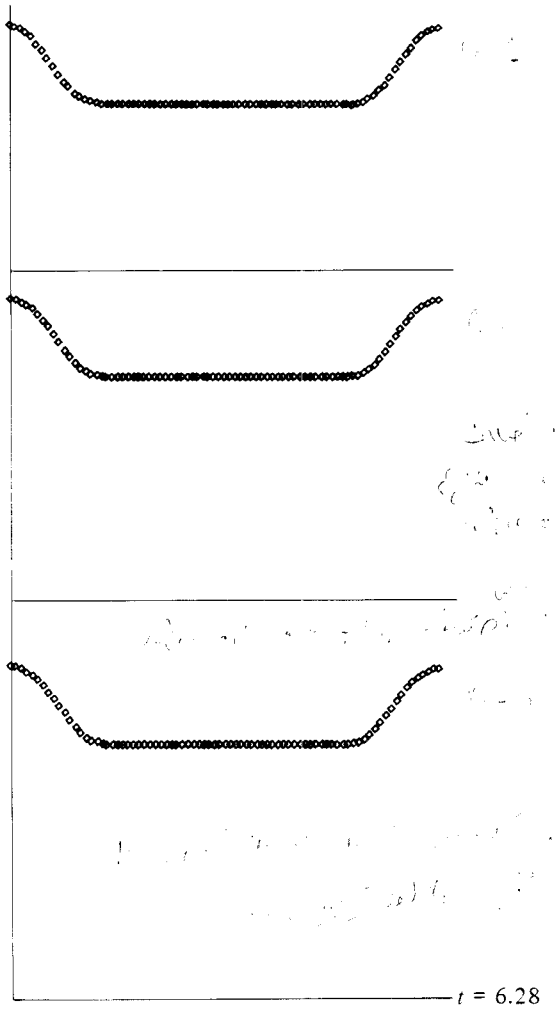

FIGURE 7.16 *Trace point height of the roller follower for* r_3/r_b = *0.1, 0.5, and 1.0, reading from top to bottom.*

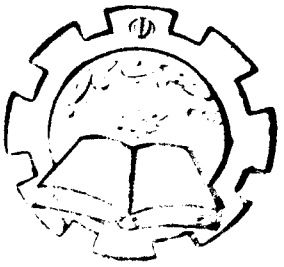

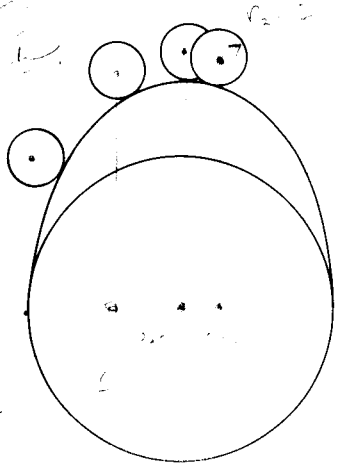

FIGURE 7.17 *The one-lobe cam with four follower rollers:* r_3/r_b = *0.2 and* a/r_b = *0, 0.2, 0.5, and 1.0.*

follower is between lobes, the connection is made, and current is sent to the appropriate cylinder. Figure 7.19a shows a four-lobe cam, a simple model of the cam in the distributor of a four-cylinder automobile. The equation used to generate this cam is

$$\rho(\phi) = r_b + r_h \cos^2(2\phi) \tag{7.33}$$

with $r_b = 10$ and $r_h = 1$. Figure 7.19b shows the response of the follower point to this cam. (In an automobile distributor, the follower is an oscillating follower, to be discussed later. The illustrative difference is not important.) The output for an automobile distributor is a little different in that inward travel of the follower is restricted and the "valleys" are flat-bottomed. Figure 7.20 shows the cam and its response when r_h is increased to 5.

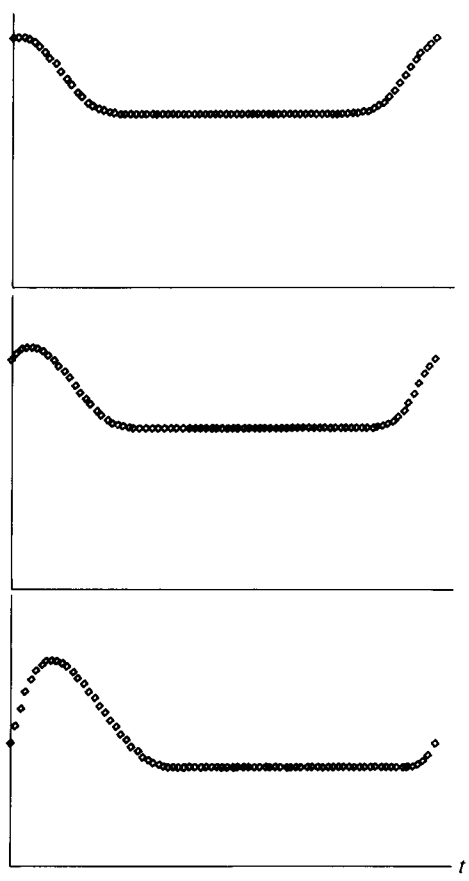

FIGURE 7.18 *Trace point height of the roller follower for* $r_3/r_b = 0.2$ *and* $a/r_b = 0.2, 0.5,$ *and* 1.0.

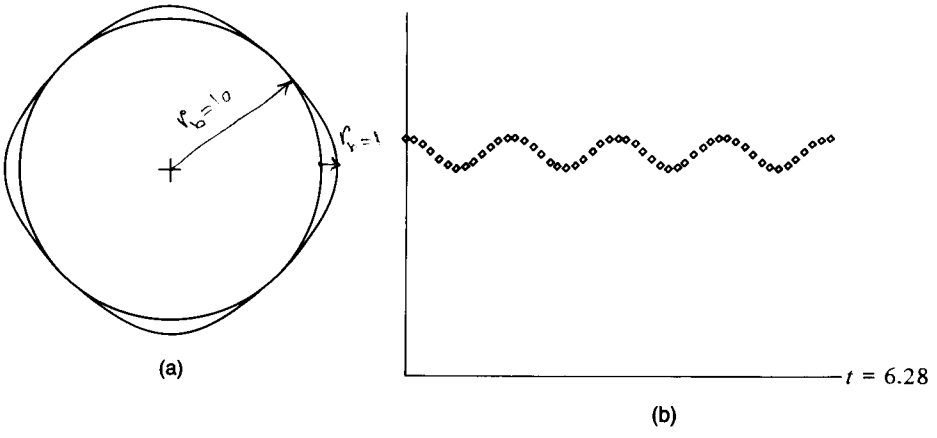

FIGURE 7.19 *A four-lobe cam and the trace point motion for one rotation of the eccentric:* $r_h/r_b = 0.1$.

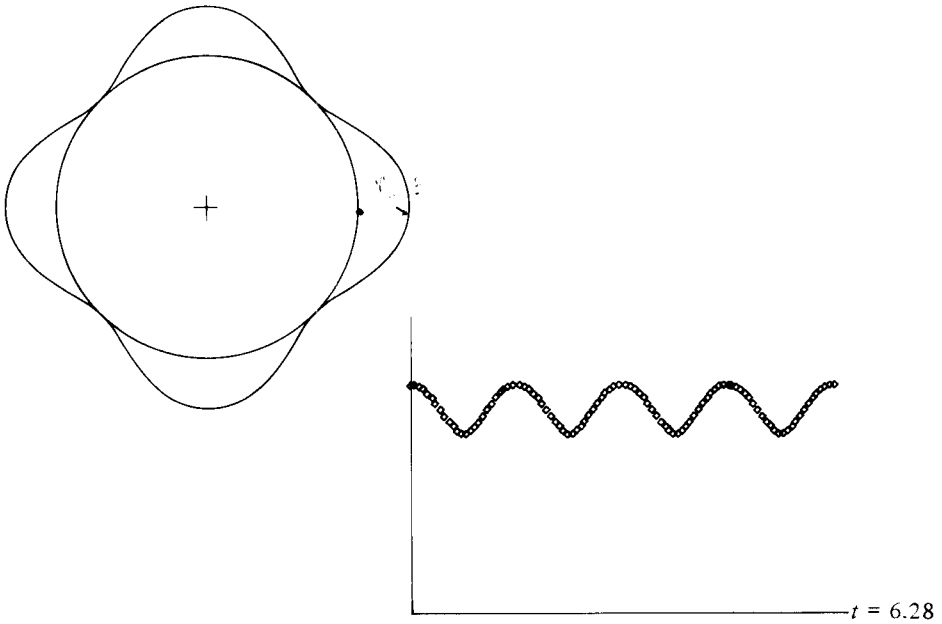

FIGURE 7.20 *A four-lobe cam and the trace point motion for one rotation of the eccentric:* $r_h/r_b = 0.5$.

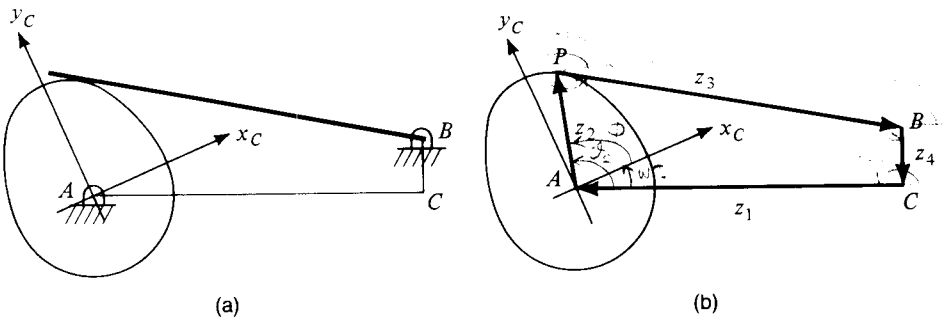

FIGURE 7.21 *A one-lobe cam with an oscillating flat follower:* (a) *a sketch of the cam pair;* (b) *a set of link variables.*

The Oscillating Follower

Figure 7.21a shows a *flat* oscillating follower, and Figure 7.21b a set of loop-closure variables. Geometry requires that the flat follower be perpendicular to the cam profile at the contact point, so that the loop-closure equation, deliberately written to resemble the four-bar-linkage loop-closure equations examined in earlier chapters, can be manipulated using the complex unit normal n which, the reader will recall, is a function

of θ_2. The two loop-closure variables z_1 and z_4 are fixed and known, z_2 is the same as the variable z_P introduced in the preceding section, and z_3 represents the pivoting follower. Its length changes, as does the length of z_2. Note, however, that the changes in length and orientation of z_2 and z_3 are related.

The loop-closure equation is

$$\begin{aligned} z_1 + z_2 + z_3 + z_4 &= 0 \\ z_1 + z_2 + r_3 n + z_4 &= 0 \end{aligned} \tag{7.34}$$

The two unknowns in Equation (7.34) are θ_2 and r_3. The latter can be eliminated by multiplying Equation (7.34) by n^*, the complex conjugate of the unit normal. The imaginary part of the resulting equation will not involve r_3 and can be solved for θ_2 using numerical techniques. The equation and its imaginary part are

$$\begin{aligned} -r_1 e^{-i\theta_n} + r_2(\theta_2 - \omega_2 t)e^{i(\theta_2 - \theta_n)} + r_3^2 + ir_4 e^{-i\theta_n} &= 0 \\ r_1 \sin\theta_n + r_2(\theta_2 - \omega_2 t)\sin(\theta_2 - \theta_n) - r_4 \cos\theta_n &= 0 = F(\theta_2) \end{aligned} \tag{7.35}$$

The function $F(\theta_2)$ and its first derivative can be inserted into Program 7.1, and the resulting code can be used to find the behavior of the flat oscillating follower cam. This is left as an exercise for the reader.

The power of the complex-variable methods becomes apparent as the system to be analyzed becomes more complex. Figure 7.22a shows an oscillating roller follower, and Figure 7.22b is a schematic sketch designed to make the individual vectors in the loop-closure equation distinct. In this diagram, z_2 and z_3 correspond to the cam and roller vectors, z_4 and $q_4 z_4$ are two vectors fixed in the follower, and these have a constant ratio q_4, as shown. Finally, z_1 and z_5 are fixed in the frame, z_5 corresponding to z_4 in Figure 7.21b.

As in the translating roller follower, z_3 must be parallel to the normal n. This can be used to write the loop-closure equation

$$z_1 + z_2 + r_3 n + q_4 z_4 + z_4 + z_5 = 0 \tag{7.36}$$

where z_1, z_5, and q_4 are known fixed complex numbers. The complex number n is a function of θ_2, so that this complex equation contains the two unknowns θ_2 and θ_4. The difficulty is separating the two unknowns so that some function $F(\theta_2)$ can be written. To do this, write the loop-closure equation with all terms containing θ_4 on the right-hand side,

$$z_1 + z_2 + r_3 n + z_5 = (q_4 + 1)z_4$$

and multiply both sides by its complex conjugate:

$$\begin{aligned} r_1^2 + r_2^2 + r_3^2 + r_5^2 - r_1 z_2^* - r_1 z_2 - ir_5 z_2^* + ir_5 z_2 \\ -r_1 r_3 n - r_1 r_3 n^* - z_2^* r_3 n - z_2 r_3 n^* + ir_5 r_3 n - ir_5 r_3 n^* = (q_4 q_4^* + 1)r_4^2 \end{aligned}$$

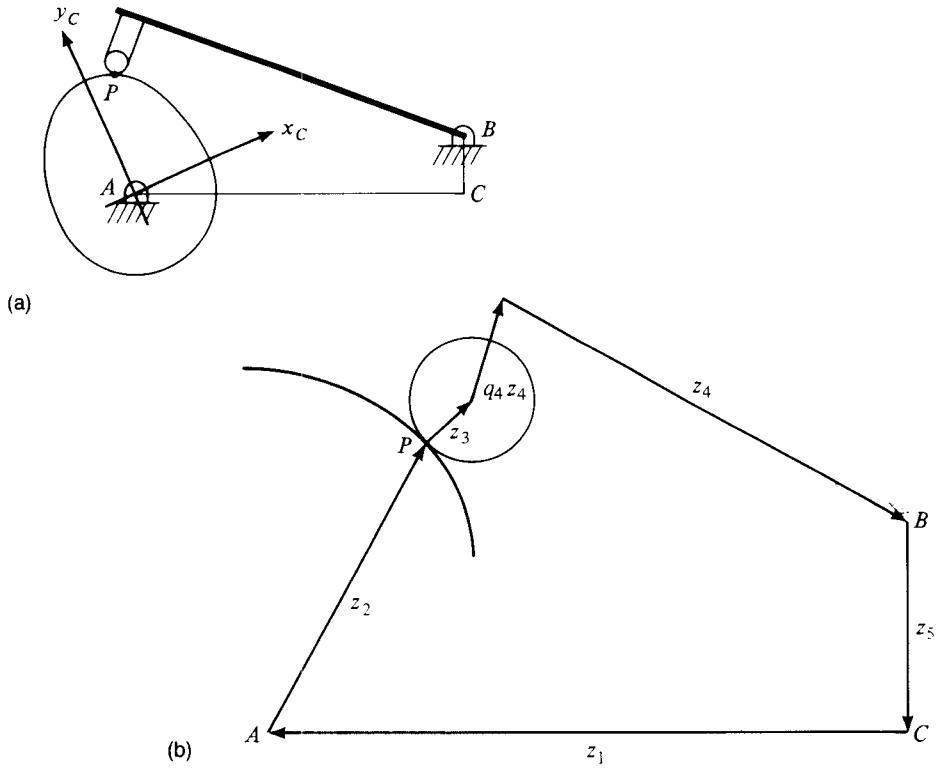

FIGURE 7.22 *A one-lobe cam with an oscillating roller follower:* (a) *a sketch of the cam pair;* (b) *a set of link variables.*

This equation is a function of θ_2 only, so that the function to be set equal to zero is

$$-r_1 z_2^* - r_1 z_2 - i r_5 z_2^* + i r_5 z_2 - r_1 r_3 n - r_1 r_3 n^*$$
$$-z_2^* r_3 n - z_2 r_3 n^* + i r_5 r_3 n - i r_5 r_3 n^* + r_1^2 + r_2^2 + r_3^2 + r_5^2 - (q_4 q_4^* + 1) r_4^2$$
$$= 0 = F(\theta_2) \tag{7.37}$$

EXERCISES

1. Consider the gear train shown in Figure 7.4:
   a. Derive Equation (7.7).
   b. If $\omega_2 = 18$ rad/s, find ω_3, assuming $r_2 = 10$ mm and $r_3 = 40$ mm.
2. Consider the system shown in Figure 7.6. Specify the rotation rate of links 1 and 2. (This is equivalent to grounding one of these links and specifying the rotation

rate of the other.) Write the velocity of point P and the velocities of links 2 and 3 with respect to P. Show that the sum of the relative velocity of each gear with the velocity of P gives the absolute velocity of the gear.

3. Applying the rules of Equation (7.3), show that the material motion of link 2 in Figure 7.6b is zero, as claimed in the text.

4. In Figure 7.6c, assume $r_2 = 100$ mm and $r_3 = 300$ mm. Find ω_2 if $\omega_1 = -15$ rad/s.

5. Take the system analyzed in Example 7.4, and repeat the analysis with link 1 grounded instead of link 5. Assume the system to be driven through the sun gear, link 2, as in the example.

6. Consider the four-link gear train shown here. Suppose the arm to rotate at 6 rad/s, and find the rotation rate of the two outside gears, assuming that $r_2 = 10$ mm, $r_3 = 35$ mm, and $r_4 = 25$ mm.

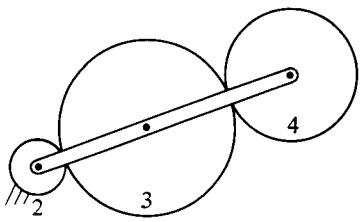

7. In the system drawn here, ground link 3, and let the arm rotate at -7 rad/s. Find the rotation rates of the remaining gears.

8. Let the arm be grounded in the illustration, and assume link 2 to rotate at 45 rpm. Find the remaining rotation rates.

9. Discuss the changes necessary to analyze a flat translating follower. Consider both the cases of an infinitely wide follower and a follower of finite width.

10. Write the pseudocode required to create the functions **F** and **F1** necessary to convert Program 7.1 to a program capable of analyzing a flat oscillating follower based on Equation (7.35).

11. Repeat Exercise 10 for the function given in Equation (7.37).

12. Implement Program 7.1, and use it to evaluate a six-lobe cam.

PART IV

Kinematics II: Synthesis

Chapter 8

Dimensional Synthesis of Four-Link Mechanisms

Mechanism synthesis is classified according to the output motion desired. If the output motion is to be a specified function of the input motion, the task is called *function generation.* If the output motion requires a point on the mechanism to trace a particular path, the task is called *path generation.* Finally, if a finite object is required to execute a specified motion, the task is called *motion generation.*

For each of these synthesis tasks—for any synthesis task—there are two stages in the synthesis: type synthesis and dimensional synthesis. *Type synthesis* is the choice of type of mechanism, including the number of elements. The choice of the number of elements is sometimes considered separately as *number synthesis.* General type synthesis is beyond the scope of this text. A recent thorough review of the subject has been given by Olson et al. (1985).

Dimensional synthesis is the task of choosing the dimensions of the elements, once a specific linkage type has been chosen. This task, at least for simpler linkages, can be reduced to an analytic procedure, hence to a computerizable algorithm. A word of warning: It will be shown that synthesis is an approximate task. The linkage synthesized will satisfy specified conditions at isolated positions. There is no guarantee that the linkage can move continuously between the design points without disassembly.

Sets of algorithms and generalized computer programs will be constructed below. First, it is useful to examine some simple cases, which can be done "by inspection." Begin by considering the classical problem of changing simple rotation into reciprocal motion, for example, asking that a point on a mechanism oscillate between two points in space separated by 100 mm. Figure 8.1 shows three possible types of mechanisms that can perform this task: in-line slider crank, offset slider crank, and crank rocker. The last is included for completeness. The motion is not straight-line motion, and usually reciprocal motion is taken to imply straight-line motion. [The production of unguided straight-line motion has long been taken as a challenge by kinematicians. Watt said of his straight-line mechanism, ". . . I am more proud of the paralel [*sic*] motion than any mechanical invention I have ever made." (Tann 1981, p. 61). Many of Chebyshev's efforts were directed toward straight-line motion (Chebyshev 1861, 1882).] A more recent summary of straight-line mechanisms has been given by Tesar and Vidosic (1965).

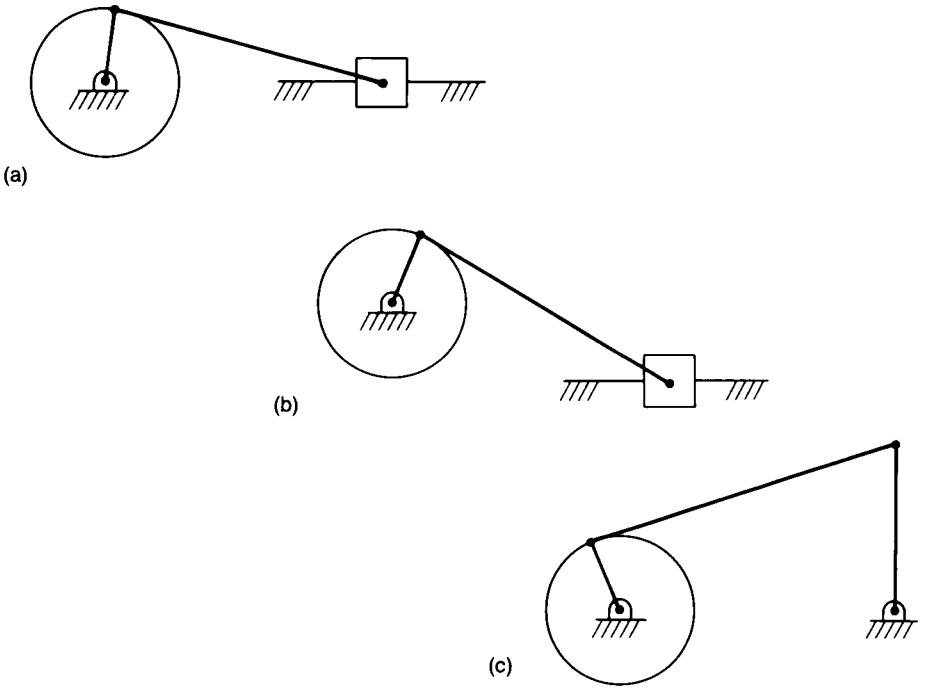

FIGURE 8.1 *Three mechanisms to produce one-dimensional displacement:* (a) *an in-line slider crank;* (b) *an offset slider crank;* (c) *a crank rocker.*

All three linkages are shown with the output link at midrange. The observant reader will note that the crank angle is different for each system. This is an example of timing, which will be discussed in context following further discussion of synthesis.

For the first case, it is clear that the length of the crank must be 50 mm, so that the difference between the extreme positions will correspond to the desired displacement of 100 mm. The coupler is only required to be longer than the crank. The coupler length determines the separation between the two ground points, or vice versa.

For the offset slider crank, the crank and the coupler lengths can be found by considering the linkage at its two extreme positions. If the vertical offset is H and the horizontal offset L, then the Pythagorean theorem applied in the extreme positions gives the sum and difference of the crank and coupler lengths as a function of the location of the origin of the crank:

$$\begin{aligned}(r_2 + r_3)^2 &= (L + d)^2 + H^2 \\ (r_2 - r_3)^2 &= (L - d)^2 + H^2 \end{aligned} \tag{8.1}$$

where the symbols are as defined in the figure. Here $d = 50$ mm, the half-stroke. One is free to choose any coupler longer than the crank.

Exactly the same analysis applies to the crank-rocker mechanism of Figure 8.1c. The equations are (8.1) with $L = 0$.

For the example given, with the stroke required to be 100 mm, the crank and coupler lengths in the three cases as drawn are

$$r_2 = 50, \qquad r_3 = 183.3$$

$$r_2 = 48.2, \qquad r_3 = 190.5$$

$$r_2 = 43.5, \qquad r_3 = 210.3$$

The stroke is always greater than, or equal to, twice the crank length.

Figure 8.2 shows the two extreme positions of an offset slider-crank mechanism. The crank rotation is positive (counterclockwise). The change in crank angle in going from the advanced position (A) to the return position (R) is less than that going from R to A. If the crank turns at a uniform rate, as is usual, the time taken for the slider to return is less than that to advance. This is an elementary example of a quick-return mechanism. The ratio of time to advance to time to return is called the timing ratio. For Figure 8.2, it is greater than unity. It clearly depends on the geometry of the linkage. The nature of the dependence will be explored in the context of the general four-element synthesis problem. If the direction of crank rotation is reversed, the timing ratio is inverted.

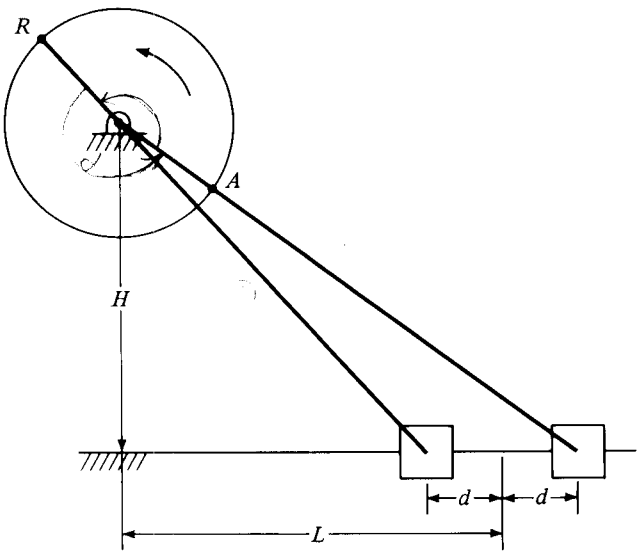

FIGURE 8.2 *An offset slider crank. For counterclockwise rotation, the return angle is the smaller angle between* A *and* R, *and the advance angle is the larger. This uneven timing gives a quick-return mechanism.*

ANALYTIC SYNTHESIS

Techniques of mechanism analysis were developed in great detail for four-link mechanisms. The idea was to introduce concepts, not to generate vast numbers of rules. The advent of digital computers and commercially available analysis and synthesis codes means that one does not need to work out example after example. On the other hand, it is crucial to understand the concepts of analysis and synthesis so that one can understand what the codes do, what one can expect them to do, and how they can generate incorrect results. The remainder of this chapter is devoted to an understanding of four-link synthesis using a direct analytic method.

The Slider Crank with Timing

Consider the offset slider crank. Figure 8.3 shows a complex vector skeleton of such a mechanism. The origin O has been chosen as shown, and the convention that z_2 is the crank and z_3 the coupler has been maintained. The loop-closure equation can be written in the usual general form

$$z_1 + z_2 + z_3 + z_4 = 0 \tag{8.2}$$

and the coordinate system allows me to rewrite this in a more instructive form:

$$r_4 = ir_1 + r_2 e^{i\theta_2} + r_3 e^{i\theta_3} \tag{8.3}$$

The synthesis task is to find r_1, r_2, r_3 such that r_4 takes on desired values for given values of θ_2. How many such pairs can be specified? Equation (8.3) represents two real equations. If θ_2 and r_4 are specified, then there are four remaining unknowns: r_1, r_2, r_3, and θ_3. I have a double redundancy. If I add a second point, I add two equations [Equation (8.3) with different values for r_4 and θ_2] and one unknown, the value of θ_3 at the new position. Thus, the new system has four equations and five unknowns, a single redundancy. Adding a third point leads to six equations in six unknowns, a complete (nonlinear) set of equations and unknowns.

If the initial position of the crank is not important, then I do not specify the initial value of θ_2 but merely specify the changes in θ_2: ϕ_{21}, the angle that the crank rotates in going from the first (initial) position to the second position, and ϕ_{22}, the angle the crank rotates in going from the first to the third position. The number of unknowns is increased by 1 (the initial crank angle), and I can specify one more point in the cycle if I choose.

The usual synthesis problem is to specify the length of the stroke and the timing ratio. Recall that the timing ratio is the ratio of the time taken to advance the slider to that taken to return it. For the usual case of uniform crank rotation, this is equal to the change in θ_2 during the advance stroke divided by that during the return stroke.

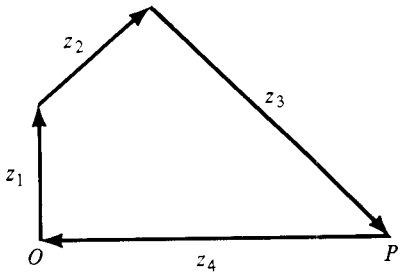

FIGURE 8.3 *A four-complex-number representation of the offset slider crank. (While the mechanism can be represented by three vectors, it is more convenient to use four.)*

In Figure 8.2, the timing ratio would be the change in θ_2 as the crank tip goes from R to A, divided by the change in θ_2 as the crank tip goes from A back to R. To solve this synthesis problem, examine the loop-closure equations for the advanced and retarded positions.

$$z_{20}\left(1 - \frac{r_3}{r_2}\right) = -z_1 - z_{40} \tag{8.4}$$

$$z_{20}\left(1 + \frac{r_3}{r_2}\right)e^{i\alpha} = -z_1 - z_{41} \tag{8.5}$$

where I have used the antiparallelism and parallelism of the crank and coupler in the two extreme positions. Angle α is the advancing angle. The timing ratio is given by

$$\beta = \frac{\alpha}{(2\pi - \alpha)} \tag{8.6}$$

so that $\alpha = 2\pi\beta/(\beta + 1)$.

Equations (8.4) and (8.5) represent four equations in five unknowns, z_{20}, H, L, and r_3/r_2. They are not linear equations, and the solution process is not immediately obvious. Begin by multiplying Equation (8.5) by $e^{-i\alpha}$ and adding the two equations. This allows the elimination of z_{20} in terms of the other variables,

$$z_{20} = -[(1 + e^{-i\alpha})z_1 + z_{40} + e^{-i\alpha}z_{41}]/2 \tag{8.7}$$

Substitution back into Equation (8.4) allows elimination of the ratio r_3/r_2,

$$r_3/r_2 = [z_{20} + z_1 + z_{40}]/z_{20} \tag{8.8}$$

Because Equation (8.8) is a complex equation, the value returned for the ratio may be complex. Thus, a *solvability condition* must be imposed: the imaginary part of the right-hand side of Equation (8.8) must be zero. The imaginary part is proportional to

the product of the numerator and the complex conjugate of the denominator. After some algebra, the solvability condition becomes

$$\sin\alpha(H^2 + L^2 - d^2) - 2Hd\cos\alpha = 0 \tag{8.9}$$

where H and L are defined in Figure 8.2 and d is the half-stroke of the slider. It can be conveniently rewritten in dimensionless form,

$$(H/d)^2 - 2\cot\alpha(H/d) + (L/d)^2 - 1 = 0 \tag{8.10}$$

L/d must be greater than unity; otherwise, the slider would be required to pass beneath the crank pivot point, and that is impossible. Equation (8.10) can be viewed as a quadratic equation determining the ratio H/d as a function of L/d and α. Its constant term, $(L/d)^2 - 1$, is greater than zero, so that there will be real roots only if the linear term is negative. Therefore, $\cot\alpha$ must be greater than zero.

It is sufficient to consider timing ratios greater than unity. As shown earlier, timing ratios less than unity can be obtained by symmetry. When $\beta > 1$, the angle α is between π and 2π. For $\cot\alpha$ to be positive, α must be less than $3\pi/2$ and the timing ratio less than 3. Finally, the discriminant for Equation (8.10) will be positive if and only if $(L/d)^2 - 1 \leq \cot^2\alpha$. If the equality holds, $H/d = \cot\alpha$. Otherwise, there are two values of H/d, one larger and one smaller than $\cot\alpha$.

Synthesis proceeds as follows. Choose the stroke $2d$ and the timing ratio $\beta < 3$. Find α. Set $L/d = [1 + \cot^2\alpha]^{1/2}$ and $H/d = \cot\alpha$. From these, find z_1, z_{40}, and z_{41}. Use these to find z_{20}, and use Equation (8.8) to find r_3. This procedure can be written out as a generic code:

PROGRAM 8.1: OFFSET SLIDER CRANK WITH TIMING

enter (d, β);

$\alpha = 2\beta\pi/[1 + \beta]$;

$L = d[1 + \cot^2\alpha]^{1/2}$;

$H = d\cot\alpha$;

$z_1 = iH$; $\quad z_{40} = -(L - d)$; $\quad z_{41} = -(L + d)$;

$z_{20} = -[(1 + e^{-i\alpha})z_1 + z_{40} + e^{-i\alpha}z_{41}]/2$;

$r_3/r_2 = (z_{20} + z_1 + z_{40})/z_{20}$;

$r_2 = |z_{20}|$; $\quad r_3 = (r_3/r_2)r_2$;

print (H, L, r_2, r_3, z_{20});

EXAMPLE 8.1

Let $d = 50$ mm, and let the timing ratio be 2. Following the program gives, in succession,

$$\alpha = 4\pi/3$$

$$\cot \alpha = 1/\sqrt{3} = 0.5774$$

$$L = 57.7350$$

$$H = 28.8700$$

$$z_{20} = -10.5700 + 39.4350i$$

$$r_2 = 40.8270$$

$$r_3 = 70.7164$$

Figure 8.4a shows the mechanism; Figures 8.4b and 8.4c show its behavior.

The detailed behavior of the linkage just synthesized can be examined using the position analysis program developed in Chapter 5.

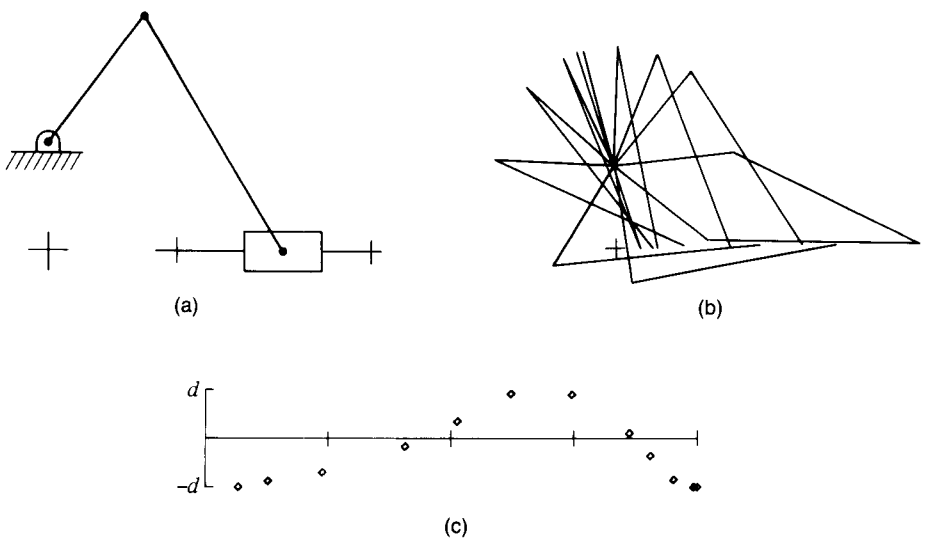

FIGURE 8.4 *The solution to Example 8.1:* (a) *a sketch of the mechanism;* (b) *a cartoon of several positions of the mechanism;* (c) *position of the slider as a function of time for a single cycle.*

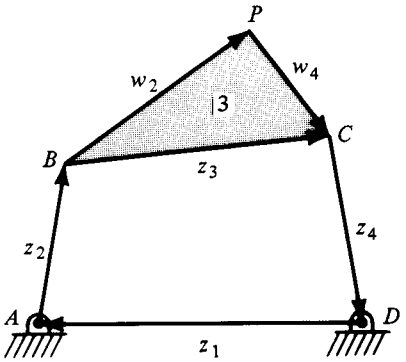

FIGURE 8.5 *A four-bar mechanism. Note the two dyad vectors* w_2 *and* w_4*. These will be used in dyad synthesis.*

Path Synthesis Using Dyads: The Direct Method

Path generation is the most general of the four-bar synthesis tasks. The other two, function generation and motion generation, can be viewed as specializations of path generation. To show this, consider the linkage shown in Figure 8.5. The task of path generation is to choose the link lengths such that point P follows a specified path. Function generation requires that θ_4 approximate a given function of θ_2. This is a special case of path generation, for which point P becomes coincident with point C and the path is a simple circular arc. Motion generation requires that a two-dimensional object take on a specific set of orientations; that is, not only must the path of one point on the object be specified, but the orientation of the object must be specified as well. If the object to be moved is attached to the coupler, this is equivalent to specifying the path that P follows, as well as the coupler angle. Thus, both function generation and motion generation are restricted cases of path generation. I will begin with a thorough exploration of the most general case, path generation, and then use these results to help with function and motion generation.

The fundamental tool for analytic depiction of linkages is the loop-closure equation. Referring to Figure 8.5 shows that I have two possible ways of writing the loop-closure equation:

$$z_1 + z_2 + z_3 + z_4 = 0 \tag{8.11a}$$

$$z_1 + z_2 + w_2 + w_4 + z_4 = 0 \tag{8.11b}$$

Both of these suffer from the fact that the complex number p associated with point P does not appear at all in the first equation and does not appear explicitly in the second. This makes the use of the first equation impossible and the second awkward. Another approach is necessary and common.

The loop-closure equation can be split into two parts, each of which involves p explicitly. The first part is the loop ABP and the second the loop $DAPC$. The corresponding loop-closure equations are

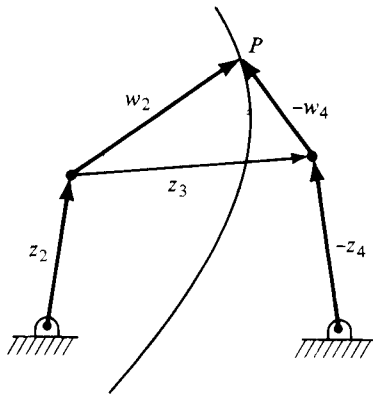

FIGURE 8.6 *The two dyads pointing to the synthesis point* P: $z_2 + w_2$ *and* $-(z_4 + w_4)$.

$$z_2 + w_2 - p = 0 \tag{8.12a}$$

$$z_1 + p + w_4 + z_4 = 0 \tag{8.12b}$$

The sum of these two equations gives Equation (8.11b).

The two-link open chains, $z_2 + w_2$ and $-(z_4 + w_4)$, are two-degree-of-freedom open chains, usually called *dyads* in the kinematic literature. In Figure 8.6, the dyads are more obvious. If the dyads were independent, they could each place point P in any location (within reach), and the synthesis problem would be trivial. It is the limitations imposed by requiring them to be assembled as shown in Figure 8.5 that restricts the apparent freedom of the dyads.

Unless the path to be followed happens to be a coupler curve, following the curve exactly is not possible. The usual procedure is to ask that P match the path exactly at a number of fixed positions; and the question arises: How many points are possible? To answer the question, it is necessary to count equations and variables.

A sequence of points, $P_0, P_1, \ldots, P_j$, with their associated complex representations, $p_0, p_1, \ldots, p_j$, will be specified. They are considered to be known quantities. Let j denote the general term in either sequence. The dyad equations for the general point are then

$$z_{2j} + w_{2j} - p_j = 0 \tag{8.13a}$$

$$z_1 + p_j + w_{4j} + z_{4j} = 0 \tag{8.13b}$$

where I have added a subscript j to all the variables that change. Because z_1 is the frame member, it does not change and it takes no subscript.

It takes 10 variables to describe the linkage. The choice of these 10 is not unique. It is only important to note that only three of these change uniquely when the linkage moves: all the lengths remain unchanged, as does the frame angle θ_1. Two more variables are necessary to locate the linkage with respect to the set of points. These variables are also invariant when the linkage executes its motion. There are thus $9 + 3N$ variables available if N linkage positions are specified, and there are $4N$ real equations. Equating these shows that the maximum number of points that can be specified is 9.

Nine points are a lot of points. The full set of equations is then 36 nonlinear equations in 36 variables. This can be reduced somewhat, and it is common to do so by subtracting the initial position from each of the other positions to produce the reduced set of equations

$$(e^{i\phi_{2j}} - 1)z_{20} + (e^{i\phi_{3j}} - 1)w_{20} = -p_j + p_0 \tag{8.14a}$$

$$(e^{i\phi_{3j}} - 1)w_{40} + (e^{i\phi_{4j}} - 1)z_{40} = p_j - p_0 \tag{8.14b}$$

where I have (1) introduced the rotations ϕ_{ij}, such that $\theta_{ij} = \theta_{i0} + \phi_{ij}$ for $i = 2, 3, 4$, so that

$$\mathbf{z}_{ij} = \mathbf{e}^{i\theta_{ij}}\mathbf{z}_{i0}$$

(2) noted that the frame link z_1 does not change and so cancels from the two equations (8.14b); and (3) noted that the rotations of w_2 and w_4 are both equal to ϕ_{3j}, as both w_2 and w_4 differ from z_3 by constant factors.

Elimination of z_1 reduces the full set to a 32×32 problem, still too large to be instructive. Rather than work down from the general case, I will begin by considering the case for three points, for which the reduced problem has only two complex equations for each dyad.

The three-point problem in its reduced form has four complex constraint equations: (8.14a) with $j = 1$ and $j = 2$, and (8.14b) with $j = 1$ and $j = 2$. These are equivalent to eight real equations and serve to determine eight unknowns. Available unknowns are

$$r_2,\ r_3,\ r_4,\ \theta_{20},\ \theta_{30},\ \theta_{40},\ a_4,\ \alpha_4,\ \phi_{21},\ \phi_{22},\ \phi_{31},\ \phi_{32},\ \phi_{41},\ \phi_{42}$$

The first eight of these determine the geometry of the linkage and its initial orientation. They can be written as four complex unknowns, z_{20}, w_{20}, z_{40}, w_{40}; and the four complex equations can be solved directly, just as if they were real.

Let $1 - e^{i\phi_{ij}} = a_{ij}$. Then the $N = 3$ equations can be written compactly in matrix notation

$$-\begin{Bmatrix} a_{21} & a_{31} \\ a_{22} & a_{32} \end{Bmatrix} \begin{Bmatrix} z_{20} \\ w_{20} \end{Bmatrix} = \begin{Bmatrix} p_1 - p_0 \\ p_2 - p_0 \end{Bmatrix} \tag{8.15a}$$

$$\begin{Bmatrix} a_{41} & a_{31} \\ a_{42} & a_{32} \end{Bmatrix} \begin{Bmatrix} z_{40} \\ w_{40} \end{Bmatrix} = \begin{Bmatrix} p_1 - p_0 \\ p_2 - p_0 \end{Bmatrix} \tag{8.15b}$$

the solutions to which are also easily written in matrix notation

$$\begin{Bmatrix} z_{20} \\ w_{20} \end{Bmatrix} = -[a_{21}a_{32} - a_{22}a_{31}]^{-1} \begin{Bmatrix} a_{32} & -a_{31} \\ -a_{22} & a_{21} \end{Bmatrix} \begin{Bmatrix} p_1 - p_0 \\ p_2 - p_0 \end{Bmatrix} \tag{8.16a}$$

$$\begin{Bmatrix} z_{40} \\ w_{40} \end{Bmatrix} = [a_{41}a_{32} - a_{42}a_{31}]^{-1} \begin{Bmatrix} a_{32} & -a_{31} \\ -a_{42} & a_{41} \end{Bmatrix} \begin{Bmatrix} p_1 - p_0 \\ p_2 - p_0 \end{Bmatrix} \tag{8.16b}$$

It is not obvious how one is to choose the six rotations ϕ_{ij}. On the face of it, any set will do. The question is clarified by working a pair of examples, two different sets of rotation angles for the same three path points.

EXAMPLE 8.2a

Find a four-bar linkage of the type shown in Figure 8.5 such that point P passes through the following three points:

$$p_0 = 3.5543 + 4.7523i, \quad p_1 = 3.7492 + 5.9084i, \quad p_2 = 2.8085 + 5.8478i$$

Choose the rotations to be

$$\phi_{21} = 1.0472, \quad \phi_{31} = -0.2660, \quad \phi_{41} = -0.0752$$
$$\phi_{22} = 1.7453, \quad \phi_{32} = -0.3669, \quad \phi_{42} = 0.0675$$

From these, one can calculate the six distinct matrix coefficients:

$$a_{21} = 0.5000 - 0.8667i, \quad a_{22} = 0.1377 - 0.9848i$$
$$a_{31} = 0.0352 - 0.2629i, \quad a_{32} = 0.0666 + 0.3587i$$
$$a_{41} = 0.0028 + 0.0751i, \quad a_{42} = 0.0023 - 0.0674i$$

Substitution of these into Equations (8.16a) and (8.16b) leads to the initial dyads

$$z_{20} = 2.0000 - 0.0003i$$
$$w_{20} = 1.5565 + 4.7534i$$
$$z_{40} = 3.0636 - 6.2936i$$
$$w_{40} = 3.3836 + 1.5429i$$

The frame link can be found from Equation (8.11b),

$$z_1 = -10.0015 - 0.0016i$$

The resulting linkage is shown in Figure 8.7a. Point P is shown at P_0 and, as the reader can verify, point A is very nearly at the origin [(− 0.0022, −0.0008)] and the other frame point D is very close to the x axis [(9.9993, 0.0008)]. The linkage satisfies the Grashof criterion, and its coupler curve can be drawn. The coupler curve is shown in Figure 8.7b, in which the circled points are the initial points for which the linkage was synthesized. It seems a quite unexceptional linkage. Is it a coincidence that A is near the origin? Is the small offset from the origin a consequence of some round-off error? What does the origin mean? To help answer these questions, another example will be useful.

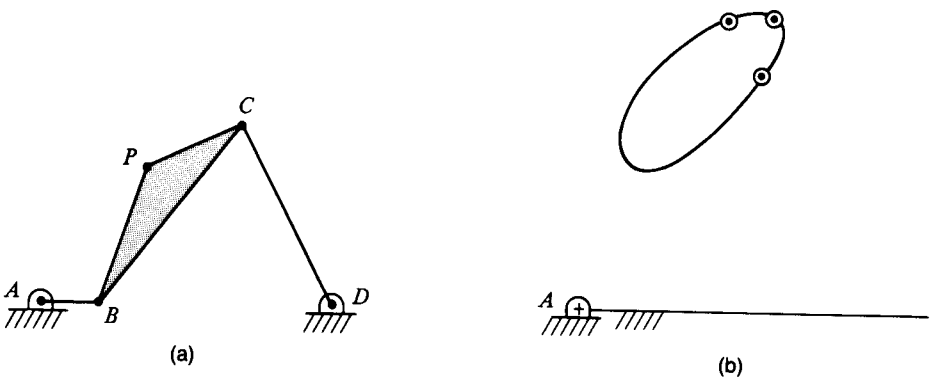

FIGURE 8.7 *The solution to Example 8.2a:* (a) *the linkage shown in its initial position;* (b) *the coupler curve.*

EXAMPLE 8.2b

Repeat the synthesis in Example 8.2a, changing only the assumed rotations. Let the new rotations be

$$\phi_{21} = 0.7854, \quad \phi_{31} = -0.4000, \quad \phi_{41} = 0.1000$$
$$\phi_{22} = 1.5078, \quad \phi_{32} = -0.6000, \quad \phi_{42} = 0.2000$$

From these, one can calculate the six distinct matrix coefficients:

$$a_{21} = 0.2929 - 0.7071i, \quad a_{22} = 1.0000 - 1.0000i$$
$$a_{31} = 0.0789 + 0.3894i, \quad a_{32} = 0.1747 + 0.5646i$$
$$a_{41} = 0.0050 - 0.0998i, \quad a_{42} = 0.0199 - 0.1987i$$

Substitution of these into Equations (8.16a) and (8.16b) leads to the initial dyads

$$z_{20} = 1.8793 + 0.6216i$$
$$w_{20} = -0.6154 + 2.9179i$$
$$z_{40} = -1.0930 - 23.4423i$$
$$w_{40} = 4.1417 - 5.6848i$$

The frame link can be found from Equation (8.11b),

$$z_1 = -4.3126 + 25.5876i$$

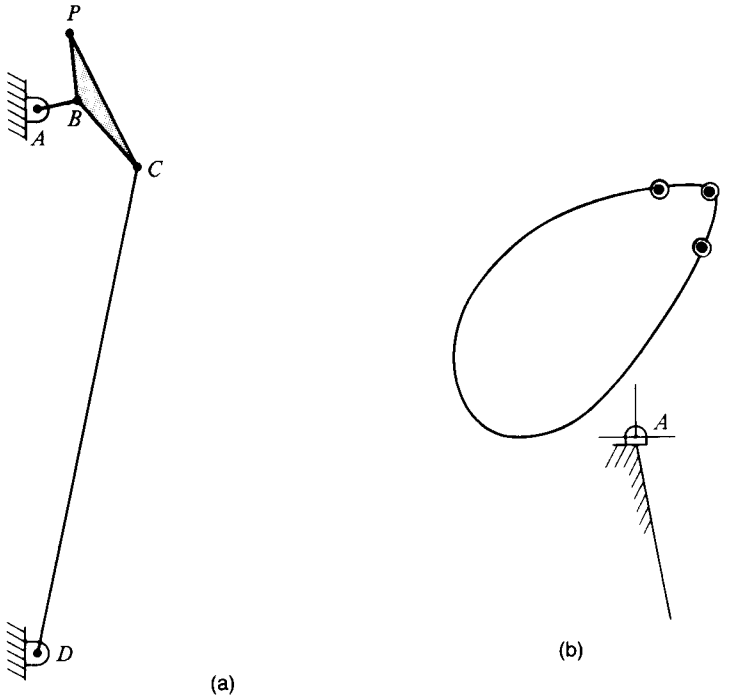

FIGURE 8.8 *The solution to Example 8.2b:* (a) *the linkage shown in its initial position;* (b) *the coupler curve.*

The resulting linkage is shown in Figure 8.8a, which is drawn to the same scale as Figure 8.7a. As in Figure 8.7a, point P is shown at p_0. This, too, is a Grashof linkage, and its coupler curve is shown in Figure 8.8b, drawn to the same scale as Figure 8.7b.

These two linkages appear radically different. The coupler shapes are different. The coupler curves are different. Most striking is the different location of the frame points A [(2.2904, 1.2128)] and D [(6.6030, −24.3748)] with respect to the precision points p_j. Evidently, the result is very sensitive to the choice of rotation angles.

Whereas this is true, the real problem arises in reducing the set of equations (8.13) to the set (8.14). When the equations for the zero position are subtracted from the equations for the other positions, this refers everything to point p_0. This is equivalent to choosing an origin for the coordinate system. Indeed, the locations of point A in both examples are found by laying out the vectors $-w_{20}$ and $-z_{20}$ from point P and finding where A lies rather than starting from A and moving out to P. Anytime one uses the set of equations (8.14a) and (8.14b) instead of the set (8.13a) and (8.13b), the origin is moved, in effect, to point p_0, and the usual convention that has been used in this text, that the origin is at A, is gone.

Ground Pivot Specification

Mechanisms do not exist in isolation. They are parts of larger systems. Because of this, the designer cannot let the frame attachment points be unconstrained functions of the solution. Such solution points may, as in Example 8.2b, be impracticably or impossibly located. It is clearly clumsy to vary the rotation angles until acceptable locations for the frame attachment points, or *ground pivots* (A,D), are found. It is very useful to have a scheme whereby the location of points A and D with respect to the precision points can be specified in advance. This can be done, but not without penalty. First, the p_0 equations are returned to the set so that, for example, the three-precision-point case that was solved so simply now involves six complex equations, and four of the six rotation angles cannot be specified but must be found from the analysis. Second, specification of the location of A and D removes four variables from the list of unknowns, reducing the freedom of the system by four, and bringing to five the maximum number of precision points that can be specified. Despite these penalties, this is sufficiently important to have a name, *ground pivot specification*, and I will now explore the analysis for path generation with ground pivot specification.

As before, I will start with the simple case of three precision points. The governing equations are taken from Equations (8.13a) and (8.13b). These are

$$\begin{aligned} z_{20} + w_{20} &= p_0 = -[z_1 + z_{40} + w_{40}] \\ e^{i\phi_{21}} \cdot z_{20} + e^{i\phi_{31}} \cdot w_{20} &= p_1 = -[z_1 + e^{i\phi_{41}} \cdot z_{40} + e^{i\phi_{31}} \cdot w_{40}] \\ e^{i\phi_{22}} \cdot z_{20} + e^{i\phi_{32}} \cdot w_{20} &= p_2 = -[z_1 + e^{i\phi_{42}} \cdot z_{40} + e^{i\phi_{32}} \cdot w_{40}] \end{aligned} \tag{8.17}$$

I am free to choose two angles; the other four must be obtained from the analysis. Let those two be the crank rotations ϕ_{21} and ϕ_{22}, arguably the ones most likely to be specified by a designer since they govern the timing of the mechanism. If, having chosen the crank rotations, I can solve the left-hand dyad, that solution will give me the values of the coupler rotations. Having the values of the coupler rotations means that I have one set of angles in the right-hand dyad, so that whatever method I used to solve the left-hand dyad will also work on the right-hand dyad. This is general. If I can solve one dyad using a set of chosen angles, I can solve the other the same way. This is assured because the coupler rotation angles, the ϕ_{3j}, appear in both dyads, coupling their motions. Thus, a thorough exploration of the left-hand dyad with the crank angles specified gives the pattern for all these synthesis solutions.

Rewrite the left-hand dyad equations, putting the unknown rotations ϕ_{31} and ϕ_{32} on the left-hand side and the known crank rotations on the right-hand side:

$$\begin{aligned} w_{20} &= p_0 - z_{20} \\ e^{i\phi_{31}} \cdot w_{20} &= p_1 - e^{i\phi_{21}} \cdot z_{20} \\ e^{i\phi_{32}} \cdot w_{20} &= p_2 - e^{i\phi_{22}} \cdot z_{20} \end{aligned} \tag{8.18}$$

Now, multiply each side of the equation by its complex conjugate. This will eliminate the coupler rotation angles ϕ_{3j}:

$$\begin{aligned} w_{20}{}^{*}w_{20} &= p_0p_0{}^{*} - z_{20}{}^{*}p_0 + z_{20}z_{20}{}^{*} \\ w_{20}{}^{*}w_{20} &= p_1p_1{}^{*} - z_{20}e^{i\phi_{21}} \cdot p_1{}^{*} - z_{20}e^{-i\phi_{21}} \cdot p_1{}^{*} + z_{20}z_{20}{}^{*} \\ w_{20}{}^{*}w_{20} &= p_2p_2{}^{*} - z_{20}e^{i\phi_{22}} \cdot p_2{}^{*} - z_{20}e^{-i\phi_{22}} \cdot p_2{}^{*} + z_{20}z_{20}{}^{*} \end{aligned} \tag{8.19}$$

The set of equations (8.19) is made up of three real equations. Subtract the first from each of the other two, and rearrange the result.

$$\begin{aligned} [e^{i\phi_{21}} \cdot p_1{}^{*} - p_0{}^{*}]z_{20} + [e^{-i\phi_{21}} \cdot p_1 - p_0]z_{20}{}^{*} &= p_1p_1{}^{*} - p_0p_0{}^{*} \\ [e^{i\phi_{22}} \cdot p_2{}^{*} - p_0{}^{*}]z_{20} + [e^{-i\phi_{22}} \cdot p_2 - p_0]z_{20}{}^{*} &= p_2p_2{}^{*} - p_0p_0{}^{*} \end{aligned} \tag{8.20}$$

Let $f_1 = [e^{-i\phi_{21}} \cdot p_1 - p_0]$ and $f_2 = [e^{-i\phi_{22}} \cdot p_2 - p_0]$. The set of equations (8.20) can be rewritten in terms of the real and imaginary parts of the variables and the coefficients

$$\begin{aligned} 2\{\mathrm{Re}[f_1]\mathrm{Re}[z_{20}] + \mathrm{Im}[f_1]\mathrm{Im}[z_{20}]\} &= p_1p_1{}^{*} - p_0p_0{}^{*} \\ 2\{\mathrm{Re}[f_2]\mathrm{Re}[z_{20}] + \mathrm{Im}[f_2]\mathrm{Im}[z_{20}]\} &= p_2p_2{}^{*} - p_0p_0{}^{*} \end{aligned} \tag{8.21}$$

Because f_1 and f_2 are known, this pair can be solved for the real and imaginary parts of z_{20} and, hence, for z_{20} itself. It is left as an exercise in complex arithmetic to show that the result is

$$z_{20} = \frac{\{f_1p_2p_2{}^{*} - f_2p_1p_1{}^{*} - [f_1 - f_2]p_0p_0{}^{*}\}}{\{f_1f_2{}^{*} - f_2f_1{}^{*}\}} \tag{8.22}$$

Once this is determined, the remainder of the unknowns can be found by back substitution as follows:

$$w_{20} = p_0 - z_{20} \tag{8.23}$$

$$e^{i\phi_{31}} = \frac{[p_1 - e^{i\phi_{21}} \cdot z_{20}]}{w_{20}} \tag{8.24a}$$

$$e^{i\phi_{32}} = \frac{[p_2 - e^{i\phi_{22}} \cdot z_{20}]}{w_{20}} \tag{8.24b}$$

Note that there is no ambiguity in finding the rotation coefficients $e^{i\phi_{31}}$ and $e^{i\phi_{32}}$ because no trigonometric inversion is required.

Once the left-hand dyad has been found, the right-hand dyad can be found in the same way. Put the terms involving ϕ_{41} and ϕ_{42} on the left-hand side, and follow the ritual just set forth. Those results will be

$$w_{40} = -\frac{\{f_3 q_2 q_2^* - f_4 q_1 q_1^* - [f_3 - f_4] q_0 q_0^*\}}{\{f_3 f_4^* - f_4 f_3^*\}} \tag{8.25}$$

$$z_{40} = q_0 - w_{40} \tag{8.26}$$

$$e^{i\phi_{41}} = \frac{[q_1 + e^{i\phi_{31}} \cdot w_{40}]}{z_{40}} \tag{8.27a}$$

$$e^{i\phi_{42}} = \frac{[q_2 + e^{i\phi_{32}} \cdot w_{40}]}{z_{40}} \tag{8.27b}$$

where $f_3 = [e^{-i\phi_{31}} \cdot q_1 - q_0]$, $f_4 = [e^{-i\phi_{32}} \cdot q_2 - q_0]$, and $q_i = p_i + z_1$. The derivation is left as an exercise for the reader. It should be easily reproduced by following the model for the left-hand dyad.

Although the derivation is complicated and tedious, the result is quite simple and lends itself to the construction of a nice deterministic algorithm.

PROGRAM 8.2: PATH GENERATION WITH TIMING AND GROUND PIVOT SPECIFICATION

enter

$(p_0, p_1, p_2, \phi_{21}, \phi_{22}, z_1)$;

$f_1 = [e^{-i\phi_{21}} \cdot p_1 - p_0], \quad f_2 = [e^{-i\phi_{22}} \cdot p_2 - p_0]$;

$z_{20} = \{f_1 p_2 p_2^* - f_2 p_1 p_1^* - [f_1 - f_2] p_0 p_0^*\} / \{f_1 f_2^* - f_2 f_1^*\}$;

$w_{20} = p_0 - z_{20}$;

$e^{i\phi_{31}} = \dfrac{[p_1 - e^{i\phi_{21}} \cdot z_{20}]}{w_{20}}$;

$e^{i\phi_{32}} = \dfrac{[p_2 - e^{i\phi_{22}} \cdot z_{20}]}{w_{20}}$;

$q_0 = p_0 + z_1, \; q_1 = p_1 + z_1, \; q_2 = p_2 + z_1$;

$g_1 = [e^{-i\phi_{31}} \cdot q_1 - q_0], \quad g_2 = [e^{-i\phi_{32}} \cdot q_2 - q_0]$;

$w_{40} = -\{g_1 q_2 q_2^* - g_2 q_1 q_1^* - [g_1 - g_2] q_0 q_0^*\} / \{g_1 g_2^* - g_2 g_1^*\}$;

$z_{40} = q_0 - w_{40}$;

$z_3 = w_2 + w_4$;

$r_2 = |z_{20}|, \quad r_3 = |z_{30}|, \quad r_4 = |z_{40}|$;

print $(z_{20}, z_{30}, z_{40}, r_2, r_3, r_4)$;

EXAMPLE 8.3

Let the three precision points be $p_0 = 3.5543 + 4.7523i$, $p_1 = 3.7492 + 5.9084i$, and $p_2 = 2.8085 + 5.8478i$. Let the frame vector $z_1 = -6$, and choose the rotations $\phi_{21} = \pi/4$ and $\phi_{22} = \pi/2$. Then,

$$f_1 = 3.2747 - 3.2255i, \quad f_2 = 2.2935 - 7.5608i$$

$$f_1 f_2^* = 31.8979 + 17.3617i$$

and

$$z_{20} = 2.3558 + 0.2605i$$

$$w_{20} = 1.1985 + 4.4918i$$

For the second half of the dyad, calculate

$$e^{i\phi_{31}} = 0.9692 - 0.2462i$$

$$e^{i\phi_{32}} = 0.8959 - 0.4442i$$

(It is worth checking that the magnitude of these is unity, as it should be.) Putting these into the second half of the dyad gives, in turn,

$$w_{40} = 3.6375 - 3.2716i$$

$$z_{40} = -1.1918 - 1.4807i$$

As a check on the solution, note that the sum $z_{20} + w_{20} + w_{40} + z_{40}$ must equal $-z_1$, here $6 + 0i$.

Figure 8.9 shows the linkage in its initial (subzero) position.

If more than three points on the path are to be specified, then either the ground pivot specification or the timing must be abandoned. If ground pivot specification is abandoned and timing retained, five points can be matched. Retaining the ground

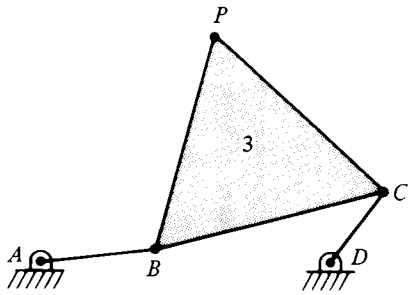

FIGURE 8.9 *The linkage synthesized in Example 8.3, shown in its initial position.*

pivots and abandoning the timing also leads to five as the maximum number of precision points. Full freedom, of course, allows nine precision points to be specified. All these cases are nonlinear.

Intricate analytic techniques exist for these more complicated five-precision-point problems. The second Sandor and Erdman (1984) volume shows some of these. It is probably more practical, however, to attack these through the use of successive approximation, using the same sort of Newton–Raphson techniques explored earlier for position analysis. This will be examined in the next chapter.

Motion and Function Generation

I noted earlier that motion- and function-generation techniques can be obtained easily once path generation is understood. It is now time to redeem that promise.

Motion generation is the placing of an object in a sequence of positions, defined by location and orientation. If the object is imagined to be attached to the coupler of a four-bar linkage in some appropriate way, then one can choose a point on the object as a coupler point P, and the motion of that point becomes a problem in path generation. The preservation of the desired orientation will be assured if the rotations of the coupler are specified; the angles ϕ_{3j} will be specified.

From this preamble, it should be clear that motion generation is exactly equivalent to path generation with timing, which has just been exhaustively covered. The entire argument just rehearsed can be repeated with the simple substitution of the set ϕ_{3j} for ϕ_{2j} in the set of givens. Five precision points are possible for a fixed ground link.

For ground pivot specification, the more common situation, an analysis parallel to that following Equation (8.17) is possible. The coupler rotations are now specified instead of the crank rotations, so that the starting point for analysis is the same for each dyad. In fact, the dyads can be solved independently, in any order. For the left-hand dyad,

$$\begin{aligned} z_{20} &= p_0 - w_{20} \\ e^{i\phi_{21}} z_{20} &= p_1 - e^{i\phi_{31}} w_{20} \\ e^{i\phi_{22}} z_{20} &= p_2 - e^{i\phi_{32}} w_{20} \end{aligned} \tag{8.28}$$

and following the steps outlined after Equation (8.18) allows one to find w_{20} and, from w_{20}, the remainder of the solution can be found by direct back substitution. The right-hand dyad is found exactly as in the path-generation problem.

Function generation is the mechanical approximation of a mathematical function. The angle of the follower is related in a specified way to that of the crank. In the notation of this text,

$$\theta_4 = \theta_{40} + \phi_4, \qquad \theta_2 = \theta_{20} + \phi_2 \tag{8.29}$$

$$\phi_4 = f(\phi_2) \tag{8.30}$$

Because angles are specified, the overall size of the mechanism is irrelevant. All geometrically similar structures are equivalent. More importantly, note that this task can be viewed as a special case of path generation. If the coupler point P is coincident with point C, the joint connecting the coupler and the follower, then P will trace a circular arc passing through the set of precision points. The angles ϕ_{4j} translate into points p_j. Thus, one need only synthesize the left-hand dyad using the techniques outlined earlier. The right-hand dyad is degenerate: the vector w_4 is identically zero, and the right-hand dyad is just the follower.

This argument has been chosen to show the connections among the three synthesis tasks. It is more restrictive than necessary. If this procedure is followed, no more than five precision points can be imposed. This is usually plenty, but it is interesting to note that more can be chosen. Sandor and Erdman (1984) state that seven is the maximum number of precision points.

What has happened? Where have the other two precision points gone? When the circle was laid out, the initial follower position z_{40} was selected. This additional constraint removes two degrees of freedom. In principle, seven precision points can be specified for function generation with a specified ground link.

With the number of precision points specified, it is possible to turn to the task of choosing them. For path and motion generation, one chooses them for performance considerations. There are usually special points that are crucial for the performance of whatever task the mechanism is to perform. For function generation, structural error should be minimized in some sense: the function should be approximated as closely as possible over some fixed interval by matching the function at fixed points. [There is another way of matching the functions, by fixing the value and some number of derivatives at one point. For a further discussion of this, see Freudenstein (1955). It will not be discussed further here.]

Function generation is mechanical *analog computation.* In this era of rapid electronic digital computation, it has little application. I have included it here for completeness. There are some interesting associated issues involved in function generation, but they are primarily of academic interest. They will be presented for the interested student at the end of Chapter 9.

EXERCISES

1. Synthesize the following slider-crank mechanisms:
   a. stroke = 10 in., timing ratio 1.5
   b. stroke = 2.3 mm, timing ratio 2.8
   c. stroke = 37 mm, timing ratio 1.15
   d. stroke = 4 in., timing ratio 1.75
2. In a coordinate system for which the crank-frame attachment point A is at (0,0) and the follower-frame attachment point is at (10,0), synthesize a linkage for which a coupler point P occupies successively points (3,4), (4, 3.5), (2,2). The time between points should be the same, represented by a crank rotation of $\pi/4$.

3. Synthesize a four-bar linkage to raise a telephone pole from the ground to the vertical, passing through the precision points shown. Pick ground pivots on the ground. (Does the pole hit the ground?)

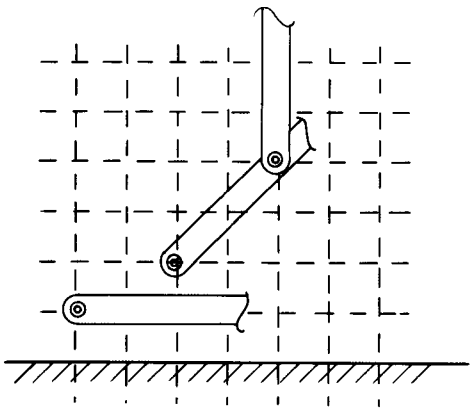

4. Write a synthesis code for slider-crank mechanisms, using stroke length and timing as the input variables. The code should: (1) check that stroke length and timing are acceptable, (2) ask the user to provide either L or H, and (3) draw a "movie" of the resulting linkage.

Chapter 9

Further Topics in Synthesis

PATH SYNTHESIS FOR FOUR-BAR LINKAGES USING INDIRECT METHODS

General Considerations

As in analysis, direct methods can be misleading. Chapter 8 presented a set of closed direct analytic calculations leading to a candidate mechanism satisfying limited constraints. As the tasks become more complicated, as more constraints are added, as the number of links is increased, direct methods become cumbersome and eventually impossible. Just as indirect methods were applied to analysis, so too can they be applied to synthesis. I will begin by examining the use of indirect methods to explore path synthesis for a four-bar mechanism, using the dyad technique presented in Chapter 8. I have chosen this limited problem because it is already familiar. As before, I will use a multidimensional Newton–Raphson (NR) method for successive approximation.

Recall that the NR technique requires finding a set of unknowns that make a set of constraint functions vanish. The technique has been discussed in detail in Chapter 5. With the ground pivot specification relaxed, the reduced version of the dyad equations, Equations (8.13a) and (8.13b) are appropriate, and the constraints can be constructed from these equations by taking the real and imaginary parts of the complex equations. For the jth set, the constraint functions will be

$$\begin{aligned} F_{1j} &= x_j - x_0 + \mathrm{Re}\{z_{20}(1 - e^{i\phi_{2j}}) + w_{20}(1 - e^{i\phi_{3j}})\} \\ F_{2j} &= y_j - y_0 + \mathrm{Im}\{z_{20}(1 - e^{i\phi_{2j}}) + w_{20}(1 - e^{i\phi_{3j}})\} \end{aligned} \tag{9.1a}$$

$$\begin{aligned} F_{3j} &= x_j - x_0 + \mathrm{Re}\{z_{40}(1 - e^{i\phi_{4j}}) + w_{40}(1 - e^{i\phi_{3j}})\} \\ F_{4j} &= y_j - y_0 + \mathrm{Im}\{z_{40}(1 - e^{i\phi_{4j}}) + w_{40}(1 - e^{i\phi_{3j}})\} \end{aligned} \tag{9.1b}$$

The four functions given by Equations (9.1a) specify the position of the left-hand dyad after the jth rotation. Those given by Equations (9.1b) specify the position of the right-hand dyad. Each of these functions vanishes when the appropriate dyad places the

coupler point at the desired location. Thus, each of the functions is an appropriate constraint function capable of being used in a Newton–Raphson scheme. These can be rewritten in a more useful real form by direct expansion and the use of the identity

$$w_{40} = -w_{30} + z_{30} \tag{9.2}$$

to obtain

$$\begin{aligned}
F_{1j} &= x_j - x_0 + r_2[\cos\theta_{20} - \cos\theta_{2j}] + r_3'[\cos(\theta_{30} + a_3) - \cos(\theta_{3j} + a_3)] \\
F_{2j} &= y_j - y_0 + r_2[\sin\theta_{20} - \sin\theta_{2j}] + r_3'[\sin(\theta_{30} + a_3) - \sin(\theta_{3j} + a_3)] \\
F_{3j} &= x_j - x_0 + r_2[\cos\theta_{40} - \cos\theta_{4j}] + r_3'[\cos(\theta_{30} + a_3) - \cos(\theta_{3j} + a_3)] \\
&\quad - r_3[\cos\theta_{30} - \cos\theta_{3j}] \\
F_{4j} &= y_j - y_0 - r_2[\sin\theta_{40} - \sin\theta_{4j}] + r_3'[\sin(\theta_{30} + a_3) - \sin(\theta_{3j} + a_3)] \\
&\quad - r_3[\sin\theta_{30} - \sin\theta_{3j}]
\end{aligned} \tag{9.3}$$

where r_3' denotes the length of w_3, and it is convenient to write these in terms of the actual position angles θ_{ij} rather than the rotations ϕ_{ij}. In the solution process, the rotations will be used.

The set (9.3) has been constructed without restriction to ground pivot specification. The original position has been subtracted. It corresponds to $j = 0$, and it is easy to see [most easily from Equation (9.1)] that the $j = 0$ constraint is automatically satisfied. Thus, $j = 1$ corresponds to the second precision point, $j = 2$ to the third, and so on up to $j = 8$. For a two-precision-point problem, only the $j = 1$ set appears, and only four variables cannot be specified in advance. For a three-precision-point problem such as those analyzed in Chapter 8, both the $j = 1$ and the $j = 2$ set appear, and eight variables cannot be specified in advance. Each precision point deducts four variables from the set, and these variables can be chosen arbitrarily.

When fewer than nine precision points are specified, the system is underdetermined: some variables become arbitrary. Which are arbitrary and which are to be determined by the constraints is a matter of choice. Table 9.1 outlines one such choice for each number of precision points.

The table shows the variables to be determined by the constraint equations. The remaining variables are arbitrary. The beginning of the table echoes what was presented in Chapter 8:

- For two precision points, the constraints determine the link lengths and the distance between P and B, the coupler point and the crank-coupler pin.
- For three precision points, the constraints determine the link lengths, the location of P on the coupler, and the initial position of the linkage.
- A fourth precision point determines two coupler and two follower rotations in addition to the variables already determined.
- A fifth precision point determines all four coupler and follower rotations.
- A sixth precision point begins to determine crank rotations.

Table 9.1 Variables to Be Determined by N Precision Points[a]

N	*Variables to Be Found*
2	r_2, r_3, r_4, r_3'
3	$r_2, r_3, r_4, r_3', \alpha_3, \theta_{20}, \theta_{30}, \theta_{40}$
4	$r_2, r_3, r_4, r_3', \alpha_3, \theta_{20}, \theta_{30}, \theta_{40}, \phi_{41}, \phi_{31}, \phi_{42}, \phi_{32}$
5	$r_2, r_3, r_4, r_3', \alpha_3, \theta_{20}, \theta_{30}, \theta_{40}, \phi_{41}, \phi_{31}, \phi_{42}, \phi_{32}, \phi_{43}, \phi_{33}, \phi_{44}, \phi_{34}$
6	$r_2, r_3, r_4, r_3', \alpha_3, \theta_{20}, \theta_{30}, \theta_{40}, \phi_{41}, \phi_{31}, \phi_{42}, \phi_{32}, \phi_{43}, \phi_{33}, \phi_{44}, \phi_{34}, \phi_{45}, \phi_{35}, \phi_{24}, \phi_{25}$
7	$r_2, r_3, r_4, r_3', a_3, \theta_{20}, \theta_{30}, \theta_{40}, \phi_{41}, \phi_{31}, \phi_{42}, \phi_{32}, \phi_{43}, \phi_{33}, \phi_{44}, \phi_{34}, \phi_{45}, \phi_{35}, \phi_{24}, \phi_{25}, \phi_{46}, \phi_{36}, \phi_{23}, \phi_{26}$
8	$r_2, r_3, r_4, r_3', \alpha_3, \theta_{20}, \theta_{30}, \theta_{40}, \phi_{41}, \phi_{31}, \phi_{42}, \phi_{32}, \phi_{43}, \phi_{33}, \phi_{44}, \phi_{34}, \phi_{45}, \phi_{35}, \phi_{24}, \phi_{25}, \phi_{46}, \phi_{36}, \phi_{23}, \phi_{26}, \phi_{47}, \phi_{37}, \phi_{22}, \phi_{27}$
9	$r_2, r_3, r_4, r_3', \alpha_3, \theta_{20}, \theta_{30}, \theta_{40}, \phi_{41}, \phi_{31}, \phi_{42}, \phi_{32}, \phi_{43}, \phi_{33}, \phi_{44}, \phi_{34}, \phi_{45}, \phi_{35}, \phi_{24}, \phi_{25}, \phi_{46}, \phi_{36}, \phi_{23}, \phi_{26}, \phi_{47}, \phi_{37}, \phi_{22}, \phi_{27}, \phi_{48}, \phi_{38}, \phi_{21}, \phi_{28}$

[a] The remaining variables may be chosen "arbitrarily."

The reader can follow the increasing complexity. It is important to note that the order in which additional variables have been introduced is not unique. The order shown in Table 9.1 is convenient only if one expects to go to nine precision points—an unlikely event.

This discussion is general, and it is useful to illustrate general principles. A more practical reduced procedure will be given later. For now, note that, with no difficulty, this can be put into the NR scheme outlined in Chapter 5.

The set of variables to be found can be symbolized by the column vector x and the constraints by the column vector $F(x)$. As usual, an iterative process is established, for which

$$x_{n+1} = x_n + \Delta x_n \tag{9.4}$$

and the Δx_n come from solving the linear system

$$\Delta_n(x_n)\Delta x_n = -F(x_n) \tag{9.5}$$

The NR correction matrix Δ_n is found, as usual, by differentiating the constraint functions with respect to the appropriate variables. In this case, the variables are those given in Table 9.1, and the constraint functions are those given by Equation (9.3) with $j = 1, 2, \ldots$. The elements of the resulting matrix are straightforward but lengthy. I will not write them out here but, by using • to denote nonzero entries, I will display the pattern of the matrix Δ_n:

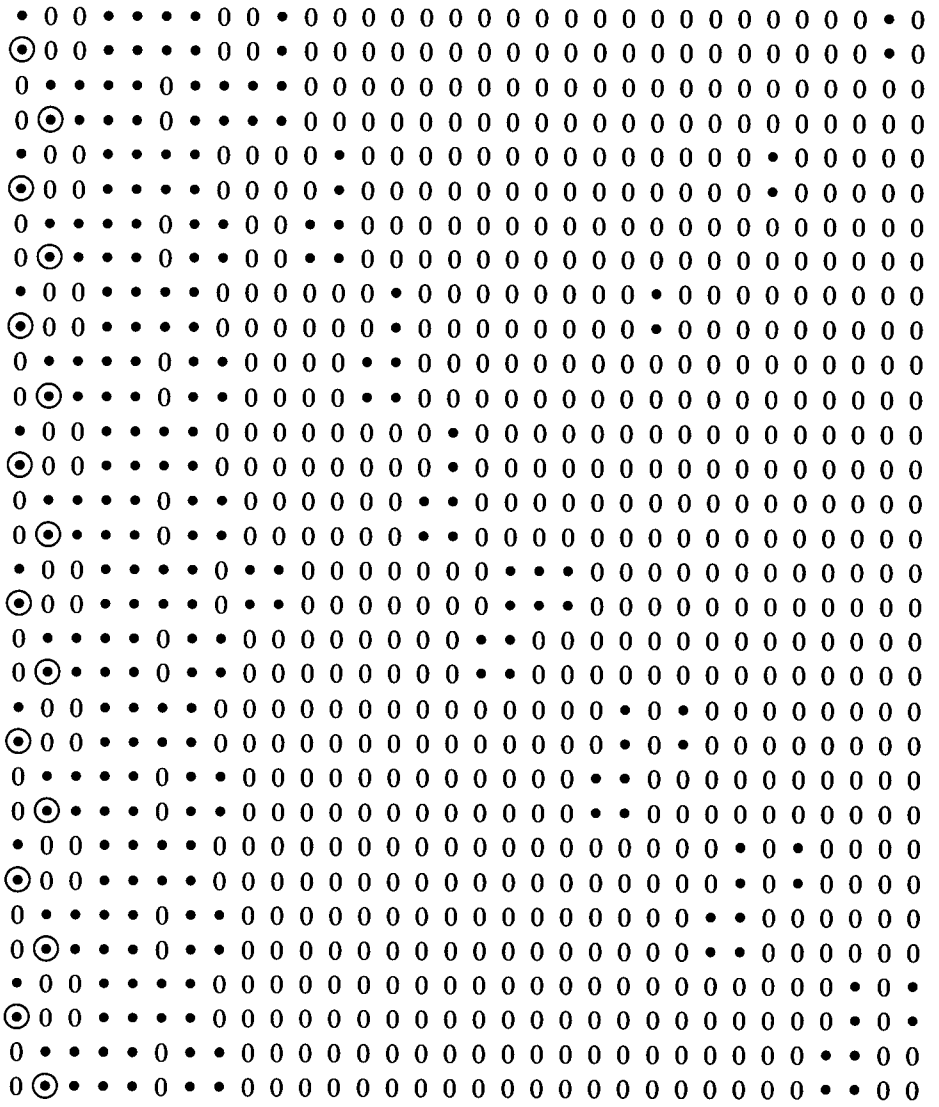

(9.6)

where I have shown the entire 32 rows and columns. The rows repeat in pairs. The first eight columns repeat in a four-row cycle as well.

The matrix is fairly sparse. The systems to be solved are square and are indicated in the diagram. The largest system is 32 × 32, for the nine-precision-point problem. Note that the circled terms in the first and second columns are easily eliminated analytically before a program to solve these systems is written. Considerable further simplification is possible by interchange of rows and columns.

Table 9.2 Variables for Ground Pivot Specification

N	*Independent Variables*	*Determinable Variables*
2	$\phi_{21}, \phi_{31}, \phi_{41}$	$r_2, r_3, r_4, a_3, \alpha_3, \theta_{20}, \theta_{30}, \theta_{40}$
3	ϕ_{21}, ϕ_{22}, or ϕ_{31}, ϕ_{32}	Above + ϕ_{41}, ϕ_{42} and $\phi_{21}\ \phi_{22}$ or ϕ_{31}, ϕ_{32}
4	One rotation angle	Above + all but one rotation angle
5	None	All

Ground Pivot Specification

Given an equation-solving routine capable of handling a 32 × 32 system (not difficult), the reader can synthesize, in principle, a four-bar linkage satisfying the nine-precision-point problem. This is, however, of only academic interest. (As will be seen later, it is easier to handle more precision points by using more complicated linkages.) Most useful at this stage is to pick up the problem of ground pivot specification and extend the results given in Chapter 8 to the case of five precision points.

First, note that the two-dyad system used so far is not general enough to be extended. How would you extend it to systems of more than four bars? Being less than general, it is a weak foundation on which to build a general analysis. Instead of considering two dyad equations for each point connected by the common coupler rotations, take the loop-closure equation itself and one dyad equation

$$\begin{aligned} z_1 + (z_2)_j + (z_3)_j + (z_4)_j &= 0 \\ (z_2)_j + q_3(z_3)_j &= p_j \end{aligned} \tag{9.7}$$

where, as earlier, q_3 is a complex proportionality constant such that $w_2 = q_3 z_3$. In Equation (9.7), $j = 0, 1, 2, \ldots$, denoting successive precision points.

Ground pivot specification implies that z_1 $(= -r_1)$ and all the p_j, including p_0, are known. Equations (9.7) yield four real equations for each precision point, and the maximum number of precision points is five—p_0, p_1, p_2, p_3, p_4—for which there will be 20 real equations and 20 unknowns, to be found using the NR method of successive approximation.

Table 9.2 shows the free variables, those that can be assigned, for ground pivot specification. The ability to specify timing or to synthesize motion vanishes (for four-bar linkages and ground pivot specification) when the number of precision points exceeds three.

Consider the five-precision-point problem in the NR successive approximation sense. It is necessary to write down the coefficients appearing in the iteration matrix Δ_n and to define the iteration vectors x_n and Δx_n. To do this, begin by ordering the dependent (determinable) variables. The ordering I will use produces the column vector x

$$x = [r_2, r_3, r_4, a_3, \alpha_3, \theta_{20}, \theta_{30}, \theta_{40}, \phi_{21}, \phi_{21}, \phi_{22}, \phi_{23}, \phi_{24}, \phi_{31}, \phi_{32}, \phi_{33}, \phi_{34}, \phi_{41}, \phi_{42}, \phi_{43}, \phi_{44}]^T \tag{9.8}$$

where the superscript T denotes transpose. The constraint function must also be numbered. F_1 will be the real part of the loop-closure equation, with $j = 0$; F_2 will be the imaginary part of that same equation. F_3 will be the real part of the dyad equation, with $j = 0$; F_4 will be the imaginary part of the same equation. The same equations with $j = 1$ serve as F_5–F_8, and this procedure is followed through to $j = 4$.

As before, the coefficients of the matrix Δ, a_{ij}, are given by

$$a_{ij} = \frac{\partial F_i}{\partial x_j}$$

To calculate these, write out Equations (9.7)

$$r_2 \cos(\theta_{20} + \phi_{2j}) + r_3 \cos(\theta_{30} + \phi_{3j}) + r_4 \cos(\theta_{40} + \phi_{4j}) - r_1 = 0 \tag{9.9a}$$

$$r_2 \sin(\theta_{20} + \phi_{2j}) + r_3 \sin(\theta_{30} + \phi_{3j}) + r_4 \sin(\theta_{40} + \phi_{4j}) = 0 \tag{9.9b}$$

$$r_2 \cos(\theta_{20} + \phi_{2j}) + a_3 r_3 \cos(\theta_{30} + \alpha_3 + \phi_{3j}) - \mathrm{Re}(p_j) = 0 \tag{9.9c}$$

$$r_2 \sin(\theta_{20} + \phi_{2j}) + a_3 r_3 \sin(\theta_{30} + \alpha_3 + \phi_{3j}) - \mathrm{Im}(p_j) = 0 \tag{9.9d}$$

There are 400 coefficients in the matrix Δ; 160 of these are nonzero. The pattern of coefficients is shown in Equation (9.10).

$$\begin{Bmatrix}
\bullet & \bullet & \bullet & 0 & 0 & \bullet & \bullet & \bullet & 0 & 0 & 0 & 0 & 0 & 0 & 0 & 0 & 0 & 0 & 0 & 0 \\
\bullet & \bullet & \bullet & 0 & 0 & \bullet & \bullet & \bullet & 0 & 0 & 0 & 0 & 0 & 0 & 0 & 0 & 0 & 0 & 0 & 0 \\
\bullet & \bullet & 0 & \bullet & \bullet & \bullet & \bullet & 0 & 0 & 0 & 0 & 0 & 0 & 0 & 0 & 0 & 0 & 0 & 0 & 0 \\
\bullet & \bullet & 0 & \bullet & \bullet & \bullet & \bullet & 0 & 0 & 0 & 0 & 0 & 0 & 0 & 0 & 0 & 0 & 0 & 0 & 0 \\
\bullet & \bullet & \bullet & 0 & 0 & \bullet & \bullet & \bullet & \bullet & \bullet & 0 & 0 & \bullet & 0 & 0 & 0 & \bullet & 0 & 0 & 0 \\
\bullet & \bullet & \bullet & 0 & 0 & \bullet & \bullet & \bullet & \bullet & \bullet & 0 & 0 & \bullet & 0 & 0 & 0 & \bullet & 0 & 0 & 0 \\
\bullet & \bullet & 0 & \bullet & \bullet & \bullet & \bullet & 0 & \bullet & \bullet & 0 & 0 & \bullet & 0 & 0 & 0 & 0 & 0 & 0 & 0 \\
\bullet & \bullet & 0 & \bullet & \bullet & \bullet & \bullet & 0 & \bullet & \bullet & 0 & 0 & \bullet & 0 & 0 & 0 & 0 & 0 & 0 & 0 \\
\bullet & \bullet & \bullet & 0 & 0 & \bullet & \bullet & \bullet & 0 & \bullet & 0 & 0 & 0 & \bullet & 0 & 0 & 0 & \bullet & 0 & 0 \\
\bullet & \bullet & \bullet & 0 & 0 & \bullet & \bullet & \bullet & 0 & \bullet & 0 & 0 & 0 & \bullet & 0 & 0 & 0 & \bullet & 0 & 0 \\
\bullet & \bullet & 0 & \bullet & \bullet & \bullet & \bullet & 0 & 0 & \bullet & 0 & 0 & 0 & \bullet & 0 & 0 & 0 & 0 & 0 & 0 \\
\bullet & \bullet & 0 & \bullet & \bullet & \bullet & \bullet & 0 & 0 & \bullet & 0 & 0 & 0 & \bullet & 0 & 0 & 0 & 0 & 0 & 0 \\
\bullet & \bullet & \bullet & 0 & 0 & \bullet & \bullet & \bullet & 0 & 0 & \bullet & 0 & 0 & 0 & \bullet & 0 & 0 & 0 & \bullet & 0 \\
\bullet & \bullet & \bullet & 0 & 0 & \bullet & \bullet & \bullet & 0 & 0 & \bullet & 0 & 0 & 0 & \bullet & 0 & 0 & 0 & \bullet & 0 \\
\bullet & \bullet & 0 & \bullet & \bullet & \bullet & \bullet & 0 & 0 & 0 & \bullet & 0 & 0 & 0 & \bullet & 0 & 0 & 0 & 0 & 0 \\
\bullet & \bullet & 0 & \bullet & \bullet & \bullet & \bullet & 0 & 0 & 0 & \bullet & 0 & 0 & 0 & \bullet & 0 & 0 & 0 & 0 & 0 \\
\bullet & \bullet & \bullet & 0 & 0 & \bullet & \bullet & \bullet & 0 & 0 & 0 & \bullet & 0 & 0 & 0 & \bullet & 0 & 0 & 0 & \bullet \\
\bullet & \bullet & \bullet & 0 & 0 & \bullet & \bullet & \bullet & 0 & 0 & 0 & \bullet & 0 & 0 & 0 & \bullet & 0 & 0 & 0 & \bullet \\
\bullet & \bullet & 0 & \bullet & \bullet & \bullet & \bullet & 0 & 0 & 0 & 0 & \bullet & 0 & 0 & 0 & \bullet & 0 & 0 & 0 & 0 \\
\bullet & \bullet & 0 & \bullet & \bullet & \bullet & \bullet & 0 & 0 & 0 & 0 & \bullet & 0 & 0 & 0 & \bullet & 0 & 0 & 0 & 0
\end{Bmatrix} \tag{9.10}$$

INTRODUCTION TO SIX-BAR SYSTEMS

The step from four to six bars is instructive. Six-bar linkages have been examined briefly in Chapter 2 and in Chapter 5 (position analysis). A general discussion of six-bar synthesis is well beyond the scope of this text, but some indication of how it would proceed is appropriate as a guide to what must underlie commercial programs capable of synthesizing linkages more complicated than the four-bar linkages already discussed.

A four-bar linkage is defined by a single loop-closure equation. A six-bar linkage requires two independent loop-closure equations. A $2n$-bar linkage (with one degree of freedom, a mobility of 1) requires $n - 1$ loop-closure equations. Synthesis requires an additional constraint, one that assures that the synthesis point passes through the specified precision points. Thus, the step to a six-bar linkage is made by adding a dyad-like equation to the two loop-closure equations.

It will become apparent that six-bar linkages are considerably more complicated than four-bar linkages. To make synthesis a conceivable task, it will be restricted to cases for which ground pivots are specified. The point to be constrained will be supposed to be attached to link 5. Figure 9.1 shows the five distinct six-bar linkages originally shown in Figure 1.17. Because ground pivot specification has been assumed, z_1 is assumed to be known in all five cases, and θ_1 is supposed to be known in the two cases for which the ground link is a ternary link.

The geometry of each link is determined by its initial position and the length of each link: $r_2 - r_6$ and $\theta_{20} - \theta_{60}$. Those linkages for which the ground link is a ternary link (Figures 9.1b and 9.1e) require four additional numbers (q_4, q_5 and q_3, q_5, respectively) to determine their geometry, for a total of 14 variables available for synthesis. The three linkages with a binary ground link require 16 numbers to determine their geometry; they have 16 variables available for synthesis. (The difference is not profound; it is a consequence of assuming q_1 to be known in Figures 9.1b and 9.1e.)

As all the linkages with binary ground links are essentially equivalent and as these have more freedom than those with ternary ground links, any one of these serves as an illustrative model for six-bar synthesis. Take the Stephenson II linkage examined in Chapter 5.

Two independent loop-closure equations are

$$z_1 + (z_2)_j + (z_3)_j + (z_4)_j + (z_6)_j = 0 \tag{9.11a}$$

$$q_3(z_3)_j - (z_4)_j + (z_5)_j + q_6(z_6)_j = 0 \tag{9.11b}$$

and a dyadlike equation is

$$(z_2)_j - (1 + q_3)(z_3)_j + q_5(z_5)_j - p_j = 0 \tag{9.12}$$

For $j = 0$, these equations provide six constraints on 16 variables (representable as the 8 complex variables z_{20}, z_{30}, z_{40}, z_{50}, z_{60} and q_3, q_5, q_6). Each additional precision point adds six constraints, the six new realizations of Equations (9.11) and (9.12). To get to that precision point requires five rotations. Thus, for n precision points, there are $6n$ constraints and $16 + 5(n - 1)$ variables. The maximum number of precision

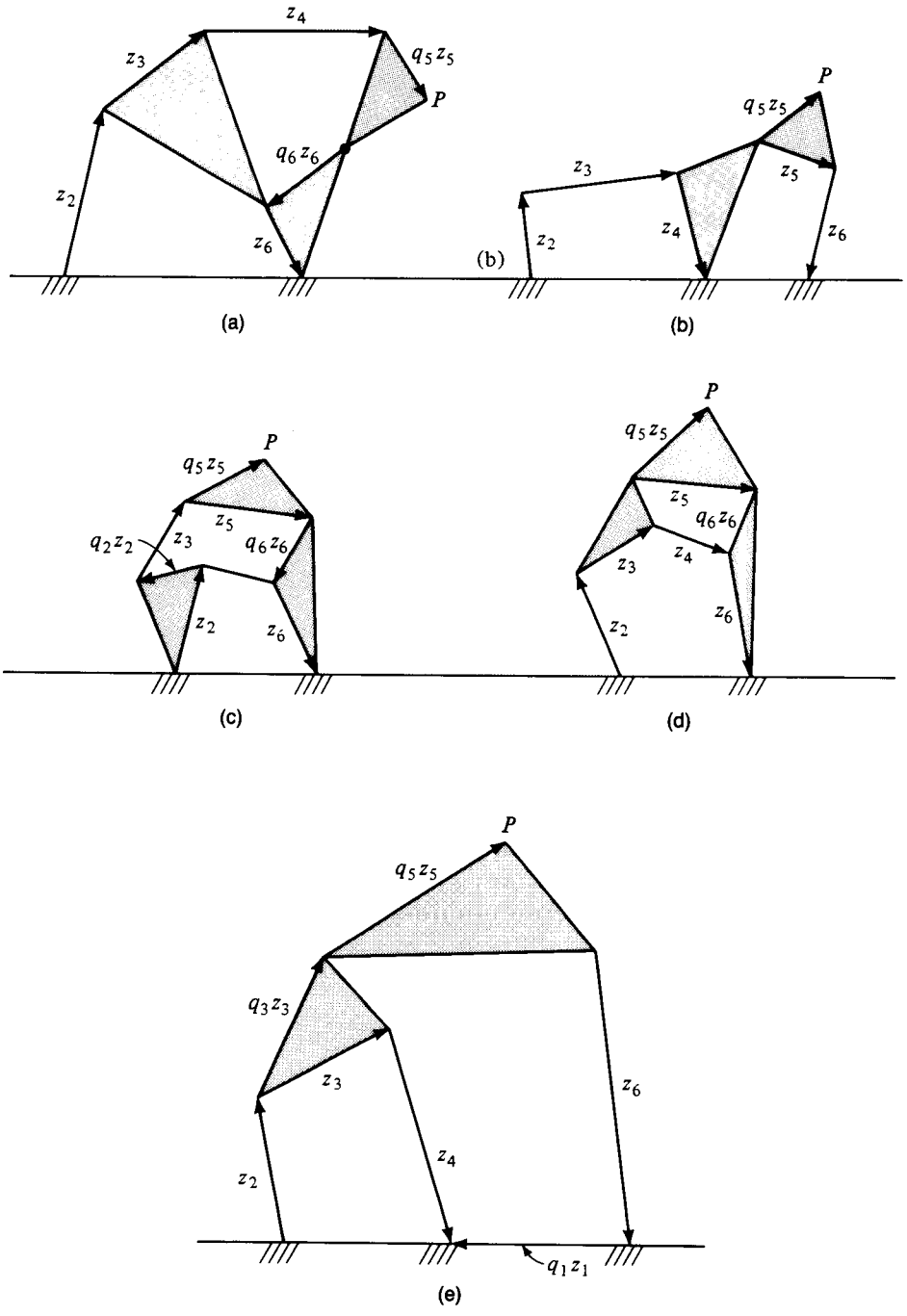

FIGURE 9.1 *The five distinct six-bar linkages showing a set of variables useful for synthesis:* (a) *the Watt I;* (b) *the Watt II;* (c) *the Stephenson I;* (d) *the Stephenson II;* (e) *the Stephenson III.*

points is obtained by equating these: 11 precision points are possible for a six-bar linkage with a specified binary ground link.

If timing or motion generation is desired, each additional link adds only four undetermined rotations, as either the crank rotation or the link-five rotation is specified. The maximum number of precision points is then determined from $6n = 16 + 4(n - 1)$: 6.

In either case, the number of equations to be solved is six times the number of precision points, 66 and 36, respectively. In the second, simpler, case, the matrix to be inverted is 36 × 36, with 1296 elements. Of these, 456 are nonzero if timing is supposed to be given, and 440 are nonzero if motion generation is the task assigned.

FUNCTION GENERATION AND THE CHOICE OF PRECISION POINTS

The question of how many precision points are possible for a given type of synthesis has been answered. How to choose them is not so easily answered. For path or motion generation, one chooses critical points, parts of the path where error is serious. For function generation, one can derive a mathematically based technique. This is primarily of academic interest, as noted earlier. I include it for completeness.

Before discussing the mechanical approximation in detail, it is instructive to consider the general problem of the representation and approximation of functions on a finite interval. Functions can be represented in functional series. A complete discussion can be found in most texts in advanced calculus, such as that by Hildebrand (1962). The following outline is well known and is stated without proof.

Let $\{F_n(x)\}$ be a complete set of functions on an interval $a < x < b$, and suppose that they are also orthogonal with respect to the weighting function $w(x)$, that is,

$$\int_a^b w(x)F_i(x)F_j(x)dx = 0, \qquad i \neq j \tag{9.13}$$

Then an arbitrary (square integrable) function $f(x)$ can be written

$$f(x) = \sum_{j=0}^{\infty} a_j F_j(x), \qquad x \in (a, b) \tag{9.14}$$

$$a_j = \frac{\int_a^b w(x)F_j(x)f(x)\,dx}{\int_a^b w(x)F_j^2(x)\,dx} \tag{9.15}$$

It can be shown that the choice of coefficients (9.15) ensures that the approximation obtained by truncating the series (9.14) minimizes the integrated error in the sense of least squares. Further, the sequence of approximations made up of the partial sums to n of Equation (9.14) converges to $f(x)$ when n tends to infinity.

[The series representation best known to engineers is the Fourier series, which represents a function in a finite interval by an infinite series of sines and cosines periodic on the interval. Other complete sets of orthogonal functions can be found by

solving Sturm-Liouville eigenvalue problems. The mathematically interested reader is directed to the classical textbook by Ince (1926). For a discussion of Fourier series, see the text by Hildebrand.]

An alternative representation of a function is the so-called Lagrangian interpolation formula. Let

$$\pi_n(x) = (x - x_1)(x - x_2) \cdots (x - x_n)$$
$$l_j(x) = (x - x_j)^{-1} \pi_n(x) / \pi_n'(x) \tag{9.16}$$

The l_j vanish for $x = x_i$ if $i \neq j$ and equal unity for $j = i$. Any function f can then be represented by a function of the form

$$L_n(x) = \sum_{j=1}^{n} f(x_j) l_j(x) \tag{9.17}$$

which is equal to the desired function at the specific points $\{x_j\}$. This is exactly what a function-generating linkage does, and so it is important to understand how good an approximation Equation (9.17) is to a given function.

First, note that $L_n(x)$ is a polynomial of degree $n - 1$. If $f(x)$ is a polynomial of lesser or equal degree, then $L_n(x)$ is exact. To assess other functions, examine the mean square error

$$\int_a^b [f(x) - L_n(x)]^2 w(x)\, dx \tag{9.18}$$

where $w(x)$ is a weighting function. If the polynomials $l_j(x)$ are orthogonal with respect to the weighting function $w(x)$ and the collocation points x_j are taken to be the zero of these polynomials, then the limit of the error as n tends to infinity is zero. That is, the sequence of partial sums converges to the desired function. [See Szego (1959).]

Such *orthogonal polynomials* form a subset of the orthogonal functions discussed earlier. There is a clear connection between the two approaches, but they are not identical. The latter recommends itself to the kinematician because only the discrete data approach is possible in constructing a function generator.

There are many sets of orthogonal polynomials. Szego's book (1959) is devoted to these. The usual polynomials used in kinematics are the Chebyshev polynomials, introduced by Chebyshev (1854) in one of his many analytic studies of mechanisms. [For more details about Chebyshev polynomials, see Hochstrasser (1965), the book by Szego (1959), and Erdelyi et al. (1953).] The Chebyshev polynomials (of the first kind—the only ones to appear here) are defined by

$$T_n(x) = T_n(\cos X) = \cos nX \tag{9.19}$$

with the weighting function

$$w(x) = [1 - x^2]^{-1} \tag{9.20}$$

and the ith zero of the nth polynomial is

$$x_{in} = \pm\cos\{[2i - 1]\pi/2n\} \tag{9.21}$$

Choosing n precision points to be the n zeros of T_n and applying a Langrangian interpolation results in a polynomial approximation of order $n - 1$

$$f(x) = a_0 + a_1T_1(x) + a_2T_2(x) + \cdots + a_nT_n(x) \tag{9.22}$$

closely related to, but not equal to, the truncated functional series based on Equations (9.14) and (9.15).

I have been unable to prove, or to find a proof for, the following conjecture. If the coefficients given by Equation (9.15) are approximated using an approximate integration scheme of the Gaussian type (Davis and Polonsky 1965), then the two expansions are equal. [In the Gaussian scheme,

$$\int_a^b g(x)\,dx = \sum W_i g(x_i) + R_n \tag{9.23}$$

where $\{W_i\}$ is a set of weighting coefficients for the integration scheme, not to be confused with the continuous weighting functions $w(x)$ associated with the set of orthogonal functions $\{F_n(x)\}$, and $\{x_i\}$ is a set of specific points on the interval (a,b).] The relevant Gaussian scheme would be that for the same weighting function and zeros

$$\int w(x)F_j(x)f(x)\,dx = \int[1 - x^2]^{1/2}F_j(x)f(x)\,dx = \sum(\pi/n)F_j(x_1) \tag{9.24}$$

if

$$x_i = \cos\{[2i - 1]/[2n]\} \tag{9.25}$$

using formula 25.4.38 in Davis and Polonsky (1965).

All the tools are now in place for function generation with up to five precision points. The only remaining task is to use the Chebyshev development to generate the precision points. For a given function-generation problem, the independent and dependent variables (x and y) must be mapped onto the rotation angles ϕ_2 and ϕ_4, and the Chebyshev collocation points (precision points) must be found. These are mapped directly onto the independent variable and, through the function being generated, onto the dependent variable. This is best illustrated by constructing an example.

Consider the task of generating the function $y = x^{2/3}$ for $1 \le x \le 2$. The limits of y are then $1 \le y \le 1.5874$. For the Chebyshev formulation to be used, the independent variable (x) must be scaled and mapped into the domain $(-1,1)$. Let $z = a + bx$. Then, $x = 1$ corresponds to $z = -1$, and $x = 2$ corresponds to $z = 1$. Solving the two linear equations gives

$$z = -3 + 2x, \qquad x = 3/2 + z/2 \tag{9.26}$$

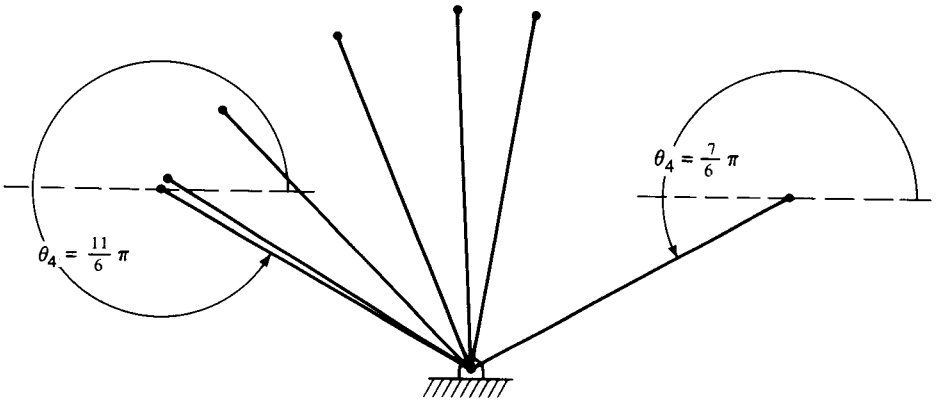

FIGURE 9.2 *The output link (the follower) for a five-point function generator synthesized for the function* $y = x^{2/3}$. *The mapping of the five Chebyshev points in* ϕ_4 *space is shown.*

Find five Chebyshev points. These will be given in z space by the five zeros

$$z_{i5} = \cos[(2i - 1)\pi/10] = \pm 0.9511, \quad \pm 0.5878, \quad 0 \tag{9.27}$$

The corresponding values of x are

$$x_i = 1.9756, \quad 1.7939, \quad 1.5, \quad 1.2061, \quad 1.0245 \tag{9.28}$$

Figure 9.2 shows the output link of the proposed mechanism. The range of the output dial is to be $2\pi/3$ (120°). Let the range be symmetrically arranged about the vertical, as shown. Thus, ϕ_4 will range from $11\pi/6$ down to $7\pi/6$. Note that the convention about the angle ϕ_4 remains unchanged. The output of y must map into this range. Thus, the mapping from y to ϕ_4 is as follows:

$$\phi_4 = -[2\pi/3]/[0.5874] \cdot (y - 1) \tag{9.29}$$

making the full range of ϕ_4 correspond to the full range of y, matching the zeros and changing the sign to make the needle move clockwise, which the dial reader's eye will see as increasing.

Let the range of ϕ_2 be $\pi/4$. The range of x is 1, so that the mapping is

$$\phi_2 = [\pi/4] \cdot (x - 1) \tag{9.30}$$

The Chebyshev points for ϕ_2 are obtained by putting those for x into Equation (9.30). The result is

$$\phi_{2i} = 0.7662, \quad 0.6235, \quad 0.3927, \quad 0.1619, \quad 0.0192 \tag{9.31}$$

The values of ϕ_4 corresponding to these are obtained by finding $y_i = x_i^{2/3}$ and then converting to ϕ_4, using Equation (8.14). That result is

$$\phi_{4i} = -1.2032, \quad -0.9978, \quad -0.6501, \quad -0.2788, \quad -0.0341 \tag{9.32}$$

The sets of rotations given by Equations (9.31) and (9.32) are now used to generate the path generation with timing problem that can be solved as outlined earlier.

Note that the Chebyshev spacing is applied to the independent variable. The values of the dependent variable are obtained from the function. They are the collocation values, called $f(x_i)$ in the theoretical development.

GENERALIZATIONS

Velocity and Acceleration Synthesis

The choice of precision points so far has been literal; they have been points through which the linkage must pass. It is also possible to specify the speed or acceleration of the coupler point, say, at a given point, instead of increasing the number of points. It is as valid to specify the values of a function and its derivatives at one point as to specify the value of a function at several points. This was touched upon in the preceding section. I will formulate these problems in this brief section.

Consider the problem of four-bar linkages with ground pivot specification and start with the basic constraint equations (9.7). Several options appear to be available for a combined path, velocity and acceleration synthesis. As in path synthesis (and the other syntheses so far examined), the crucial issue is the number of variables and of constraints. In the case of path synthesis (re-examine Table 9.2), five complex constraints can be applied. The situation is a little more complicated in the case of mixed synthesis because of the nature of the additional variables introduced by the additional constraints.

In the case of path synthesis, each new position introduced two new dependent variables, the two rotations. Each new position also required four new constraints, so that each new point added more constraints than independent variables. The number of points one could specify was therefore determined by the number of points at which the supply of new variables was exhausted by the increasing number of constraints. A similar situation applies if one is to specify velocity and/or acceleration at one or more points.

The velocity constraint introduces only one additional dependent variable, the crank rotation rate, in contrast to the two introduced by a new position. However, four constraints are introduced from both the velocity and acceleration equations obtained by differentiating the constraint Equations (9.7). Differentiating Equations (9.7) once [Equations (9.33)] and twice [Equations (9.34)] with respect to time gives the governing equations for the motion of the entire linkage and of the single dyad:

$$\begin{aligned} \{i\omega_2 z_2 + i\omega_3 z_3 + i\omega_4 z_4\}_j &= 0 \\ \{i\omega_2 z_2 + i\omega_3 q_3 z_3\}_j &= \dot{p}_j = v_j \end{aligned} \tag{9.33}$$

$$\{(i\dot{\omega}_2 - \omega_2^2)z_2 + (i\dot{\omega}_3 - \omega_3^2)z_3 + (i\dot{\omega}_4 - \omega_4^2)z_4\}_j = 0$$
$$\{(i\dot{\omega}_2 - \omega_2^2)z_2 + (i\dot{\omega}_3 - \omega_3^2)q_3 z_3\}_j = \ddot{p}_j = a_j \tag{9.34}$$

Thus, even three-point ground pivot specification cannot be managed if one adds a velocity constraint at one of the three points. The best one can do is to specify two points and the velocity at one of them. The case for acceleration is apparently better because acceleration introduces not only the crank rotation but its derivative, so that, in principle, one could solve for these two as well as the two unspecified rotations (see Table 9.2) and synthesize a linkage that passed through three points and that gave a specified acceleration at one of these points. In practice, the linkage would be hard to realize, as realizing a specified rate of change in crank rotation is not easy to do in the real world.

The solution to this problem is, of course, to add more links to gain additional freedom. This text is not the place to explore this in any depth, although it is probably appropriate to mention another approach to synthesis problems, so-called *optimum design.*

Optimum Design

I cannot cover the field of optimum design in this short section, but I would be remiss in not mentioning the subject in a book dealing with design (synthesis). The reader who wants to know more about this important subject is directed to any of the texts available in this area, such as the relatively modern book by Vanderplaats (1984).

In all the synthesis problems discussed so far, the solution has been exact: that is, a number of constraints were specified, and the number of dependent variables available was greater than or equal to the number of constraints. Therefore, if the problem had a solution, that solution would be exact. The difficulty in solving large systems of nonlinear algebraic equations may have obscured this point, but it is important. If the synthesis problem posed had a solution, that solution would be exact.

This restriction to exact solutions severely limits the number of constraints that can be applied. Alternatively, specifying many constraints leads to very complicated mechanisms. Optimum design provides an alternative approach that avoids this difficulty by relaxing the requirement that the solution be exact. (This is only one way of viewing optimum design, and one with which all optimum designers may not agree. Nevertheless, it is appropriate to this setting.) Consider ground pivot specification as a model from which to move to optimum design considerations. The synthesis problem can be viewed as the satisfaction of a set of synthesis criteria: that the linkage pass through some fixed points, that it be subject to a set of constraints, and that the ground pivots be assigned. This is a little different from what has gone before because I am distinguishing two different kinds of constraints, one associated directly with the synthesis problem, and the other, the ground pivot specification, associated with exterior considerations. In a real problem, there will be other considerations external to the synthesis problem, considerations of materials, cost, and the like. In the language of optimal design, the synthesis constraints, say, the path specification, would be

specified by an *objective function.* This would be a quantitative expression of the difference between the linkage position and the desired linkage position at each of the precision points. The task would be to make this objective function equal to zero under the constraints of specified ground pivots.

The generalization is in the objective function. Rather than ask it to be the very special function just described, let it be the mean-square distance of the coupler point from some specified curve. The path synthesis problem was to make the coupler path fit exactly on a given curve at a specified number of points. The new optimum design path synthesis problem is to minimize the mean-square discrepancy from the given path. The average distance cannot be made equal to zero, but it can be minimized, and the coupler curve giving the minimum discrepancy is the optimal coupler curve in the sense of the specific objective function.

Unfortunately, a disquisition on how to do this is beyond the scope of this text. This is, however, an important synthesis technique, and interested readers should explore this on their own. It can also be generalized further. For example, one could ask for a minimum weight mechanism satisfying one of the exact coupler curve problems explored throughout the text. The objective function would then be the weight of the mechanism, and the path synthesis, old style, would function as one of the constraints.

EXERCISES

1. Write a set of constraint equations for the eight-bar linkage shown in Figure 2.9, assuming the path point P to be on link 5.
2. How many precision points can be specified for the linkage of Figure 2.9
   a. with ground pivot specification?
   b. with ground pivot specification and timing?

PART V

Forces and Moments

Chapter 10

Fundamentals of Kinetic Analysis

The analysis and synthesis so far explored has been purely geometrical and kinematical. Mechanisms have been synthesized that (approximately) follow specified motions. No mention has been made of the power required to drive these mechanisms nor of the forces required in the various links. The even simpler question of the speed with which the members move has been only very lightly touched on, in the context of timing and the synthesis of quick return mechanisms. These are important topics if one is to design a real mechanism.

Any link is a real extended physical object, obeying the laws of dynamics. In the design of mechanisms, links are usually taken to be rigid bodies, so that the relevant laws are those of rigid-body dynamics: the conservation of momentum and the conservation of moment of momentum (angular momentum). These basic principles, laid down by Euler over 200 years ago, are covered in any elementary dynamics text (e.g., Beer and Johnston 1984), and the reader might well review that material, although the presentation here is self-contained.

The kinetics of a mechanism can be studied at many levels of approximation. The lowest level of approximation is that already covered: total neglect. To deduce other useful levels of approximation, consider the dynamic behavior of a link in a bar mechanism. The general link is rotating and translating, and it is connected to the rest of the mechanism by two or more joints. It may also be connected, directly or indirectly, to the output of the mechanism. Figure 10.1 shows an isolated coupler. There will be forces at B and C from the rest of the mechanism, and there may be a force at P if the coupler is connected to a load. Let $\mathbf{V}$ denote the translational velocity of the coupler and $\boldsymbol{\Omega}$ its instantaneous rotation. Let $\mathbf{F}_B$, $\mathbf{F}_C$, and $\mathbf{F}_P$ denote the forces at the three positions, and let $\mathbf{R}_{BP}$, $\mathbf{R}_{BC}$ denote the vectors from B to P and C, respectively. Let M denote the mass of the coupler and I_B its moment of inertia with respect to B. Using a dot to denote differentiation with respect to time, the dynamic equations may be written

$$M\dot{\mathbf{V}} = \mathbf{F}_B + \mathbf{F}_C + \mathbf{F}_P \tag{10.1a}$$

$$I_B\dot{\boldsymbol{\Omega}} = \mathbf{R}_{BP} \times \mathbf{F}_P + \mathbf{R}_{BC} \times \mathbf{F}_C \tag{10.1b}$$

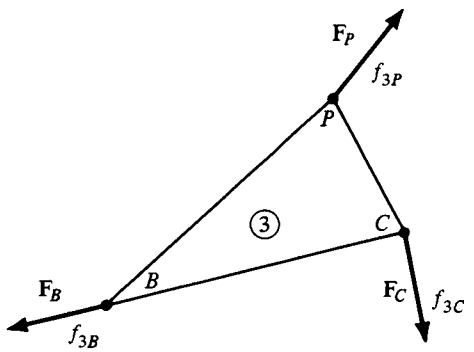

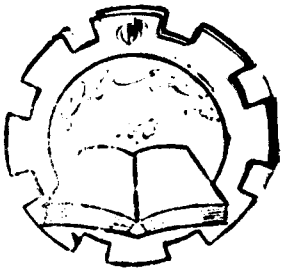

FIGURE 10.1 *The free-body diagram of a coupler showing the forces on the coupler from the crank* F_B*, the follower* F_C*, and whatever load is at point* P, F_P.

I have returned briefly to vector notation to introduce this new material. These equations are valid in three dimensions, and they should be familiar. They will be recast in complex variable notation in the next section, and that notation will then be used throughout the rest of the book.

An important approximation is the *quasistatic approximation,* for which the left-hand side of each equation is negligible compared to the right-hand side, and the dynamics problem reduces to a statics problem: the sum of the forces and the sum of the moments both vanishing. This approximation is appropriate if either the linear and angular accelerations, or the mass and moment of inertia, are small enough to justify neglecting the left-hand sides.

Most mechanisms are required to transmit forces to provide a useful output from a given input. The forces required to drive the mechanism itself ought to be small. Any forces used to move the links require additional input for a given output. Thus, properly designed mechanisms will satisfy the quasistatic approximation. In designing mechanisms, then, the quasistatic approximation will be assumed. *It is important to verify, after the fact, that the assumption was justified.* You must calculate the inertial forces and moments [the left-hand sides of Equations (10.1a) and (10.1b)] and compare these to the others to be sure that they are negligible.

In the quasistatic analysis of mechanisms, then, the problems reduce to analysis of free-body diagrams and the calculation of resultant forces. These familiar things need only be put into complex-variable language to be integrated into the developing kinematic lore of this text. To that end, it is necessary to look at complex forces and to develop expressions for velocity, acceleration, and their angular counterparts. This will be done in the next two sections.

FORCES, MOMENTS, RESULTANTS, AND THE FREE-BODY DIAGRAMS

This section deals with the calculation of static forces and moments using the complex-variable notation for bar linkages. The extension to dynamics is straightforward; one needs merely to include the inertial reaction forces. This will be considered in Chapter

11. Some general principles are worth noting. A pin joint cannot transmit moments. Just as in statics, a two-force member, one loaded only through two pins, is loaded along a line connecting the two pins. This will be of immense help in performing analyses. It is necessary to distinguish between free pins and driving pins. In a crank-rocker mechanism, for instance, the pins connecting the crank to the coupler, pin B in our standard notation, and the pin connecting the coupler to the follower, pin C, are all free pins and cannot support moments. (This changes if friction is allowed. That will be considered in Chapter 11.) The pin connecting the crank to the frame, pin A, is not free. In a real crank-rocker mechanism, the prime mover—some motor, perhaps—is connected to the crank at A in a way that allows the transmission of torque to the mechanism, perhaps through a keyed shaft. In performing a force analysis, it is important to be careful about this distinction. Most, but not all, pins are free.

Some additional notation is required for this section. A force on link j will be denoted by the complex number f_j. I will use η to denote the argument of f, subscripted if necessary to resolve ambiguity. That is, $f = |f|e^{i\eta}$. A second subscript will be used to denote the application point of a force: f_{jP} represents a force on link j acting at point P.

Figure 10.1 is a free-body diagram of a link. Let it be a coupler, and denote it by link 3. There are forces at points B, C, and P, so that the quasistatic version of Equation (10.1a) is just

$$0 = f_{3B} + f_{3C} + f_{3P} \tag{10.2}$$

The sum of the moments about B requires some additional thought and manipulation, using what has already been derived. First, recall that

$$\begin{aligned} \mathbf{R}_{PB} &\rightleftarrows z_P - z_B \\ \mathbf{R}_{CP} &\rightleftarrows z_C - z_B \end{aligned} \tag{10.3}$$

Then, note that

$$\mathbf{R}_{PB} \times \mathbf{F}_P \rightleftarrows \text{Im}\{(z_P - z_B)^* f_{3P}\} \tag{10.4}$$

so that Equation (10.1b) has the specific realization

$$0 = \text{Im}\{(z_P - z_B)^* f_{3P}\} + \text{Im}\{(z_C - z_B)^* f_{3B}\} \tag{10.5}$$

Euler's equations of motion for a single link referred to an arbitrary point O are then

$$0 = f_A + f_B + \cdots + f_N \tag{10.6a}$$

$$0 = \text{Im}\{(z_A - z_O)^* f_A\} + \text{Im}\{(z_B - z_O)^* f_B\} + \cdots + \text{Im}\{(z_N - z_O)^* f_N\} \tag{10.6b}$$

Application of these equations can be illustrated by finding the moment (torque) at the crank base, point A in a standard four-bar linkage, for an arbitrary force applied

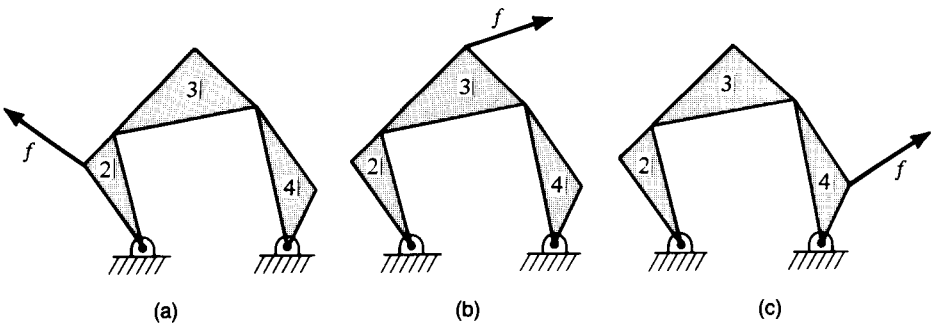

FIGURE 10.2 *A four-bar mechanism loaded at each of its three moving links:* (a) *loaded crank;* (b) *loaded coupler;* (c) *loaded follower.*

to any link in a four-bar linkage. Figure 10.2 shows the various possibilities. If the force is applied to the crank, a very simple problem results. Taking moments about A leads directly to the moment at A,

$$M_A + \text{Im}(z_{PA}{}^*f) = 0 \tag{10.7}$$

where z_{PA} is the complex vector at P with respect to A. In general, I will write $z_P - z_{P'} = z_{PP'}$ in direct analogy to the vector notation introduced in Chapter 3.

If f is applied to the coupler (link 3), summing the moments about B gives the scalar reaction force at C, $f_{3C}e^{-i\theta_4}$, and force equilibrium then gives the total force at B, f_{3B}. The force on the crank at B is then $f_{2B} = -f_{3B}$, and the sum of the moments about A then gives the moment required for equilibrium. The sequence of calculations is as follows. Diagrams are shown on Figure 10.3.

First, take the sum of the moments about B,

$$\text{Im}(z_{PB}{}^*f) + \text{Im}(z_{CB}{}^*) = 0 \tag{10.8}$$

Link 4 is a two-force member, so that the forces f_{4C} and f_{4D} are both parallel to z_4. The force on the coupler at C, $f_{3C} = -f_{4C}$, and so it too is parallel to z_4. Thus,

$$f_{3C} = \pm|f_{3C}|e^{i\theta_4}$$

It is inconvenient to carry the $\pm$ sign around. To avoid that, note that

$$f_{3C} = f_{3C}e^{-i\theta_4}e^{i\theta_4} = [f_{3C}e^{-i\theta_4}]e^{i\theta_4}$$

Because f_{3C} is parallel to z_4, the quantity in square brackets is a real number equal to $\pm\,|f_{3C}|$. This decomposition will be used any time the direction of a force is

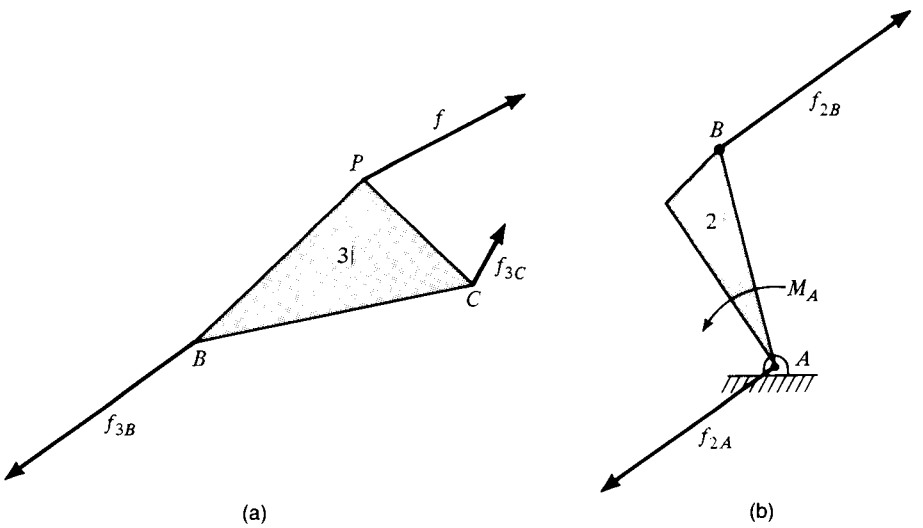

FIGURE 10.3 *Free-body diagrams for the coupler and the crank, assuming a uniform force on the coupler point* P: (a) *the coupler;* (b) *the crank.*

known, and the real number will be called the *scalar force.* Solving for the scalar force and recombining give

$$f_{3C} = -\{\text{Im}(z_{PB}{}^*f)/\text{Im}(z_{CB}{}^*e^{i\theta_4})\}\, e^{i\theta_4} \tag{10.9a}$$

$$= -\{\text{Im}(z_{PB}{}^*f)/\text{Im}(z^*z_4)\}\, z_4 \tag{10.9b}$$

In the second line, I have multiplied by r_4/r_4 and noted that $z_{CB} = z_3$.

Force equilibrium on link 3 can be written

$$f + f_{3B} + f_{3C} = 0 \tag{10.10}$$

so that the unknown force

$$f_{3B} = -f - f_{3C} = -f + \{\text{Im}(z_{PB}{}^*f)/\text{Im}(z_3{}^*z_4)\}\, z_4 \tag{10.11}$$

This can be transferred to the crank because $f_{2B} = -f_{3B}$, and then taking moments about A gives

$$M_A + \text{Im}[z_2{}^*f_{2B}] = 0 \tag{10.12}$$

from which

$$M_A = \text{Im}\{z_2{}^*[f - \{\text{Im}(z_{PB}{}^*f)/\text{Im}(z_3{}^*z_4)\}\, z_4]\}$$

$$= \text{Im}[z_2{}^*f] - \{\text{Im}(z_{PB}{}^*f)/\text{Im}(z_3{}^*z_4)\}\, \text{Im}[z_2{}^*z_4] \tag{10.13}$$

If f is applied to link 4, there is one more step in the analysis. The coupler is a free link, and $f_{3C} = [f_{3C}e^{-i\theta_3}]e^{i\theta_3}$. The sum of the moments about D can be written

$$\text{Im}\{z_{PD}{}^*f\} + \text{Im}\{(-z_4{}^*)(-[f_{3C}e^{-i\theta_3}]e^{i\theta_3})\} = 0 \tag{10.14}$$

from which

$$[f_{3C}e^{-i\theta_3}] = -\frac{\text{Im}\{z_{PD}{}^*f\}}{\text{Im}\{z_4{}^*e^{i\theta_3}\}}$$

The sum of the forces on the coupler can be written

$$f_{3C} + f_{3B} = 0$$

from which

$$f_{3B} = \frac{\text{Im}\{z_{PD}{}^*f\}}{\text{Im}\{z_4{}^*e^{i\theta_3}\}}e^{i\theta_3} = \frac{\text{Im}\{z_{PD}{}^*f\}}{\text{Im}\{z_4{}^*z_3\}}z_3$$

and

$$f_{2B} = -f_{3B} = \frac{\text{Im}\{z_{PD}{}^*f\}}{\text{Im}\{z_4{}^*z_3\}}z_3 \tag{10.15}$$

Finally, the moment balance about A can be written

$$M_A + \text{Im}(z_2{}^*f_{2B}) = 0$$

from which

$$M_A = \{\text{Im}[z_{PD}{}^*f] \cdot \text{Im}[z_2{}^*z_3]\}/\text{Im}[z_4{}^*z_3] \tag{10.16}$$

The quasistatic analysis neglects the mass of the links, and that approximation will be maintained through this chapter. However, forces in a running linkage are generated by the need to accelerate the load—whatever the mechanism is driving. This is done using D'Alembert's principle, according to which minus the product of the mass and its acceleration appears as an *inertial force* applied to the linkage.

INERTIAL FORCES

The first application will be to a general four-bar linkage that is supposed to be driving a mass m along some path. To simplify the moment analysis, the mass will be assumed to be a point mass. The path will be a coupler curve, and the notation will be the standard notation used in discussing coupler curves. Figure 10.4 will refresh the reader's memory. In the spirit of quasistatic analysis, the masses of the links will be neglected. The mechanism will be supposed to be driven by uniform rotation of the crank at a

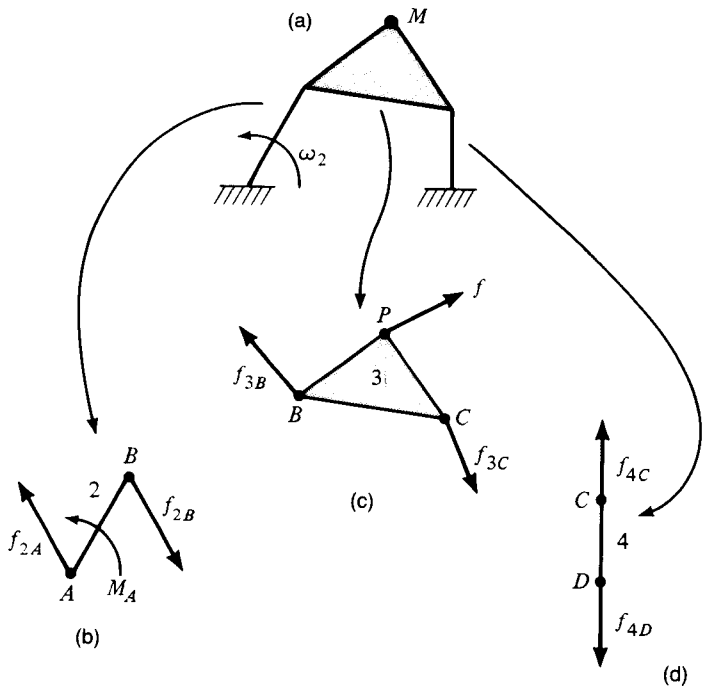

FIGURE 10.4 *A four-bar mechanism with a point mass attached to the coupler:* (a) *the mechanism;* (b) *free-body diagram of the crank;* (c) *free-body diagram of the coupler;* (d) *free-body diagram of the follower.*

rate $\dot{\theta}_2 = \omega_2$. The task is to find the torque required to drive the mechanism as a function of position and, hence, time.

The position of the mass as a function of time is given by $z_P = z_2 + w_2 = z_2 + q_3 z_3$. The velocity and acceleration of the mass are obtained by differentiation:

$$\dot{z}_P = \dot{z}_2 + \dot{w}_2 = i\omega_2 z_2 + i\omega_3 w_2 \tag{10.17a}$$

$$\dot{z}_P = \dot{z}_2 + \dot{w}_2 = -[\omega_2^2 + i\dot{\omega}_2]z_2 - [\omega_3^2 + i\dot{\omega}_3]w_2 \tag{10.17b}$$

The mass is being driven by the coupler, so that the coupler feels the reaction force $-m\ddot{z}_P$.

Figures 10.4b–10.4d shows the free-body diagrams for all three links. The mass on link 3 provides an inertial force to load link 3. Link 3 is not a free link. The analysis is exactly parallel to that for a static load on link 3, presented earlier, from Equations (10.8)–(10.13), with $f = -m\ddot{z}_P$. That is, one proceeds as follows:

1. Note that link 4 is a two-force member to obtain the direction of f_{3C}.
2. Take moments about B to find the magnitude of f_{3C}.
3. Use force equilibrium on link 3 to find f_{3B}.
4. Apply $f_{2B} = -f_{3B}$ to the crank to find M_A.

The result of these steps is

$$M_A = \text{Im}\{z_2{}^* m\ddot{z}_P\} - \frac{\text{Im}[z_2{}^* z_4]}{\text{Im}[z_3{}^* z_4]} \text{Im}[w_2{}^* m\ddot{z}_P] \tag{10.18}$$

where $\ddot{z}_P$ is given by Equation (10.17b).

To evaluate that expression, the rates of change of θ_3, $\dot{\theta}_3$, and $\ddot{\theta}_3$ are needed. These can be obtained using the algorithms outlined in Chapter 9. Thus, the solution given in Equation (10.18) is really the last step in a chain of algorithms, not a formula into which one would plug values. Actual calculation will be discussed in Chapter 11. I have displayed it to emphasize a geometric property of four-bar linkages. Note that the moment at A is formally infinite for almost any applied force if $\text{Im}\{z_3{}^* e^{i\theta_4}\} = 0$. This term is zero when the coupler and follower are aligned. The condition of alignment is called a *change point* or a *toggle point.* The angle between the coupler and the follower is called the *transmission angle.* At a toggle point, the transmission angle is zero or π.

Not only is the driving torque formally infinite at a change point, but the path of the mechanism is ambiguous. Figure 10.5 shows a mechanism at a change point and the two paths available to it near the change point. Change points are tricky and require considerable thought on the part of the designer. Sometimes it is necessary to provide guidance through the change points to prevent the system from reversing the sense of the output (follower) rotation. In other circumstances, the inertia of the system is adequate to carry the mechanism smoothly through the change point. A one-time common linkage with change points was the drive mechanism for the steam locomotive. [For a wealth of information on steam locomotives and their mechanics, see Tann (1981) and Warren (1970).]

If the load is applied to the follower, either as a force somewhere on the linkage or as a torque at D, the expressions simplify. Point P moves to C, and the effective force f_{3P} is now parallel to z_3, because the coupler is now loaded only through its pins. Again, the analysis follows the static analysis given in the preceding section. A free-body analysis of the follower gives the force at C in terms of the output torque M_D.

$$[f_{4C} e^{-i\theta_3}] = -M_D / \text{Im}\{z_4{}^* e^{i\theta_3}\} \tag{10.19}$$

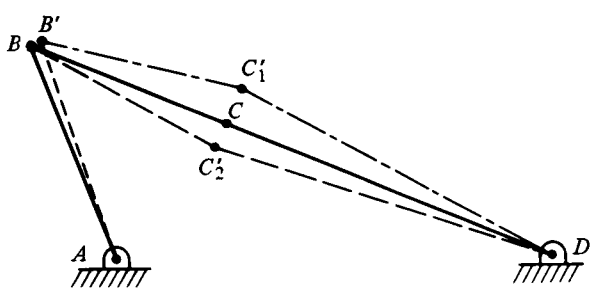

FIGURE 10.5 *A four-bar mechanism shown passing through a change point. As the crank moves from* B *to* B′, *point* C *may move to either* C_1' *or* C_2'.

The effective f_{3P} is the negative of the force on the follower at C,

$$f_{3P} = M_D e^{i\theta_3} / \text{Im}\{z_4^* e^{i\theta_3}\} \tag{10.20}$$

and this is balanced by the force at B, so that

$$f_{3B} = -M_D e^{i\theta_3} / \text{Im}\{z_4^* e^{i\theta_3}\} \tag{10.21}$$

Finally, the torque balance at A gives

$$\begin{aligned} M_A &= -M_D \text{Im}\{z_2^* e^{i\theta_3}\} / \text{Im}\{z_4^* e^{i\theta_3}\} \\ &= -M_D [r_2 \sin(\theta_3 - \theta_2)] / [r_4 \sin(\theta_3 - \theta_4)] \end{aligned} \tag{10.22}$$

Equation (10.22) can be obtained directly from (10.18) by putting f_{3P} equal to the expression (10.20) and letting point P move to C. The first term on the right-hand side of Equation (10.18) is then identical to the right-hand side of Equation (10.22), and the second term vanishes because, when P moves to C, w_2 becomes equal to z_3 and, thus, $\text{Im}\{w_2^* f_{3P}\} = 0$ because the two vectors are parallel.

The ratio of the output torque to the input torque, here M_D/M_A, is called the *mechanical advantage* of the linkage. It is given by

$$\begin{aligned} M_D/M_A &= -\text{Im}\{z_4^* e^{i\theta_3}\} / \text{Im}\{z_2^* e^{i\theta_3}\} \\ &= -[r_4 \sin(\theta_3 - \theta_4)] / [r_2 \sin(\theta_3 - \theta_2)] \end{aligned} \tag{10.23}$$

Note that this is equal to ω_2/ω_4. In crank follower pairs, $\omega_2 M_A = \omega_4 M_D$; the power in is equal to the power out. This is consistent with the neglect of the inertia of the links and friction in the joints.

As in the more general case, the mechanical advantage is zero when the coupler and follower are parallel, or *in toggle*. For this special case, the mechanical advantage can be seen to be infinite when the crank and coupler are in toggle. Both the auto window mechanism (Figure 1.6) and the vise-grip pliers (Figure 1.7) introduced in Chapter 1 take advantage of this. The window linkage uses both toggle positions. The "inner" toggle, with z_2 and z_3 antiparallel, is used to lock the window closed. The "outer" toggle, with z_2 and z_3 parallel, is used to resist the wind pressure trying to close the window when it is open. When the vise grips are locked, the crank and coupler are in the outer toggle position.

THE SLIDER CRANK

The analysis so far has been formulated in terms of the four-bar mechanism. The slider-crank can be fit into the same format. The obvious problem is to find the torque

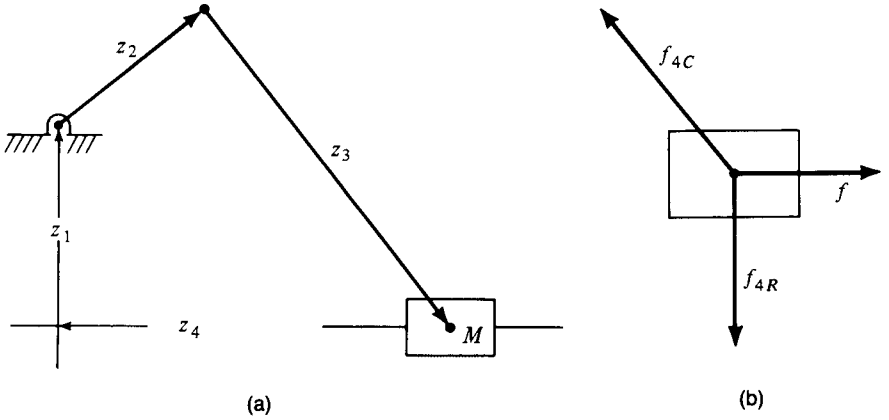

FIGURE 10.6 *A slider-crank mechanism, taking account of the mass of the slider:* (a) *the mechanism;* (b) *free-body diagram of the slider.*

required to drive the slider. Note that there are two levels of approximation available: the output force can be considered to be constant, or the output can be supposed to drive a point mass. If the system is operating in "reverse," like an engine, then the force at the slider can be specified as a function of time, and the torque at the crank can be found. In this problem, there must also be a load on the crank or the dynamics cannot be solved. This problem will be addressed in Chapter 11. Figure 10.6 is a definition sketch of the slider-crank mechanism.

The initial quasistatic analysis doesn't care what the imposed force on the slider is, an inertial force or an externally generated force. Figure 10.6b shows a free-body diagram of the slider. In addition to the imposed force f, there are reaction forces from link 3 and the guide that constrains the slider to move horizontally, the former parallel to link 3 and the latter perpendicular to the direction of motion of the slider, here defined as parallel to z_1. In general, there will also be friction forces from the guide. These will be assumed to be negligible for the present analysis.

As the forces on the slider all act at the slider center of reaction, point C, the notation already developed needs some help.

Let the force on the slider be f_4, and write

$$f_4 = [f] + [f_{4C}e^{-i\theta_3}]e^{i\theta_3} + [f_{4R}e^{-i3\pi/2}]e^{i3\pi/2} \tag{10.24}$$

where $[f]$ is the scalar imposed force and the other two terms on the right-hand side represent the reaction forces from link 3 and the guide, respectively.

In the quasistatic approximation, f_4 equals zero and Equation (10.24) can be solved for the two scalar reaction forces $[f_{4C}e^{-i\theta_3}]$ and $[f_{4R}e^{-i3\pi/2}]$. If f is an inertial force, caused by the motion, then f_4, as written in Equation (10.24), is still zero, but f will then depend on the position of the linkage. This issue will be deferred, and f

will be assumed to be constant. Then, considering, in turn, $e^{-i\theta_3}$ and $e^{-i3\pi/2}$ times Equation (10.24) and taking the imaginary part gives

$$[f_{4C}e^{-i3\pi/2}] = -[f]\{\sin(3\pi/2)/\sin(3\pi/2 - \theta_3)\} \tag{10.25a}$$

$$[f_{4R}e^{-i\theta_3}] = [f]\{\sin\theta_3/\sin(3\pi/2 - \theta_3)\} \tag{10.25b}$$

The remainder of the analysis is simple. The coupler merely transmits the force at C to B:

$$f_{3C} = -f_{4C}, \quad f_{3B} = -f_{3C} = f_{4C}, \quad f_{2B} = -f_{3B} = f_{3C} = -f_{4C} \tag{10.26}$$

EXERCISES

1. Find the moment at A required to maintain the six-bar linkage shown in the sketch in equilibrium (motionless).

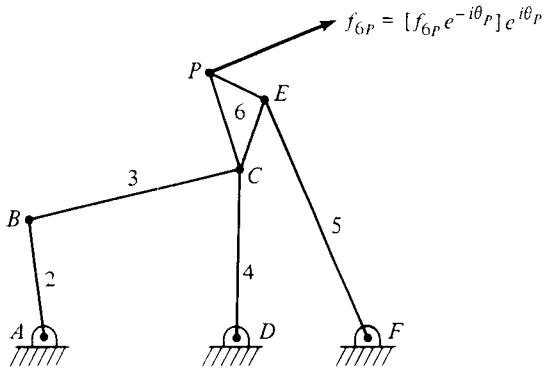

2. What is the reaction force at A for the four-bar linkage shown in the sketch?

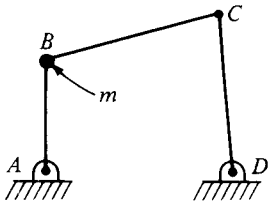

3. If the linkage of Exercise 1 is to be held in equilibrium by a moment (torque) at D, what is its magnitude?

4. For a complete cycle, $0 < \theta_2 < 2\pi$, for the slider-crank mechanism shown, plot the following quantities: position, velocity, and acceleration of point C; the force on link 3 at point C; and the moment at A (the shaft torque) required to drive the

mechanism. Let the mass of link 4 be 1 kg, and let the crank rotate at 900 rpm. Neglect gravity, friction, and the inertia of the other links.

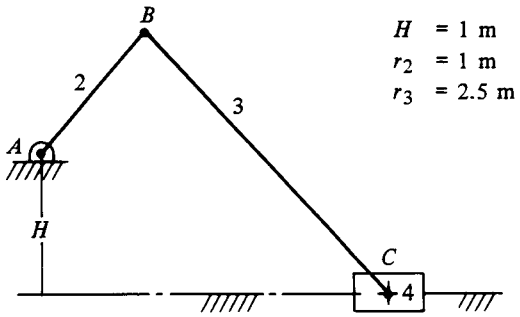

5. Let the mass at P be 5 kg, and let the crank rotation rate be 1 Hz. Plot the coupler curve, and plot both components of velocity and acceleration of point P for a complete cycle. Find the components of the force on link 3 at P. Assume the dimensions to be (in mm): $r_1 = 300$; $r_2 = 100$, $r_3 = 175$, and $r_4 = 175$, and let $w_2 = 0.8e^{i\pi/6}z_3$.

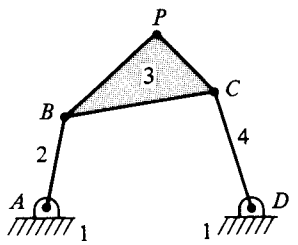

6. The crank shown is 1.4 m long. The angle $\theta_2 = at^2 + 3\pi/2$, where t denotes the time in seconds. The mass is 4 kg. The acceleration of gravity points down on the page and is equal to 9.8 m/s^2. Find the torque (moment) at A, at $t = 0.5$ s, if $a = 2.4$ rad/s^2.

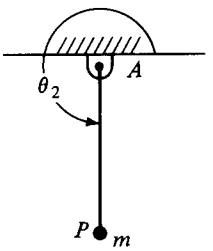

7. The force in a linear spring is equal to k times the difference between the stretched and relaxed length of the spring. This force is parallel to the spring. The spring shown is such a spring, and it has a relaxed length of 5. The link lengths are:

$r_1 = 4$, $r_2 = 1$, $r_3 = 5$, and $r_4 = 4$. Outline the procedure for calculating the torque at A for a complete crank cycle.

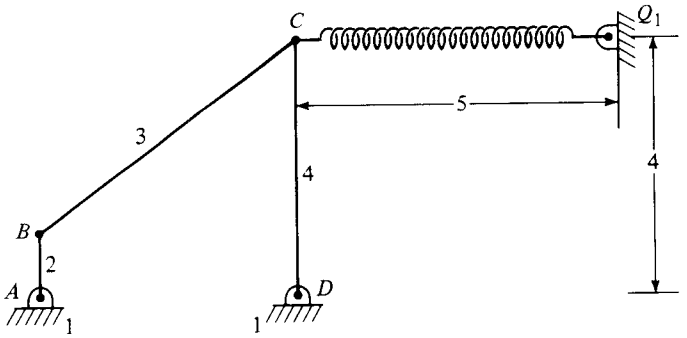

8. Find the moment at A for the preceding linkage when $\theta_2 = \theta_3 + \pi = 4.1888$ (240°).

Chapter 11

Friction and Inertia

In Chapter 10, forces and torques were considered for "perfect" mechanisms: frictionless mechanisms with massless links. Mechanisms were made to move with no care as to how this movement might be driven. A torque was needed; a torque was supposed to be available. These restrictions will be progressively relaxed in this chapter, and more realistic problems and tasks will be examined. In order to keep the new phenomena in clear focus, the mechanisms involved will be restricted to four-link mechanisms: four-bar linkages and slider-crank mechanisms. This chapter as a whole is designed to show just how far one can get with the simple tools introduced earlier in the text. It can be read as an introduction to further work in the dynamics of machinery and the design of moving systems.

Figures 11.1 and 11.2 show the most general four-bar linkage and the most general slider-crank systems with which this chapter will be concerned. All links will be supposed to have masses m_j and moments of inertia I_j, where j denotes the link number, as has been the case throughout the text. The moments of inertia will be taken with respect to the same point with respect to which the link angle is measured. That is, I_2 is measured with respect to A, I_3 with respect to B, and I_4 with respect to C. The four-bar linkage is assumed to be loaded through either the coupler or the follower, or both, by forces. Point moments at points P_3 and P_4 are excluded, although it should be reasonably clear how they could be added.

The slider crank is loaded through the slider, which is supposed not to rotate. Clearly, there are normal forces and torques developed at the sliding joint between the slider and the frame. Moments will not be considered in this chapter, and normal forces will be deferred until the final section. Because moments are neglected, the moment of inertia of the slider is irrelevant to this analysis.

The dynamics of the individual links are controlled by the general equations given at the beginning of Chapter 10, Equations (10.1a) and (10.1b). The complex two-dimensional forms of these equations can be written out for each individual link. The first line represents the balance of forces, where the force on link j at joint J is denoted by f_{jJ}. The second represents the balance of moments. The result for the four-bar linkage is

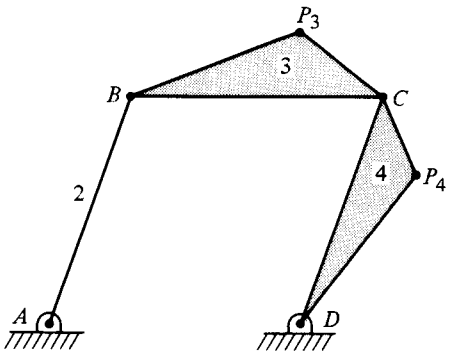

FIGURE 11.1 *Sketch of a four-bar linkage defining the notation used in this chapter. The notation is consistent with the notation used earlier.*

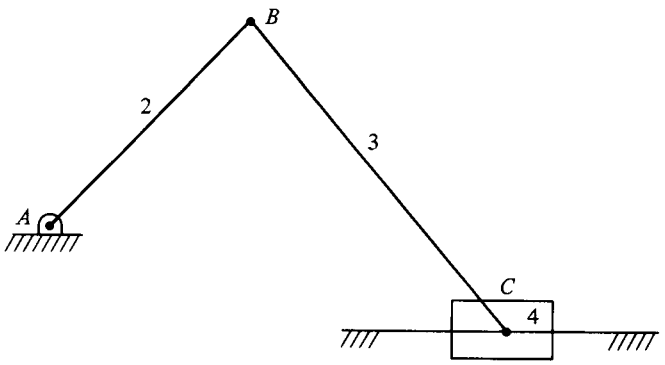

FIGURE 11.2 *Sketch of a slider-crank linkage defining the notation used in this chapter. The notation is consistent with the notation used earlier.*

Crank:

$$m_2\ddot{\zeta}_2 = f_{2A} + f_{2B}$$
$$I_2\ddot{\theta}_2 = M_{2A} + M_{2B} + \mathrm{Im}(z_2{}^* f_{2B}) \tag{11.1a}$$

Coupler:

$$m_3\ddot{\zeta}_3 = f_{3B} + f_{3C} + f_{3P_3}$$
$$I_3\ddot{\theta}_3 = M_{3B} + M_{3C} + \mathrm{Im}(z_3{}^* f_{3C}) + \mathrm{Im}(q_3{}^* z_3{}^* f_{3P_3}) \tag{11.1b}$$

Follower:

$$m_4\ddot{\zeta}_4 = f_{4C} + f_{4D} + f_{4P_4}$$
$$I_4\ddot{\theta}_4 = M_{4C} + M_{4D} + \mathrm{Im}(z_4{}^* f_{4D}) + \mathrm{Im}(q_4{}^* z_4{}^* f_{4P_4}) \tag{11.1c}$$

and, for the slider crank,

Crank:

$$m_2\ddot{\zeta}_2 = f_{2A} + f_{2B}$$
$$I_2\ddot{\theta}_2 = M_{2A} + M_{2B} + \mathrm{Im}(z_2{}^* f_{2B}) \tag{11.2a}$$

Coupler:

$$m_3\ddot{\zeta}_3 = f_{3B} + f_{3C}$$
$$I_3\ddot{\theta}_3 = M_{3B} + M_{3C} + \mathrm{Im}(z_3{}^* f_{3C}) \tag{11.2b}$$

Slider:

$$0 = \mathrm{Im}(f_{4C} + f_L + f_S)$$
$$m_4\,\mathrm{Re}(\ddot{\zeta}_4) = \mathrm{Re}(f_{4C} + f_L + f_S) \tag{11.2c}$$

where the ζ_j denote the vectors from A to the center of mass of the link, that is,

$$\zeta_4 = z_2 + z_3 + q_4 z_4$$

and similarly for the others. The complex number q_j in each expression is analogous to the number q_3 introduced previously to specify a coupler point in terms of z_3. For simple rods or bars, each q_j is simply 1/2.

The slider-crank equations can be obtained by reduction from the four-bar-linkage equations. The only slider-crank equations calling for comment are the last pair, Equation (11.2c). I have divided the force on the slider into two parts, f_L and f_S. The former includes any load attached to the slider or, if the mechanism is driven by the slider as in an internal combustion engine (to be explored at length later), the force applied to the slider, as well as the frame reaction force. The latter has a frictional component, directed parallel to link 4, and a side force directed perpendicular to the slider. In general, there will be a moment on the slider as well, as was noted earlier. Its computation is beyond the scope of this text, and further discussion would merely cloud the picture.

These equations are the general versions of those given in Chapter 10. Equations like (10.6) can be obtained from these general equations by elimination of the joint moments M_{jP} and the inertial terms on the left-hand sides.

FRICTION

Friction is a dissipative force acting to oppose motion. All real linkages have friction. The friction in a corkscrew is large and obvious. Friction in other mechanisms may be quite small. Commonly, one designs mechanisms to have little friction, as friction is

usually a loss. Zero friction is, of course, impossible; any mechanism without friction, once set in motion, would run forever, and this is contrary to intuition and experience. Friction makes such perpetual motion impossible.

Friction can be divided into *dry friction* and *lubrication.* For lightly loaded, noncritical, and inexpensive mechanisms, the trouble and expense of adding lubricated bearings is not worthwhile. In most other circumstances, lubrication is well worth the effort.

Dry friction is frequently characterized using the Amonton–Coulomb friction rule (*Coulomb friction*): the friction force is proportional to the normal force and independent of the contact area. The proportionality constant is called the coefficient of friction, usually symbolized by μ. Frequently, a distinction is made between the coefficient of static friction and the coefficient of sliding friction, the latter being smaller when they are different. The image usually presented in statics (cf. Beer and Johnson 1977) is that of a block on an inclined plane. If the plane is inclined steeply enough, the block will slide. The coefficient of static friction is the tangent of the angle at which sliding just begins. The coefficient of sliding friction is less than, or equal to, the static coefficient. It can be determined, in principle, by the final equilibrium sliding speed down an infinite inclined plane. This point will not be pursued further here.

Lubricated mechanisms can be analyzed using standard lubrication analyses based on the Reynolds equation. [The Reynolds equation was first derived by Osbourne Reynolds (1886). Its derivation can be found in any modern book on lubrication theory, e.g. Gross (1980).] In such circumstances, the friction force is relatively insensitive to the load but is proportional to the sliding speed between the two moving surfaces. I will use a simplified model of both sliding and rotating friction, assuming the friction force (or torque) to be proportional to the relative speed between two links, either rotational or sliding. Friction opposes the motion. For rotational friction, the friction acts as a moment; for sliding friction, it acts as a force. The reader familiar with the language of applied differential equations will recognize this form of friction as being identical to the *damping terms* introduced in simple dynamical systems, such as the harmonic oscillator or the one-dimensional wave equation.

Rotational friction depends on the speed with which the angle between two links is changing, on the rate of change of the *difference* between two link angles. If the angle between links 2 and 3 is increasing, then friction, which acts to retard the motion, appears as a positive moment on link 2 and a negative moment on link 3. This is, of course, general. If the joint moments appearing in Equations (11.1) and (11.2) are restricted to frictional moments, as they will be for all the joints except A, they can be written out as

$$M_{2B} = -M_{3B} = \mu_B(\dot{\theta}_3 - \dot{\theta}_2) = \mu_B(\omega_3 - \omega_2) \tag{11.3}$$

$$M_{3C} = -M_{4C} = \mu_C(\dot{\theta}_4 - \dot{\theta}_3) = \mu_C(\omega_4 - \omega_3) \tag{11.4}$$

$$M_{4D} = -\mu_D\dot{\theta}_4 = -\mu_D\omega_4 \tag{11.5}$$

where the three coefficients μ_B, μ_C, and μ_D denote effective friction coefficients for the bearings, and ω denotes the derivative with respect to time of θ, the notation intro-

duced in Chapter 6. The effective friction coefficients have the units of moment times time. In SI units, these are N-m-s, or kg-m^2/s.

Sliding friction opposes the motion of the slider, so that its action on the slider is negative when the slider is moving to the right and positive when the slider is moving to the left. Rightward motion corresponds to increasing r_4, and vice versa, and so the sliding friction for a slider-crank mechanism can be written

$$f_S = -\mu_S \dot{r}_4 = -\mu_S v_4 \tag{11.6}$$

when the subscript S denotes *sliding* and v_4 the rate of change of r_4. The coefficient μ_S has the dimensions of force divided by velocity. In SI units, this is N-s/m, or kg/s.

Some Friction Examples

The Four-Bar Linkage

The simplest four-bar friction analysis is one for which only μ_D is nonzero. This is also a model for a system in which the output torque of the follower is proportional to the rotation rate of the follower. More complicated output forces are possible, but I will not address them here. Two cases can be examined for this simple case: a fixed shaft rotation rate, ω_2, or a fixed torque applied at the shaft, M_{2A}. In the former case, the problem is to determine the required torque; in the latter, the shaft rotation. Both of these will be functions of time. The analysis is the same in this special simple case. Shaft rotation and torque turn out to be proportional, and all that is necessary is to find the relation connecting the two.

In this simple case, the reduced version of the second of Equations (11.1a) shows that the shaft torque M_{2A} depends only on f_{2B} and the position of the linkage. (As with all analyses beyond the simple position analysis, it is assumed that a position analysis routine is available, so that it is enough to specify the dimensions of the linkage and the behavior of the crank to know the position, velocity, and acceleration of all the links. Programs like those developed in Chapter 5 will serve.) Because inertia has been neglected and no external forces are applied to any of the links, all the forces are equal in magnitude and direction and are alternating in sign. Thus,

$$f_{2B} = f_{3C} = f_{4D} \tag{11.7}$$

Because there is no frictional moment at B or C, the technique used in Chapter 10 to isolate two-force members can be applied to the coupler, link 3. That is, link 3 is a two-force member, and the link force can be written in terms of the scalar force representation, namely,

$$f_{3C} = [f_{3C}e^{-i\theta_3}]e^{i\theta_3} = f_{4D} \tag{11.8}$$

Substituting this into the reduced version of the second of Equations (11.1c) gives an expression for the scalar force

$$[f_{3C}e^{-i\theta_3}] = -\frac{M_{4D}}{r_4 \sin(\theta_3 - \theta_4)} = \frac{\mu_D \omega_4}{r_4 \sin(\theta_3 - \theta_4)} \tag{11.9}$$

where the second right-hand side is obtained by substituting for the frictional moment from Equation (11.5). The force is now known, and it is easy to find the moment at A:

$$M_{2A} = -\mu_D \omega_4 \frac{r_2 \sin(\theta_3 - \theta_2)}{r_4 \sin(\theta_3 - \theta_4)} \tag{11.10}$$

The techniques explored in Chapter 6 can be used to find ω_4. Substituting for ω_4 from Equation (6.7) gives the final expression for the shaft torque in terms of the shaft rotation rate

$$M_{2A} = \mu_D \omega_2 \frac{r_2^2 \sin^2(\theta_3 - \theta_2)}{r_4^2 \sin^2(\theta_3 - \theta_4)} \tag{11.11}$$

If the crank rotation ω_2 is given, the shaft torque M_{2A} can be found; if M_{2A} is given, ω_2 can be found.

The behavior of the torque (or of the rotation) depends on the nature of the linkage and varies with position during each cycle. The torque required to keep the linkage moving goes to infinity when the linkage moves into toggle. Friction cannot resolve this difficulty. It is inherent in the geometry. Figure 11.3 shows the torque as a function of crank angle for three crank-rocker linkages, identical except for the follower length. The common lengths are: $r_1 = 100$, $r_2 = 10$, and $r_3 = 80$. The follower lengths for the three cases, a, b, and c, are $r_{4a} = 40$, $r_{4b} = 50$, and $r_{4C} = 60$. The figures were prepared using a realization of the pseudocode given later as Program 11.1. (Some additional friction examples will be presented in the next section.) As the follower length increases, the minimum difference between the coupler and follower angles decreases. That is, the linkage moves further and further from a change point (from being in toggle), and the magnitude of the maximum moment decreases. There are two maxima, approximately 180° apart, one corresponding to the follower moving to the right and one to the follower moving to the left. Note also that the position of the maxima changes somewhat with linkage geometry, although the effect is small for the small changes in geometry explored here. The reader is encouraged to construct a personal code and explore a wider variety of cases at leisure.

The problem is made somewhat more complicated if all three undriven joints are allowed to have frictional torques, so that all three μ are nonzero. There are now no two-force members; both the coupler and the follower have moments applied to their ends. The analysis is still fairly simple. It can be done directly, without need for successive approximations, because all the force balance equations still involve only two forces so that, as previously, the forces all have equal magnitude and alternating sign. In this case, however, the direction is not known a priori but must be found from the analysis.

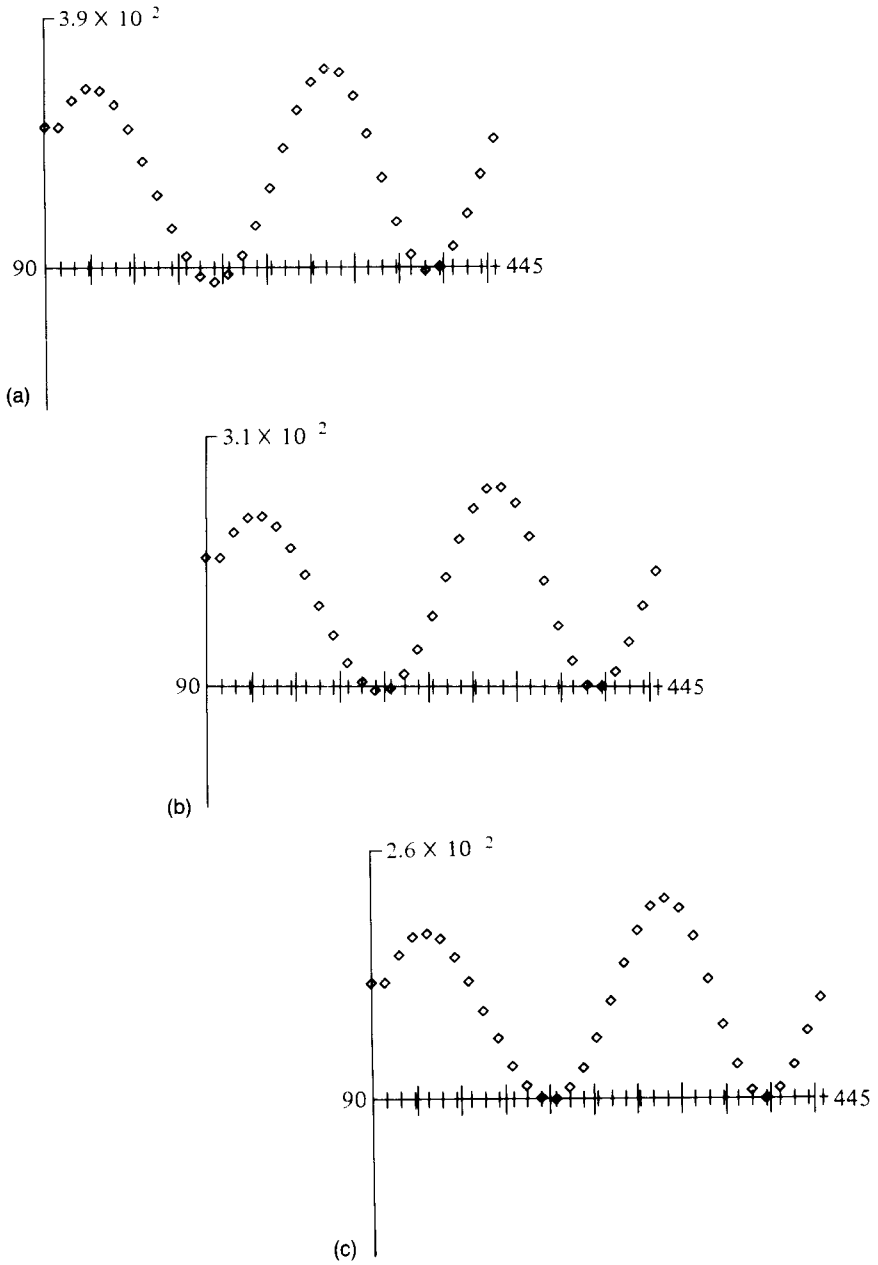

FIGURE 11.3 *Shaft torque as a function of follower length during one crank revolution:* (a) *follower length = 40;* (b) *follower length = 50;* (c) *follower length = 60. Crank length = 10, coupler length = 80, and shaft to output (frame) distance = 100. Torque units are arbitrary; the crank angle varies from 90 to 450° (see text).*

To simplify the notation, let the joint friction coefficients be equal, so that

$$\begin{aligned} M_{2B} &= M_B = -M_{3B} \\ M_{3C} &= M_C = -M_{4C} \\ M_{4D} &= M_D \end{aligned} \tag{11.12}$$

and

$$f_{2B} = f_{3C} = f_{4D} = f = -f_{3B} = -f_{4C} \tag{11.13}$$

With these definitions, the three force equations are satisfied identically, and the three moment equations become

$$0 = M_{2A} + M_{2B} + \text{Im}(z_2{}^*f) \tag{11.14}$$

$$\begin{aligned} 0 &= -M_{2B} + M_{3C} + \text{Im}(z_3{}^*f) \\ 0 &= -M_{3C} + M_{4D} + \text{Im}(z_4{}^*f) \end{aligned} \tag{11.15}$$

The first of these will serve to determine the required driving moment, once the force has been determined. The two equations (11.15) can be viewed as giving the value of two projections of f: one along z_3 and one along z_4. As long as the two links are not parallel—a situation that has already been seen to be singular—these two projections are independent and can be used to determine f. Let

$$f = \text{Re}(f) + i\,\text{Im}(f)$$

In terms of this Cartesian notation, the two equations (11.15) can be rewritten as the algebraic pair

$$\begin{aligned} -r_3 \sin\theta_3\,\text{Re}(f) + r_3 \cos\theta_3\,\text{Im}(f) &= M_{2B} - M_{3C} \\ -r_4 \sin\theta_4\,\text{Re}(f) + r_4 \cos\theta_4\,\text{Im}(f) &= M_{3C} - M_{4D} \end{aligned} \tag{11.16}$$

from which the Cartesian components (the real and imaginary parts) of f can be determined. These can be substituted into Equation (11.14) and, after some manipulation and simplification, the moment at A can be written

$$M_A = -M_B + \frac{r_2 \sin(\theta_2 - \theta_4)}{r_3 \sin(\theta_3 - \theta_4)}(M_B - M_C) + \frac{r_2 \sin(\theta_3 - \theta_2)}{r_3 \sin(\theta_3 - \theta_4)}(M_C - M_D) \tag{11.17}$$

All three moments are proportional to the first time derivatives of the link angles, as shown in Equations (11.3)–(11.5), and all the derivatives can be related to ω_2 using Equations (6.6) and (6.7), so that Equation (11.17) can be rewritten as a relation between the shaft torque M_{2A} and the shaft rotation rate ω_2.

The following program will calculate the shaft torque as a function of crank position, assuming that the procedures at the beginning to find velocity and position are available. It is an obvious implementation of Equations (11.3)–(11.5). This pseudocode assumes the existence of (1) a position code such as that outlined in pseudocode as Program 5.5, or its Newton–Raphson equivalent, Program 5.8; and (2) a velocity and acceleration program such as that outlined as Program 6.1. The moment procedure is shown explicitly.

PROGRAM 11.1: SHAFT TORQUE FOR FOUR-BAR LINKAGE WITH VISCOUS FRICTION

procedure velocity $(\theta_2, \omega_2, r_1, r_2, r_3, r_4, \omega_3, \omega_4)$

procedure position $(\theta_2, r_1, r_2, r_3, r_4, \theta_3, \theta_4)$

procedure moments $(\theta_2, r_1, r_2, r_3, r_4, \theta_3, \theta_4, \mu_B, \mu_C, \mu_D, M_{2B}, M_{3C}, M_{4D})$

begin

$M_{2B} = \mu_B(\omega_3 - \omega_2)$

$M_{3C} = \mu_C(\omega_4 - \omega_3)$

$M_{4D} = -\mu_D\omega_4$

end

enter $(\omega_2, r_1, r_2, r_3, r_4)$

enter $(\theta_2, \delta\theta_2, n)$

enter (μ_B, μ_C, μ_D)

for $i = 1$ to n **do**

$\theta_2 = \theta_2 + \delta\theta_2$

position $(\theta_2, r_1, r_2, r_3, r_4, \theta_3, \theta_4)$

velocity $(\theta_2, \omega_2, r_1, r_2, r_3, r_4, \omega_3, \omega_4)$

moments $(\theta_2, r_1, r_2, r_3, r_4, \theta_3, \theta_4, \mu_B, \mu_C, \mu_D, M_{2B}, M_{3C}, M_{4D})$

$$M_{2A} = -M_{2B} + [r_2 \sin(\theta_2 - \theta_4)/r_3 \sin(\theta_3 - \theta_4)](M_{2B} - M_{3C}) + [r_2 \sin(\theta_3 - \theta_4)/r_4 \sin(\theta_3 - \theta_4)](M_{3C} - M_{4D})$$

repeat the loop

end

The Slider Crank

The analysis for the simple friction-loaded slider crank is very similar to that for the four-bar linkage. The basic equations can be written out by simplifying Equations (11.2), as was done for the four-bar linkage. The crank and coupler force equations are automatically satisfied by setting

$$f_{2B} = f_{3C} = f = -f_{4C}$$

in direct analogy to Equation (11.13). There remain two moment equations and one force equation, and these are analogous to the three moment equations (11.14) and (11.15):

$$0 = M_{2A} + M_{2B} + \text{Im}(z_2{}^*f) \tag{11.18}$$

$$0 = -M_{2B} + M_{3C} + \text{Im}(z_3{}^*f)$$

$$0 = \text{Re}(f_L) + [f_S e^{-i\theta_4}]e^{i\theta_4} - \text{Re}(f) \tag{11.19}$$

The square-bracket notation is that of the scalar force introduced in the preceding chapter. [Note that $\theta_4 = \pi$, so that $\exp(\pm i\theta_4) = -1$, and Equation (11.19) can be written in the alternative form

$$0 = \text{Re}(f_L) - [f_S e^{-i\theta_4}] - \text{Re}(f)$$

so that $\text{Re}(f)$ is determinable from this equation.]

As in the four-bar case, the two equations (11.19) can be solved for f, and Equation (11.18) can then be solved for M_{2A}. That result, in terms of the forces and moments, is

$$M_{2A} = -M_{2B} + \frac{r_2 \cos\theta_2}{r_3 \cos\theta_3}(-M_{2B} + M_{3C}) + \frac{r_2 \sin(\theta_2 - \theta_3)}{r_3 \cos\theta_3}(\text{Re}(f_L) + [f_S]) \tag{11.20}$$

where $[f_S]$ is short for $-[f_S e^{-i\pi}]$. As in the four-bar case, the friction force and the moments can all be written in terms of ω_2, and Equation (11.20) then becomes a relation among M_{2A}, ω_2, and the load (or driving force) $\text{Re}(f_L)$. [The reaction force $\text{Im}(f_L)$ can be found from the second of Equations (11.2c).]

Four cases can be recognized. The first two have $[f_L]$ equal to zero and so are analogous to the two cases discussed for the four-bar linkage. We can specify the crank rotation speed and find the torque required, or we can specify the torque available and find the rotation speed possible. The other two cases assume that a load on the slider, or possible driving motion from the slider, $[f_L]$, is nonzero. The two possibilities still arise. One can still ask what torque is needed for a specified rotation rate, or what rotation rate will follow from a given shaft torque, if $[f_L]$ is a load. If $[f_L]$ is a driving force, such as would be found if the slider crank were being used to model an internal combustion engine, as will be done later, then the load is at the shaft, joint A, and can

be specified as a torque, or as a required speed, and we can ask what driving force $[f_L]$ is required to meet the specified torque or speed at the shaft. This is an interesting problem, which I will defer until inertia has been considered.

The analog of the example of a simple friction-loaded four-bar linkage is a slider crank for which $\mu_B = 0 = \mu_C$ and $\mathrm{Re}(f_L) = 0$. Then,

$$M_{2A} = \frac{r_2 \sin(\theta_2 - \theta_3)}{r_3 \cos \theta_3}[f_S] = \mu_S \dot{r}_4 \frac{r_2 \sin(\theta_2 - \theta_3)}{r_3 \cos \theta_3}[f_S] \tag{11.21}$$

Compare this to Equation (11.10). The methods of Chapter 6 can be used to eliminate r_4 (see Exercise 6.3). This leads to the analog of Equation (11.11)

$$M_{2A} = \mu_S \frac{r_2^2 \sin^2(\theta_2 - \theta_3)}{r_3 \cos \theta_3}[f_S] \tag{11.22}$$

and the interested student is encouraged to write the code necessary to explore the behavior of this simple system.

INERTIA

All the dynamic analysis presented so far neglects inertia of the links, although the inertia of specifically added masses was considered in Chapter 10. Link inertia was formally neglected by neglecting the mass and moments of inertia in the dynamical Equations (11.1) and (11.2). To include inertia, it is merely necessary to include these terms. This is a generalization of the inertial force analysis presented in Chapter 10.

Two classes of problems present themselves: (1) the crank rotation is specified, and the problem is to find the reaction forces and moments; (2) the crank moment (torque) or some other forcing function is specified, and the problem is to find the motion. The first problem is much easier than the second. If the motion is specified, then velocities and accelerations can be found using the programs of Chapter 6, and the inertial forces can be calculated as in Chapter 10. In the latter case, the dynamical equations are actually ordinary differential equations, with time as the independent variable and the various linkage parameters as dependent variables. These equations must be integrated, subject to the constraints imposed by the loop-closure equation(s). I will begin with the first, simpler, problem.

If ω_2 and its derivative with respect to time are specified, then Program 6.1 can be used to find all the rates of change of angle and position with time, so that everything in Equations (11.1) is known except the shaft torque M_{2A} and the joint forces. The three force equations can eliminate three of the four independent forces in terms of the fourth. Letting f_{2B} be the remaining undetermined force gives

$$\begin{aligned} f_{2A} &= m_2 \ddot{\zeta}_2 - f_{2B} \\ f_{3C} &= m_3 \ddot{\zeta}_3 + f_{2B} \\ f_{4D} &= m_4 \ddot{\zeta}_4 + m_3 \ddot{\zeta}_3 + f_{2B} \end{aligned} \tag{11.23}$$

and the three moment equations are

$$M_{2A} = I_2\dot{\omega}_2 - M_{2B} - \text{Im}(z_2{}^*f_{2B}) \tag{11.24}$$

$$\text{Im}(z_3{}^*f_{2B}) = I_3\dot{\omega}_3 + M_{2B} - M_{3C} - \text{Im}(z_3{}^*m_3\ddot{z}_3) \tag{11.25}$$

$$\text{Im}(z_4{}^*f_{2B}) = I_4\dot{\omega}_4 + M_{3C} - M_{4D} - \text{Im}(z_4{}^*m_4\ddot{z}_4) - \text{Im}(z_4{}^*m_3\ddot{z}_3) \tag{11.26}$$

As in the previous section, Equations (11.25) and (11.26) can be solved for two independent components of the unknown force f_{2B}, assuming that the linkage is not in toggle. Once f_{2B} is known, Equation (11.24) can be solved for the shaft torque M_{2A}. All this could be written out in one grand formula. It would occupy an entire page of the text and be of little use to anyone. Once again, an algorithm is preferable, and Program 11.2 is an algorithm for finding the shaft torque for this problem.

PROGRAM 11.2: SHAFT TORQUE FOR A FOUR-BAR LINKAGE (WITH SHAFT ROTATION SPECIFIED)

procedure velocity $(\theta_2, \omega_2, r_1, r_2, r_3, r_4, \omega_3, \omega_4, z_2, z_3, z_4, \dot{z}_2, \dot{z}_3, \dot{z}_4)$
procedure position $(\theta_2, r_1, r_2, r_3, r_4, \theta_3, \theta_4)$
procedure moments $(\theta_2, r_1, r_2, r_3, r_4, \theta_3, \theta_4, \mu_B, \mu_C, \mu_D, M_{2B}, M_{3C}, M_{4D})$
begin
enter $(\omega_2, r_1, r_2, r_3, r_4)$
enter $(\theta_2, \delta\theta_2, n)$
enter $(\mu_B, \mu_C, \mu_D, I_2, I_3, I_4, q_2, q_3, q_4)$
for $i = 1$ to n **do**
    $\theta_2 = \theta_2 + \delta\theta_2$
    position $(\theta_2, r_1, r_2, r_3, r_4, \theta_3, \theta_4)$
    velocity $(\theta_2, \omega_2, r_1, r_2, r_3, r_4, \omega_3, \omega_4, z_2, z_3, z_4, \dot{z}_2, \dot{z}_3, \dot{z}_4)$
    moments $(\theta_2, r_1, r_2, r_3, r_4, \theta_3, \theta_4, \mu_B, \mu_C, \mu_D, M_{2B}, M_{3C}, M_{4D})$
    $a11 = -r_3 \sin\theta_3, \quad a12 = r_3 \cos\theta_3$
    $a21 = -r_4 \sin\theta_4, \quad a22 = r_4 \cos\theta_4$
    $J = a11{}^*a22 - a12{}^*a21$
    $b1 = I_3\omega_3 + M_{2B} - M_{3C} - \text{Im}(z_3{}^*m_3q_3z_3)$
    $b2 = I_4\omega_4 + M_{3C} - M_{4D} - \text{Im}(z_4{}^*m_4q_4z_4) - \text{Im}(z_4{}^*m_3q_3z_3)$

$\text{Re}(f_{2B}) = (a22*b1 - a12*b2)/J$

$\text{Im}(f_{2B}) = (-a21*b1 + a22*b2)/J$

$M_{2A} = I_2\omega_2 - M_{2B} + r_2 \sin\theta_2 \text{Re}(f_{2B}) - r_2 \cos\theta_2 \text{Im}(f_{2B})$

repeat the loop

end

The same sort of analysis can be done for the slider crank. If either the crank motion or the slider motion is specified, all the forces and torques can be found. Treat f_{2B} as the unknown force, as I just did for the four-bar linkage. The remaining two forces can be written down directly from Equations (11.23), which apply equally to both situations:

$$f_{2A} = m_2\ddot{\zeta}_2 - f_{2B}$$
$$f_{3C} = m_3\ddot{\zeta}_3 + f_{2B} = -f_{4C} \tag{11.27}$$

The components of f_{2B} can then be determined by solving the second moment equation in the set (11.2) and the final force equation. Then the moment can be found from the first moment equation in the same set. Once again, writing out the algebra is not productive, and the procedure is best expressed as an algorithm, given below as Program 11.3.

PROGRAM 11.3: SLIDER-CRANK MOMENTS WITH MOTION SPECIFIED

procedure velocity $(\theta_2, \omega_2, r_1, r_2, r_3, r_4, \omega_3, \omega_4, z_2, z_3, z_4, \dot{z}_2, \dot{z}_3, \dot{z}_4)$

procedure position $(\theta_2, r_1, r_2, r_3, r_4, \theta_3, \theta_4)$

procedure moments $(\theta_2, r_1, r_2, r_3, r_4, \theta_3, \theta_4, \mu_B, \mu_C, \mu_D, M_{2B}, M_{3C})$

begin

enter $(\omega_2, r_1, r_2, r_3, r_4, q_2, q_3)$

enter $(\theta_2, \delta\theta_2, n)$

enter (μ_B, μ_C, I_2, I_3)

for $i = 1$ to n **do**

$\theta_2 = \theta_2 + \delta\theta_2$

position $(\theta_2, r_1, r_2, r_3, r_4, \theta_3)$

velocity $(\theta_2, \omega_2, r_1, r_2, r_3, r_4, \omega_3, \omega_4, z_2, z_3, z_4, \dot{z}_2, \dot{z}_3, \dot{z}_4)$

moments $(\theta_2, r_1, r_2, r_3, r_4, \theta_3, \theta_4, \mu_B, \mu_C, M_{2B}, M_{3C})$

$a11 = -r_3 \sin\theta_3, \quad a12 = r_3 \cos\theta_3$

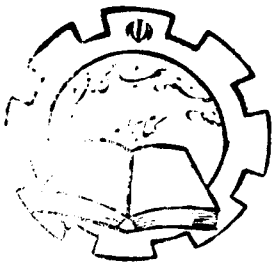

$a21 = 1, \quad a22 = 0$

$J = a11*a22 - a12*a21$

$b1 = I_3\omega_3 + M_{2B} - M_{3C} - \text{Im}(z_3*m_3q_3z_3)$

$b2 = m_4 \text{Re}(z_4) - \text{Re}(f_S)$

$\text{Re}(f_{2B}) = (a22*b1 - a12*b2)/J$

$\text{Im}(f_{2B}) = (-a21*b1 + a22*b2)/J$

$M_{2A} = I_2\omega_2 - M_{2B} + r_2 \sin\theta_2 \text{Re}(f_{2B}) - r_2 \cos\theta_2 \text{Im}(f_{2B})$

repeat the loop

end

The reader will note that the structure of Program 11.3 is the same as that of Program 11.2. The input data are different, and the motion, velocity, and moment procedures needed to be changed to those for the slider crank. The actual calculation shown here has retained the algebraic manipulation used in the other code. Only the coefficients change; the operations can be left the same. This is a precursor to building larger codes for which the algebra will be more clearly separated from the analysis.

It is instructive to examine the nature of the forces and moments. The equations are sufficiently complicated to put a thorough exploration of the behavior of linkages, even limited to only four-bar linkages, well beyond the scope of a general text. Interested readers are urged to construct their own programs and to explore at leisure the behavior of linkages. In this space, I will look at three relatively simple four-bar linkages, parameters of which are given in Table 11.1. I will look at the reaction forces as well as the driving torque. The slider crank will be examined later as a model of a one-cylinder internal combustion engine.

These three four-bar linkages are taken from linkages explored earlier in the text: the motorcycle foot brake (Figures 11.4 and 11.7) and the car window mechanism (Figures 11.5 and 11.8) from Chapter 1 viewed as crank-rocker mechanisms, and the mechanism shown in Figure 6.4 (Figures 11.6 and 11.9). All three linkages will be treated as if made up of rods so that, using the parallel-axis theorem (cf. Beer and Johnston 1977), the moment of inertia of each link with respect to its end is

$$I_j = \frac{1}{12} m_j r_j^2 + \frac{1}{4} m_j r_j^2 = \frac{1}{3} m_j r_j^2$$

and the mass of each link will be taken to be proportional to the length of the link. The first three are friction-free examples, and the second three are inertialess frictional examples. The forces depend linearly on the masses and friction, so that these examples can be added, even though the problems are nonlinear. The code used to generate these curves is based on the pseudocode Program 11.2.

Table 11.1 Parameters for Figures 11.4–11.9

	Figure 11.4	*Figure 11.5*	*Figure 11.6*	*Figure 11.7*	*Figure 11.8*	*Figure 11.9*
r_1	100	100	110	100	100	110
r_2	16.2	2.6	60	16.2	2.6	60
r_3	98.6	4.1	100	98.6	4.1	100
r_4	20.4	100	100	20.4	100	100
m_2	16.2	2.6	60	0	0	0
m_3	98.6	4.1	100	0	0	0
m_4	20.4	100	100	0	0	0
I_2	87.480	2.253	1200	0	0	0
I_3	3240.65	5.604	3333.33	0	0	0
I_4	138.72	3333.33	3333.33	0	0	0
μ_B	0	0	0	1	1	1
μ_C	0	0	0	1	1	1
μ_D	0	0	0	1	1	1

The first curve in each figure is the shaft torque, the second is reaction force at A, with diamonds denoting the horizontal component and crosses the vertical component, and the third is the reaction force at D. The horizontal axis shows the crank angle from 90° to 445.2°, the distinct part of a full cycle. These motions are periodic, so that the moment and forces at 450° equal those at 90°. (The choice of 90° to 450° instead of 0° to 360° is simply an artifact of the choice of reference angle. When the crank angle is at zero, the linkage is in toggle, and the program will not start. Thus, I have done all the calculations starting with the crank vertical, corresponding to a crank angle of 90°.) The inertia figures are scaled. The force scale used is $(1/2)m_2r_2\omega_2^2$, and the moment scale is $I_2\omega_2^2$. The friction pictures are unscaled. In all cases, ω_2 is fixed at unity.

The reader should note that the reaction forces are variable and that they vary over a wide range, as does the driving torque. All diagrams show a single spike corresponding to the minimum value of $\sin(\theta_3 - \theta_4)$. This is in contrast to the double spikes appearing in Figure 11.3. The difference is that $\sin(\theta_3 - \theta_4)$ never gets very small for the cases shown in Figure 11.3. These latter examples lead one to wonder about constant-speed mechanisms. Is it really necessary to have a wildly varying shaft torque? How do the reaction forces shake the mechanism? These questions will be examined in more detail after the questions of torque-driven systems and of loads have been examined.

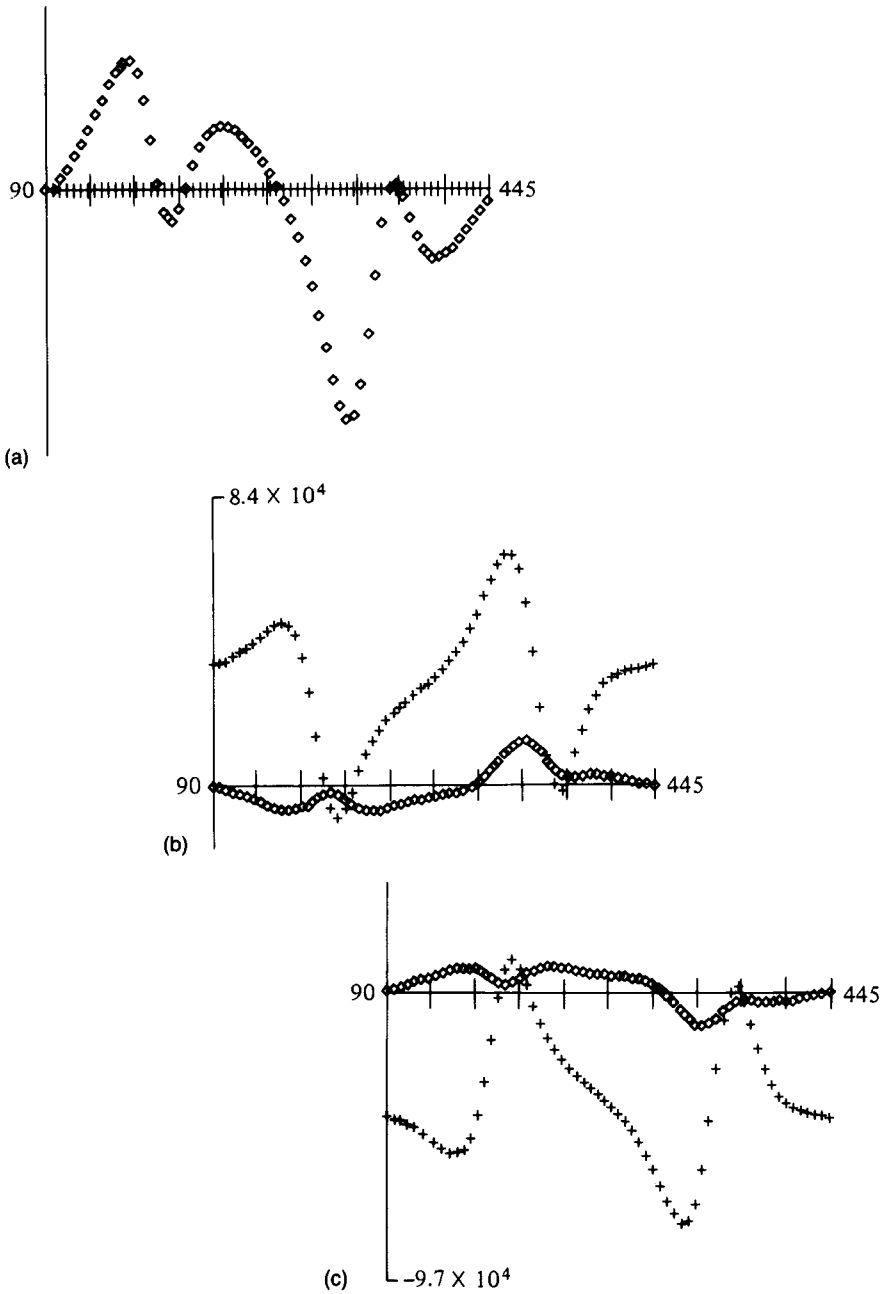

FIGURE 11.4 *The motorcycle foot-brake linkage with inertial resistance:* (a) *shaft torque, arbitrary units;* (b) *shaft reaction force, arbitrary units (diamonds denote the horizontal component, plus signs the vertical);* (c) *follower reaction force (at* D*), arbitrary units (diamonds denote the horizontal component, plus signs the vertical).*

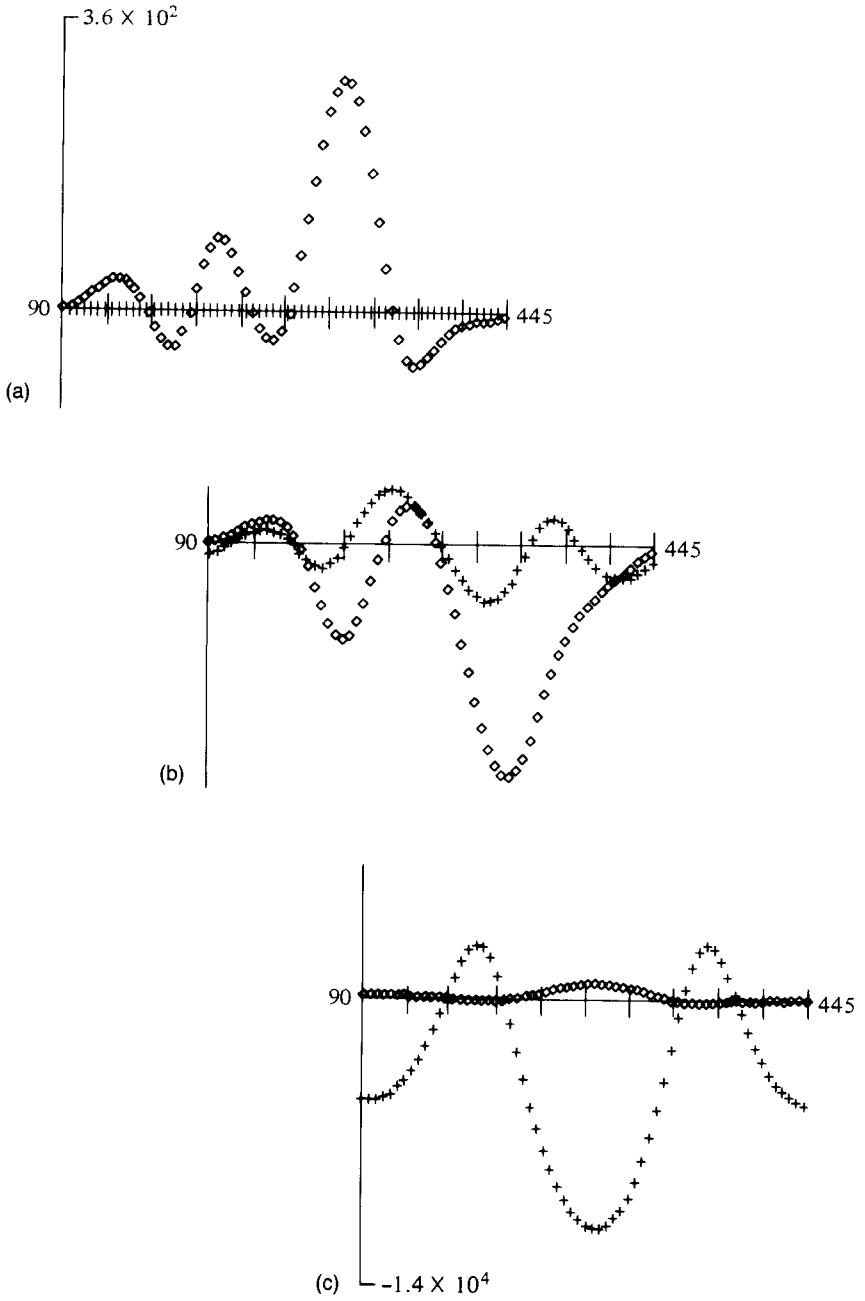

FIGURE 11.5 *The car window linkage with inertial resistance:* (a) *shaft torque, arbitrary units;* (b) *shaft reaction force, arbitrary units (diamonds denote the horizontal component, plus signs the vertical);* (c) *follower reaction force (at* D*), arbitrary units (diamonds denote the horizontal component, plus signs the vertical).*

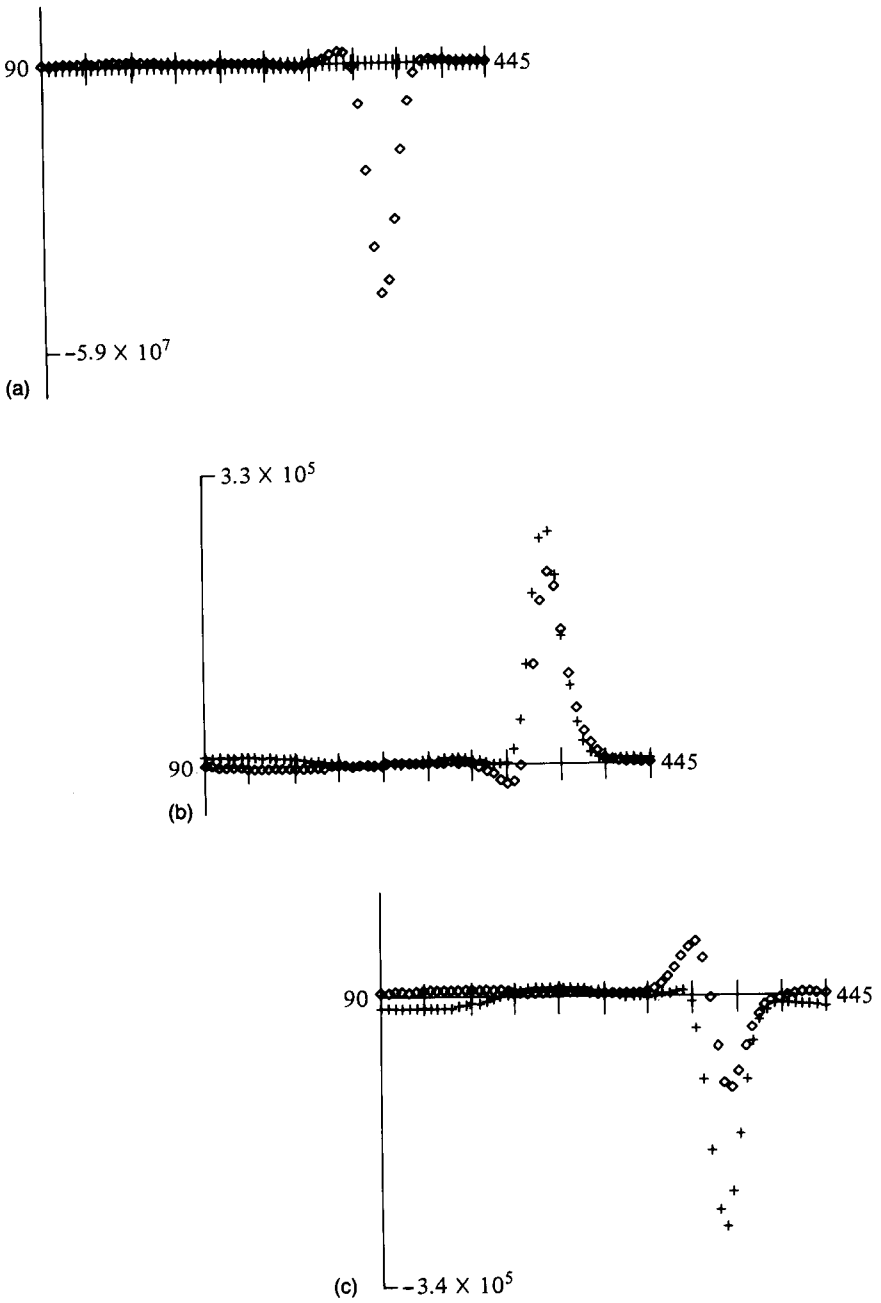

FIGURE 11.6 *The linkage shown in Figure 6.4 with inertial resistance:* (a) *shaft torque, arbitrary units;* (b) *shaft reaction force, arbitrary units (diamonds denote the horizontal component, plus signs the vertical);* (c) *follower reaction force (at* D*), arbitrary units (diamonds denote the horizontal component, plus signs the vertical).*

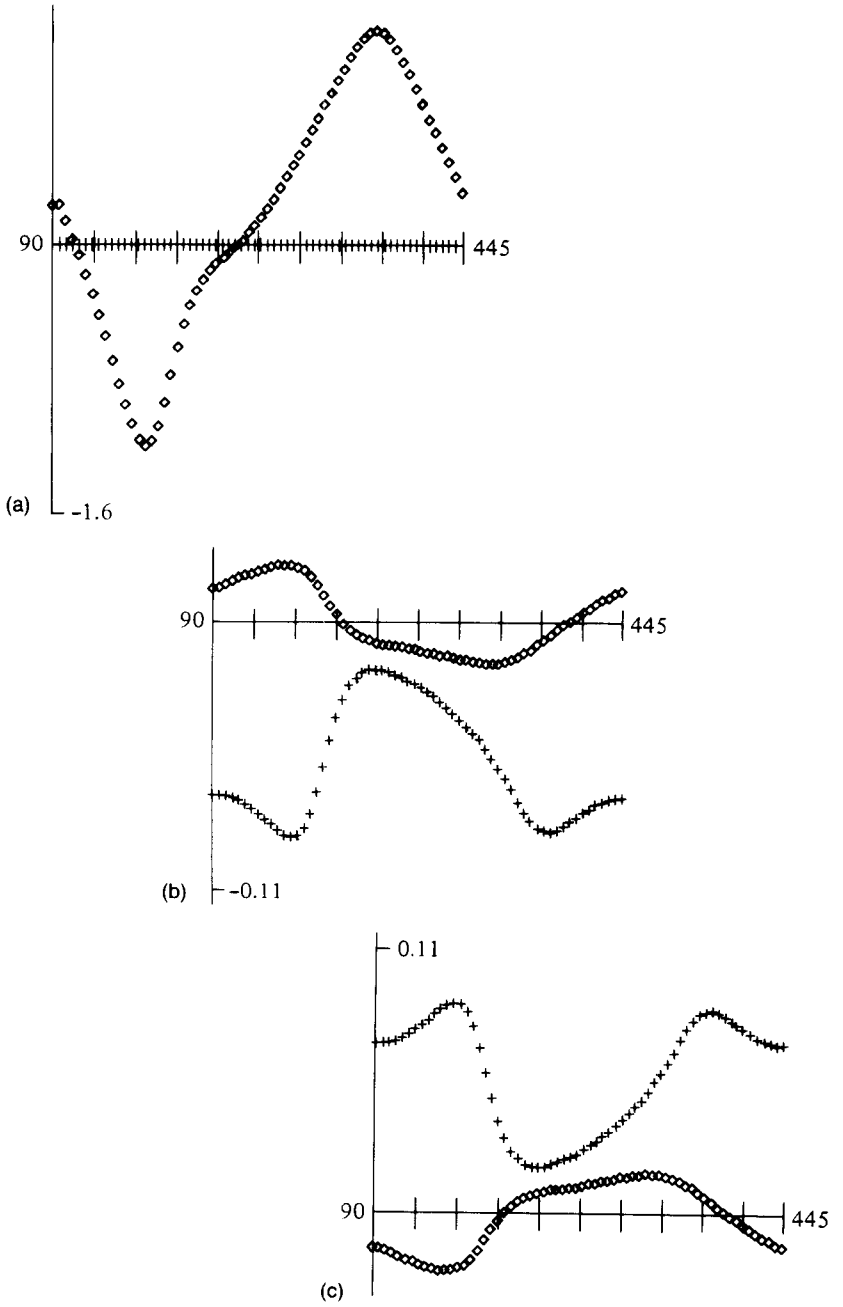

FIGURE 11.7 *The motorcycle foot-brake linkage with frictional resistance:* (a) *shaft torque, arbitrary units;* (b) *shaft reaction force, arbitrary units (diamonds denote the horizontal component, plus signs the vertical);* (c) *follower reaction force (at* D*), arbitrary units (diamonds denote the horizontal component, plus signs the vertical).*

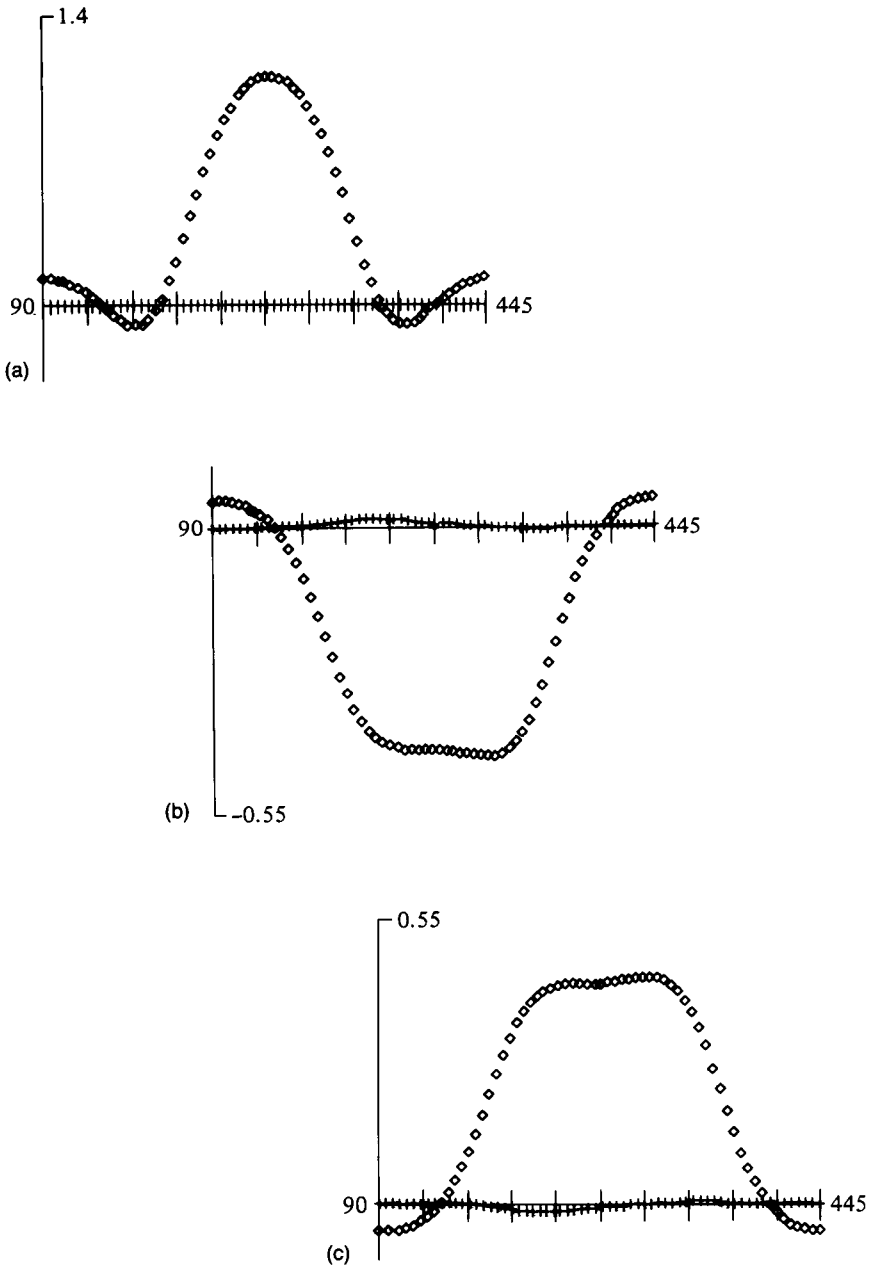

FIGURE 11.8 *The car window linkage with frictional resistance:* (a) *shaft torque, arbitrary units;* (b) *shaft reaction force, arbitrary units (diamonds denote the horizontal component, plus signs the vertical);* (c) *follower reaction force (at* D*), arbitrary units (diamonds denote the horizontal component, plus signs the vertical).*

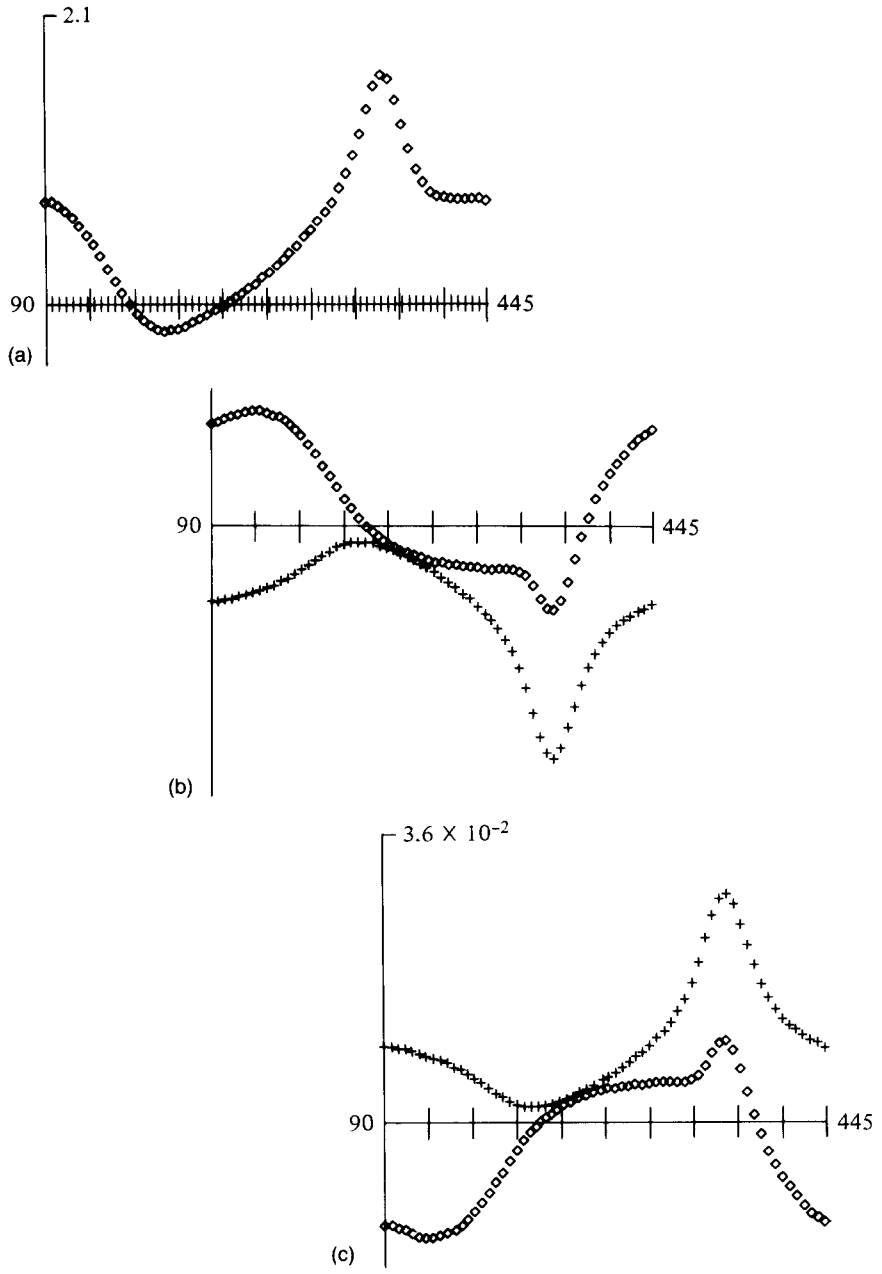

FIGURE 11.9 *The linkage shown in Figure 6.4 with frictional resistance:* (a) *shaft torque, arbitrary units;* (b) *shaft reaction force, arbitrary units (diamonds denote the horizontal component, plus signs the vertical);* (c) *follower reaction force (at* D*), arbitrary units (diamonds denote the horizontal component, plus signs the vertical).*

FORCE- AND TORQUE-DRIVEN SYSTEMS

Any four-bar linkage or slider-crank system must satisfy the appropriate governing equations, Equations (11.1) or Equations (11.2), respectively. In the cases examined so far, the crank rotation has been specified. With the crank rotation specified, the equations reduce to algebraic equations. They are nonlinear algebraic equations and need to be solved numerically, but they are algebraic; no integration is necessary.

As written, with the crank rotation unspecified, they are second-order ordinary differential equations. The dependent variables are the link angles, and the independent variable is time. To find the motion of the system, the set of differential equations must be solved. The differential equations are nonlinear, and they are constrained by the loop-closure equation in each case. (As demonstrated in Chapter 6, all the rates of change are connected. If one is known, all the others are known as well.) Analytic solutions to these strongly nonlinear differential equations are not known. It is necessary to solve them numerically. How to do this is explained in detail in both Carnahan et al. (1969) and Press et al. (1986). I will outline the underlying principles here and demonstrate some of the preliminary algebraic steps necessary before the numerical methods can be used.

The problem for either the four-bar linkage or the slider crank can, in principle, be reduced to a single second-order differential equation for θ_2. The velocity and acceleration equations can be used to eliminate the derivatives of the other link angles in favor of θ_2. The resulting differential equation can be solved formally, again in principle, for the second derivative of θ_2, leading to a quasilinear second-order ordinary differential equation:

$$\ddot{\theta}_2 = \dot{\omega}_2 = F(\theta_2, \theta_3, \theta_4, \dot{\theta}_2, \dot{\theta}_3, \dot{\theta}_4, r_1, r_2, r_3, r_4) \tag{11.28}$$

This single second-order equation can be written as a pair of first-order equations

$$\begin{aligned} \dot{\omega}_2 &= F(\theta_2, \theta_3, \theta_4, \dot{\theta}_2, \dot{\theta}_3, \dot{\theta}_4, r_1, r_2, r_3, r_4) \\ \dot{\theta}_2 &= \omega_2 \end{aligned} \tag{11.29}$$

so it is really only necessary to understand how to solve a single nonlinear first-order ordinary differential equation.

Newton–Raphson methods were introduced in Chapter 5 for one-dimensional systems before extending them to multidimensional problems. The same thing can be done here. If one equation can be solved, the extension to a pair, and then to a system of arbitrary size, is straightforward.

Consider the equation

$$\dot{y} = f(y,t) \tag{11.30}$$

The derivative can be approximated using the definition of the derivative

$$\dot{y} \approx \frac{y(t + \Delta t) - y(t)}{\Delta t}$$

and an approximate version of Equation (11.30) can be written as one step in an iterative scheme,

$$y^{n+1} = y^n + \Delta t f(y,t) \tag{11.31}$$

Equation (11.31) is called the *simple Euler* scheme with *forward differences*. Unless the time steps are very small, the scheme is unstable, and this scheme is almost never suitable for numerical integration. More stable and accurate schemes are created by improving the approximation of the derivative.

A very common class of direct integration schemes is the *Runge–Kutta* method. Different orders of Runge–Kutta integration approximate the derivative to different order. A fourth-order Runge–Kutta technique, the most commonly used, approximates the derivative using the value of the function at four points. It is *fourth-order accurate*, which means that the error in integration can be represented by a constant times $(\Delta t)^5$. For well-behaved systems, the constant is not large. For pathological systems, the constant can be very large; for fourth-degree polynomials, the constant is zero. In the latter case, the Runge-Kutta scheme gives the correct answer within numerical accuracy. I will use the fourth-order scheme to generate solutions in this text. The actual code is adapted from that given in Press et al. (1986). [The reader should note that the fourth-order Runge–Kutta scheme, while common, is not the only scheme for integration in time. There are problems for which it is unsuited. Decisions about the nature of numerical methods are in many cases artistic—whence the name of the Press volume just cited. The interested reader is referred to either Carnahan (1969) or Press et al. (1986).]

A system of first-order ordinary differential equations can be solved using the vector equivalent of the single equation system. That is, if the unknowns are $y_1, y_2, \ldots, y_n$, then the system to be solved is

$$\begin{aligned}
\dot{y}_1 &= f_1(y_1, y_2, \ldots, y_n, t) \\
\dot{y}_2 &= f_2(y_1, y_2, \ldots, y_n, t) \\
&\vdots \\
\dot{y}_n &= f_n(y_1, y_2, \ldots, y_n, t)
\end{aligned} \tag{11.32}$$

At their most complicated, the algebraic equations cannot be solved symbolically and, thus, one cannot write the equations with the various derivatives isolated as in Equation

(11.32). In that case, the governing system must be written

$$A_{ij}\dot{y}_i = f_j(y_1, y_2, \ldots, y_n, t) \tag{11.33}$$

where A_{ij} is a coefficient matrix depending on all the components of the vector y_j and the time t. The elements of the matrix will be denoted by a_{ij}. In the simple case in which the second derivatives can be separated, the equations can be manipulated so that the off-diagonal elements are all zero. In the general case, this cannot be done in closed form, and the algebraic equations corresponding to Equations (11.33) need to be solved numerically at each time step. Program 11.4 outlines the procedure.

PROGRAM 11.4: INTEGRATION OF A SYSTEM OF EQUATIONS

procedure invert (A_{ij}, A_{ij}^{-1})
procedure calculate (y_j, A_{ij}, f_i)
procedure time step $(y_j, A_{ij}^{-1}, f_i, \delta y_j)$
begin
  enter (physical parameters)
  enter (initial values of y_j)
  enter ($t$max)
  while $t < t$max **do**
    begin
    calculate (y_j, A_{ij}, f_i)
    invert (A_{ij}, A_{ij}^{-1})
    time step $(y_j, A_{ij}^{-1}, f_i, \delta y_j)$
    $y_i = y_i + \delta y_i$
  repeat the loop
end

In this program, the procedure **invert** and **time step** are general procedures taken from text or from software available at whatever computation center is being used. The procedure **calculate** must be provided by the user. It will contain the dynamic (or other) equations to be solved. The physical parameters include all the linkage parameters and any external forces and torques, and $t$max is the upper limit of integration.

How does all this apply to the problems at hand? To explicate this question, I will convert Equations (11.1) into a form that can be integrated using the vector Runge–Kutta scheme. This can be done in several ways. The breakdown is not unique. As written, the equations already have all the second derivatives with respect to time on the left-hand side. However, the constraint provided by the loop-closure equation has not been applied, and some manipulation is necessary. The degree of manipulation is a matter of taste.

For the four-bar analysis, I imagine that the shaft torque M_{2A} is given, or required, and that the load can be represented by M_{2D}. These are specified functions of time, and the task is to find the position of the linkage as a function of time. As in the simpler case worked earlier, the three force equations can be used to eliminate all but one of the forces. That one remaining force can be any of the joint forces. I will let f_{2B} be the unknown force.

To find f_{2B}, I solve the second and third moment equations for the two components of f_{2B} in terms of the rates of change of the angles. It is convenient to use the expressions in Chapter 6 to eliminate the link accelerations in favor of the angular accelerations:

$$\ddot{z}_j = (i\dot{\omega}_j - \omega_j^2)z_j \tag{11.34}$$

This can be generalized in an obvious fashion to find the rates of change of the ζ_j, which are sums of z_j, each of which can be differentiated using Equation (10.34). The two equations determining f_{2B}, the reduced moment equations from Equations (11.1b) and (11.1c), are

$$\begin{aligned} I_3\ddot{\theta}_3 = {} & -\mu_B(\omega_3 - \omega_2) + \mu_C(\omega_4 - \omega_3) \\ & + m_3 \operatorname{Im}\{(i\dot{\omega}_3 - \omega_3^2)z_3{}^*\zeta_3\} + \operatorname{Im}\{z_3{}^*f_{2B}\} \end{aligned} \tag{11.35}$$

and

$$\begin{aligned} I_4\ddot{\theta}_4 = {} & -\mu_C(\omega_4 - \omega_3) - \mu_D\omega_4 + m_3 \operatorname{Im}\{(i\dot{\omega}_3 - \omega_3^2)z_4{}^*\zeta_3\} \\ & + m_4 \operatorname{Im}\{(i\dot{\omega}_4 - \omega_4^2)z_4{}^*\zeta_4\} + \operatorname{Im}\{z_4{}^*f_{2B}\} \end{aligned} \tag{11.36}$$

Enough information is available to construct an algorithm, but that algorithm would be quite complicated, obscuring essential points in a fog of algebra. To avoid this for now, neglect the bearing friction at B, C, and D as small compared to the load, and neglect the inertia of the crank and coupler. This combination of assumptions does not change the problem in any serious way but makes it possible to proceed further analytically, which is useful if one wants to understand what is happening.

Under these assumptions, the coupler is a two-force member. That is, only the ends of the coupler are loaded, and the loads are applied through pins, so that no moments are applied to the coupler. Then f_{3B}, and hence f_{2B}, is parallel to the coupler. This could have been deduced directly from Equation (11.35). Equation (11.36) becomes

$$(I_4 - m_4 q_4 r_4^2)\dot{\omega}_4 = r_4[f_{2B}e^{-i\theta_3}]\sin(\theta_3 - \theta_4) \tag{11.37}$$

determining f_{2B} in terms of ω_4. Substitution into the moment equation obtained from Equation (11.1a) by eliminating μ_B, μ_C, μ_D, and the inertias of the crank and coupler gives the dynamical equation

$$I_2\dot{\omega}_2 = M_{2A} + \frac{r_2(I_4 - m_4 q_4 r_4^2)\sin(\theta_3 - \theta_2)}{r_4\sin(\theta_3 - \theta_4)}\dot{\omega}_4 \tag{11.38}$$

The rate of change of follower angle can be found from Equation (6.10),

$$\dot{\omega}_4 = \frac{r_2\sin(\theta_2 - \theta_3)}{r_4\sin(\theta_4 - \theta_3)}\dot{\omega}_2 - \frac{r_2\cos(\theta_2 - \theta_3)}{r_4\sin(\theta_4 - \theta_3)}\omega_2^2$$

$$-\cot(\theta_4 - \theta_3)\omega_4^2 - \frac{r_3}{r_4\sin(\theta_4 - \theta_3)}\omega_3^2 \tag{11.39}$$

The pair of equations (11.38) and (11.39) form a fourth-order system. This is obvious once the two supplementary equations,

$$\dot{\theta}_2 = \omega_2, \qquad \dot{\theta}_4 = \omega_4 \tag{11.40}$$

are added. This system can be solved in two ways: either one can address the full system, using a 4×4 matrix, or one can use Equation (11.39) to eliminate ω_4 from the system, reducing it to a second-order system in the crank angle. The former method is much to be preferred. It makes use of the numerical techniques just developed and is relatively easily adapted to "canned" numerical integration schemes, which generally expect to be presented with a system of first-order equations.

The behavior of the slider crank is calculated in the same way, just as I showed in the earlier sections on friction and inertia. The internal combustion engine is a common example of a mechanism that can be abstracted as a slider-crank mechanism, driven by the slider. Because it is such a common example, I think it informative to address the question of force-driven slider cranks through the specific example, an example that can be further extended to look at the forces that shake a mechanism and its frame.

A Model for a Four-Stroke Engine

A four-stroke internal combustion engine has four independent components of its cycle. (Any mechanical engineering thermodynamics book will give you more detail than I include here, but I think it useful to construct the model here.) There is an *intake stroke,* during which the piston moves to increase the cylinder volume, and air (as well as fuel) is drawn into the cylinder. This is followed by a *compression stroke,* during which the volume decreases and the mixture is compressed. At the end of the compression cycle, the mixture is ignited, and it expands, driving the piston in the *power stroke.* This is followed by the *exhaust stroke,* during which the volume decreases again and

the products of combustion are expelled. Anyone familiar with internal combustion engines will realize that this is simplified; issues of timing, partial combustion, and other real phenomena are totally neglected. This is, however, adequate to construct a model for dynamic analysis.

The piston cylinder crankshaft system can be modeled as a centered (zero-offset) slider crank. The total motion of the slider, $2d$ in the notation used in this text, is equal to the stroke of the cylinder. Because the mechanism is centered (that is, there is zero offset, $H = 0$), the crank must be d units long: $r_2 = d$. The connecting rod joining the crank shaft to the piston plays the role of coupler. The load being driven is connected to the crank and enters the analysis as the shaft torque, M_{2A}.

The important aspects of this problem are the load, the driving force of combustion, and the inertia of the linkage. The last will be dominated by the inertia of the load and flywheel, appearing in the analysis as I_2. To isolate these phenomena, I will neglect all friction forces, assuming them to be small compared to the load, as they will be in any well-designed piece of machinery. I will neglect all forces at the piston except that during the power stroke, assuming that the other three strokes have forces small compared to the load (the additional analysis to add the compression stroke, clearly the next effect, is straightforward, and I will leave it to any reader interested enough to construct a personal code), and I will assume that all the linkage inertia is in the crank through its connection to the flywheel. That is, the inertia of the piston and of the connecting rod are both negligible. It remains only to construct a model of the power stroke.

The combustion and subsequent expansion is a rapid process, and it is sufficient for the present purpose to assume an adiabatic expansion, so that the pressure on the piston face is proportional to the gas density to the γ power, where γ is used to denote the ratio of specific heats. The expanding gas is mostly air, and I will take $\gamma = 1.4$. The gas density is inversely proportional to the volume of the cylinder, which varies linearly with the position of the cylinder, hence with the slider. If p_0 denotes the pressure at the minimum volume, a measure of the energy being dumped by combustion, and V_0 denotes the minimum volume of the cylinder, then the pressure can be written as a function of r_4 during the power stroke and taken to be zero during the other strokes. Thus,

$$\frac{p}{p_0} = \left(\frac{V_0}{V}\right)^{\gamma} = \left(\frac{V_0}{\pi a^2[(V_0/\pi a^2) + r_2 + L - r_4]}\right)^{\gamma} \tag{11.41}$$

where a denotes the radius of the piston, L the coupler length (in this zero-offset case), and r_4 the instantaneous length of the standard slider-crank vector z_4. The force is equal to p times the piston area.

To apply this in the present circumstance, write the reduced versions of the slider-crank equations (11.2), which are

Crank:

$$\frac{1}{2} m_2 \ddot{z}_2 = f_{2A} + f_{2B}$$

$$I_2 \ddot{\theta}_2 = M_{2A} + \mathrm{Im}(z_2{}^* f_{2B}) \tag{11.42}$$

Coupler:

$$0 = f_{3B} + f_{3C}$$
$$0 = \mathrm{Im}(z_3{}^* f_{3C}) \tag{11.43}$$

Slider:

$$0 = \mathrm{Re}(f_{4C} + f_L) \tag{11.44}$$

and f_L is given by the power stroke relation, Equation (11.41), during the power stroke and is zero otherwise. The factor of 1/2 in Equation (11.42) is the value of q_2 for this problem.

Neglecting the joint friction at B and C, and the inertia of the coupler makes it possible to consider the coupler a two-force member, and the coupler force can be found directly in terms of the driving force f_L. This is enough to allow all the kinematic variables to be solved explicitly in terms of the crank angle, so that the dynamics can be reduced exactly to a second-order system constructed from the crank moment equation.

The governing equations become, written in their standard form as a pair of first-order equations:

$$I_2\dot{\omega}_2 = M_{2A} + \left[f_{2B}e^{-i\theta_3}\right] r_2 \sin(\theta_3 - \theta_2) \tag{11.45a}$$
$$\dot{\theta}_2 = \omega_2 \tag{11.45b}$$

where

$$\left[f_{2B}e^{-i\theta_3}\right] = -\frac{\mathrm{Re}(f_L)}{\cos\theta_3} \tag{11.46}$$

The slider crank always has θ_3 between $-\pi/2$ and $\pi/2$, so that its cosine is always positive. The loop-closure equations can thus be used to find $\cos\theta_3$ unambiguously in terms of trigonometric functions of θ_2, so that the pair of equations (11.45) can be integrated without the need for successive approximations in the position location routine. Indeed, the position location can be incorporated directly into the integration scheme. This is simple enough to be left as an exercise for the reader.

A thorough exploration of the behavior of this model is another task that is beyond the scope of this text. The question of reaction forces will be addressed in the following section. Some simple observations are in order at this point. Equation (11.45a) states that the angular acceleration of the crank is equal to the difference between the driving force of the piston and the load. Steady rotation is possible only for an exact balance between the two, and this would be possible only for a very peculiar load because the force is a function of time and is zero for about three quarters of the time. Note, however, that the larger the inertia of the system, the smaller the angular accelerations necessary to balance differences between the load and the driving force.

This thought can be extended. The relative behavior of any linkage cannot depend on the units of measurement. In Parts I–IV of this text, I noted that all that was important was the relative lengths of the links. With forces and torques added to the system, things are more complicated, but the idea that the nature of the behavior depends only on ratios remains. The relative contributions of inertia, load, and driving force to Equation (11.45a) determine the behavior of the linkage. The actual values become important only at the next level of design requirements—making sure the system is strong enough.

For the sake of discussion, assume a frictional load, so that

$$M_{2A} = -\mu_{2A}\omega_2 \tag{11.47}$$

Let time be measured in units τ. Substitute Equation (11.47) into Equation (11.45a), introduce the time scale explicitly, separate the dimensional and nondimensional parts of the driving force, and divide the resulting equation by μ_{2A}. The resulting nondimensional equation, written as Equation (11.48), shows the important ratios governing the behavior of this one-cylinder engine model.

$$I\dot{\omega}_2 = -\omega_2 + Fg(\theta_2) \tag{11.48}$$

where

$$I = \frac{I_2}{\mu_{2A}\tau}, \qquad F = \frac{\pi p_0 a^2 r_2 \tau}{\mu_{2A}}$$

and the function $g(\theta)$ describes the variation of the piston force as the mechanism turns. It is obtainable from Equations (11.44) and (11.46).

[This approach to general understanding through scaling is an example of *dimensional analysis.* For a thorough discussion of the principles and practices of this art, the interested reader is directed to Sedov (1959) or to the appropriate sections of most texts in fluid dynamics or heat transfer.]

Figures 11.10 and 11.11 show some simple results, which I hope are sufficiently intriguing to motivate readers to build a code and explore these situations further. These results are based on the formulation shown in Equation (11.48). The geometry is given in unspecified units, although modeled on a 100-ml displacement, "square" (bore = stroke) cylinder. The geometry of the linkage is the same for all the illustrations: $d = 2.515$ and $r_3 = 8.0$. The offset is zero. I take τ to be unity. The system inertia ratio I is 50 for all cases. Note that the mass of the crank is irrelevant for the computation of the rotation. It enters only in the computation of the reaction forces, to be considered in the next section. Variables are the initial rotation rate of the crank (the load) and the force ratio F. Figure 11.10 shows two different individual conditions for the same force ratio, $F = 150$.

There are a total of five distinct sets of results in the two composite figures (Figures 11.10 and 11.11). Each part of the figures has a plot of crank rotation rate as a function of time and a plot of piston position as a function of time. Separating the

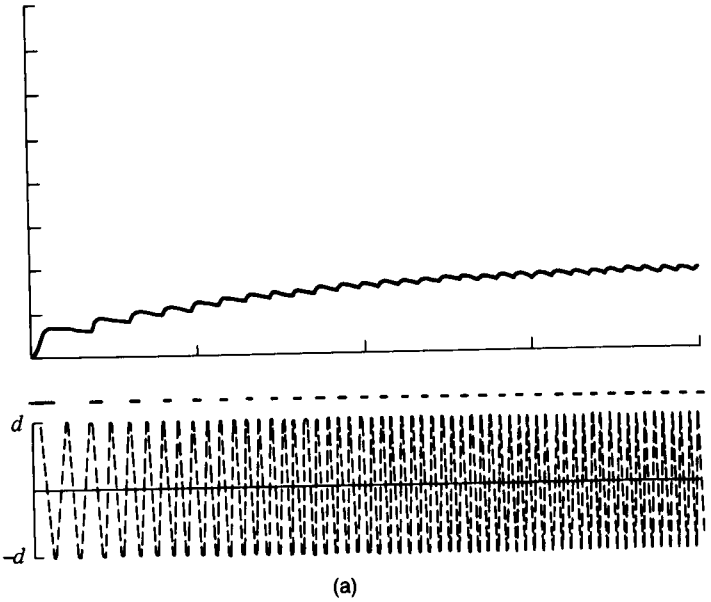

(a)

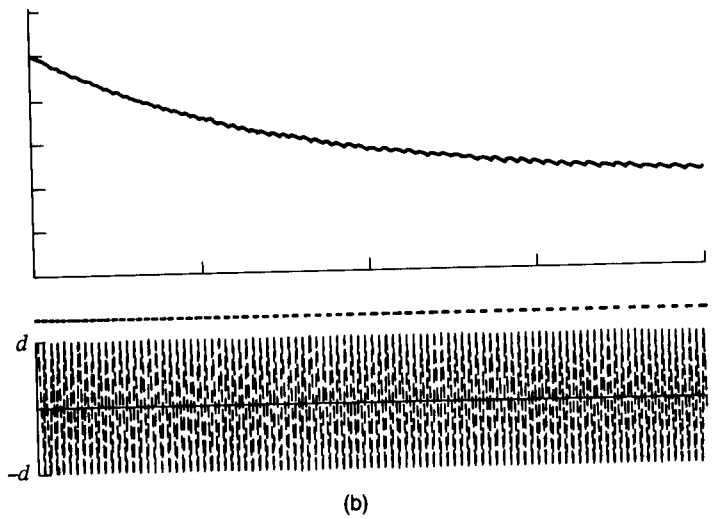

(b)

FIGURE 11.10 *The one-cylinder engine with force ratio 150 and inertia ratio 50:* (a) *start-up from rest;* (b) *start-up at speed higher than the equilibrium speed. Upper plot in each part is dimensionless rotation rate vs. time; the lower is piston displacement vs. time. The dashed line between the two shows when the cylinder is firing, the duration of the power stroke.*

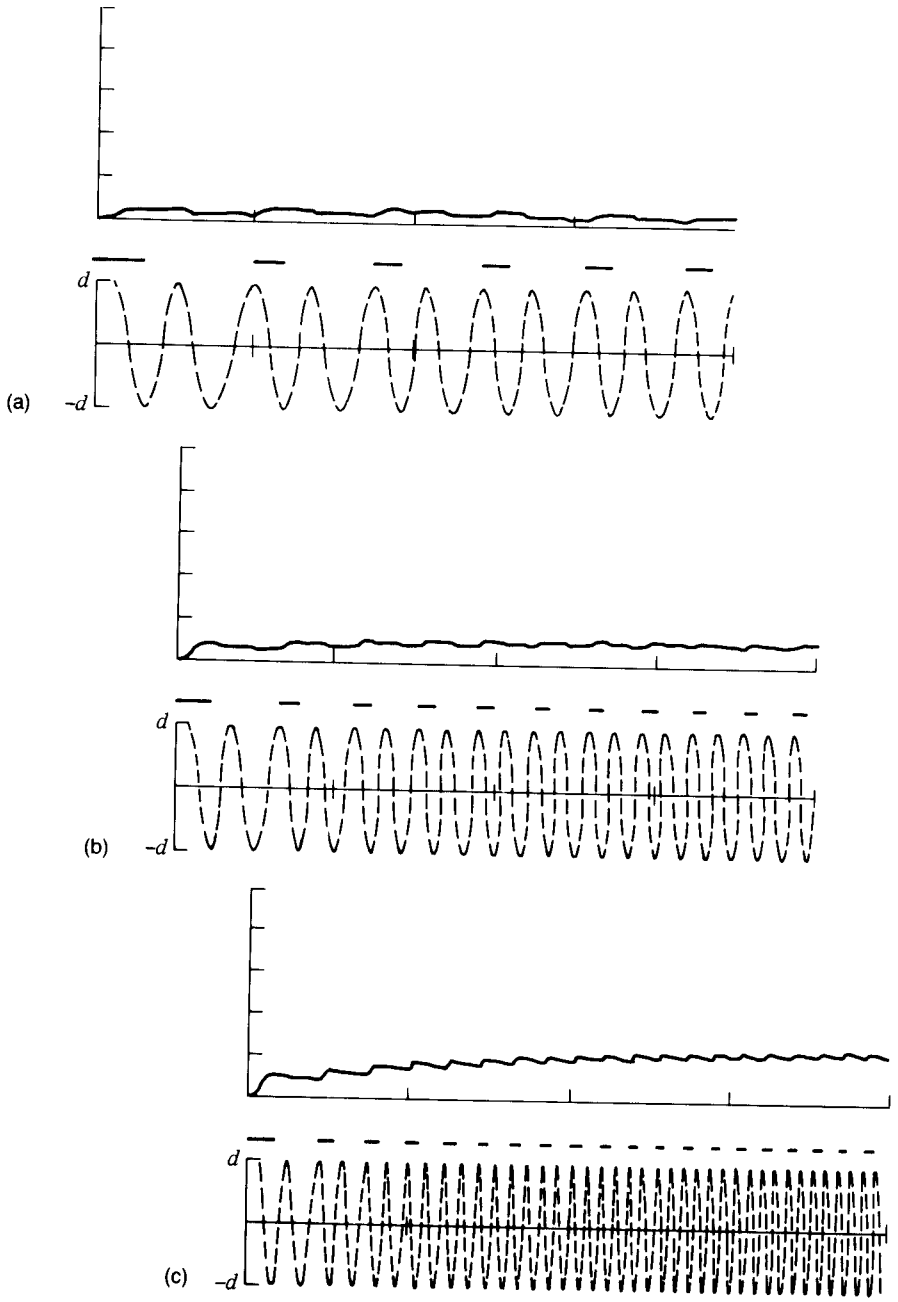

FIGURE 11.11 *The one-cylinder engine, start-up from rest at three different force ratios:* (a) *force ratio = 50;* (b) *force ratio = 100;* (c) *force ratio = 150. The inertia ratio is 50, as in the previous figure. Each figure has the same three components as Figure 11.10.*

two is a dashed line indicating the power stroke. When the line is dark, the cylinder is firing; when the line is absent, the cylinder is in one of the other three strokes. Time runs from 0 to 257.41 in dimensionless units in all figures. The ticks on the ordinate are at intervals of 2 rad/unit time, and the piston moves between $\pm d$.

Figure 11.10a shows start-up from rest, and Figure 11.10b start-up from a speed higher than the equilibrium speed. The figures, taken together, demonstrate effectively that there is an equilibrium speed and that it is not exactly constant. It can be found formally by integrating Equation (11.48) with respect to θ_2 from 0 to 2π and setting the right-hand side equal to zero, so that the mean imbalance is zero. This would be done by setting the mean dimensionless rotation rate equal to the negative of the mean dimensionless force.

Figure 11.11 illustrates this qualitatively. Figure 11.11a shows the start-up from rest of the system with one-third the force, $F = 50$; Figure 11.11b shows the same thing for two-thirds the force, $F = 100$; Figure 11.11c is a redrawing of Figure 11.10a.

It is worth noting that the centered slider crank has one toggle point during each cycle. This is not a problem because the inertia of the system carries the linkage through smoothly. It could be a problem during start-up, however, because at the top dead center position the linkage is in toggle. When the linkage is in toggle it can withstand, in principle, an infinite force and will not start. (The computer program used to generate the figures will never move if this condition is used as an initial condition. I have taken 1° to be the initial value of θ_2 for all the start-up figures, both here and later.) In practice, this is an example of unstable equilibrium. The unavoidable departures from perfect alignment will allow it to move, but it is equally likely to move in a clockwise direction as in the supposed counterclockwise direction. (This is not a problem in real engines, which are not started from rest, although I am told by friends that this is the cause for the occasional "kickback" when a motorcycle is kick-started.)

REACTION FORCES, INERTIA, AND BALANCE

It is fairly easy to add a calculation of the reaction forces to the simple model just explored. The motion of the linkage is independent of the force equations, and so they can be solved after the motion is known. The first equation of the pair of equations (11.27) determines the reaction force at A, the crank bearing, and the first of Equations (11.2c) can be used to find the imaginary part of f_L, which is the reaction force on the cylinder walls.

The reaction force on the cylinder walls is directly proportional to the load force, with a proportionality constant that varies with the position of the linkage. For the simple case of a massless coupler, the maximum is near the beginning of the power stroke. It increases with θ_2 because of geometry, the component of the force in the coupler perpendicular to the slider track increasing as θ_3 decreases from 0 while, at the same time, it decreases because the magnitude of the force drops as the cylinder expands. The actual maximum depends on the relative magnitudes of these two effects.

If the coupler angle remains between $\pm\pi/2$, the side force component remains less than the driving force component. In the examples to be explored, it will remain considerably less.

The crank bearing force f_{2A} can be found by a series of substitutions into Equation (11.2a). This can be written as

$$f_{2A} = \frac{1}{2}(i\dot{\omega}_2 - \omega_2{}^2)m_2 z_2 - f_{2B} \tag{11.49}$$

and f_{2B} can be found from Equation (11.46). I have assumed that the center of mass is that of a simple bar crank, halfway between the two ends, introducing a factor of 1/2 for q_2. For the simple idealization addressed here, f_{2B} is zero when F_L is zero. Thus, there are three components to the bearing force. Two of these depend on the asymmetry of the crank mass distribution. Of these, one, the part with the real coefficient, is a simple centripetal acceleration term, and the other, the part with the imaginary coefficient, a tangential acceleration term. (The distinction between these terms is explained in detail in Chapter 6.) Both of these can, in principle, be eliminated by proper balancing of the crank.

The third term is that transmitted through the coupler from the firing of the cylinder. This one cannot be balanced out, although the apparent effects can be reduced by using multiple cylinders, and it is well known that multicylinder engines are "smoother" than single-cylinder engines of the same power. Each individual "kick" of a cylinder firing is smaller, and the frequency of kicks is higher, each cylinder still firing every other revolution of the crankshaft.

Smoothness is also a function of the steadiness of the rotation rate of the output shaft (the crankshaft). Figures 11.10 and 11.11 show that the rotation rate is not constant, but they show only a small fluctuation. This is because the moment of inertia of the load is relatively large. Smaller inertias lead to much larger variations in output shaft speed. This is illustrated in Figure 11.12, which shows start-up from rest of the same linkage used in the preceding section with $F = 150$, but with I_2 reduced to that associated with the crank alone, $I_2 = I_{\min}$ (Figure 11.12a), followed by slowly increasing inertia, I_2 equal to two, three, and four times the minimum inertia. In general, the less inertia, the more rapid the start-up and the larger the fluctuation in the output rotation rate. Note the change of time scale between Figures 11.12c and 11.12d. The first three figures show the first 100 time units, and the last shows the first 200 time units.

Figure 11.13a shows the reaction forces at A and D for the history shown in Figure 11.12a. The reader can observe that the transients vanish quickly and that the reaction forces are periodic (but not sinusoidal) at the end of perhaps 30 time units. Figure 11.13b shows a massive system running in a steady state. Not only are the reaction forces periodic, but they are nearly sinusoidal. The momentary shock of the piston firing is negligible compared to the centripetal forces, and the large inertia means that tangential accelerations are also negligible. Finally, Figure 11.14 shows the steady running of one of the intermediate cases, that corresponding to Figure 11.12c.

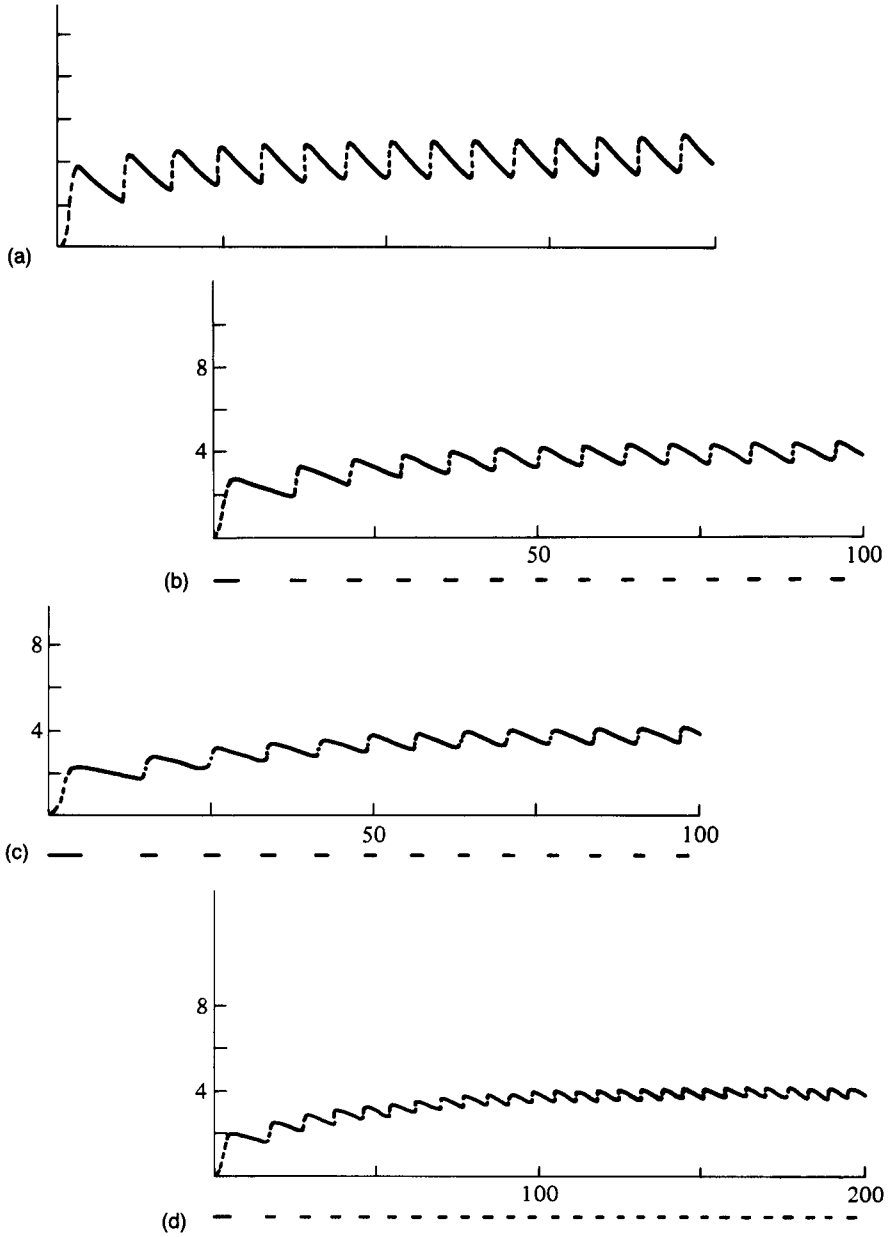

FIGURE 11.12 *The effects of inertia on start-up, rotation rate vs. time:* (a) *shaft inertia only, first 100 time units shown;* (b) *inertia equal to twice the shaft inertia, first 100 time units shown;* (c) *inertia equal to three times the shaft inertia, first 100 time units shown;* (d) *inertia equal to four times the shaft inertia, first 200 time units shown. Force ratio = 150.*

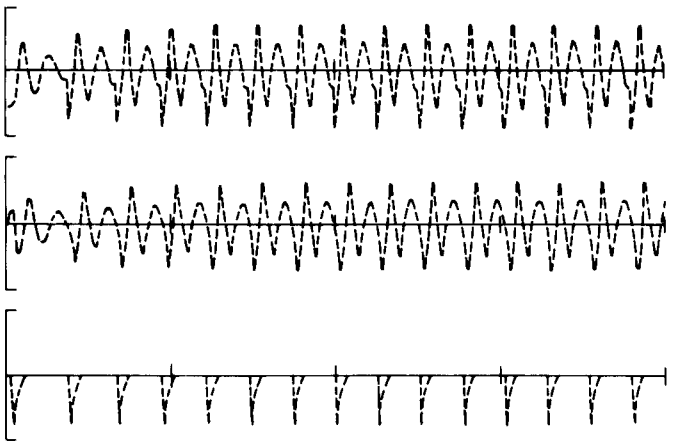

(a)

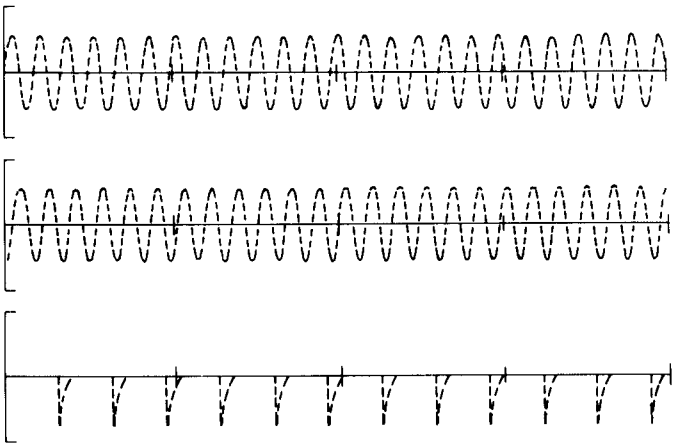

(b)

FIGURE 11.13 *Shaking: reaction forces (arbitrary units) at the shaft (first two curves) and side force (arbitrary units) at the piston (third line) as a function of time. The pulses in the side force correspond to the firing of the cylinder.* (a) *The "light" system of Figure 10.12a;* (b) *a massive (high-inertia) version of this system.*

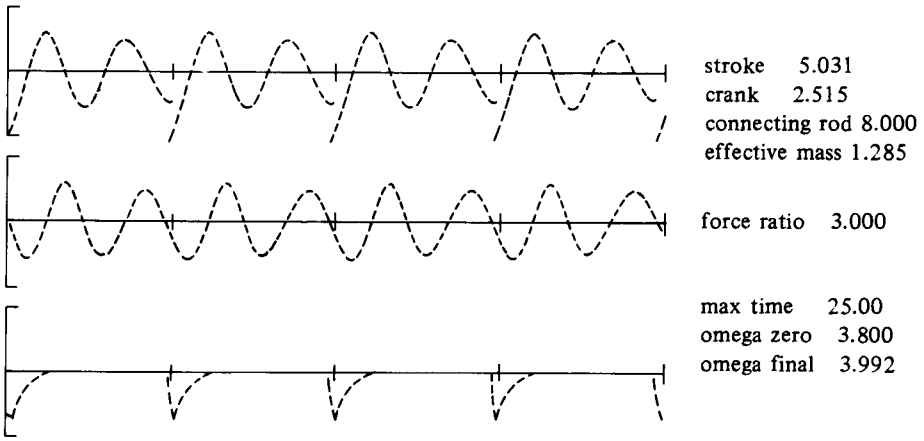

FIGURE 11.14 *Steady running of the one-cylinder engine whose start-up is shown in Figure 10.12c: reaction forces at the shaft (first two curves) and side force at the piston (third line) as a function of time. The spikes visible in the figure correspond to the firing of the cylinder.*

EXERCISES

1. Synthesize the dyad shown below. Let $p = 1 + 3i$ (in m), and let $\dot{p} = -2 + 2i$ (in m/s). Let $\omega_2 = 1$ rad/s and $\omega_3 = 2$ rad/s.

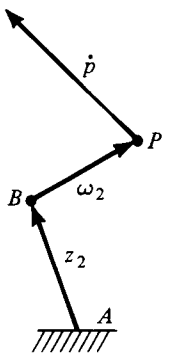

2. Formulate the constraint(s) necessary to use shaft torque as a synthesis parameter, assuming ground pivot specification. Does this make sense at the level of four-bar synthesis? Explain.

3. What variables would you need to specify to design a ball-throwing machine? Write the relevant constraint equations. How complex a mechanism seems necessary? Discuss.

4. How do piston mass, coupler mass, and compression stroke forces affect the reaction forces at A and D for the one-cylinder engine model?

5. The load on an automobile at highway speeds is dominated by air drag, which is proportional to the square of the vehicle speed. Adapt the one-cylinder engine model to investigate the effect of output loading proportional to the square of output rotation rate.

6. In a real vehicle, the inertia of the system includes that of the vehicle. Translate vehicular inertia into an equivalent flywheel inertia. Does this help you understand how a car with "rough idle" can seem quite smooth at highway speeds? Explain.

7. Suppose that the slider-crank mechanism is used to model a piston pump. Construct a model for the shaft torque required to drive the pump at a constant rotation speed. Assume two-stroke pumping, and make some appropriate assumption(s) about the force required to pump the fluid.

References

Beer, F.P., and Johnston, E.R., Jr. 1977. *Vector Mechanics for Engineers: Statics and Dynamics*, 3rd ed. New York: McGraw-Hill.

Bell, E.T. 1956. The prince of mathematicians. In *The World of Mathematics*, ed. J.P. Newman, Volume 1, pp. 295–339. New York: Simon & Schuster.

Carnahan, B., Luther, H.A., and Wilkes, J.O. 1969. *Applied Numerical Methods*. New York: Wiley.

Chakraborty, J., and Dhande, S.G. 1977. *Kinematics and Geometry of Planar and Spatial Cam Mechanisms*. New York: Wiley.

Chebyshev, P.L. 1854. Theorie des mecanismes connus sous le nom de parallèlogrammes. *Memoires l'Academie Imperiale des Sciences de St. Petersbourg* 7:539–568. [Reprinted in *Oeuvres de P.L. Tchebychef*. New York: Chelsea, 1961.]

Chebyshev, P.L. 1861. Sur une modification de parallèlogramme articule de Watt. *Bulletin physico-mathematique de l'Academie Imperiale des Sciences de St. Petersbourg* **4**: 433–438. [Reprinted in *Oeuvres de P.L. Tchebychef*. New York: Chelsea, 1961.]

Chebyshev, P.L. 1882. Sur les plus simples parallèlogrammes qui fournissent un mouvement rectiligne aux termes de quatrième ordre prés. [Reprinted in *Oeuvres de P.L. Tchebychef*. New York: Chelsea, 1961.]

Chironis, N.P., ed. 1965. *Mechanisms, Linkages and Dynamical Controls*. New York: McGraw-Hill.

Courant, R., and Robbins, H. 1947. *What is Mathematics?* 4th ed. Oxford: Oxford Univ. Press.

Davis, P.J., and Polonsky, I. 1965. Numerical interpolation, differentiation and integration. In *Handbook of Mathematical Functions*, eds. M. Abramowitz and I.A. Stegun. New York: (NBS) Dover.

Erdelyi, A., Magnus, W., Oberhettinger, F., and Tricomi, F.G. 1953. *Higher Transcendental Functions*, Volume II, Chapter 10. New York: McGraw-Hill.

Erdman, A.G., and Sandor, G.N. 1984. *Mechanism Design: Analysis and Synthesis*, Volume 1. Englewood Cliffs, NJ: Prentice-Hall.

Freudenstein, F. 1955. Approximate synthesis of four-bar linkages. *Trans ASME* **77**: 853–861.

Freudenstein, F., and Dobrjanskyj, L. 1966. On a theory for the type synthesis of mechanisms. *Proceedings of the XIth International Congress of Applied Mechanics*, ed. H. Goertler, pp. 420–428. Berlin: Springer-Verlag.

Gnudi, M.T., ed. 1972. *The Various and Ingenious Machines of Agostino Ramelli (1588)*. Baltimore: Johns Hopkins Press.

Greenspan, H.P., and Benney, D.J. 1973. *Calculus. An Introduction to Applied Mathematics*. New York: McGraw-Hill.

Gross, W.A. 1980. *Fluid Film Lubrication*. New York: Wiley.

Hildebrand, F.B. 1962. *Advanced Calculus for Applications*. Englewood Cliffs, NJ: Prentice-Hall.

Hochstrasser, U.W. 1965. Orthogonal polynomials. In *Handbook of Mathematical Functions*, eds. M. Abramowitz and I. Stegun. New York: (NBS) Dover.

Hrones, J.A., and Nelson, G.L. 1951. *Analysis of the Four-Bar Linkage.* New York: MIT/ Wiley.

Ince, E.L. 1956. *Ordinary Differential Equations.* New York: Dover.

McGill, D.J., and King, W.W. 1984. *An Introduction to Dynamics.* Monterey, CA: Brooks/ Cole.

Meirovitch, L. 1970. *Methods of Analytical Dynamics.* New York: McGraw-Hill.

Olson, D.G., Erdman, A., and Riley, D.R. 1985. A systematic procedure for type synthesis of mechanisms with literature review. *Mechanism and Machine Theory* **20**(4): 285–295.

Prager, F.D., and Scaglia, G. 1972. *Mariano Taccola and His Book "De Ingeneis."* Cambridge, MA: MIT Press.

Press, W.H., Flannery, B.P., Teukolsky, S.A., and Vetterling, W.T. 1986. *Numerical Recipes. The Art of Scientific Computing.* Cambridge: Cambridge Univ. Press.

Raven, F.H. 1959. Analytical design of disk cams and three dimensional cams by independent position equations. *ASME J. Appl. Mech.* **26**(1): 18–24.

Reuleaux, F. 1876. *The Kinematics of Machinery,* transl. A.B.W. Kennedy. London: MacMillan.

Reynolds, O. 1886. On the theory of lubrication and its application to Mr. Beauchamp Tower's experiments including an experimental determination of the viscosity of olive oil. *Phil. Trans. Roy. Soc. A* **177**: 157–234.

Sandor, G.N., and Erdman, A.G. 1984. *Advanced Mechanism Design: Analysis and Synthesis,* Volume 2. Englewood Cliffs, NJ: Prentice-Hall.

Sedov, I. 1959. *Similarity and Dimensional Methods in Mechanics,* transl. M. Friedman. New York: Academic Press.

Shigley, J.E. 1977. *Mechanical Engineering Design.* 3rd ed. New York: McGraw-Hill.

Strang, G. 1986. *Introduction to Applied Mathematics.* Wellesley, MA: Wellesley-Cambridge.

Szego, G. 1959. *Orthogonal Polynomials,* American Math Society Colloquium Publ Volume 23. New York: American Mathematics Society.

Tann, J., ed. 1981. *The Selected Papers of Boulton and Watt.* Cambridge, MA: MIT Press.

Tesar, D., and Vidosic, J.P. 1965. Analysis of approximate four-bar straight-line mechanisms. *ASME J. Engineering for Industry* **87**: 291–297.

Truesdell, C. 1968. The mechanics of Leonardo da Vinci (1955). In *Essays in the History of Mechanics,* ed. C. Truesdell, pp. 1–84. New York: Springer-Verlag.

Usher, A.P.A. 1929. *History of Mechanical Inventions.* New York: McGraw-Hill.

Vanderplaats, G.N. 1984. *Numerical Optimization Techniques for Engineering Design with Applications.* New York: McGraw-Hill.

Warren, J.G.H. 1970. *A Century of Locomotive Building by Robert Stephenson & Co.* New York: Augustus Kelly [Originally published by Andrew Reid, London, 1923].

Woo, L.S. 1967. Type synthesis of plane linkages. *ASME J. Engineering for Industry* **89**(1): 153–158.

Author Index

Subject Index